

I. Enantioselective Synthesis of Cyclohexa-2,4-dien-1-ones and Cyclohex-2-en-1-ones from Phenols

II. Cyclobutanes through S_Ni' Ring Closure, a Mechanistic Study

Dissertation

zur

Erlangung der naturwissenschaftlichen Doktorwürde
(Dr. sc. nat.)

vorgelegt der

Mathematisch-naturwissenschaftlichen Fakultät

der

Universität Zürich

von

Martin A. Lovchik

von Zürich ZH

Promotionskomitee

Prof. Dr. Georg Fráter
Prof. Dr. Heinz Heimgartner

Zürich, 2006

To my advisor

Prof. Dr. Georg Fráter

in great appreciation of his constant encouragement, support
and guidance throughout this work and my entire chemistry education.

Table of Contents

Part I and Part II

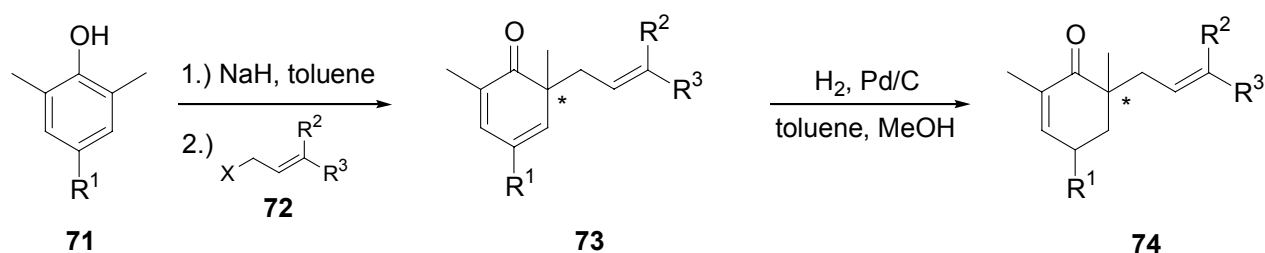
1. ABSTRACT	1
1.1 ABSTRACT PART I.....	1
1.2 ABSTRACT PART II.....	2
2. ZUSAMMENFASSUNG	3
2.1 ZUSAMMENFASSUNG TEIL I	3
2.2 ZUSAMMENFASSUNG TEIL II.....	4
3. PART I. ENANTIOSELECTIVE SYNTHESIS OF CYCLOHEXA-2,4-DIEN-1-ONES AND CYCLOHEX-2-EN-1-ONES FROM PHENOLS.....	5
3.1 INTRODUCTION	5
3.2 OBJECTIVES.....	9
3.3 RESULTS AND DISCUSSION	13
3.3.1 Selective hydrogenation of cyclohexadienones	13
3.3.2 By-products formed during the phenol alkylation	14
3.3.3 Determination of the enantiomeric excess	16
3.3.4 Phenol alkylation in the presence of (-)-sparteine	17
3.3.5 Screening for chiral auxiliaries	19
3.3.6 Alkylation of phenols under solvent free conditions	22
3.3.7 Alkylation of asymmetric phenols	24
3.3.8 Absolute configuration of naphthalenones 66 and 70	26
3.3.9 Vibrational Circular Dichroism (VCD) spectroscopic studies on 66	26
3.3.10 VCD spectroscopic studies on naphthalenone 70	28
3.4 CONCLUSIONS.....	31
3.5 EXPERIMENTAL	33
3.6 REFERENCES.....	46
4. PART II. CYCLOBUTANES THROUGH S_NI' RING CLOSURE, A MECHANISTIC STUDY	48
4.1 INTRODUCTION	48
4.1.1 Summary of different S _N 2' reactions from the literature	53
4.1.2 Stereochemical analysis of the S _N 2' reaction by MO considerations.....	55
4.1.3 Synthetic routes leading to optically active cyclobutanones	60

4.2	OBJECTIVES	63
4.3	RESULTS AND DISCUSSION	67
4.3.1	Synthetic intermediates	67
4.3.2	Cyclobutanone formation through S _N i' ring closure.....	71
4.3.3	Cyclobutanone vs. oxetane, the HSAB theory.....	73
4.3.4	Synthesis of the S _N i' precursor (<i>S</i>)-(<i>E</i>)- 139	75
4.3.5	X-ray crystallography of the camphanoate derivative of (+)-(<i>E</i>)- 178	75
4.3.6	Determination of the absolute configuration of secondary alcohols by Horeau.....	76
4.3.7	Searching for suitable leaving groups.....	78
4.3.8	Chiral cyclobutanones through stereoselective S _N i' reaction	79
4.3.9	Absolute configuration of (<i>E</i>)- and (<i>Z</i>)-cyclobutanones with VCD and ROA	81
4.3.10	Mechanism of the S _N i' reaction	83
4.4	TOTAL SYNTHESIS OF JUNIONONE.....	86
4.4.1	Introduction.....	86
4.4.2	Synthetic intermediates	87
4.4.3	Determination of the absolute configuration of keto-epoxide (<i>E</i>)- 190	90
4.4.4	ROA spectroscopy of (<i>E</i>)- 190	92
4.4.5	Cyclization of epoxyketone (<i>R,R</i>)-(<i>E</i>)- 190	93
4.4.6	Cyclization experiments with β-keto-ester (<i>R,R</i>)-(<i>E</i>)- 241	101
4.4.7	Total synthesis of (-)-(<i>S</i>)-junionone	104
4.4.8	Total synthesis of (+)-(<i>R</i>)-junionone.....	104
4.4.9	Isolation of natural junionone from <i>juniperus communis</i> L.....	105
4.5	CONCLUSIONS	108
4.6	EXPERIMENTAL	111
4.6.1	Mechanistic studies on the S _N i' reaction.....	113
4.6.2	Synthesis of (-)- and (+)-junionone (<i>E</i>)- 189	127
4.7	REFERENCES.....	142
5.	TABLES.....	144
6.	FIGURES.....	145
7.	SCHEMES	147
8.	ACKNOWLEDGMENTS	150
9.	CURRICULUM VITAE.....	151

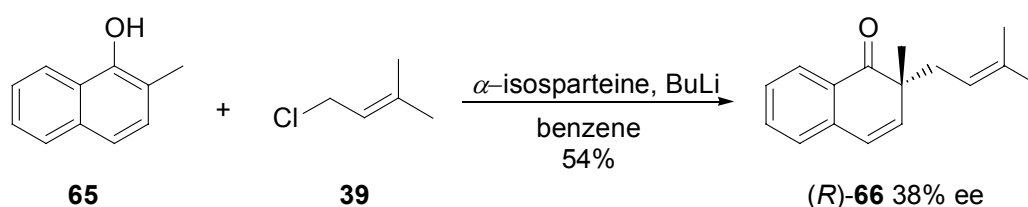
1. Abstract

1.1 Abstract Part I

Construction of quaternary stereogenic carbon centers in α -position of cyclic ketones has been subject of numerous research publications over the last decades [1].¹ In this dissertation a new method for the enantioselective synthesis of 2,6,6-trisubstituted cyclohexa-2,4-dien-1-ones **73** and 2,6,6-trisubstituted cyclohex-2-en-1-ones **74** is presented. The method involves C-alkylation of phenols **71** with allyl halides **72** followed by subsequent selective hydrogenation of the intermediate cyclohexadienone **73** [2][3].



The objective of this research was to investigate whether the phenoxide ion could undergo complexation with an optically active bidentate ligand, forcing the incoming nucleophile to approach predominantly from one stereotopic face, leading preferentially to the formation of one enantiomer. The newly developed method was then extended to asymmetric phenols and naphthols. The synthesis of (*R*)-**66** illustrated below is the best example using a lithium- α -isosparteine complex as a chiral base [4].

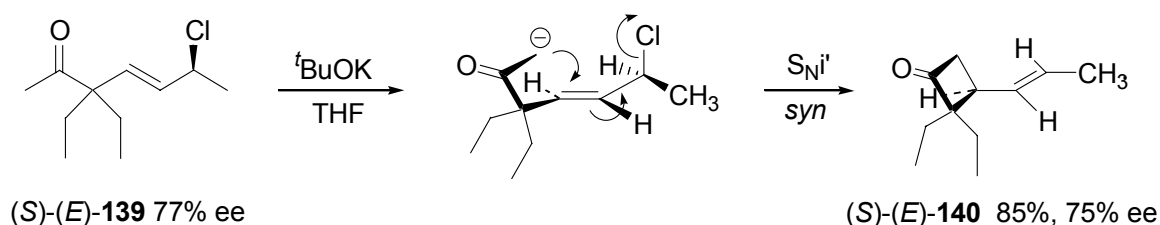


Several substituted phenols and naphthols were alkylated in the presence of different chiral ligands bearing tertiary nitrogen atoms. The influence of solvent and phenoxide counter ions on the outcome of the reaction was investigated.

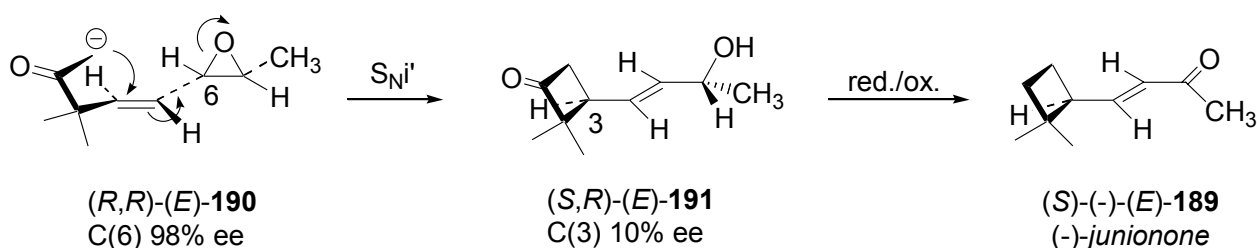
¹ Literature references to Part I are listed on p.46.

Abstract Part II

The S_N2' reaction has first been postulated independently by Hughes and by Winstein [38][39]. The mechanistic course of the reaction was found to depend on both the nature of the nucleophiles and that of the leaving groups [49]. Stereoelectronic requirements of the reaction were analyzed by Liotta based on orbital symmetry considerations [55]. The intramolecular variant, the S_{Ni}' reaction, was reviewed by Paquette and Stirling [41]. Part II of this dissertation reports the results of mechanistic studies on the S_{Ni}' reaction and reports a new stereoselective access to substituted cyclobutanones. Optically active β,γ -unsaturated ketone (*S*)-(*E*)-**139** was selectively cyclized to (*S*)-(*E*)-**140** with complete transfer of chirality. The absolute configuration of (*S*)-(*E*)-**139**, and of the resulting vinyl-cyclobutanone (*S*)-(*E*)-**140**, was determined by X-ray diffraction analysis and Raman Optical Activity (ROA) spectroscopy.



The absolute configuration of (*S*)-(*E*)-**139** and (*S*)-(*E*)-**140** allowed the conclusion that the reaction mechanism proceeded by an intramolecular, allylic substitution of the leaving group, taking place in *syn*-fashion relative to the incoming nucleophile. The method was extended to the allylic epoxide (*R,R*)-(*E*)-**190**, where the expected S_{Ni}' reaction initially failed under the usual reaction conditions. Activation of the epoxide with Lewis acid such as $\text{BF}_3 \cdot \text{Et}_2\text{O}$ led to the formation of cyclobutanone (*S,R*)-(*E*)-**191**. Under these reaction conditions, substantial loss of chiral information was observed at the newly formed ring-carbon. These results led to the conclusion that the reaction involved an allyl cation intermediate, formed by Lewis acid catalyzed epoxide opening, followed by nucleophilic attack of the ketone enolate.

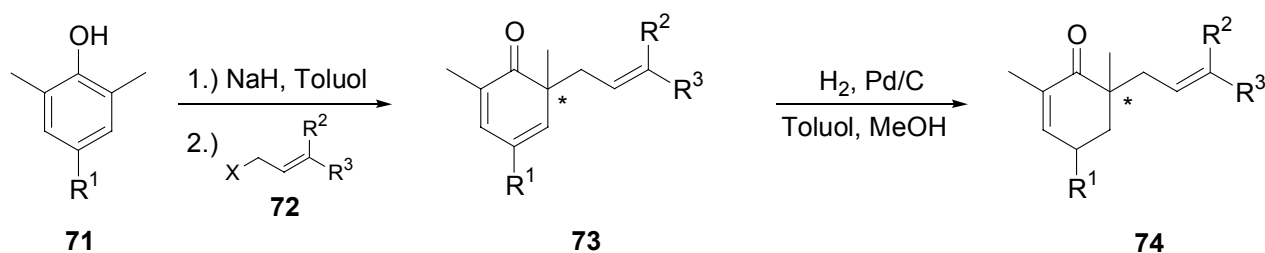


Junione, an olfactorily interesting cyclobutane monoterpene from *Juniperus communis*, L. was synthesized in two steps from (*S,R*)-(*E*)-**191** and compared to authentic material isolated from natural juniper-berry oil [77].

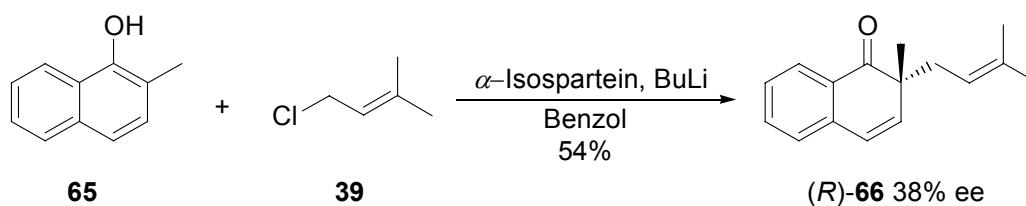
2. Zusammenfassung

2.1 Zusammenfassung Teil I

Die Synthese quartärer stereogener Zentren in der α -Stellung cyclischer Ketone war schon das Thema vieler Publikationen [1].² In dieser Dissertation wird eine neue, enantioselektive Methode vorgestellt, um 2,6,6-trisubstituierte Cyclohexa-2,4-dien-1-one und 2,6,6-trisubstituierte Cyclohex-2-en-1-one zu synthetisieren. Alkalisalze der Phenole **71** können mit Allyl-halogeniden **72** in *ortho*-Stellung alkyliert werden. Die resultierenden Cyclohexa-2,4-dien-1-one **73** können durch regioselektive Hydrierung in die entsprechenden Cyclohex-2-en-1-one **74** übergeführt werden [2][3].



Das Ziel dieser Forschung war, den Einfluss optisch aktiver Auxiliare auf die Konfiguration des neu gebildeten quartären Zentrums zu studieren. Optische Induktion sollte durch Komplexieren des Phenolat-Ions mit einem chiralen Auxiliar erreicht werden. Dazu wurden verschiedene Alkaloide sowie kommerziell erhältliche Liganden untersucht. Die chirale Umgebung hatte zur Konsequenz, dass der elektrophile Angriff bevorzugt aus einer bestimmten Richtung erfolgen konnte, was zu Anreicherung eines Enantiomers im Produkt führte [4]. In der folgenden Abbildung ist als bestes Beispiel die asymmetrische Alkylierung von Naphthol **65** mit Prenylchlorid **39**, in Gegenwart von α -Isosparteine illustriert.

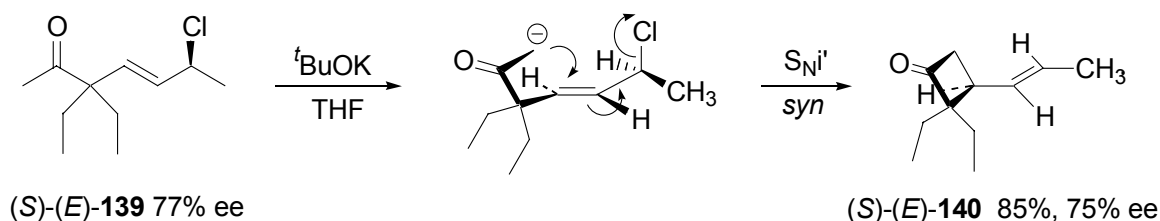


Verschiedene substituierte Phenole und Naphthole wurden in Gegenwart unterschiedlicher chiraler Auxiliare alkyliert. Der Einfluss von Lösungsmitteln und Phenolat-Gegenionen auf den Reaktionsverlauf wurde untersucht.

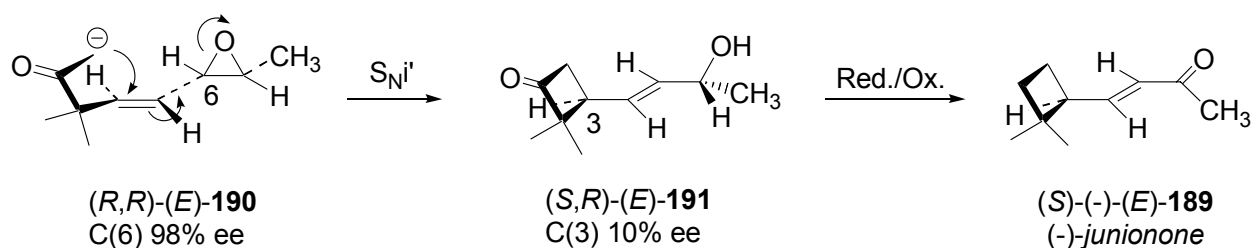
² Literaturreferenzen für Teil I sind im Verzeichnis auf Seite 46 aufgeführt.

2.2 Zusammenfassung Teil II

Die S_N2' Reaktion wurde erstmals von Hughes und von Winstein, unabhängig von einander postuliert [38][39]. Der mechanistische Ablauf der Reaktion wird von den Eigenschaften des Nukleophils sowie der Abgangsgruppe beeinflusst [49]. Die stereoelektronischen Voraussetzungen für die Reaktion wurden von Liotta aus dem Gesichtspunkt der Orbitalsymmetrie analysiert [55]. Die intramolekulare Variante der S_N2' Reaktion, die sogenannte S_{Ni}' Reaktion, wurde von Paquette and Stirling zusammengefasst [41]. Teil II dieser Dissertation präsentiert die Resultate neuer mechanistischer Studien der S_{Ni}' Reaktion und berichtet von einem neuen, stereoselektiven Zugang zu substituierten Cyclobutanonen. Optisch aktives β,γ -ungesättigtes Keton (*S*)-(*E*)-**139** wurde selektiv, mit vollständigem Chiralitätstransfer, zu Cyclobutanon (*S*)-(*E*)-**140** cyclisiert. Die absolute Konfiguration von (*S*)-(*E*)-**139** und (*S*)-(*E*)-**140** wurde durch Röntgenstrukturanalyse und "Raman Optical Activity" (ROA) Spektroskopie bestimmt.



Die Bestimmung der absoluten Konfigurationen von (*S*)-(*E*)-**139** und (*S*)-(*E*)-**140** lies den Schluss zu, dass es sich um eine konzertierte, intramolekulare, allylische Substitution handelte, wobei der Angriff des Nukleophils, relativ zur Abgangsgruppe, *syn*-selektiv erfolgt. Die Methode wurde auf das allylische Epoxid (*R,R*)-(*E*)-**190** ausgedehnt. Zwar scheiterten erste Zyklisierungsversuche, aber die Aktivierung des Epoxids mit Lewis Säuren wie zum Beispiel $\text{BF}_3 \cdot \text{Et}_2\text{O}$, führte schliesslich zum Cyclobutanon. Bei der Umsetzung von (*R,R*)-(*E*)-**190** unter diesen Bedingungen wurde ein weitgehender Verlust der chiralen Information am neu gebildeten, stereogenen Zentrum beobachtet. Diese Resultate deuten darauf hin, dass die Lewis Säure katalysierte Öffnung des Epoxides zur Bildung eines allylkationischen Zwischenproduktes führt, bevor der Ringschluss erfolgen kann.

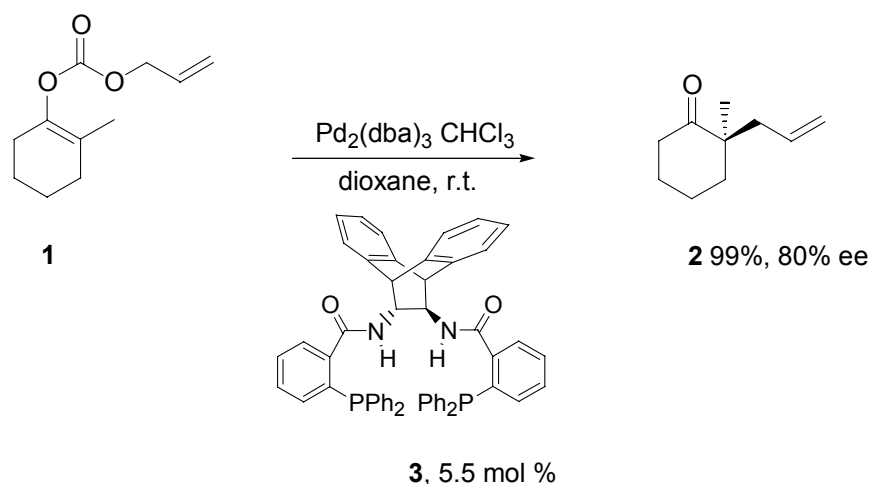


Im weiteren wurde *Junione*, ein olfaktorisch interessantes Cyclobutanon-Monoterpen aus *Juniperus communis* L., in zwei Stufen aus (*S,R*)-(*E*)-**191** synthetisiert und mit einer authentischer Referenzsubstanz, die aus dem Öl der Wacholderbeere isoliert wurde, verglichen [77].

3. Part I. Enantioselective Synthesis of Cyclohexa-2,4-dien-1-ones and Cyclohex-2-en-1-ones from Phenols

3.1 Introduction

Construction of quaternary stereogenic centers has become an important goal in modern organic synthesis. Over the last decades, numerous articles were published, reporting various methods to construct quaternary stereogenic centers with high enantioselectivity. For a review of recently developed methods see Barriault et al. and the references cited therein [1]. The need for stereochemical control of quaternary stereogenic centers in α -position to carbonyl groups arises in the synthesis of natural products and compounds with polycyclic carbon structures [2][19]. The asymmetric alkylation of ketone enolates has mostly been restricted to structurally biased molecules, with covalently attached chiral auxiliaries, in which only one enolate is possible. Bulky substituents block one diastereotopic face, leading to enantiomeric discrimination due to the energy difference of the transition states [5]. Lately, Trost et al. reported a regio- and enantioselective Pd-catalyzed allylic alkylation of cyclic ketones via allyl enol carbonates **1** [6], *Scheme 1*.

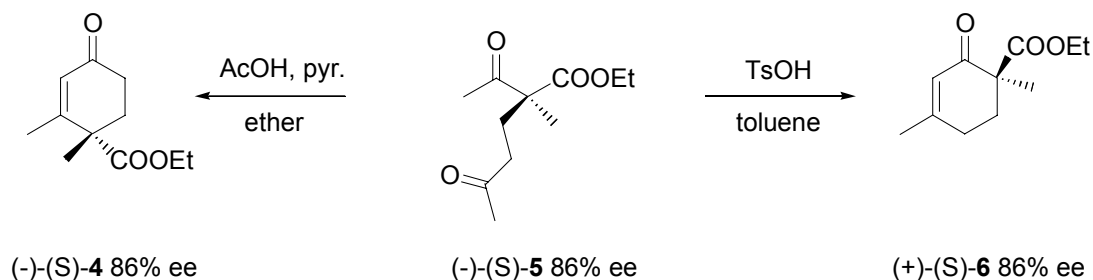


Scheme 1. Regio- and enantioselective ketone alkylation of allyl enol carbonates by Trost.

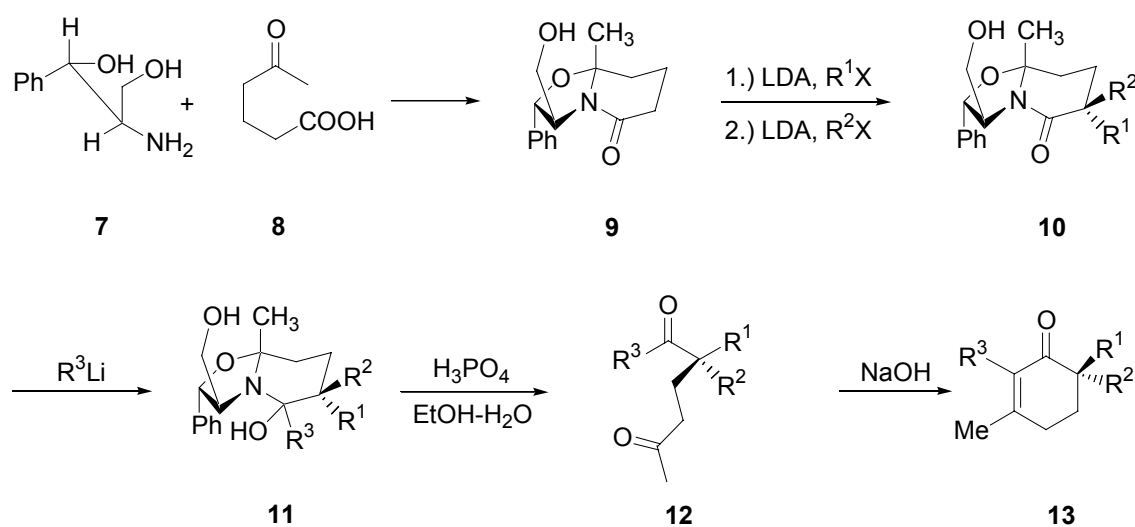
Chiral 3,6,6-trialkylated and 3,4,4-trialkylated cyclohex-2-en-1-ones are accessible through intramolecular aldol condensation of chiral α,α -disubstituted-2,6-heptane-diones **5**, as reported by Fráter [7], *Scheme 2*. The chemoselectivity is controlled by choosing appropriate reaction conditions leading to **4** or **6** respectively. Similar results were reported by Kreiser et al. [8].

A modified approach to chiral cyclohexenones, allowing the introduction of a broad range of alkyl groups, involving intramolecular aldol condensation of the chiral dicarbonyl compound **12**, was reported by Meyers and Lefker [9], *Scheme 3*. The bicyclic lactam **9** was easily prepared from γ -ketoacid **8** and commercially available (*S,S*)-aminodiol **7**. Successive diastereoselective alkylation led to the intermediate **10** with a quaternary center in α -position to the carbonyl carbon.

Treatment of **10** with alkyl lithium allowed the insertion of an alkyl substituent in 2-position of the final product. Hydrolysis and subsequent basic cyclization led to the optically active cyclohexenone **13**, *Scheme 3*.

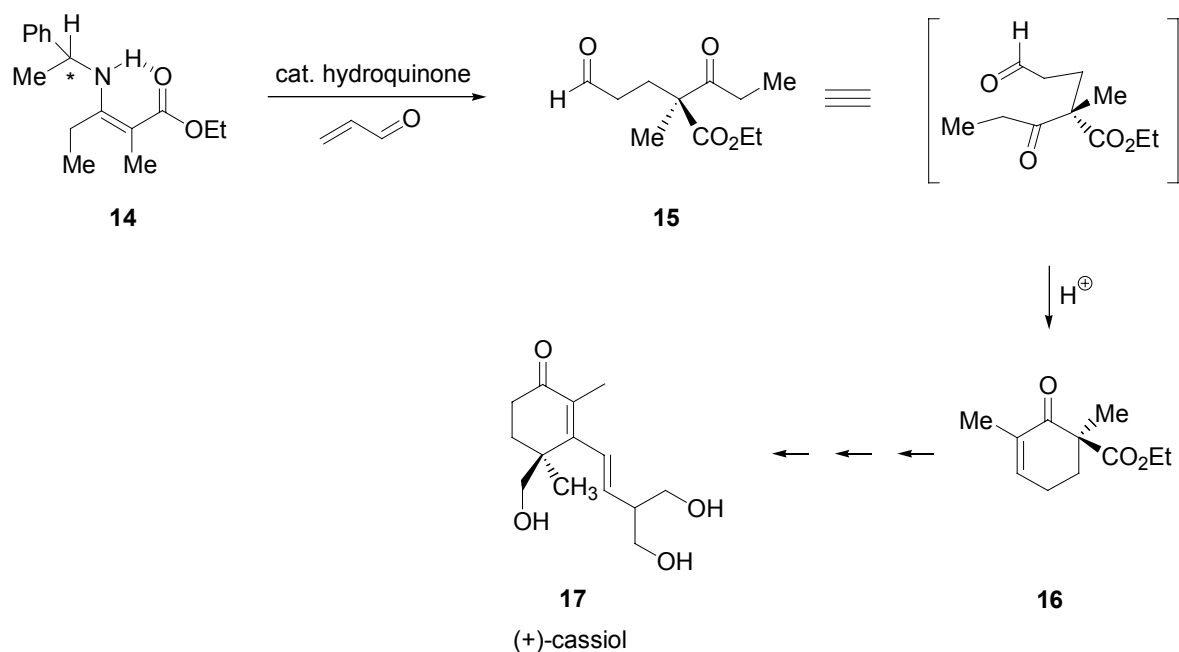


Scheme 2. Synthesis of chiral, substituted cyclohexenones by Fráter.



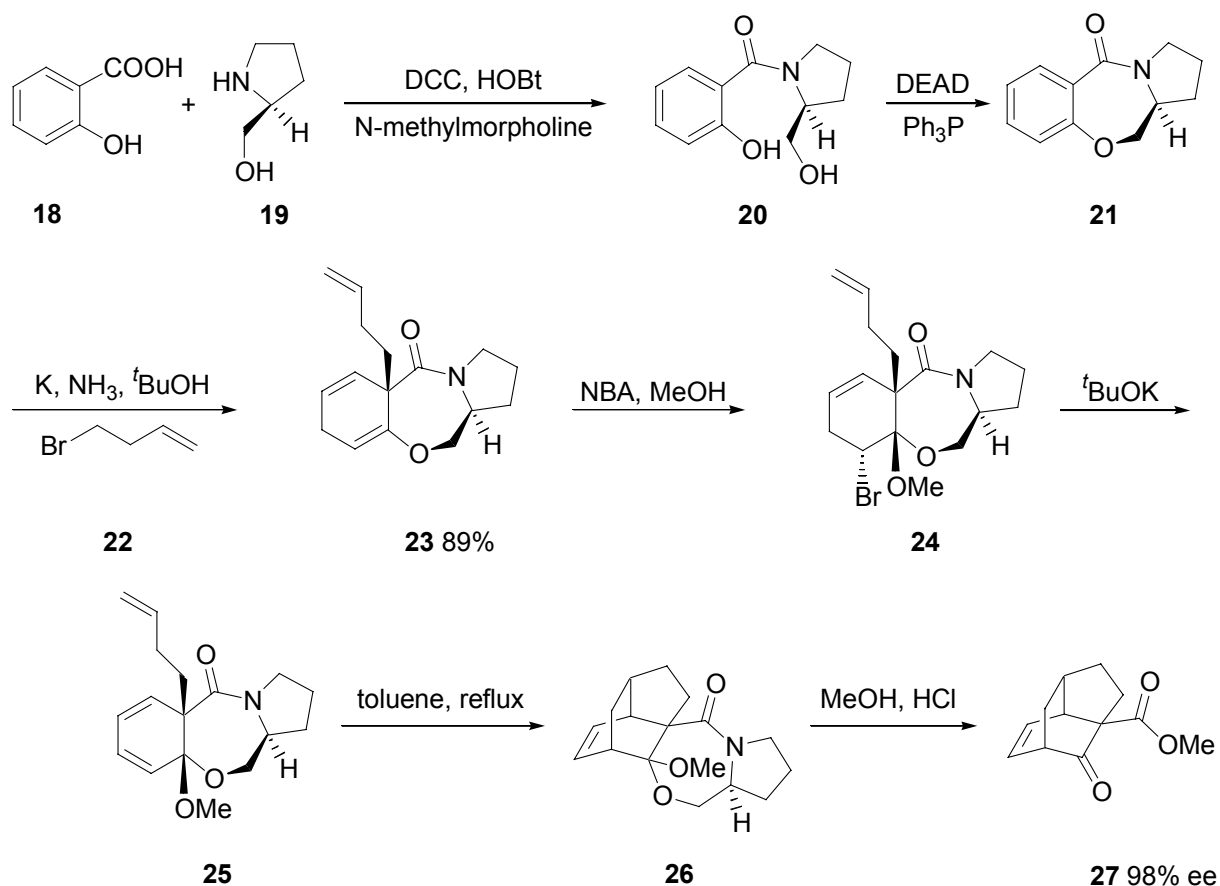
Scheme 3. Diastereoselective synthesis of cyclohexenones by Meyers et al.

A disadvantage of the method is the mandatory methyl substituent in 3-position of **13**, resulting from the keto-acid. A related procedure was reported by Maiti et al. in the diastereoselective synthesis of (+)-cassiol **17** [10], *Scheme 4*. The synthesis required the enantiomerically pure intermediate **16**, prepared by intramolecular Aldol reaction of (+)-**15**. The chirality was introduced by acrolein condensation with the chiral enamine of an acyclic β -ketoester **14**. This strategy results in one of the substituents in 6-position being a carboxylate group.



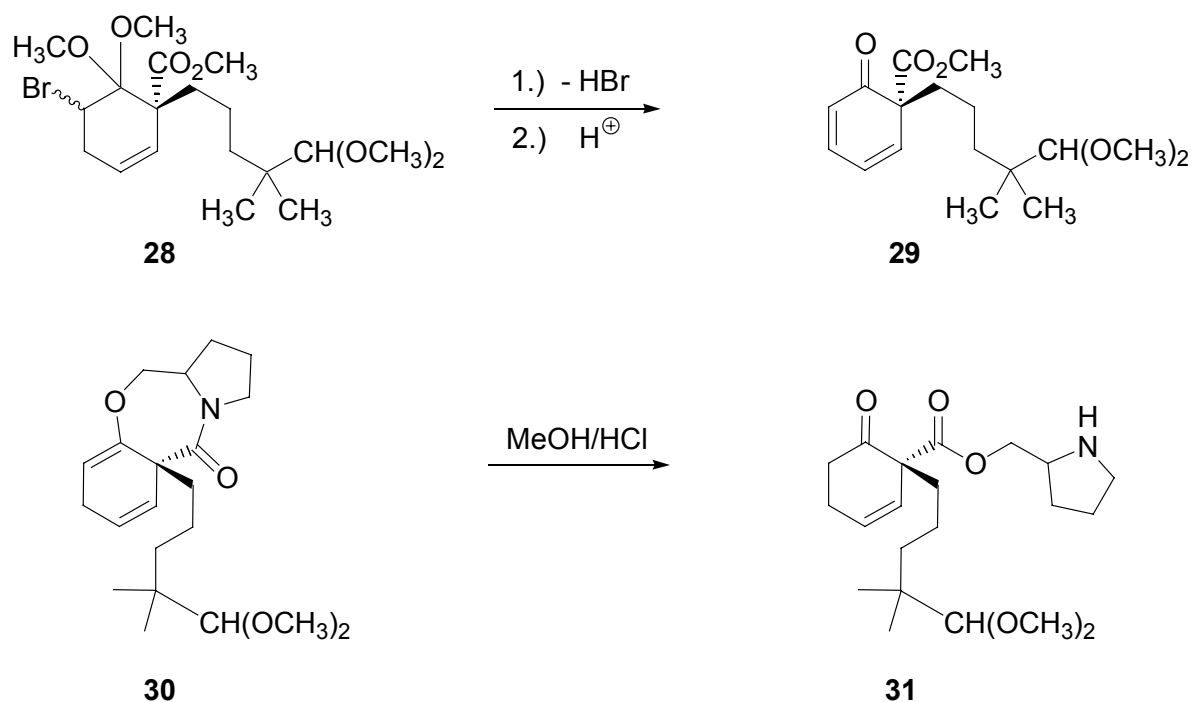
Scheme 4. Diastereoselective synthesis of cyclohexenones by Maiti et al.

Methods for the direct synthesis of optically active cyclohexa-2,4-dien-1-ones of type **29** have not been reported until now. A multistep route was described by Schultz et al. The authors reported that optically active cyclohexadienones are accessible by an asymmetric variation of the Birch reduction-alkylation reaction, using a covalently bound chiral auxiliary [11], *Scheme 5*.



Scheme 5. Diastereoselective Birch reduction alkylation reaction by Schultz et al.

Compound **21**, readily available from salicylic acid **18** and *L*-prolinol **19**, undergoes a Birch reduction-alkylation sequence with 4-bromo-1-buten **22** to give **23** in 89% yield and 98% diastereoselectivity. Bromohydrine formation in **24** was accomplished by treating enol ether **23** with *N*-bromoacetamide in MeOH. Dehydrobromination then led to **25**. Diels-Alder reaction of **25** followed by hydrolysis of the intermediate **26** led to the tricyclic compound **27**. Alternatively, hydrolysis of **25** will lead to an optically active cyclohexadienone. Although this reaction was not performed, examples reported by the same authors show that **28** can be converted to **29** by hydrolysis on acidic silica gel and that **30** will rearrange to the carboxylic ester **31** upon treatment with hydrochloric acid in methanol, *Scheme 6*.

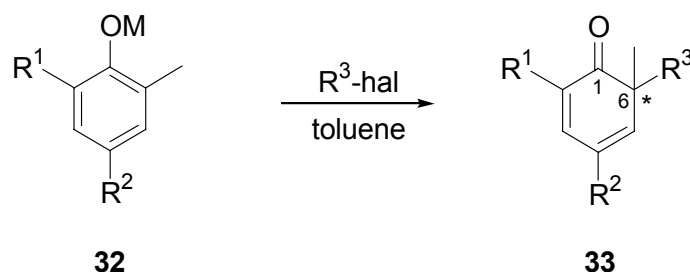


Scheme 6. Dehydrobromination- and rearrangement-reaction reported by Schulz et al.

To this day, it remains a challenge to synthesize substituted cyclohexa-2,4-dien-1-ones and cyclohex-2-en-1-ones enantioselectively. It was the goal of this research to find a straight forward synthetic strategy to access such compounds through asymmetric alkylation of substituted phenols [12].

3.2 Objectives

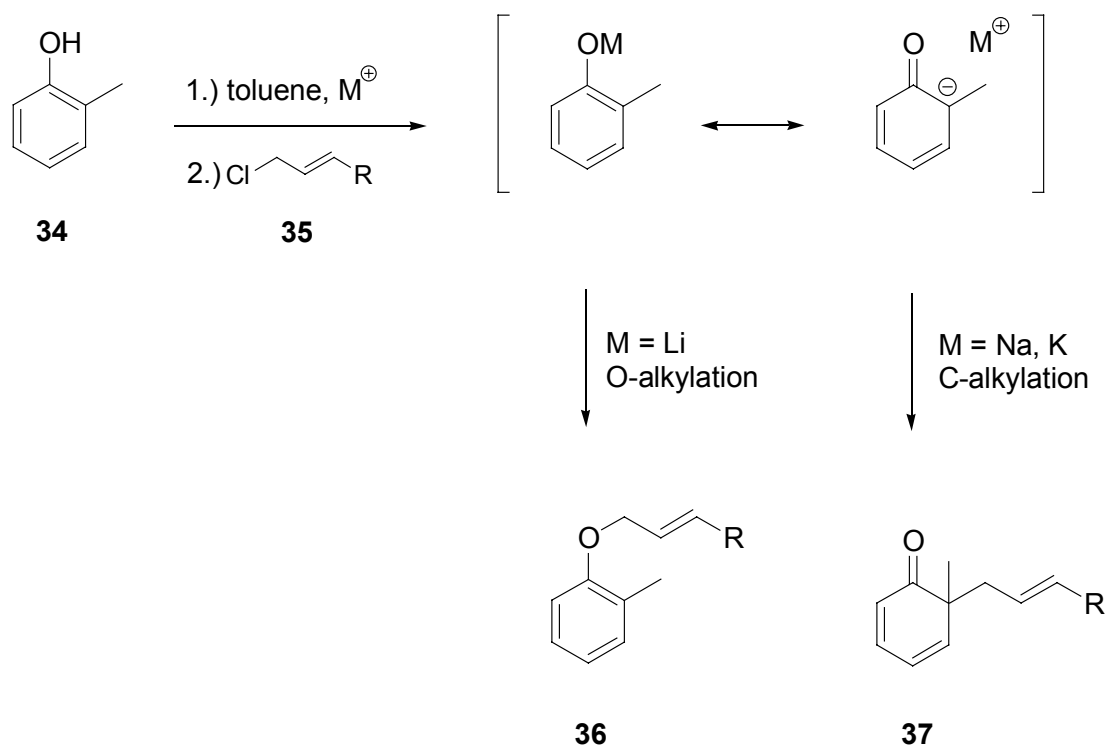
Phenoxide ions **32** may act like ambident cyclic ketone enolates and can be C-alkylated under certain conditions. This results in the formation of cyclohexadienones **33** with a new quaternary stereogenic center formed at C(6), *Scheme 7*.



Scheme 7. Alkylation-dearomatization of phenols.

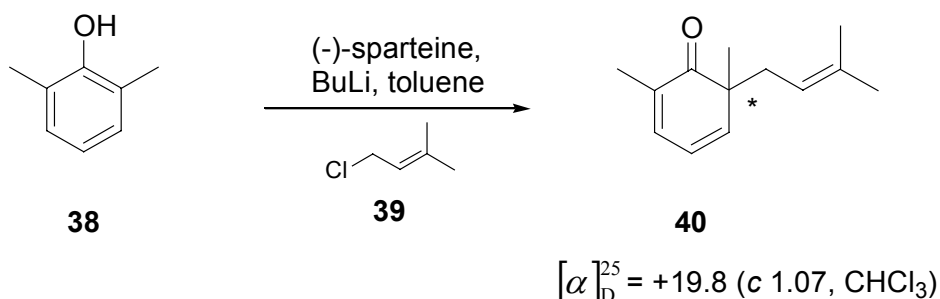
The chemoselective outcome of the reaction depends largely on the nature of the solvent. In the 1960's several controversial studies on the effect of solvents on the regioselectivity of the phenol alkylation were published. Curtin et al. reported that C-alkylation of 2,6-dimethylphenol was best performed in heterogeneous suspensions of sodium phenoxide in toluene. The authors reasoned, that less dissociated phenoxide ions were more likely to be alkylated at the *ortho*-carbon [13]. At the same time, Kornblum and his co-workers found that C-alkylation of phenols with allyl bromide and benzyl chloride was effectively performed in protic solvents such as water, phenol and fluorinated alcohols [14]. The authors proposed, that solvation of the phenoxide ion through hydrogen bonding with the solvent was responsible for the formation of C-alkylated products in as much as 78% yield.

The nature of the phenoxide counter ion also has a significant effect on the regioselective outcome of the reaction, *Scheme 8*. Sodium was found to be suited best, leading to formation of cyclohexadienone **37** in 80% yield. The aluminum- and bromomagnesium salts reacted too slowly to be useful. On the other hand, alkylation of lithium phenoxide afforded the O-alkylated product **36** almost exclusively [15]. This observation can also be related to the HSAB theory. The lithium cation being the harder acid than the sodium cation is expected to coordinate more closely with the oxygen atom, thereby removing negative charge from the carbon atom. The softer sodium counter ion allows a better distribution of the negative charge, which makes alkylation at the *ortho* carbon possible, *Scheme 8*.



Scheme 8. C- and O-alkylation of phenoxide ion.

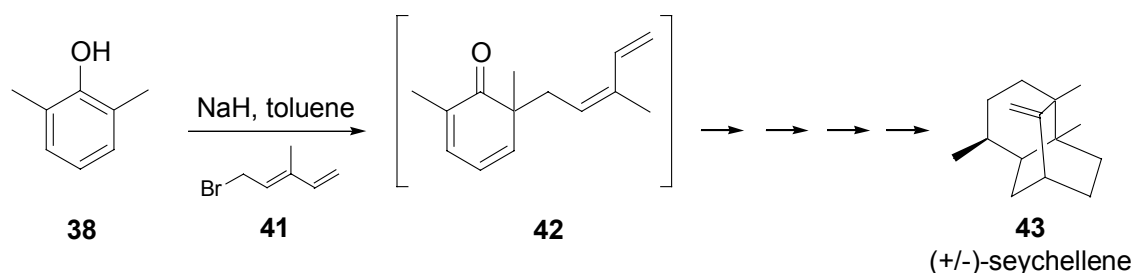
The C-alkylation product **37** can readily undergo acid catalyzed dienone-phenol rearrangement leading to substituted phenols. The different rearrangement reactions of **37** will be discussed in detail in *Chapter 3.3.2*. Unpublished results by Goeke et al. showed that when 2,6-dimethylphenol **38** was deprotonated with a (-)-sparteine-lithium complex and then treated with 1-chloro-3-methylbut-2-ene (prenyl chloride) **39**, enantiomerically enriched cyclohexadienone **40** of unknown enantiomeric excess was obtained, exhibiting an optical rotation of +19.8 at 589 nm, *Scheme 9*. This indicated that chiral information had been transferred from (-)-sparteine to the newly formed quaternary stereogenic center in **40**. It was the objective of this research to learn more about the effects that influence the stereoselectivity of this reaction.



Scheme 9. Unpublished phenolate alkylation experiment with (-)-sparteine.

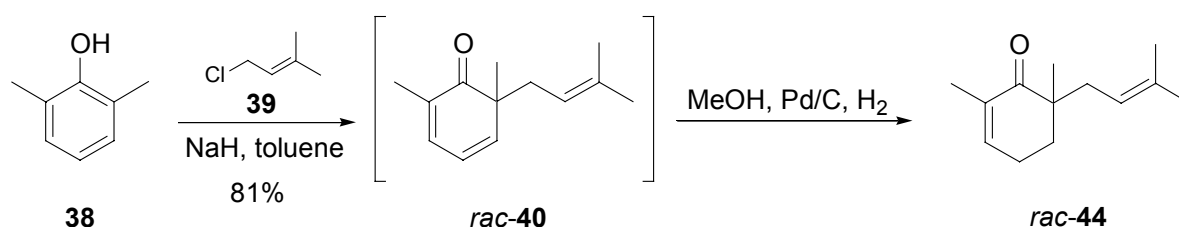
Cyclohexadienones are useful intermediates for a variety of applications including cycloadditions, in which the diene unit functions as a two-electron or four-electron donor, and photochemical rearrangements to bicyclo[3.1.0]hex-3-en-2-ones [16][17].

Some practical applications of cyclohexadienones can be found in the literature. During research performed on the rearrangement of dienyl-mesityl ethers in 1972, Fráter et al. found that tricyclic homotwistanone derivatives were formed by an in-situ intramolecular Diels-Alder reaction of a cyclohexadienone intermediate [18]. Based on these results, the authors published the total synthesis of (\pm)-seychellene **43** in four steps from 2,6-dimethylphenol **38** [19]. The first step involves the alkylation of **38** with bromodiene **41**, *Scheme 10*. Intramolecular Diels-Alder reaction of the resulting cyclohexadiene **42** furnished a tricyclic ketone which upon hydrogenation, methylation and subsequent rearrangement gave (\pm)-seychellene **43**.



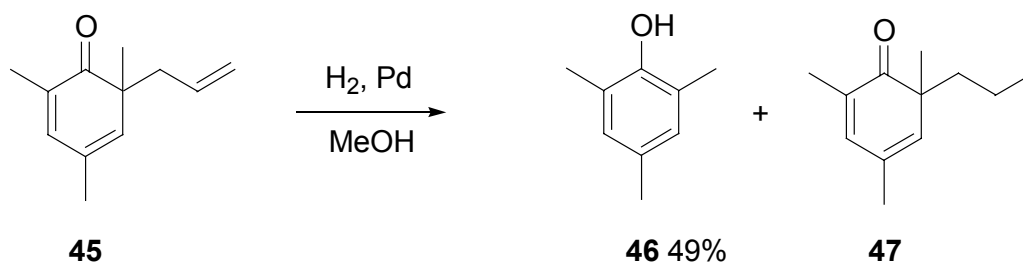
Scheme 10. Synthesis of (+/-)-seychellene by Fráter et al.

Some allyl substituted cyclohexenones have interesting olfactory properties and exhibit strong grapefruit-like odors, accompanied by floral and fresh green aspects. Goeke published a regioselective in-situ hydrogenation of cyclohexadienone *rac*-**40** to give the stable cyclohexenone *rac*-**44** [3], *Scheme 11*.



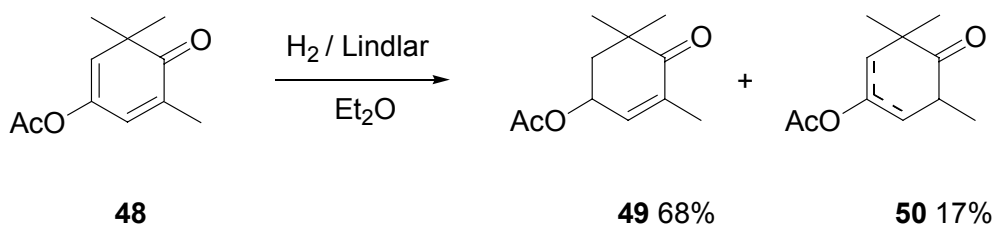
Scheme 11. Regioselective in-situ hydrogenation by Goeke.

Preliminary results showed, that the in-situ hydrogenation did no longer function in the presence of (-)-sparteine. Presumably, the nitrogen containing auxiliary poisoned the palladium catalyst. For this reason, it was necessary to develop a method to regioselectively hydrogenate isolated cyclohexadienones. No method for the direct, regioselective hydrogenation of the 4,5-double bond in cyclohexa-2,4-diene-1-ones has been published to date. Miller et al. reported that hydrogenation of cyclohexadienones can not be achieved under standard conditions [20]. The authors stated, that hydrogenation of allyl cyclohexadienones leads to appreciable hydrogenolytic cleavage of the allyl group and no evidence for ring hydrogenation was observed. A typical example was the hydrogenation of **45**, leading to the hydrogenolysis product **46** and the side chain hydrogenation product **47**, *Scheme 12*.



Scheme 12. Hydrogenolysis of cyclohexadienones by Miller et al.

Regioselective hydrogenation in a cyclohexadienone system was first described by Soukup et al. for the Lindlar catalyzed hydrogenation of 4-oxoisophorone enol acetate **48**, *Scheme 13*. Mixed enol acetate **50** was formed as a by-product during the hydrogenation [21].

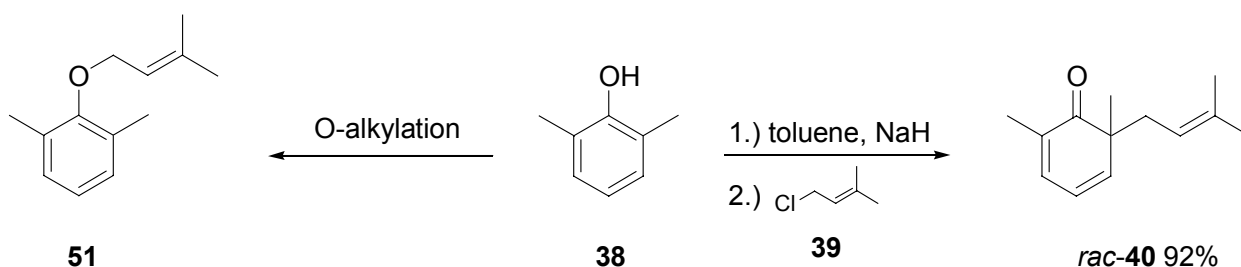


Scheme 13. Regioselective hydrogenation of 4-oxoisophorone enol acetate by Soukup.

Ten years later Scalone et al. published an asymmetric reduction of **48** to **49** using chiral Rh and Ir catalysts [22].

3.3 Results and Discussion

Alkylation of 2,6-dimethylphenol with 1-chloro-3-methylbut-2-ene (prenyl chloride) **39** was chosen as the model reaction for the initial studies on the chiral alkylation of phenols. **38** was deprotonated in toluene with NaH at 0 °C to give a bright green suspension of sodium phenoxide, *Scheme 14*. Alkylation with prenyl chloride went smoothly and the α -disubstituted cyclohexadienone *rac*-**40** was obtained in good yield (92%) and high purity [2][3]. Phenylether **51**, being the major side product, was prepared by a conventional method and used as a reference for GC and TLC analysis.



Scheme 14. O- and C-alkylation of 2,6-dimethylphenol.

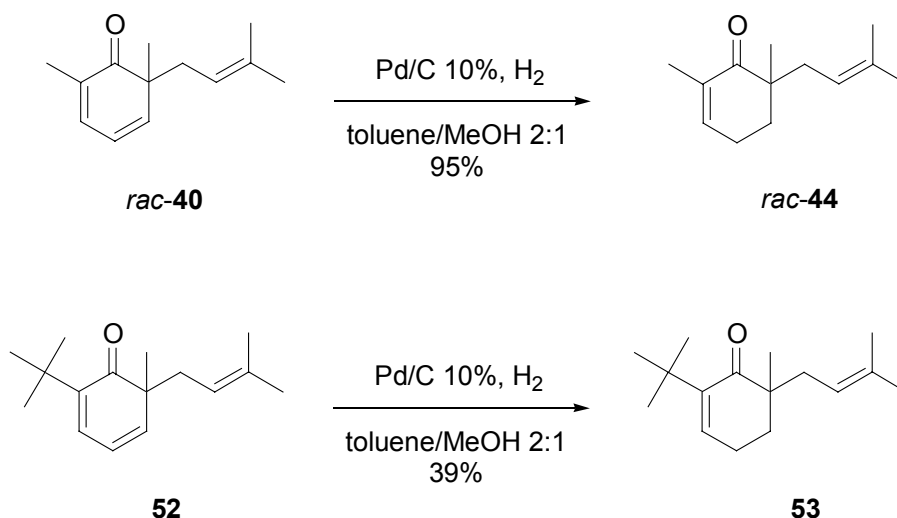
Cyclohexa-2,4-dien-1-ones are somewhat difficult to handle, because they undergo thermal and acid catalyzed rearrangement leading to more stable *meta*- and *para*-phenols. They readily form dimers by a Diels-Alder reaction even at room temperature [15]. Nevertheless, *rac*-**40** could be isolated after chromatography on basic aluminum oxide and distilled under mild short path conditions (50 °C, 0.05 mbar). The slightly yellow oil could be stored in the refrigerator for several days.

3.3.1 Selective hydrogenation of cyclohexadienones

After the alkylation reaction of **38** was complete, 50%_[vol.] of methanol and palladium 10% on activated charcoal was added to the crude reaction mixture and stirring was continued under a hydrogen atmosphere at room temperature [3]. Under these conditions the hydrogenation of *rac*-**40** took 2 h and resulted in selective reduction of the sterically less hindered 4,5-double bond leading to *rac*-**44**. It was found that, when (-)-sparteine was present in the reaction mixture, the palladium catalyst was poisoned and hydrogenation no longer took place. When pure *rac*-**40** was hydrogenated in MeOH with Pd/C 10%, a mixture of phenols was obtained, possibly resulting from hydrogenolysis [20] and palladium catalyzed Cope rearrangements [23].

It was found that the polarity of the solvent mixture was the key factor and that selective hydrogenation of the 4,5-double bond in the cyclohexadienone ring was favored in a mixture of toluene/MeOH 2:1. By applying this simple procedure, it was possible to convert the cyclohexadienones *rac*-**40** and **52** into their cyclohexenone analogues *rac*-**44** and **53** respectively.

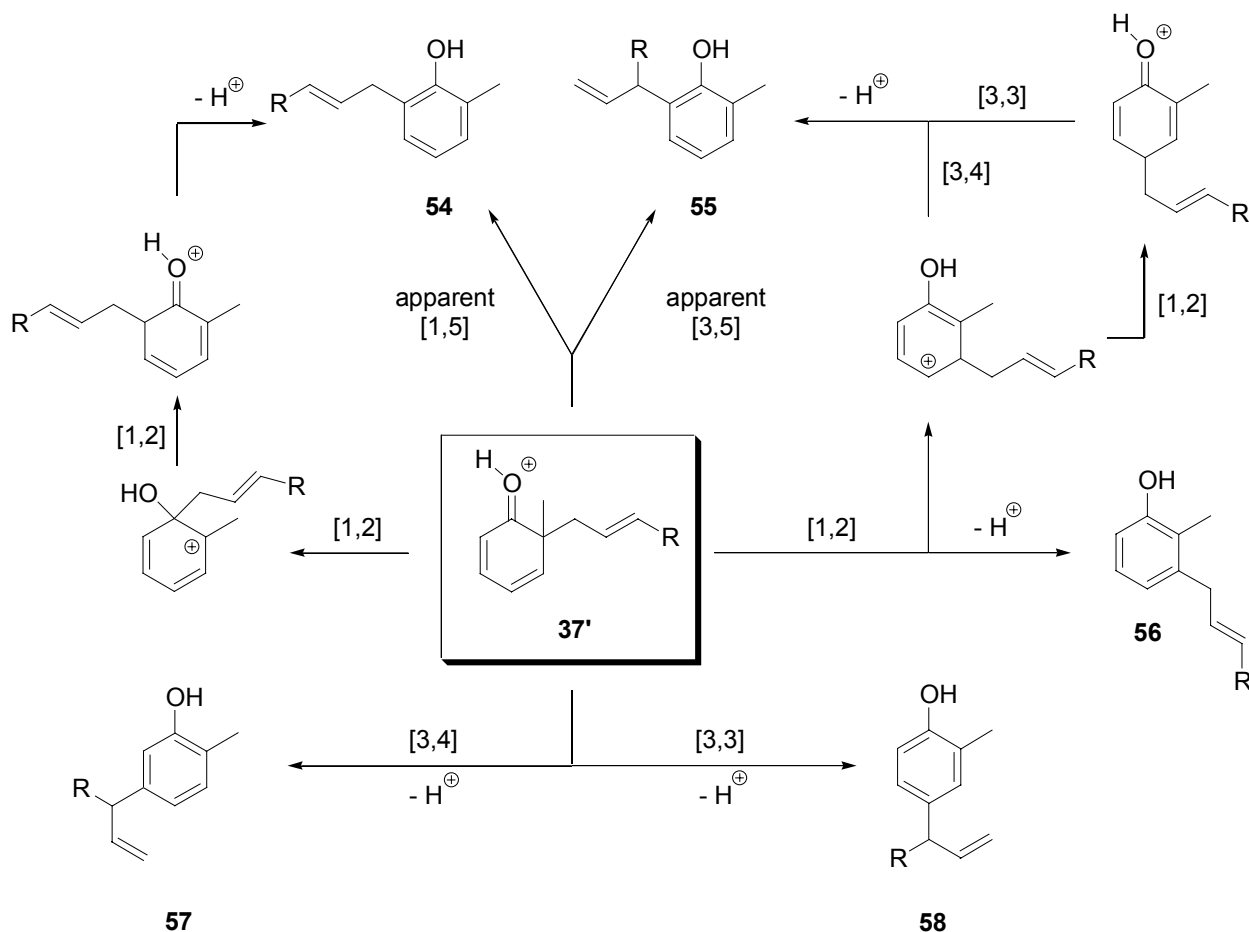
Selective hydrogenation of **52** was performed on micro scale resulting in a low yield due to product loss during sample handling, *Scheme 15*.



Scheme 15. Selective hydrogenation of the cyclohexadienone 4,5-double bonds.

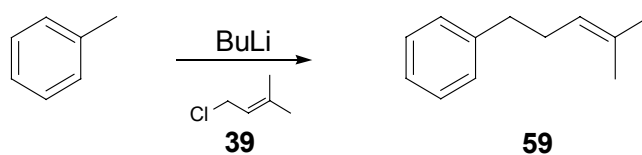
3.3.2 By-products formed during the phenol alkylation

As a consequence of the ambident character of phenolate anions and the instability of the corresponding products, alkylation often generated complex product mixtures [24][25]. After more than a decade of research on cyclohexadienones Miller wrote an article called: “Too many rearrangements of cyclohexadienones” [17]. When the rearrangement of cyclohexa-2,4-diene-1-ones of type **37'** are carried out in protic solvents, the allyl group usually undergoes [3,3] shifts. Smaller amounts of [1,2] migration products were also obtained [26][27]. [1,2] and [3,4] migrations became more important when the rearrangements were carried out in acid anhydrides as the solvent, although the [3,3] migration still predominated. Presumably, acyl groups react with the carbonyl oxygen, thereby removing electron density from the ring resulting in more “carbonium ion type” migration. Small amounts of rearrangement products resulting from apparent [1,5] and [3,5] migrations were observed in some cases. For instance, it was suggested that compounds **54** and **55** were formed either by a series of [1,2] and [3,3]/[3,4] shifts or by [1,5] and [3,5] shifts [28], *Scheme 16*.



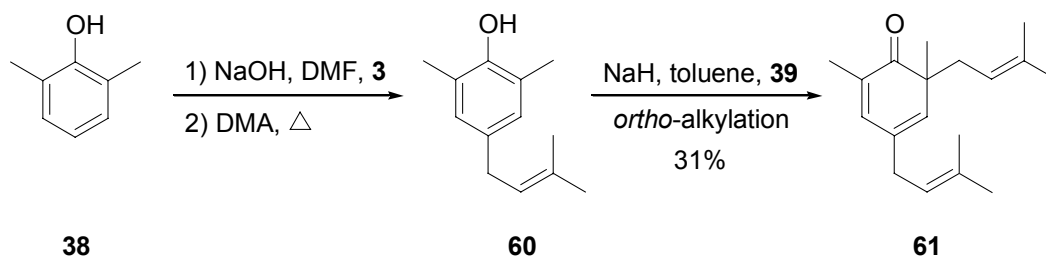
Scheme 16. Acid catalyzed rearrangement of cyclohexadienones.

Under the current phenol alkylation and subsequent work-up conditions mainly by-products resulting from acid catalyzed [3,3] allyl migration had to be expected. However, these rearrangement reactions can be suppressed by avoiding acidic conditions resulting from contaminated glassware and silica gel. During the investigation of the phenol alkylation in the presence of (-)-sparteine (*Chapter 3.3.4*), the analysis of the crude products revealed three generally occurring contaminants, the major one being the O-alkylated phenol-ether **51**, *Scheme 14*. In addition, two unknown products were detected, one of which turned out to be the BuLi/toluene adduct **59** as the reactions were originally carried out in toluene, *Scheme 17*. After this discovery, all further experiments were performed in benzene, thus eliminating this side reaction.



Scheme 17. By-product from BuLi and toluene.

The third side product was very troubling, because it was not possible to remove it from **40** by column chromatography. NMR spectroscopy of enriched samples suggested that it was the dialkylated product **61** resulting from alkylation of **60**, formed by initial *para*-alkylation of **38**. *Para*-C-alkylation of phenols can take place to a significant degree, if the 4-position is not blocked by a bulky substituent [14][24][29], *Scheme 18*.



Scheme 18. By-product resulting from dialkylation of 2,6-dimethyl naphthol.

In order to confirm the structure of **61**, phenol-ether **51** was synthesized and heated in *N,N*-dimethyl aniline at 170 °C for 24 h, leading to the thermally more stable **60** by a Claisen-Cope rearrangement. Subsequent alkylation with prenyl chloride under the usual conditions furnished **61**. The integration of two distinctive ^1H -NMR signals (300 MHz, CDCl_3) resulting from the two protons on the cyclohexadienone ring at 6.65 and 5.81 ppm, showed that up to 10% of **61** was present in a typical product from sparteine/lithium assisted alkylation of **38** after column chromatography.

Phenolic side products such as **60**, as well as residual 2,6-dimethylphenol **38**, were removed from the product mixture by washing the organic solutions with Claisen-base (sat. KOH in MeOH) during the work-up procedure.

3.3.3 Determination of the enantiomeric excess

Several analytical methods were considered to determine the ee of the products obtained from the chiral auxiliary assisted alkylation reactions. ^1H -NMR spectroscopy with chiral shift reagents was found to be a suitable method. Compared to CDCl_3 , deuterated benzene resulted in higher resolution in the down-field region of the spectrum. Different chiral shift reagents were tested and the best results were obtained with $\text{Eu}(\text{TFC})_3$ ³. In deuterated benzene the C(6) methyl group of **40** gives rise to a sharp singlet (1.14 ppm, 300 MHz) in the ^1H -NMR spectrum. When $\text{Eu}(\text{TFC})_3$ is added, this signal splits into two, representing the two different diastereomeric complexes, *Figure 1*. The ratio of the peak areas represents the enantiomeric distribution. The ee was calculated according to the following equation: % ee = $(A_1 - A_2 / A_1 + A_2) \cdot 100$. The NMR analysis revealed

³ $\text{Eu}(\text{TFC})_3$ = Tris[3-(trifluoromethylhydroxymethylene)-D-camphorato] Europium.

that the optical rotation of +19.8 of the initially prepared **40** (Scheme 9) corresponds to an ee of 7%.

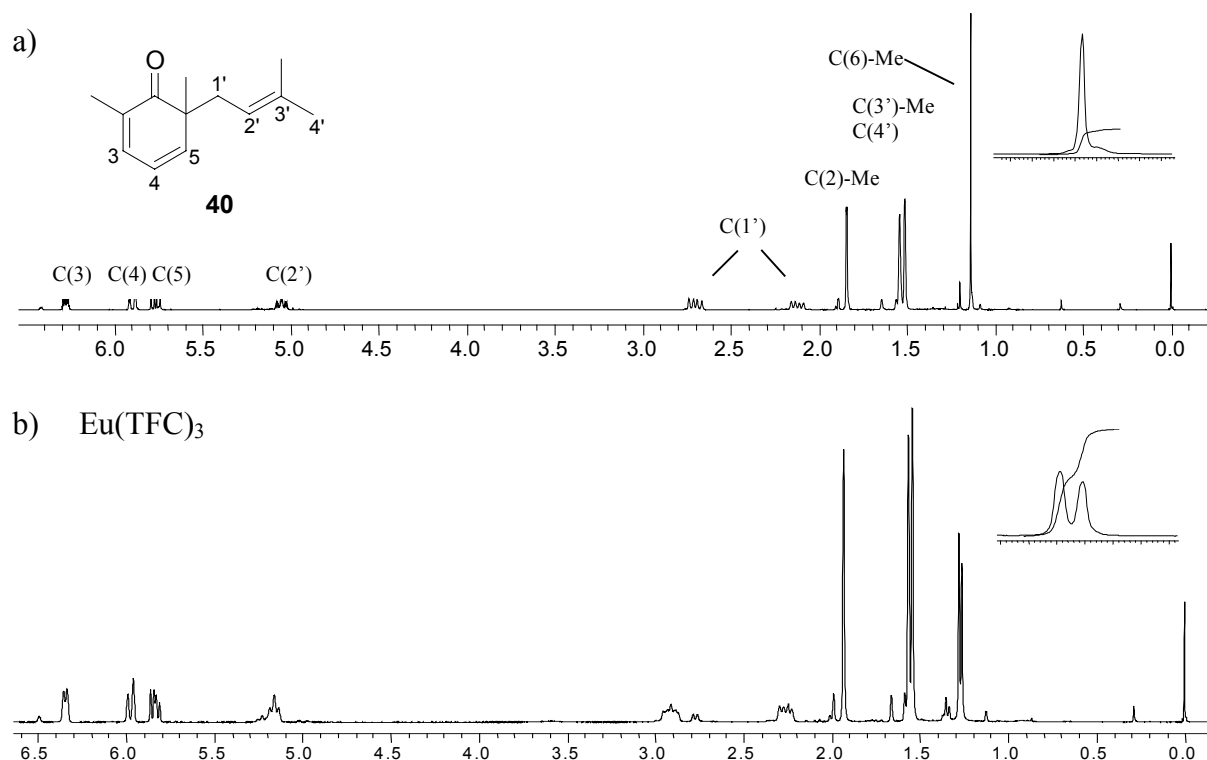


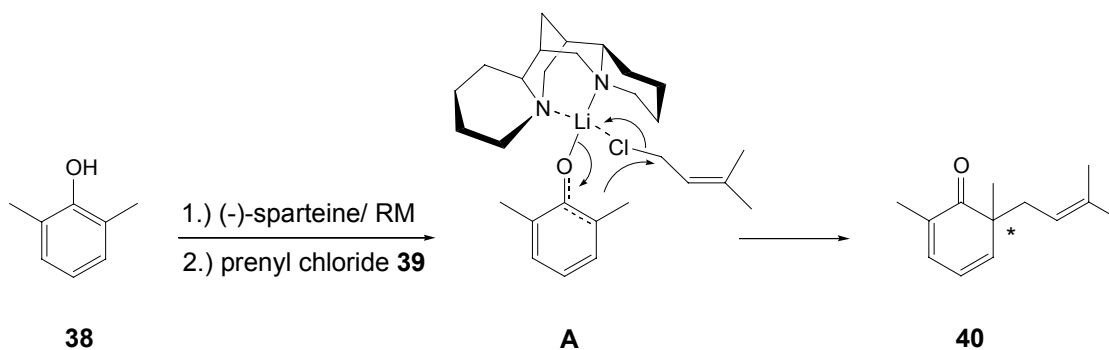
Figure 1. a) 300 MHz NMR spectrum of *rac*-**40**. b) *rac*-**40** with chiral shift reagent.

3.3.4 Phenol alkylation in the presence of (-)-sparteine

Although sodium proved to be the most effective cation for the C-alkylation of phenolate ions, it was not capable of forming a useful complex with (-)-sparteine and no enantiomeric discrimination occurred. When (-)-sparteine was treated with butyl lithium in benzene, the solution turned bright yellow indicating the formation of a sparteine-lithium complex. However, using this complex as the base resulted in the formation of a large amount of phenol ether **51** and the chemical yield of the desired cyclohexadienone **40** was at most 20-25%. Although Li⁺ is known to have a significantly stronger binding affinity to nitrogen containing ligands than Na⁺ [30], the lithium counter ion is also the harder acid. As a consequence it will withdraw negative charge from the *ortho* carbon, leading to longer reaction times and the formation of significant amounts of O-alkylated products. When dimethylphenol **38** was added to the bright yellow (-)-sparteine-lithium complex at 0-5 °C a white suspension was formed. After addition of prenyl chloride **39**, the progress of the reaction was monitored by TLC. At ice bath temperature, no alkylation reaction took place. Once the mixture had reached room temperature, formation of cyclohexadienone **40** was detected. In an attempt to understand what the complex could look like, *transition state A* in Table 1 was postulated. Next, it was investigated whether the alkyl group on the lithium reagent

and molar equivalents had an influence on the reaction, and if metals other than lithium could be used as well. The results are summarized in *Table 1*.

Table 1. Phenol alkylation with (-)-sparteine using different bases.



Reagent	Sparteine	Yield (%)	% ee	$[\alpha]_D^{25}$
Li met.	1 equiv.	25	5.5	+21.73
BuLi	1 equiv.	29	4.0	+16.60
BuLi	2 equiv.	14	8.4	+31.90
BuLi	3 equiv.	3	8.1	+26.69 ⁴
BuLi 2 equiv.	2 equiv.	1	0.9	+3.31
sec. BuLi	1 equiv.	26	4.2	+17.50
Phenyllithium	1 equiv.	10	4.9	+21.78
MeLi	1 equiv.	4	6.6	+28.48
EtMgBr	1 equiv.	decomposition after 2 d		
Et ₃ Al	1 equiv.	decomposition after 48 h		
DIBAH	1 equiv.	no reaction		
Et ₂ Zn	1 equiv.	5	1.4	+7.12

Although the yields of **40** differed drastically, significant changes of selectivities were not observed. When alkyl lithium was used in excess, the formation of O-alkylated product was favored. In an attempt to raise the yield of C-alkylated product **40**, a variety of different organo-metallic reagents was tested. Ethyl-Grignard reagent, triethylaluminum, dibutylaluminum hydride and diethylzinc were applied as well as metallic lithium. Except for diethylzinc, that gave the desired product in 5% yield, all of the transition metal reagents led to intractable materials. Using 2 equivalents of (-)-sparteine with 1 equivalent of BuLi led to an improvement of the enantioselectivity of the reaction, resulting in an enantiomeric excess of 8% in the product. Using

⁴ The value of the optical rotation was lowered due to residual (-)-sparteine in the product.

three equivalents of (-)-sparteine complicated the isolation of the product from the reaction mixture and did not improve the yield nor the enantioselectivity.

3.3.5 Screening for chiral auxiliaries

A part from (-)-sparteine, several commercially available, chiral natural products and ligands were tested for their ability to induce optical activity in **40**, *Figure 2*. In most cases, the chiral auxiliary was dissolved in benzene and treated with BuLi in hexane. The resulting complex was then used to deprotonate 2,6-dimethylphenol followed by alkylation with prenyl chloride. The highest enantiomeric excess was obtained with α -isosparteine **IV** followed by (-)-sparteine **VII**. It was interesting to observe that, when quinine **II** was treated with two equivalents of alkyl lithium, the optical rotation of the product changed signs. *Table 2* shows the results obtained from alkylating **38** with prenyl chloride **39** in the presence of the different chiral auxiliaries illustrated in *Figure 2*. Unfortunately, it was not possible to obtain an enantiomeric excess above 10%. However, the results do show that, for the first time, it has been possible to influence the enantioselectivity of the C-alkylation of phenols to a considerable degree by using chiral bidentate auxiliaries.

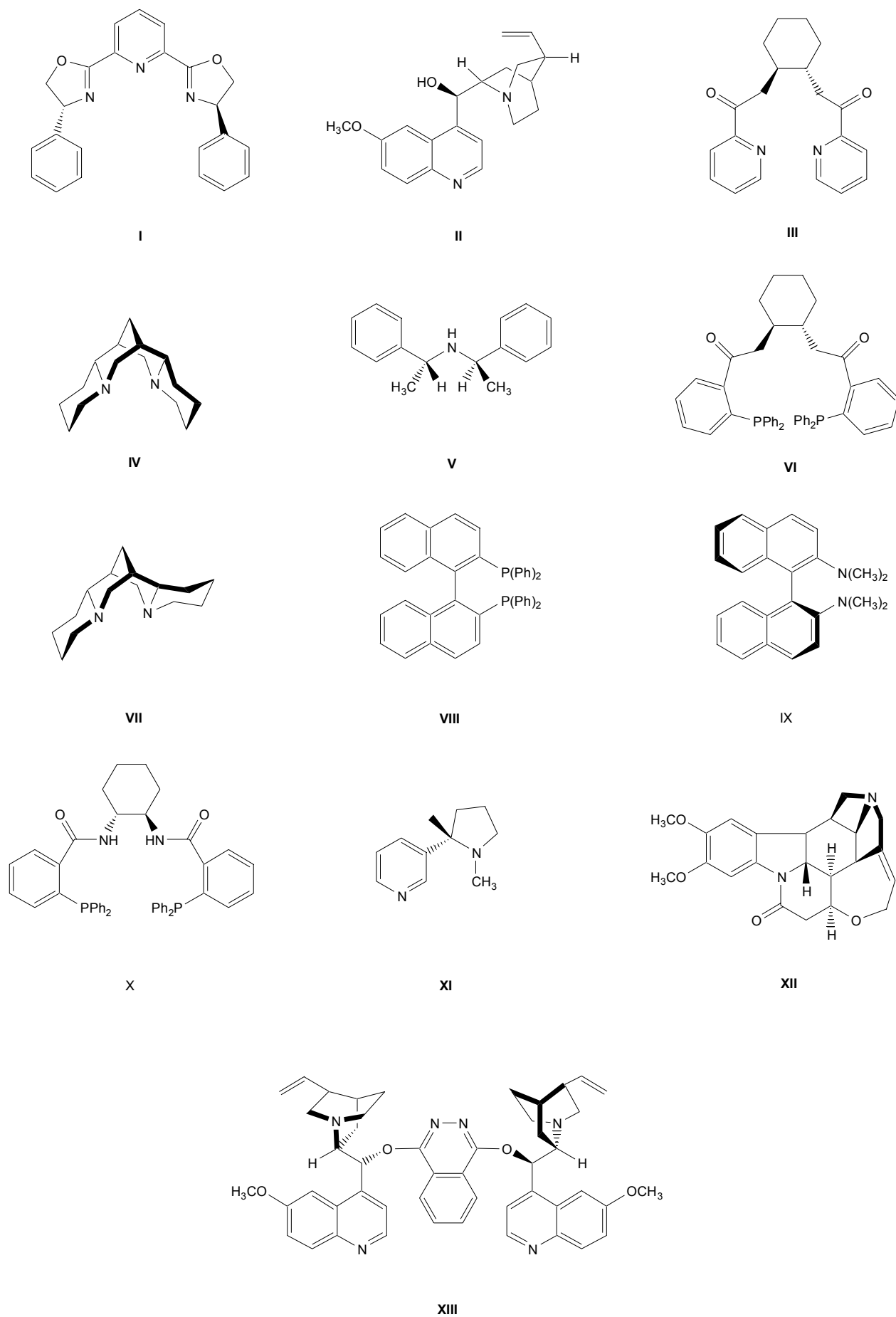
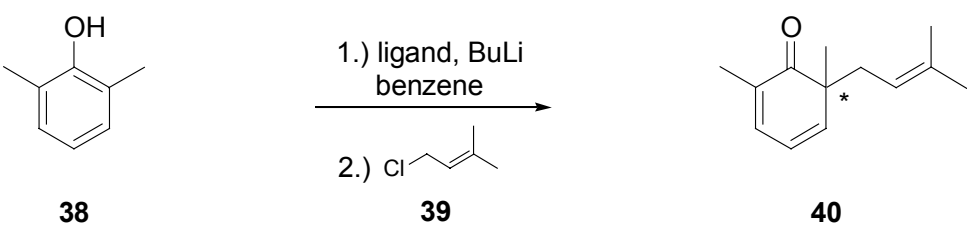


Figure 2. Chiral auxiliaries used for the alkylation of 2,6-dimethyl phenol.

Table 2. Experimental results with different chiral auxiliaries.



Auxiliary	Alkyl lithium	Yield (%)	% ee	$[\alpha]_D^{25}$
I	BuLi	1	0.0	0.00
II	BuLi	12	2.0	-8.31
II	2 equiv. BuLi	9	7.5	+28.83
III	BuLi	O-alkylation only		
IV	BuLi	17	8.9	+36.97
V	BuLi	29	0.0	0.00
VI	BuLi	O-alkylation only		
VII	BuLi	29	4.0	+16.60
VII 2 equiv.	BuLi 1 equiv.	14	8.4	+31.90
VII 3 equiv.	BuLi 1 equiv.	3	8.1	+26.70 ⁶
VIII	BuLi	37 ⁷	5.1	+11.03
IX	BuLi	18	0.0	0.00
X	BuLi	O-alkylation only		
XI	BuLi	13	0.0	0.00
XII	BuLi	3	0.0	0.00
XIII	BuLi	5	1.9	+1.97

Instead of the two cyclohexane rings found in (-)-sparteine and α -isosparteine, Tröger's base contains two benzene rings, *Figure 3*. Due to the geometric constraints, the lone pairs on the nitrogen atoms in Tröger's base point away from the molecules cavity. Therefore, they should be to far apart from each other to form a complex with the lithium phenoxide ion, as postulated in *transition state A*, *Table 1*. Indeed, the yield of C-alkylated product was very low (0.9%), indicating that Tröger's base did not form a stable complex with alkali metals and was not effective in shielding the oxygen anion from electrophilic attack.

⁶ The value of the optical rotation was to low, presumably due to residual (-)-sparteine in the product.

⁷ These results were obtained using 2,4,6-trimethylphenol as starting material. The yield is higher because the para position is blocked reducing the amount of side products formed by dimerization and *para*-alkylation.

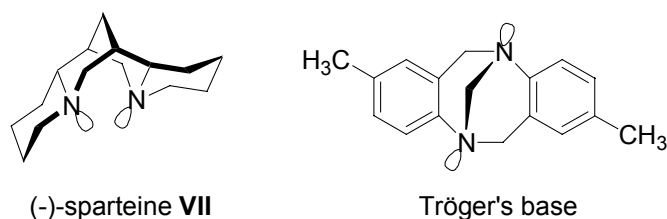
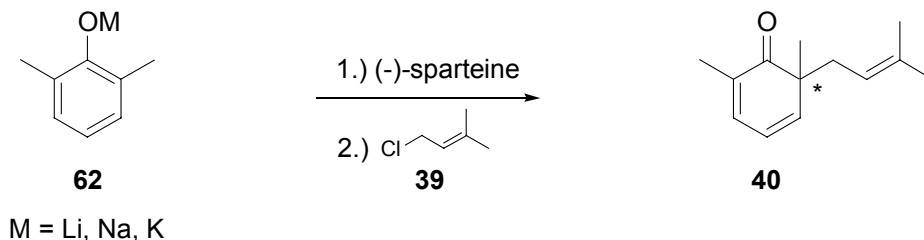


Figure 3. (-)-sparteine vs. Tröger's base.

3.3.6 Alkylation of phenols under solvent free conditions

Because the outcome of the phenol alkylation strongly depends on the solvent and has been reported to work best in heterogeneous mixtures of the phenoxide ions in an aprotic solvent, it was an obvious decision to try performing the reaction in the solid state [31]. Sodium, potassium and lithium phenoxide was prepared by treating 2,6-dimethyl phenol with NaH, KH and BuLi, respectively, and then removing the solvent under vacuum. The pastel colored pink and blue phenoxides could be stored under water- and air-free conditions. The solid phenoxides were mixed with (-)-sparteine, a colorless viscous liquid, to result in a dark green readily stirred mixture. After the addition of prenyl bromide the mixture was stirred at room temperature for 20 h, *Table 3*.

Table 3. Results from solid-state alkylation reactions.



Phenoxide	Alkylation agent	% C-alkylation	% O-alkylation	% ee	$[\alpha]_D^{25}$
Li	prenyl bromide	18	28	0.0	0.00
Na	prenyl bromide	50	12	10.7	+52.56
Na	prenyl bromide	33	13	2.8	+7.95
Na	prenyl bromide	31	15	6.9	+27.70
K	prenyl bromide	39	25	0.0	+0.00

Although the solvent free reaction of sodium phenoxide showed a good tendency towards higher yields and enantioselectivities, the experimental results were not reproducible.

Based on these results, another strategy came to mind: (-)-sparteine could react with the alkylating agent to yield a quaternary ammonium salt **63** [32]. It was imaginable that an allylic halide would

attach reversibly to the lone pairs of the nitrogen atoms leading to intermediates **63a** and **63b** with rapid interchange of the allylic system between the two nitrogen atoms, *Figure 4*.

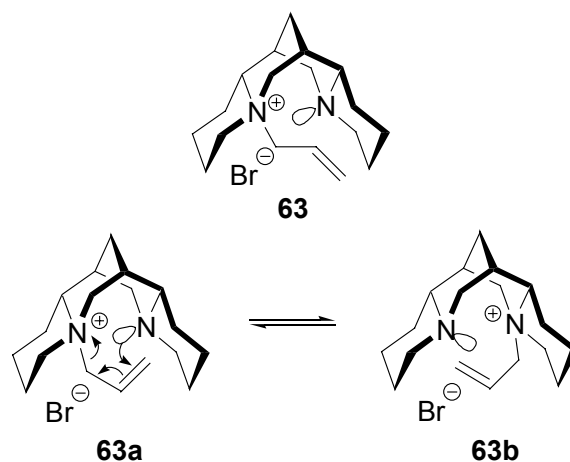


Figure 4. Postulated structure of the allyl bromide/ α -isosparteine salt **63**.

It was speculated that, such an ally halide/sparteine intermediate could result in high enantiomeric discrimination due to the chiral environment of the alkylating agent. Possibly such a mechanism could have gone undetected, because addition of the allyl halide was usually the last step in the reaction, therefore, the reaction conditions did not offer sufficient time for the formation of the intermediate **63**. *Transition state 1* and *transition state 2* in *Figure 5* were postulated for the alkylation of **62** in the presence of an allyl bromide/(-)-sparteine salt.

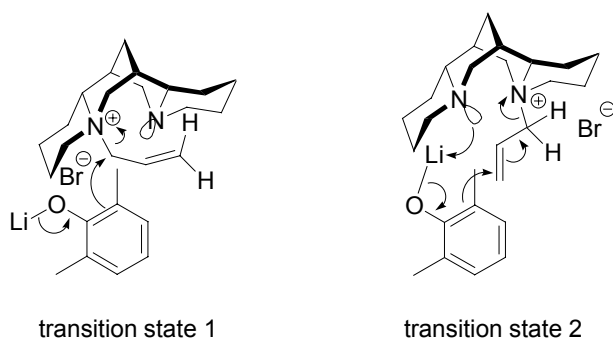


Figure 5. Postulated transition state for the phenol alkylation with **63**.

In order to determine whether such a mechanism is in effect, (-)-sparteine and α -isosparteine were treated with allyl bromide in toluene solution. The solvent was removed under reduced pressure and the resulting (-)-sparteine salts were analyzed by NMR. The products gave rise to complicated NMR spectra not suited for structure determination. Luckily, the quaternary allyl bromide/ α -isosparteine salt **63** gave fine colorless crystals upon standing and could be analyzed by X-ray diffraction analysis [33]. The structure of **63** was solved and refined successfully with no unusual features. The crystals were enantiomerically pure and the absolute configuration of the molecule

was determined independently by the diffraction experiment. The asymmetric unit contains one cation, one anion and two benzene molecules, *Figure 6*.

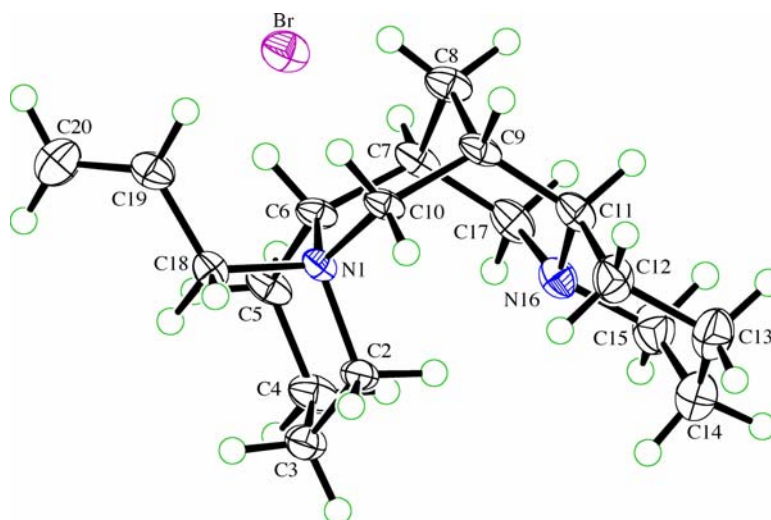


Figure 6. ORTEP plot of allyl bromide/ α -isosparteine salt **63**, benzene molecules omitted.

It was disappointing, but also interesting, to find that allyl bromide/ α -sparteine salt **63** was indeed present, but the allyl bromide moiety was attached on the outside of the sparteine cavity and had promoted inversion of configuration at the involved nitrogen center. **63** was prepared in larger amounts and reacted with solid sodium and lithium phenoxides in the solid state as well as in benzene solution. The results of these experiments showed that **63** was no longer capable of alkylating the phenoxide. Therefore the formation of the allyl bromide-sparteine salt can be considered a side reaction that results in loss of alkylating reagent and auxiliary compound.

3.3.7 Alkylation of asymmetric phenols

2,6-Dimethylphenolate is a symmetrical molecule and offers four equivalent sites for electrophilic attack. Approach from (1) and (4) as well as (2) and (3) lead to the formation of the same enantiomer. For this reason, the chiral ligand must effectively shield two sites *anti* to each other in order to provide a chiral environment that will lead to the formation of one single enantiomer, *Figure 7*.

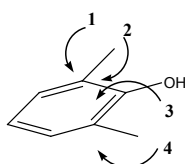
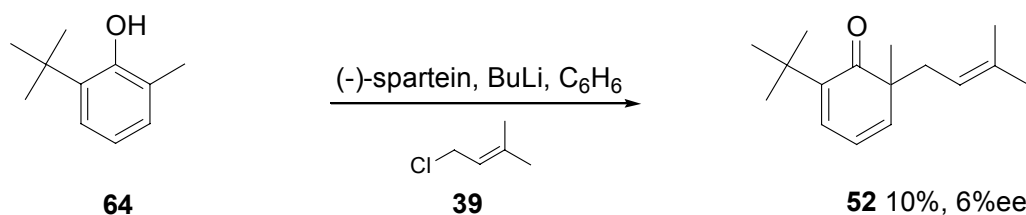


Figure 7. Possible sites of attack on 2,6-dimethyl phenol.

If one of the sites at C(2) or C(6) is blocked, either by a bulky group or by using naphthol derivatives, the enantioselectivity should be increased significantly. The 2-methyl-6-*tert*-

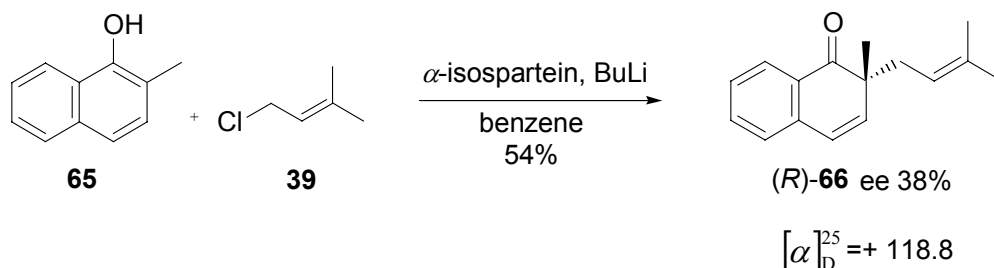
butylphenol **64** is commercially available and was considered a good candidate to study the effect of bulky groups on one of the two reactive sites, *Scheme 19*.



Scheme 19. Alkylation of asymmetric 2-methyl-6-*tert*-butylphenol **64**.

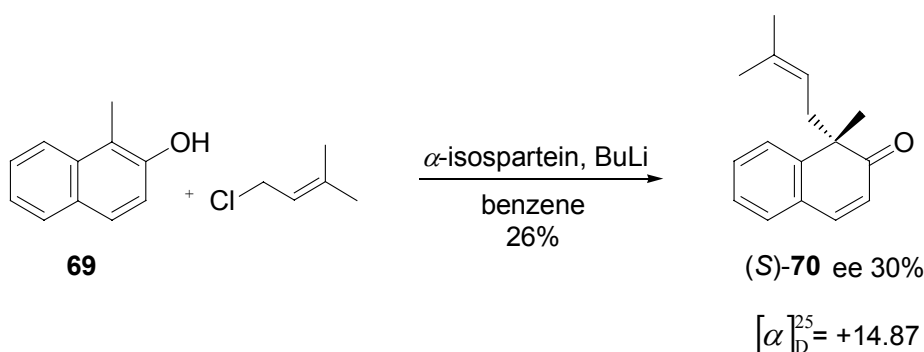
However, **64** gave bad yields and an impure product, and it was assumed that the *tert*-butyl group prevented the formation of a stable complex with (-)-sparteine and therefore was not suitable for our reaction conditions.

Due to the more extensive delocalization of charge, naphthols are more reactive than phenols and alkylation is more rapid. For this reason 2-methyl-1-naphthol **65** was alkylated with prenyl chloride **39** in the presence of α -isosparteine as the chiral auxiliary, *Scheme 21*. The reaction proceeded with significantly higher stereoselectivity and afforded (*R*)-**66** in acceptable yield (54%).



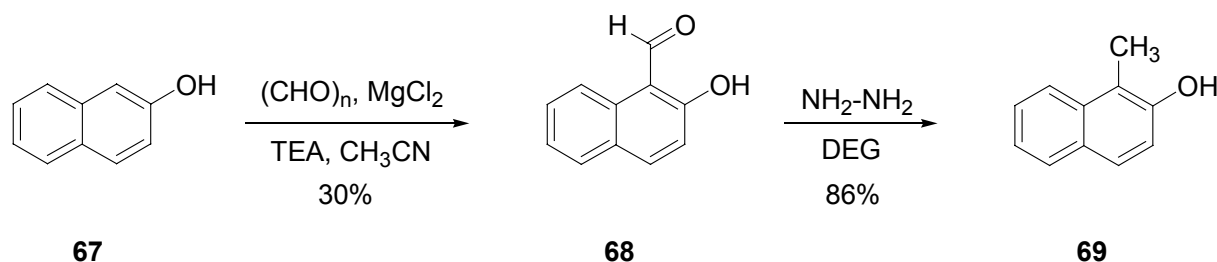
Scheme 21. Enantioselective alkylation of 2-methyl-1-naphthol **65**.

In order to assess the observed result, 1-methyl-2-naphthol **69** was alkylated under the same reaction conditions, leading to (*S*)-**70** with 26% yield and 30% ee, *Scheme 20*.



Scheme 20. Enantioselective alkylation of 1-methyl-2-naphthol **69**.

69 was not commercially available and had to be synthesized by formylation of 2-naphthol **67** in 1-position followed by Wolff-Kishner reduction of the aldehyde moiety in **68** with hydrazine to give 1-methyl-2-naphthol **69** [34][35], *Scheme 22*.



Scheme 22. Synthesis of 1-methyl-2-naphthol 69.

3.3.8 Absolute configuration of naphthalenones **66** and **70**

The prenyl chromophore is under a weak chiral influence. In a first approach its chiroptical contribution to the CD spectrum can be neglected. **66** contains a separated “acetophenone type” and a “styrene type” chromophore. Both of them can be slightly distorted. **70** contains an enone chromophore in conjugation with the benzene chromophore. The CD spectrum of this molecule is expected to be dominated by the contribution of the inherently chiral enone chromophore. The CD spectrum of enones is characterized by two bands (*R*- and *K*-bands) of opposite sign. The *R*-band appears above ~320 nm and the *K*-band near 250 nm. The sign pattern of the bands (+/- or -/+) depends on the helicity (torsion angle) of the enone chromophore: *M* helicity gives rise to a +/-, while *P*-helicity to a -/+ sign pattern.

The CD spectrum of **66** in acetonitrile contains only positive bands with fine structures in the 250-400 nm region. Below 250 nm the spectrum is governed by the positive $^1\text{L}_a$ band at ~230 nm and a negative one below 200 nm. These bands result mostly from the phenyl chromophore. Applying the sector rule of the saturated ketones to the positive long-wavelength band at 333 nm results in (*R*)-configuration of the chiral center assuming the axial position of the Me group. (Perturbation by the equatorial prenyl group is neglected.)

As expected, the CD spectrum of **70** in acetonitrile contains a broad asymmetric *positive* band with two maxima above 320 nm and a *negative* one near 300 nm. The +/- sign pattern is compatible with an *M*-helicity of the enone chromophore. Again, if assuming the axial position of the methyl group, this gives rise to an (*S*)-configuration.

3.3.9 Vibrational Circular Dichroism (VCD) spectroscopic studies on **66**

The small sample of compound **66** did not permit to obtain a full VCD spectrum ($1800\text{ cm}^{-1} - 900\text{ cm}^{-1}$), with high signal/noise ratio, from a neat liquid film. The VCD and IR spectra were recorded in acetonitrile- d_3 solution ($c = 50\text{ mg/mL}$) at room temperature with a Bruker Equinox55/PMA37

FT-VCD system, *Figure 8*. The spectra were recorded with an average of 5 blocks of 1800 scans and 4 cm^{-1} resolution, using a CaF_2 liquid cell of 0.05 mm pathlength. The spectrum of solvent (baseline), obtained under identical conditions, was subtracted from the spectrum.

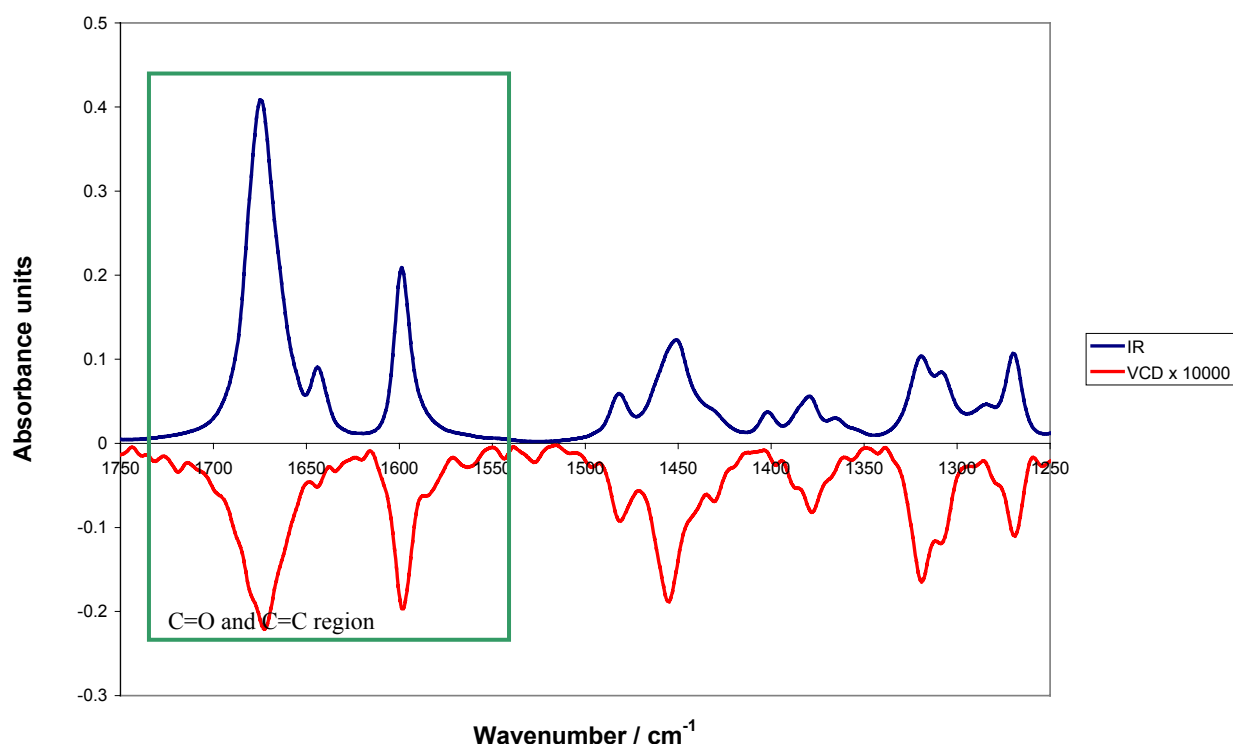


Figure 8. IR and VCD spectrum of (*R*)-**66** in acetonitrile- d_3 .

A number of 6 conformers of **66** have been computed with the Gaussian 03 quantum chemical program at the 6-31G(d)/B3LYP level of theory for the vacuum state. The differences in relative energies of these conformers are small, due to the rotational freedom of the 3-methyl-2-buten-1-yl side-chain.

Due to the high conformational mobility of the side-chain, only VCD signals resulting from stretching vibrations of the C=O group and the C=C double bonds (the 1750 – 1550 cm^{-1} region) can be interpreted. The $\nu\text{C=O}$ and $\nu\text{C=C}$ (side-chain) modes are coupled in several conformers. From the sign of calculated VCD spectra of (*R*)- and (*S*)- **66** (*Figure 9*), one can conclude that the investigated molecule is the (*R*)-enantiomer, *Figure 10*.

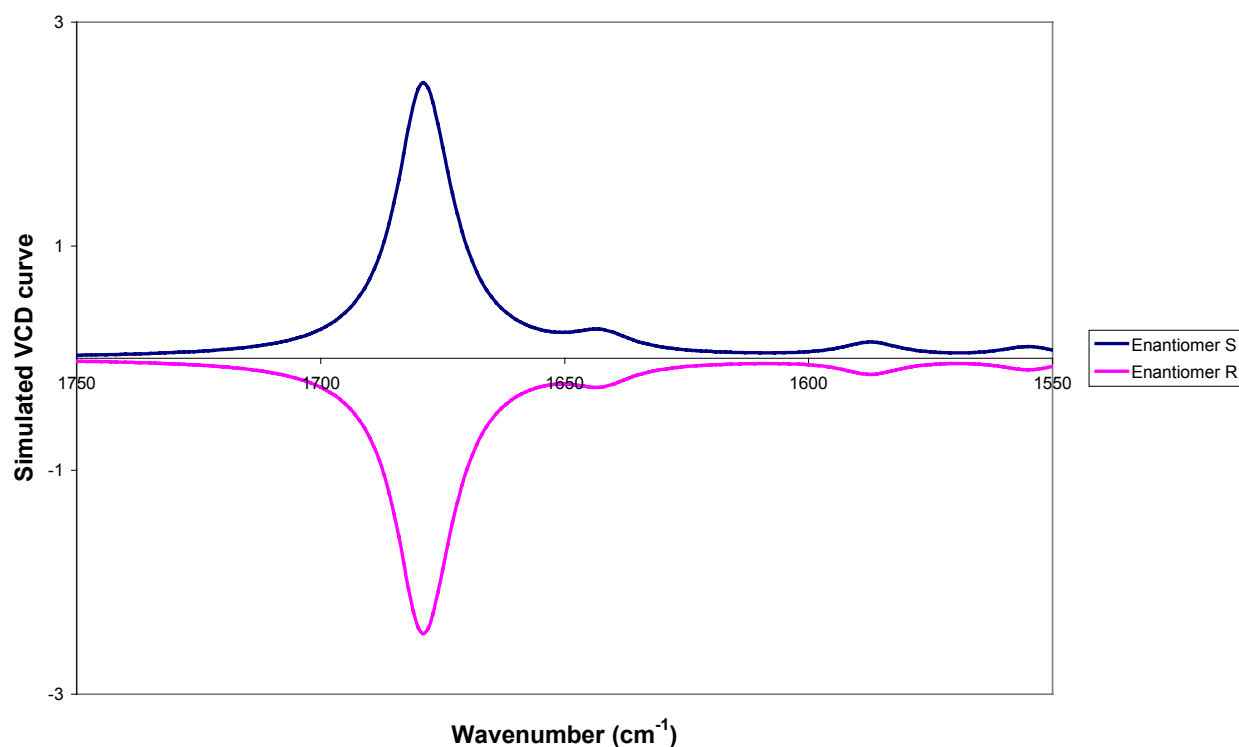


Figure 9. Simulated VCD curves of the two enantiomers of **66**.

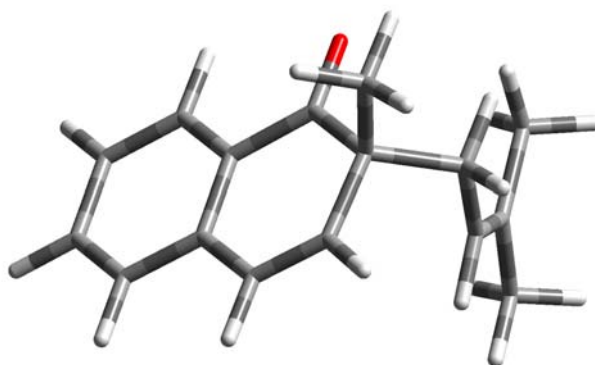


Figure 10. Proposed structure of (*R*)-**66**.

3.3.10 VCD spectroscopic studies on naphthalenone **70**

VCD and IR spectra of **70** were obtained under similar conditions as for **66**, *Figure 11*. Unfortunately, the sample was impure, which is revealed by the band at 1716 cm^{-1} , not compatible with an α,β -unsaturated or aromatic ketone structure. The number of bands in the $1750\text{--}1550\text{ cm}^{-1}$ region is higher than expected. Molecular modeling and calculation of VCD spectra of **70** followed the procedure described for **66**, *Figure 12*.

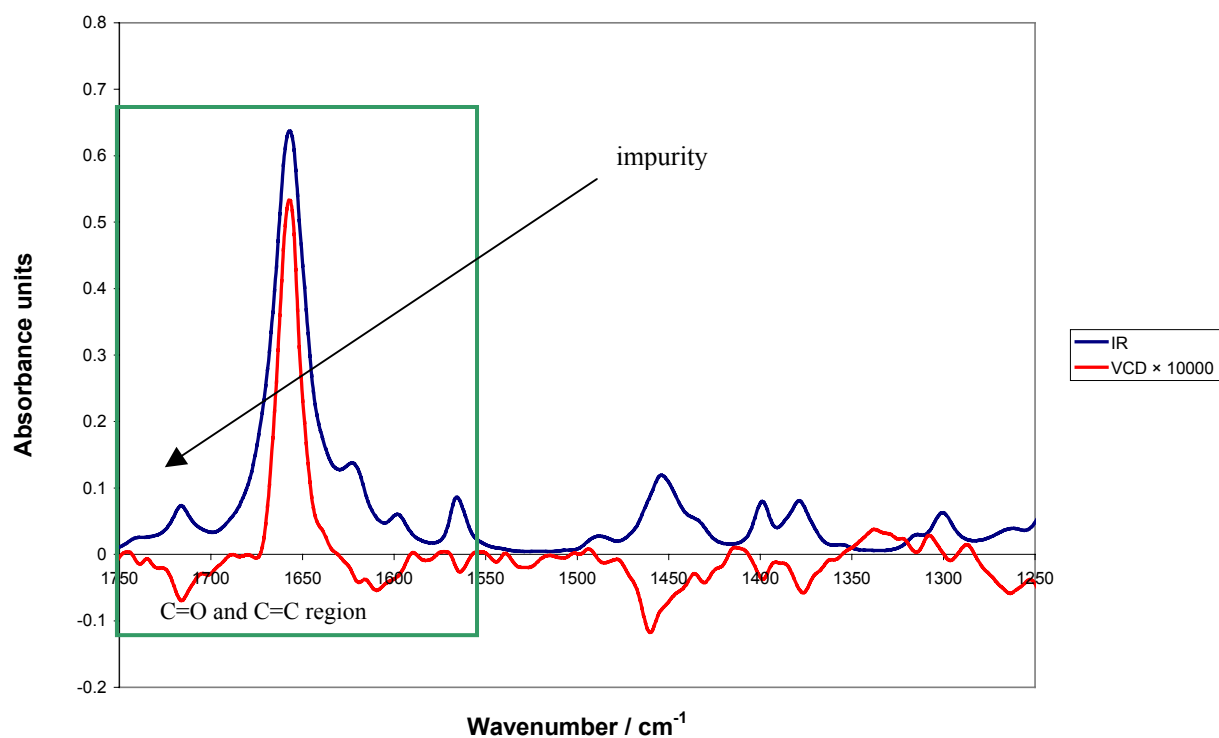


Figure 11. IR and VCD spectrum of **70** in acetonitrile- d_3

Apart from the contribution of some impurity to the IR and VCD spectrum, the region of C=O and C=C stretching vibrations can be interpreted. From the sign of the calculated VCD spectra of (*R*)- and (*S*)-**70** it can be concluded, that the investigated molecule is the (*S*)-enantiomer, *Figure 13*.

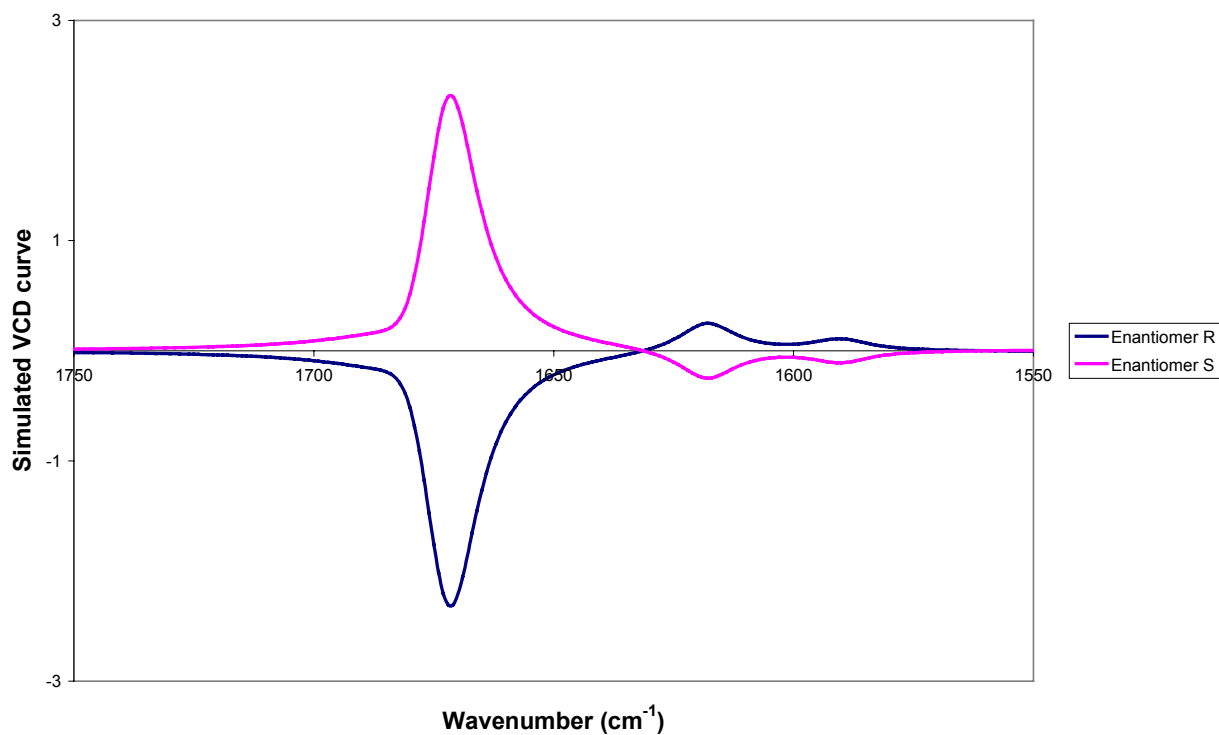


Figure 12. Simulated VCD curves of the two enantiomers of **70**.

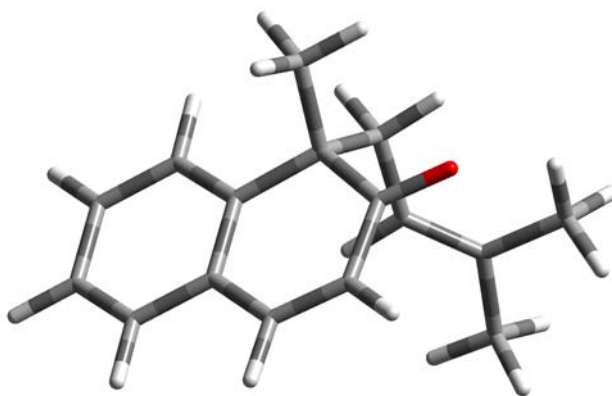
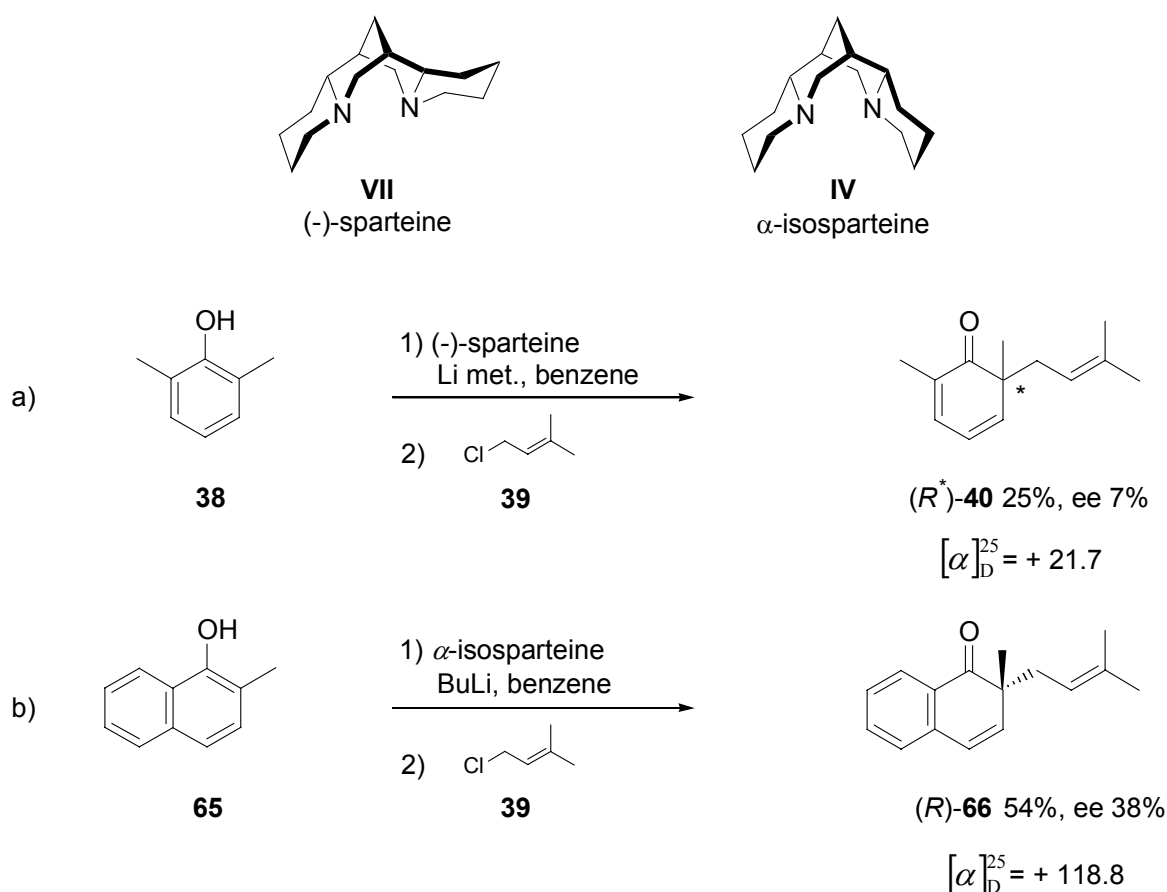


Figure 13. Proposed structure of (*S*)-70 based on the VCD spectrum.

3.4 Conclusions

Ambident phenolate ions can be alkylated with alkyl- and allyl halides leading to cyclohexadienones [13][14][15]. The current research has shown, for the first time, that it is principally possible to influence the enantioselectivity of the phenol alkylation by employing nitrogen containing, bidentate ligands as chiral auxiliaries. Out of thirteen different chiral auxiliaries, tested during this research, (-)-sparteine **VII** and α -isosparteine **IV** gave the best results, leading to an enantiomeric excess of up to 38% in the cyclohexadienone product. Experimental results showed that C-alkylation of the ambident phenolate ion was favored and side reactions were minimized when performing the reactions in benzene. Contrary to the results reported in the non-asymmetric alkylation protocols, lithium was found to be the most suitable counter ion in the asymmetric variant. Presumably, it has a stronger binding affinity to the neutral ligand than sodium and it still enables sufficient electron distribution for a reasonable amount of C-alkylation to take place, *Scheme 23*.



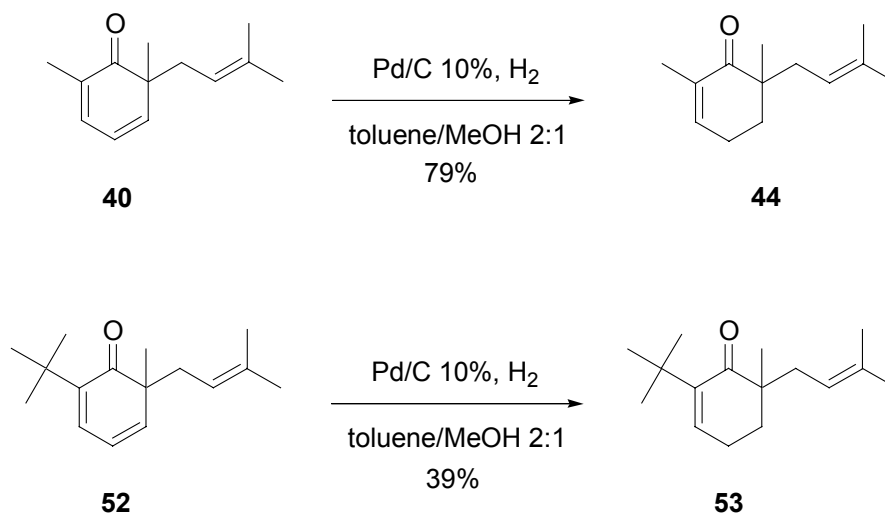
Scheme 23. Enantioselective phenol and naphthol alkylation with sparteine.

The screening experiments in *reaction a* showed that quinine **II** (9% yield, 6% ee) and *R*-(+)-2,2'-bis(diphenylphosphino)-1,1'-binaphthalene **VIII** (37% yield⁸, 5% ee) also resulted in moderate

⁸ These results were obtained using 2,4,6-trimethylphenol as starting material.

optical activity of the resulting cyclohexadienone **40**. Alkylation of 2-*tert*-butyl-6-methylphenol **64** with prenyl chloride led mostly to the O-alkylated product. The asymmetric nature of the phenol did not lead to an improvement of the enantiomeric excess in product **52**, isolated in 10% yield.

It was found, that the 4,5-double bond in the cyclohexa-2,4-dienone system could be reduced selectively with Pd/C 10% in toluene/MeOH 2:1, without any hydrogenation of the 2,3-double bond or the allylic side chain. This method offers a straight forward access to cyclohexenones **44** and **53**, *Scheme 24*.



Scheme 24. Regioselective hydrogenation of cyclohexadienones.

(-)-Sparteine and α -isosparteine were reacted with allyl and prenyl chloride and bromide to give the corresponding quaternary ammonium salts. X-ray diffraction analysis of the α -isosparteine/allyl bromide salt **63** led to the conclusion, that the allyl group attaches to the outside of the molecular cavity of the α -isosparteine molecule, resulting in inversion of configuration at the involved nitrogen center, *Figure 14*.

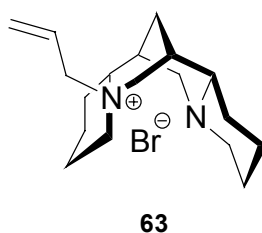


Figure 14. Allyl bromide/ α -isosparteine salt **63.**

Alkylation experiments using these salts as nucleophiles failed. To avoid the formation of the inactive sparteine salts, the addition of the allyl halide was always the last step in the reaction.

Naphthols, being more reactive than phenols, were readily alkylated and led to the highest enantiomeric enrichment. VCD spectroscopy of the products indicated that alkylation of 2-methyl-1-naphthol **65** with prenyl chloride, in the presence of one equivalent of α -isosparteine, led to 38% enantiomeric excess of (*R*)-**66**, *Scheme 23 reaction b*.

3.5 Experimental

Abbreviations

abs.	absolut
aq.	aqueous
DEG	diethylenglycol
dil.	diluted
DMF	dimethylformamide
hex	hexane
M	mol/liter
min.	minutes
MS	mass spectrometry
MtBE	<i>tert</i> -butylmethyl ether
r.t.	room temperature
TEA	triethylamine
THF	tetrahydrofuran
TLC	thin layer chromatography

General procedures.

¹H-NMR-Spectra: Routine NMR-spectra were measured on *Bruker AC300* and *Bruker ARX300* (both 300 MHz) spectrometers. Experiments using chiral shift reagents were carried out on *Bruker DPX-400* and *Bruker AVANCE 500* instruments. Deuterated chloroform and benzene were used as solvent with tetramethylsilane as an internal standard. The chemical shifts are indicated in ppm and the values of the J_{HH} -coupling constants are given in Hz. Multiplicities are specified by abbreviations, *s* = singlet, *d* = doublet, *t* = triplet, *m* = multiplet and *td* = triplet of doublets.

¹³C-NMR-Spectra: *Bruker AC300*, *Bruker DPX-400* and *Bruker AVANCE 500*. The solvent itself served as the internal standard: CDCl_3 ($\delta(\text{C}) = 77.00$ ppm, *t*, $J_{\text{CD}} = 31.5$ Hz). DEPT (Distortionless Enhancement by Polarization Transfer) experiments were performed to determine the multiplicity of the carbon nuclei. The multiplicity is designated *q* (quartet) for CH_3 , *t* (triplet) for CH_2 , *d* (doublet) for CH and *s* (singlet) for fully substituted carbon atoms.

Mass Spectrometry: GC/MS was measured routinely on a *HP MSD 5973* instrument with a 30m *HP5/MS* or *Varian VF5ms* column. High resolution mass spectrometry was performed on a *Finnigan MAT 95* (*Finnigan MAT95*, San Jose, CA; USA) double-focusing magnetic sector mass spectrometer (geometry BE). Mass spectra were measured in electron impact (EI) mode at 70 eV,

with a source temperature of 200 °C, an acceleration voltage of 5 kV, and a resolution of 10'000. The instrument was scanned between m/z 30 und 900 at 2 scan min.⁻¹. Perfluorokerosene (PFK, ICN Pharmaceutical Inc, Plainview, NY, USA) served for calibration.

Infrared Spectrometry: *Spectrum One FT-IR-* and *Bruker Vector 22 FT-IR*-spectrometers. Liquids were measured 5% in chloroform (0.05 mm cell) and solids were measured as KBr pellets (1mg substance/100mg KBr). The background spectrum was recorded either from the pure solvent or the empty sample path. The relative intensities of the absorption bands are indicated as νs = very strong (> 90%), s = strong (70-90%), m = medium (40-70%), w = weak (< 40%).

Thin Layer Chromatography: Silica gel pre-coated plastic sheets *Macherey-Nagel Polygram SIL G/UV₂₅₄* or aluminum oxide pre-coated plastic sheets *Macherey-Nagel Polygram N/UV₂₅₄*. Substances were made visible under UV-light (254 nm or 366 nm) or with staining reagents. KMnO_4 reagent was prepared by dissolving 5g of KMnO_4 and 15g of K_2CO_3 in 250.0 mL of water. Cesium reagent contained 25g phosphorous molybdenum acid, 13g $\text{Ce}(\text{SO}_4)_2 \times 4 \text{ H}_2\text{O}$ and 60.0 mL H_2SO_4 98% per liter of aqueous solution.

Column Chromatography: Silica gel *Chemie Uetikon ZEOCHEM C-Gel C-560*, particle size 40-63 μm or aluminum oxide *Fluka type 5016 basic*, particle size 50-150 μm ; pH 9.5 +/- 0.5 Act. III (*Brockmann*).

Short Path Distillation: Most products were short path distilled by the „kugelrohr“-method. A modified rotary evaporator motor was utilized and the bulb was heated by means of a *Büchi* kugelrohr oven or a hot air gun for micro scale amounts. The vacuum was provided either by a rotary slide pump (0.05 mbar) or by a water-jet vacuum pump (10 mbar).

Gas Chromatography: Standard GC analysis was performed on a *HP 5890* instrument with *HP 3396A* integrator and a DB5 30m, 0.53 mm column. Split ratio 1:100, initial temperature 80 °C, rate 10 °C/min.

2,6-Dimethyl-6-(3-methylbut-2-enyl)cyclohexa-2,4-dienone (rac-40).

2,6-Dimethylphenol **38** (2.50 g, 20.80 mmol) was placed in a reactor and 18.0 mL of toluene were added, resulting in a 1M solution. The solution was stirred and cooled to 5 °C by means of an ice/water bath. Sodium hydride 60% in paraffin oil (0.85 g, 21.30 mmol) was added over 10 min., keeping the temperature below 10 °C. The mixture was stirred for 45 min. at 5 °C. At the end of this period the reaction mixture had become bright green. A solution of prenyl chloride **39** (2.62 g, 25.20 mmol) in 4.0 mL of toluene was added dropwise at 5 °C over 1 h. The mixture was left to reach r.t. and stirring was continued for 1 h. The reaction was quenched with water and extracted with MtBE. The organic layers were washed with water and brine, dried over MgSO₄ and evaporated. Chromatography of the residue over silica gel, with a mixture of hex/MtBE 9:1 and 0.5% TEA, followed by short path distillation (50°C, 0.05mbar) gave *rac-40* (3.60 g, 92%) as a colorless oil.

IR (CCl₄): 3034_w, 2969_m, 2923_m, 1627_{vs}, 1642_s, 1582_w, 1450_m, 1377_m, 742_m.

¹H-NMR (300 MHz, C₆D₆): 6.27 (m, 1 H); 5.90 (m, 1 H); 5.76 (dd, *J* = 5.9, 9.5 Hz, 1 H); 5.05 (m, 1 H); 2.7 (m, 1 H); 2.12 (m, 1H); 1.84 (m, 3 H); 1.54 (d, *J* = 1.1 Hz, 3 H); 1.51 (s, 3 H); 1.14 (s, 3 H).

¹³C-NMR (75 MHz, CDCl₃): 206 (s); 145.1 (d); 137.8 (d); 134.1 (s); 133.0 (s); 120.1 (d); 118.8 (d); 51.1 (q); 38.9 (t); 25.6 (q); 24.0 (q); 17.8 (q); 15.3 (q).

EI-MS (GC/MS): 190 (1, *M*⁺), 175 (4), 122 (100), 107 (28), 91 (14), 69 (25), 41 (29).

2,6-Dimethyl-6-(3-methyl-but-2-enyl)-cyclohex-2-enone (rac-44).

2,6-Dimethylphenol **38** (2.50 g, 20.80 mmol) was alkylated with prenyl chloride **39** as described for *rac-40*. Once the reaction had gone to completion, the mixture was diluted with 10.0 mL of methanol and palladium 10% on activated carbon (25mg) was added. The mixture was hydrogenated under a hydrogen atmosphere at room temperature. After 2 hours the reaction mixture was filtered over celite and washed with water and Claisen base (sat. KOH in MeOH) to remove any phenols present. After chromatography over silica gel with hex/MtBE 9:1 and short path distillation (100 °C, 0.05 mbar), *rac-44* (1.45 g, 37%) was obtained as a colorless oil.

IR (CCl₄): 2966_m, 2922_m, 1665_s, 1449_m, 1375_m, 1356_m, 1189_w, 1074_w, 1032_m, 979_w, 942_w, 876_w, 840_w.

¹H-NMR (400 MHz, CDCl₃): 6.11 (m, 1 H); 5.25 (m, 1 H); 2.33 (m, 2 H); 1.91-1.83 (m, 5 H); 1.73 (m, 1 H); 1.67 (s, 3 H); 1.54 (s, 3 H); 1.47 (m, 1 H); 1.09 (s, 3 H).

¹³C-NMR (75 MHz, CDCl₃): 204.3 (s); 143.4 (d); 134.1 (s); 134.0 (s); 119.8 (d); 45.1 (s); 35.0 (t); 33.5 (t); 26.0 (q); 23.0 (t); 21.9 (q); 17.9 (q); 16.5 (q).

CI-MS (GC/MS, NH₃): 193.1 (100, [*M*+H]⁺), 194.1 (14).

High res. EI-MS calculated for C₁₃H₂₀O: 192.1514; *found*: 192.1513.

1,3-Dimethyl-2-(3-methylbut-2-enyloxy)benzene (51).

2,6-Dimethylphenol **38** (20.00 g, 0.16 mol) was placed in a reactor and dissolved in 135.0 mL of DMF. Sodium hydroxide (7.20 g, 0.18 mol) in 15.0 mL of water was added in portions. The temperature rose slowly to 40 °C and a clear, green solution was obtained. After stirring for additional 15 min. prenyl chloride **39** (30.00 g, 0.16 mol) was added at once. The solution turned brown and some solid precipitated, the temperature rose to 45 °C. After stirring for 3 h the reaction was quenched with 200.0 mL of water and extracted with MtBE. The organic layers were washed with Claisen base (sat. KOH/MeOH), then with water and brine. After concentration the residue was purified by chromatography over silica gel with hex/MtBE 95:5 and dried in vacuo. The phenol ether **51** (25.00 g, 82%) was obtained as a light yellow liquid.

IR (CCl_4): 2918w, 1475m, 1470m, 1378m, 1262m, 1198s, 1090m, 976s, 856w, 765s.

$^1\text{H-NMR}$ (400 MHz, CDCl_3): 6.99 (m, 2 H); 6.90 (m, 1 H); 5.59 (m, 1 H); 4.29 (d, $J = 6.5$ Hz, 2 H); 2.29 (s, 6 H); 1.80 (s, 3 H); 1.70 (s, 3 H).

$^{13}\text{C-NMR}$ (75 MHz, CDCl_3): 155.0, 137.4, 131.0 (4 s); 128.6, 123.6, 120.6 (4 d); 68.8 (t); 25.7, 17.9, 16.2 (4 q).

EI-MS (GC/MS): 190 (2, M^+), 175 (3), 123 (9), 122 (100), 121 (7), 107 (14), 91 (7), 77 (7), 69 (22), 53 (3), 41 (16).

2,6-Dimethyl-4-(3-methylbut-2-enyl)phenol (60).

1,3-Dimethyl-2-(3-methylbut-2-enyloxy)benzene **51** (4.00 g, 21.00 mmol) was placed in a glass ampoule and *N,N*-dimethyl aniline (8.00 g, 66.00 mmol) was added. The ampoule was evacuated, sealed and heated in an oven at 170 °C for 24 h. After cooling to room temperature the ampoule was opened and the light yellow contents mixed with 100.0 mL of water. Hexane was added and the mixture was acidified with H_3PO_4 to remove the *N,N*-dimethyl aniline and extracted three times with hexane. The combined organic solutions were washed with Claisen base to remove phenolic contaminants. Then the organic solution was set to pH 5 with H_3PO_4 , washed with water and brine and concentrated. The phenol **60** was dried in vacuo (2.45 g, 61%) and alkylated without further purification.

2,6-Dimethyl-4,6-bis(3-methylbut-2-enyl)cyclohexa-2,4-dienone (61).

2,6-Dimethyl-4-(3-methylbut-2-enyl)phenol **60** (2.45 g, 12.89 mmol) was placed in a reactor and 30.0 mL of benzene were added. The solution was cooled to 0 °C and NaH 60% in paraffin oil (516 mg, 12.89 mmol) was added in portions. The reaction was exothermic and hydrogen gas evolved. After stirring at 0 °C for 30 min. prenyl chloride **39** (2.23 g, 12.89 mmol) was added dropwise. The mixture was stirred for 20 h at room temperature resulting in a bright yellow suspension. TLC analysis showed that the reaction had gone to completion. Water and hexane

were added to the reaction mixture and the layers were separated. The aq. layer was extracted two times with hexane. The combined organic layers were washed with Claisen base and then with water and brine. After drying and concentrating the hexane solution, the product was purified by chromatography over silica gel with hex/MtBE 95:5. After short path distillation (150 °C, 0.05 mbar) **61** (1.03 g, 31%) was obtained as a light yellow oil.

IR (CCl_4): 2974 m , 2917 m , 1647 m , 1479 m , 1448 m , 1375 m , 1214 s , 1125 vs , 1000 w , 917 s , 868 s , 770 w , 697 w .

$^1\text{H-NMR}$ (300 MHz, CDCl_3): 6.65 (m , 1 H); 5.81 (m , 1 H); 5.14 (m , 1 H); 4.88 (m , 1 H); 2.86 (d , J = 7.4 Hz, 2 H); 2.45 (m , 1 H); 2.13 (m , 1 H); 1.85 (m , 3 H); 1.75 (d , J = 0.7 Hz, 3 H); 1.67 (s , 3 H); 1.62 (d , J = 0.7 Hz, 3 H); 1.55 (s , 3 H); 1.14 (s , 3 H).

$^{13}\text{C-NMR}$ (75 MHz, CDCl_3): 205.9 (s); 141.4, 138.8 (2 d); 133.8, 133.7, 132.7, 130.8 (4 s); 121.2, 119.1 (2 d); 50.2 (s); 39.3, 33.7 (2 t); 25.6, 24.2, 17.6, 15.3 (6 q).

EI-MS (GC/MS): 258 (1, M^+), 190 (56), 175 (100), 160 (9), 122 (8), 91 (10), 69 (23), 41 (23).

General procedure for the alkylation of 2,6-dialkylphenols in the presence of chiral auxiliaries

A 0.3 M solution of the chiral auxiliary in anhydrous toluene was placed in a reactor and one molar equivalent of butyl lithium *Fluka* (1.6 M in hexane) was added dropwise at -10 °C. The mixture was stirred at -10 °C for 30 min. and then a 15% solution of the dialkylphenol in toluene (1 molar equivalent) was added dropwise. Stirring was continued at -10 °C and the reaction was monitored by GC and TLC. Commercially available (-)-sparteine-sulfate was converted to (-)-sparteine **VII** by dissolving in water, treating the solution with K_2CO_3 and extracting the free amine with MtBE. The viscous, colorless product was short path distilled (160 °C, 0.05 mbar) and stored under argon. (-)-Sparteine **VII** has a limited shelf life and turns brown over time. For some experiments, it was necessary to stir the mixture at r.t. over night for the reaction to go to completion. Silica gel was added to the reaction mixture and the suspension was filtered. The clear organic solution was washed with Claisen base to remove any phenols present in the mixture. After washing with water and brine, the organic solution was dried over MgSO_4 and concentrated. The residue was purified by chromatography over aluminum oxide with hex/MtBE. The column was capped with 5 cm of silica gel to retain the basic chiral auxiliaries. The enantiomeric excess of the product was determined by comparing the optical rotation and by NMR experiments with chiral shift reagents, *Chapter 3.3.3*.

α -Isosparteine (**IV**).

Neutral, dry aluminum oxide (18.00 g) was mixed under argon with aluminum chloride (7.56 g, 56.80 mmol). The mixture was divided into six 20.0 mL ampoules and then (-)-sparteine **VII** (2.00

g, 8.55 mmol) was added to each tube. The contents were mixed with a spatula and the ampoules sealed under vacuum. The ampoules were placed in an oven and heated to 230 °C for 6 h. After the ampoules had cooled to r.t., they were smashed and the orange solid was placed in a beaker. Diluted HCl was added until all of the organic material was in solution and only aluminum oxide and broken glass remained. The solution was filtered and extracted with MtBE. The aq. layers were made basic with 30% NaOH and extracted again with MtBE. The organic layers from the second extraction were washed with brine, dried over MgSO₄ and concentrated. The crude α -isosparteine was short path distilled under high vacuum at (150 °C, 0.05 mbar) and then dissolved in acetone. Several drops of water were added to the acetone solution. α -Isosparteine hydrate (3.35 g, 26%) precipitated in large white crystals from the solution. The required amounts of α -isosparteine **IV** for the following experiments were dehydrated by short path distillation (120 °C, 0.05 mbar) immediately before performing the reaction. α -Isosparteine hydrate could be stored in the refrigerator for extended periods of time whereas the anhydrous material was much less stable and turned orange after a couple of days in the refrigerator.

M.p α -isosparteine hydrate = 108-110°C, lit. 104-105.

Opt. rot. (α -isospartein hydrate): $[\alpha]_{\text{D}}^{25}$ - 55.00 (*c* 1.275, MeOH), lit. -32.6 [36].

2,6-Dimethyl-6-(3-methylbut-2-enyl)cyclohexa-2,4-dienone (40).

α -Isosparteine (0.60 g, 2.46 mmol) was dissolved in 6.0 mL of toluene. The solution was cooled to -10 °C and BuLi 1.6 M in hexane (1.50 mL, 2.46 mmol) was added dropwise. The originally colorless solution turned bright yellow. After stirring at -10 °C for 30 min., 2,6-dimethylphenol **38** (300 mg, 2.46 mmol) was added dropwise as a solution in 1.5 mL of toluene. The solution discolored immediately after the addition and then turned yellow again after stirring for 30 min. at -10 °C. Prenyl chloride **38** (256 mg, 2.46 mmol) was added and the mixture was slowly warmed to r.t. and stirred for 14 h. After chromatography with Hex/MtBE 95:5 and short path distillation (~50 °C, 0.05 mbar) **40** (80 mg, 17%) was obtained as yellow oil.

Opt. rot.: $[\alpha]_{\text{D}}^{25}$ + 36.97 (*c* 0.825, EtOH).

Enantiomeric excess (¹H-NMR, Eu(TFC)₃): 7.8%.

2-tert-Butyl-6-methyl-6-(3-methylbut-2-enyl)cyclohexa-2,4-dienone (52).

(-)-Sparteine **VII** (2.00 g, 8.20 mmol) was placed in the reactor and 20.0 mL of benzene were added. The solution was cooled to -15 °C and BuLi 1.6 M in hexane (5.12 mL, 8.20 mmol) was added dropwise, resulting in a bright yellow solution. 2-tert-Butyl-6-methyl-phenol **64** (1.34g, 8.20 mmol) was added dropwise as a solution in 4.0 mL of benzene over 15 min. The resulting homogenous, bright green solution was stirred at room temperature over night. The mixture turned

dark green and a fine precipitate formed. TLC analysis showed a product spot with an R_f value of 0,8 and still a significant amount of unreacted starting material. The mixture was stirred at room temperature for another 24 h. TLC analysis showed only very little change. Silica gel was added to the reaction mixture and the solids were removed by filtration and washed with hex/MtBE 95:5. The combined filtrates were washed with Claisen base and then with water and brine. Chromatography of the crude material over silica gel with hex/MtBE 95:5 afforded **52** (190mg, 10%), after solvent removal under vacuum.

Enantiomeric excess ($^1\text{H-NMR}$, $\text{Eu}(\text{TFC})_3$): 6.2%.

$^1\text{H-NMR}$ (300 MHz, C_6D_6): 6.47 (dd, $J=1.9, 6.1$ Hz, 1 H); 5.94 (dd, $J=1.9, 9.3$ Hz, 1 H); 5.84 (dd, $J=6.1, 9.3$ Hz, 1 H); 5.06 (m, 1 H); 2.73 (m, 1 H); 2.07 (m, 1 H); 1.54 (d, $J=7.2$ Hz, 6 H); 1.28 (s, 9 H); 1.14 (s, 3 H).

$^{13}\text{C-NMR}$ (75 MHz, CDCl_3): 204.0 (s); 145.1 (d); 144.4 (s); 134.5 (d); 133.6 (s), 120.6, 119.9 (2 d); 52.2 (s); 39.4 (t); 34.3 (s); 29.3, 24.5, 24.2, 17.9 (6 q).

EI-MS (GC/MS): 232 (5, M^+), 164 (37), 149 (100), 121 (41), 91 (12), 69 (9).

High res. EI-MS calculated for $\text{C}_{16}\text{H}_{24}\text{O}$: 232.1827; *found*: 232.1831.

2-tert-Butyl-6-methyl-6-(3-methylbut-2-enyl)cyclohex-2-enone (53).

2-tert-Butyl-6-methyl-6-(3-methylbut-2-enyl)cyclohexa-2,4-dienone 52 (150mg, 0.65 mmol) was mixed with 6.0 mL of toluene and 3.0 mL of MeOH. 25mg of palladium 10% on activated charcoal were added and a hydrogen atmosphere was applied by attaching a hydrogen filled balloon to the reactor. The mixture was stirred under the hydrogen atmosphere for 12 h. The mixture was filtered over celite and concentrated. Chromatography over silica gel with hex/MtBE 95:5 and short path distillation (60 °C, 0.05 mbar) afforded **53** (60 mg, 39%) as a colorless oil. NMR experiments with chiral shift reagents showed no splitting of prochiral proton signals.

IR (CCl_4): 2958s, 2913s, 2867s, 1673s, 1453m, 1363m, 1149w, 946w, 882m, 850w, 773w.

$^1\text{H-NMR}$ (500 MHz, C_6D_6): 6.23 (t, $J=4.1$ Hz, 1 H); 5.21 (m, 1 H); 2.27 (m, 2 H); 1.96-1.81 (m, 2 H); 1.63 (s, 3 H); 1.50 (s, 3 H); 1.47-1.40 (m, 2 H); 1.29 (s, 9 H); 1.05 (s, 3 H).

$^{13}\text{C-NMR}$ (125 MHz, CDCl_3): 202.7, 145.4 (2 s); 139.6 (d); 133.5 (s); 120.8 (d); 46.1 (s); 35.6 (t); 34.8 (s); 33.1 (t); 29.7 (3 q); 26.1 (q); 23.1 (t); 22.1, 17.9 (2 q).

EI-MS (GC/MS): 234 (11, M^+), 219 (9), 206 (14), 191 (10), 165 (63), 151 (31), 123 (63), 108 (100), 80 (37), 68 (33), 56 (69).

High res. EI-MS Calculated for $\text{C}_{16}\text{H}_{26}\text{O}$: 234.1984; *found*: 234.1983.

2-Hydroxynaphthalene-1-carbaldehyde (68).

2-Naphthol 67 (28.80 g, 0.20 mol) and MgCl_2 (28.56 g, 0.30 mol) were suspended in 500.0 mL of acetonitrile containing triethylamine (75.75 g, 0.75 mol). Paraformaldehyde (40.50 g, 1.35 mol)

was added at once. After stirring for 30 min. the temperature reached 50 °C. The reactor was equipped with a reflux condenser and the mixture was heated to reflux (75 °C) and stirred at that temperature over night. The reaction was quenched with 5% HCl and extracted with MtBE. The ether layers were combined, washed with water and brine and dried over MgSO₄. Some white solids precipitated during concentration of the solvent. The material was identified as paraformaldehyde and removed by filtration. The light yellow product **68** was crystallized from hex/MtBE and dried in vacuo. Light beige crystals (10.50 g, 30%) were obtained. M.p = 61-63 °C
IR (CCl₄): 3076-1703 (broad signal), 1621s, 1589s, 1518m, 1463s, 1398m, 1310s, 1274m, 1245s, 1177m, 1162s, 968w, 949w, 863m, 793s, 775s, 743s, 714s, 678m, 653m.

¹H-NMR (300 MHz, CDCl₃): 13.13 (s, 1 H); 10.77 (s, 1 H); 8.30 (d, *J* = 8.4 Hz, 1 H); 7.94 (d, *J* = 8.8 Hz, 1 H); 7.77 (m, 1 H); 7.59 (m, 1 H); 7.41 (m, 1 H); 7.11 (d, *J* = 9.2 Hz, 1 H).

¹³C-NMR (75 MHz, CDCl₃): 193.1 (d); 164.8 (s); 139.0 (d); 132.8 (s); 129.4, 129.0 (2 d); 127.7 (s); 124.4, 119.1, 118.5 (3 d); 111.2 (s).

EI-MS (GC/MS): 172 (100, *M*⁺), 171 (61), 144 (52, [*M*-CO]⁺), 126 (16), 115 (91), 89 (17), 63 (20).

High res. EI-MS Calculated for C₁₁H₈O₂: 172.0524; *found*: 172.0518.

Anal. calc. for C₁₁H₈O₂ (172): C 76.73 H 4.68; *found*: C 76.73 H 4.65.

1-Methylnaphthalen-2-ol (69).

2-Hydroxynaphthalene-1-carbaldehyde **68** (5.00 g, 29.10 mmol) was dissolved in 250.0 mL diethylen glycol and hydrazine hydrate 80% (18.18 mL, 291.00 mmol) was added. The mixture was heated at 100 °C for 2.5 hours. After cooling to room temperature, KOH (10.40 g, 185.70 mmol) was added and the temperature was gradually raised to 210 °C while removing the volatiles by distillation. Once the desired temperature was reached (210 °C) the mixture was refluxed for 1 h. The reaction mixture was cooled to r.t. and set to pH 2 with dil. HCl. 250.0 mL of water were added and the biphasic mixture was extracted with MtBE. The combined organic layers were washed with water and brine, dried and concentrated. The residue was dissolved in boiling hexane and then cooled to 5 °C. 1-Methylnaphthalen-2-ol **69** crystallized in fine white needles and was isolated by filtration. The filtrate was concentrated and the residue was crystallized once more. The combined product was dried in vacuo (3.97 g, 86%). M.p = 109-111 °C, lit. 111-112 °C [37].

IR (CCl₄): 3281s, 1628w, 1606w, 1583m, 1511m, 1455m, 1428m, 1348s, 1260m, 1211m, 1168m, 1140m, 1060m, 1016m, 888m, 806s, 767m, 741s, 687m.

¹H-NMR (300 MHz, CDCl₃): 7.90 (m, 1 H); 7.75 (m, 1 H); 7.60 (d, *J* = 8.8 Hz, 1 H); 7.48 (m, 1 H); 7.32 (m, 1 H); 7.03 (d, *J* = 8.8 Hz, 1 H); 4.85 (-OH, 1 H); 2.52 (s, 3 H).

¹³C-NMR (75 MHz, CDCl₃): 150.4, 133.8, 129.2 (3 s); 128.4, 127.3, 126.2, 123.1, 117.5 (6 d); 115.2 (s); 10.3 (q).

EI-MS: 159 (11, [*M*+1]⁺), 158 (100, *M*⁺), 157 (30), 140 (8), 129 (24), 128 (20), 127 (9), 115 (6).

High res. EI-MS calculated for $C_{11}H_{10}O$: 158.0732; found: 158.0725.

Anal. calc. for $C_{11}H_{10}O$ (158): C 83.51 H 6.37; found: C 83.35 H 6.40.

(2R)-2-Methyl-2-(3-methylbut-2-enyl)-2H-naphthalen-1-one ((R)-66).

A solution of α -isosparteine **IV** (440 mg, 1.80 mmol) in 5.0 mL of toluene was cooled to -10 °C. Butyl lithium (1.10 mL, 1.80 mmol) was added dropwise. A bright yellow solution was obtained and stirred for 30 min. at -10 °C. 2-methyl-naphthalen-1-ol **65** (284 mg, 1.80 mmol) was added dropwise as a solution in 2.0 mL of toluene. After stirring at -10 °C for 30 min., solids precipitated and the mixture turned grey/green. Additional 2.0 mL of toluene were added to maintain a movable suspension. Prenyl chloride **39** (234 mg, 1.80 mmol) was added and the mixture turned darker. The reaction was left stirring at r.t. for 15 h. More solids formed and analysis of the reaction mixture by TLC showed that all the starting material had been consumed. Silica gel and hexane was added to the reaction mixture. The solids were removed by filtration and washed with hex/MtBE 1:1. The filtrate was concentrated and the residue was purified by chromatography over Aluminum oxide with hex/MtBE 95:5. After short path distillation (120 °C, 0.05 mbar), (R)-**66** (220 mg, 54%) was isolated as a light-yellow oil.

Opt. rot.: $[\alpha]_D^{25} + 118.80$ (c 1.005, EtOH).

Enantiomeric excess (1H -NMR, $Eu(TFC)_3$): 37.9%

IR (CCl_4): 2968w, 1673s, 1644w, 1598m, 1483w, 1317w, 1268w, 981w, 790vs, 691m.

1H -NMR (300 MHz, C_6D_6): 8.26 (m, 1 H); 7.08 (m, 1 H); 6.93 (m, 1 H); 6.82 (m, 1 H); 6.30 (d, $J = 9.7$ Hz, 1 H); 5.84 (d, $J = 9.9$ Hz, 1 H); 5.09 (m, 1 H); 2.78 (dd, $J = 8.0, 14.0$, 1 H); 2.19 (m, 1 H); 1.51 (s, 3 H); 1.43 (d, $J = 1.1$ Hz, 3 H); 1.20 (s, 3 H).

^{13}C -NMR (75 MHz, C_6D_6): 202.1 (s); 140.1 (d); 138.5 (s); 134.2 (s); 134 (d); 130.0 (s); 127.9, 127.2, 127.0, 214.1, 119.6 (5 d); 49.6 (s); 39.0 (t); 25.6, 24.5, 17.9 (3 q).

EI-MS (GC/MS): 226 (1, M^+), 211 (1, $[M-CH_3]^+$), 158 (100), 128 (24), 115 (10), 69 (19), 41 (20).

Anal. calc. for $C_{16}H_{18}O$ (226): C 84.91, H 8.02; found: C 84.96, H 8.26.

(1S)-1-Methyl-1-(3-methylbut-2-enyl)-1H-naphthalen-2-one ((S)-70).

α -Isosparteine **IV** (1.00 g, 4.10 mmol) was dissolved in 10.0 mL of benzene. The solution was cooled to 0 °C and BuLi 1.6 M in hexane (2.56 mL, 4.10 mmol) was added dropwise. After stirring at 0 °C for 30 min., 1-methyl-naphthalen-2-ol **69** (647 mg, 4.1 mmol) was added as solution in 3.0 mL of benzene. The bright yellow α -isosparteine lithium complex discolored and some solids precipitated. After 30 min. at 0-5 °C prenyl chloride **39** (533 mg, 4.10 mmol) was added at once. The reaction mixture was stirred over night allowing it to gradually reach room temperature. TLC analysis showed that the reaction had gone to completion. Silica gel and hexane

was added to the reaction mixture and the solids were removed from the suspension by filtration and washed with hex/MtBE 1:1. The filtrate was concentrated and the residue separated by chromatography over basic aluminum oxide with hex/MtBE 9:1. After short path distillation (*S*)-**70** (240 mg, 26%) was obtained as light yellow oil.

Opt. rot.: $[\alpha]_{\text{D}}^{25} + 14.87$ (*c* 1.035, EtOH).

Enantiomeric excess ($^1\text{H-NMR}$, Eu(TFC)_3): 30%

IR (*neat*): 2970w, 2913w, 1655vs, 1621w, 1597w, 1449m, 1397w, 1376w, 1299w, 1239w, 1207w, 835m, 755s.

$^1\text{H-NMR}$ (300 MHz, CDCl_3): 7.42-7.23 (*m*, 5 H); 6.14 (*d*, $J = 9.9$ Hz, 1 H); 4.66 (*m*, 1 H); 2.77 (*m*, 1 H); 2.45 (*m*, 1 H); 1.49 (*m*, 3 H); 1.47 (*s*, 3 H); 1.40 (*s*, 3 H).

$^{13}\text{C-NMR}$ (75 MHz, CDCl_3): 204.4 (*s*); 146.3 (*s*); 145.0 (*d*); 134.7 (*s*); 130.0 (*s*); 129.9, 129.4, 126.9, 126.7, 125.4, 118.8 (6 *d*); 52.03 (*s*); 41.8 (*t*); 25.8, 17.9 (3 *q*).

EI-MS (*GC/MS*): 226 (1, M^+), 211 (1, $[M-\text{CH}_3]^+$), 158 (100), 128 (22), 115 (9), 69 (20), 41 (20).

X-ray crystallographic data for the allyl bromide/ α -isopartaine salt **63.****Definition of Terms**

Function minimized:		$\Sigma w(F_o^2 - F_c^2)^2$
w	=	$[\sigma^2(F_o^2) + (aP)^2 + bP]^{-1}$ and $P = (F_o^2 + 2F_c^2)/3$
F_o^2	=	$S(C - RB)/Lp$ and $\sigma^2(F_o^2) = S^2(C + R^2B)/Lp^2$
S	=	Scan rate
C	=	Total integrated peak count
R	=	Ratio of scan time to background counting time
B	=	Total background count
Lp	=	Lorentz-polarization factor
R-factors:	R_{int}	= $\Sigma <F_o^2> - F_o^2 / \Sigma F_o^2$ summed only over reflections for which more than one symmetry equivalent was measured.
	$R(F)$	= $\Sigma F_o - F_c / \Sigma F_o $ summed over all observed reflections.
	$wR(F^2)$	= $[\Sigma w(F_o^2 - F_c^2)^2 / \Sigma w(F_o^2)^2]^{1/2}$ summed over all reflections.

Standard deviation of an observation of unit weight (goodness of fit):

$$[\Sigma w(F_o^2 - F_c^2)^2 / (N_o - N_v)]^{1/2}$$

where N_o = number of observations; N_v = number of variables

Crystal-Structure Determination. A crystal $C_{18}H_{31}BrN_2 \cdot 2C_6H_6$ **63**, obtained from benzene/ CH_2Cl_2 , was mounted on a glass fiber and used for low-temperature X-ray structure determination. All measurements were made on a *Nonius KappaCCD* area-detector diffractometer⁹ using graphite-monochromated Mo $K\alpha$ radiation ($\lambda = 0.71073$ Å) and an *Oxford Cryosystems Cryostream 700* cooler. The unit cell constants and an orientation matrix for data collection were obtained from a least-squares refinement of the setting angles of 59793 reflections in the range $4^\circ < 2\theta < 55^\circ$. The mosaicity was $1.093(2)^\circ$. A total of 434 frames were collected using ϕ and ω scans with κ offsets, 112 seconds exposure time and a rotation angle of 1.5° per frame, and a crystal-detector distance of 30.0 mm.

Data reduction was performed with *HKL Denzo* and *Scalepack*¹⁰. The intensities were corrected for Lorentz and polarization effects, and an absorption correction based on the multi-scan method¹¹ was applied. Standard reflection intensities were not monitored. The space group was determined

⁹ R. Hoof, *KappaCCD Collect Software*, Nonius BV, Delft, The Netherlands, 1999.

¹⁰ Z. Otwinowski, W. Minor, in *Methods in Enzymology*, Vol. 276, *Macromolecular Crystallography*, Part A, Eds. C.W. Carter Jr., R.M. Sweet, Academic Press, New York, 1997, pp. 307-326.

¹¹ R.H. Blessing, *Acta Crystallogr., Sect A* **1995**, 51, 33-38.

from the systematic absences, packing considerations, a statistical analysis of intensity distribution, and the successful solution and refinement of the structure. Equivalent reflections, other than Friedel pairs, were merged. Data collection and refinement parameters are given in *Table 1*. A view of the molecule is shown in *Chapter 3.3.6, Figure 6*.

The structure was solved by direct methods using *SIR92*¹², which revealed the positions of all non-hydrogen atoms. The non-hydrogen atoms were refined anisotropically. All of the H-atoms were placed in geometrically calculated positions and refined using a riding model where each H-atom was assigned a fixed isotropic displacement parameter with a value equal to 1.2U_{eq} of its parent atom. Refinement of the structure was carried out on F^2 using full-matrix least-squares procedures, which minimized the function $\sum w(F_o^2 - F_c^2)^2$. The weighting scheme was based on counting statistics and included a factor to down weight the intense reflections. Plots of $\sum w(F_o^2 - F_c^2)^2$ versus $F_c / F_c(\text{max})$ and resolution showed no unusual trends. A correction for secondary extinction was applied. Refinement of the absolute structure parameter¹³ yielded a value of 0.05(1), which confidently confirms that the refined coordinates, as listed in *Table 2*, represent the true enantiomorph.

Neutral atom scattering factors for non-hydrogen atoms were taken from Maslen, Fox and O'Keefe^{14a}, and the scattering factors for H-atoms were taken from Stewart, Davidson and Simpson¹⁵. Anomalous dispersion effects were included in F_c ¹⁶; the values for f' and f'' were those of Creagh and McAuley^{14b}. The values of the mass attenuation coefficients are those of Creagh and Hubbel^{14c}. All calculations were performed using the *SHELXL97*¹⁷ program.

¹² A. Altomare, G. Cascarano, C. Giacovazzo, A. Guagliardi, M.C. Burla, G. Polidori, M. Camalli, *SIR92*, *J. Appl. Crystallogr.* **1994**, *27*, 435.

¹³ a) H.D. Flack, G. Bernardinelli, *Acta Crystallogr., Sect. A* **1999**, *55*, 908-915; b) H.D. Flack, G. Bernardinelli, *J. Appl. Crystallogr.* **2000**, *33*, 1143-1148.

¹⁴ a) E.N. Maslen, A.G. Fox, M.A. O'Keefe, in 'International Tables for Crystallography', Ed. A.J.C. Wilson, Kluwer Academic Publishers, Dordrecht, 1992, Vol. C, Table 6.1.1.1, pp. 477-486; b) D.C. Creagh, W.J. McAuley, *ibid.* Table 4.2.6.8, pp. 219-222; c) D.C. Creagh, J.H. Hubbell, *ibid.* Table 4.2.4.3, pp. 200-206.

¹⁵ R.F. Stewart, E.R. Davidson, W.T. Simpson, *J. Chem. Phys.* **1965**, *42*, 3175-3187.

¹⁶ J.A. Ibers, W.C. Hamilton, *Acta Crystallogr.* **1964**, *17*, 781-782.

¹⁷ G.M. Sheldrick, *SHELXL97, Program for the Refinement of Crystal Structures*, University of Göttingen, Germany, 1997.

Crystallographic Data for 63

Crystallized from	benzene / CH ₂ Cl ₂
Empirical formula	C ₁₈ H ₃₁ BrN ₂ ·2C ₆ H ₆
Formula weight [g mol ⁻¹]	511.59
Crystal colour, habit	colorless, prism
Crystal dimensions [mm]	0.10 × 0.20 × 0.22
Temperature [K]	160 (1)
Crystal system	monoclinic
Space group	<i>P</i> 2 ₁ (#4)
<i>Z</i>	2
Reflections for cell determination	59793
2 θ range for cell determination [°]	4–55
Unit cell parameters	
<i>a</i> [Å]	9.6338 (2)
<i>b</i> [Å]	8.4978 (2)
<i>c</i> [Å]	16.9348 (4)
α [°]	90
β [°]	96.8364 (9)
γ [°]	90
<i>V</i> [Å ³]	1376.53 (5)
<i>F</i> (000)	544
<i>D_x</i> [g cm ⁻³]	1.234
μ (Mo <i>K</i> α) [mm ⁻¹]	1.517
Scan type	ϕ and ω
2 $\theta_{\text{(max)}}$ [°]	55
Transmission factors (min; max)	0.661; 0.745
Total reflections measured	31067
Symmetry independent reflections	6276
<i>R</i> _{int}	0.060
Reflections with <i>I</i> > 2 σ (<i>I</i>)	5456
Reflections used in refinement	6276
Parameters refined; restraints	300; 1
Final <i>R</i> (<i>F</i>) [<i>I</i> > 2 σ (<i>I</i>) reflections]	0.0476
<i>wR</i> (<i>F</i> ²) (all data)	0.1255
Weights:	$w = [\sigma^2(F_o^2) + (0.0659P)^2 + 1.0981P]^{-1}$ where $P = (F_o^2 + 2F_c^2)/3$
Goodness of fit	1.065
Secondary extinction coefficient	0.007 (2)
Final $\Delta_{\text{max}}/\sigma$	0.001
$\Delta\rho$ (max; min) [e Å ⁻³]	0.78; -0.578
$\sigma(d_{\text{C-C}})$ [Å]	0.005–0.01

3.6 References

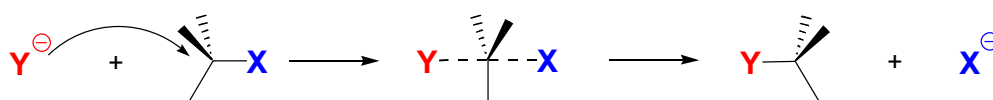
- [1] I. Denissova, L. Barriault, *Tetrahedron*, **2003**, 59, 10105-10146 and references cited therein.
- [2] A. Goeke, D. Mertl, G. Brunner, *Angew. Chem. Int. Ed.*, **2005**, 44, 99-101.
- [3] A. Goeke, EP 1213276, priority 5.12.2000 to Givaudan.
- [4] D. Hoppe, T. Hense, *Angew. Chem. Int. Ed.*, **1997**, 36, 2282-2316.
- [5] See for example: C. Cavé, D. Desmaële, J. d'Angelo, *J. Org. Chem.*, **1996**, 61, 4361-4368; M. J. Lucero, K. N. Houk, *J. Am. Chem. Soc.*, **1997**, 119, 826-827.
- [6] B. M. Trost, J. Xu, *J. Am. Chem. Soc.*, **2005**, 127, 2846-2847.
- [7] G. Fráter, *Tetrahedron Lett.*, **1981**, 22, 425-428.
- [8] W. Kreiser, P. Below, *Tetrahedron Lett.*, **1981**, 22, 429-432.
- [9] A. I. Meyers, B. A. Lefker, *Tetrahedron*, **1987**, 43, 5663-5676.
- [10] S. Maiti, B. Achari, A. K. Banerjee, *Synlett*, **1998**, 2, 129-130.
- [11] A. G. Schultz, P. Sundaraman, *Tetrahedron Lett.*, **1984**, 25, 4591-4594.
- [12] M. Lovchik, G. Fráter, A. Goeke, preliminary results were presented at the fall meeting of the Swiss Chemical Society in 2003; *Chimia*, **2003**, 7, 427.
- [13] D. Y. Curtin, D. H. Dybvig, *J. Am. Chem. Soc.*, **1962**, 84, 225-232.
- [14] N. Kornblum, P. J. Berrigan, W. J. Le Noble, *J. Am. Chem. Soc.*, **1963**, 85, 1141-1147.
- [15] D. Curtin, R. R. Fraser, *J. Am. Chem. Soc.*, **1958**, 80, 6016-6020.
- [16] A. G. Schultz, J. P. Dittami, F. P. Lavieri, C. Salowey, P. Sundararaman, M. B. Szymula, *J. Org. Chem.*, **1984**, 49, 4429-4440.
- [17] B. Miller, *Acc. Chem. Res.*, **1975**, 8, 245-256.
- [18] G. Fráter, H. Greuter, H. Schmid, *Helv. Chim. Acta*, **1972**, 55, 526-531.
- [19] G. Fráter, *Helv. Chim. Acta*, **1974**, 57, 172-179.
- [20] B. Miller, L. Lewis, *J. Org. Chem.*, **1974**, 39, 2605-2607.
- [21] M. Soukup, T. Lukáč, R. Zell, F. Roessler, K. Steiner, E. Widmer, *Helv. Chim. Acta*, **1989**, 72, 365-369.
- [22] E. A. Broger, W. Burkart, M. Hennig, M. Scalone, R. Schmid, *Tetrahedron: Asymmetry*, **1998**, 9, 4043-4054.
- [23] H. Nakamura, H. Iwama, M. Ito, Y. Yamamoto, *J. Am. Chem. Soc.*, **1999**, 121, 10850-10851.
- [24] J. Borgulya, *Dissertation, University of Zurich*, **1965**.
- [25] H.-J. Hansen, *Dissertation, University of Zurich*, **1968**.
- [26] B. Miller, *J. Am. Chem. Soc.*, **1965**, 87, 5115-5120.

- [27] J. Borgulya, R. Madeja, P. Fahrni, H.-J. Hansen, H. Schmid, R. Barner, *Helv. Chim. Acta*, **1973**, *56*, 14-75; U. Widmer, J. Zsindely, H.-J. Hansen, H. Schmid, *Helv. Chim. Acta*, **1973**, *56*, 75-105.
- [28] B. Miller, *J. Am. Chem. Soc.*, **1969**, *91*, 2170-2172.
- [29] B. Miller, M. P. McLaughlin, *J. Org. Chem.*, **1982**, *47*, 5204-5207.
- [30] S. Woodward, *Tetrahedron*, **2002**, *58*, 1017-1050.
- [31] D. Bradley, *Chem. Brit.*, **2002**, 42-45; G. W. V. Cave, C. L. Raston, J. L. Scott, *Chem. Com.*, **2001**, 2159-2169; G. W. V. Cave, C. L. Raston, *Chem. Com.*, **2000**, 22, 2199-2200; J. R. Radja, G. Sankar, M. Thomas, *J. Am. Chem. Soc.*, **2001**, *123*, 8153-8154; A. McClusky, P. J. Robinson, T. Hill, J. L. Scott, J. K. Edwards, *Tetrahedron Lett.*, **2002**, *43*, 3117-3120; J. Long, J. Hu, X. Shen, B. Ji, J. Ding, *J. Am. Chem. Soc.*, **2002**, *124*, 10-11; C.-J. Li, C. Wei, *Chem. Commun.*, **2002**, 268-269.
- [32] A. Farina, S. V. Meille, M. T. Messina, P. Metrangolo, G. Resnati, *Acta Cryst.*, **1999**, *C55*, 1710-1711; M. F. Simeonov, S. L. Spassov, H. Duddeck, U. Majchrzak-Kuczyńska, J. Skolik, *Mag. Res. Chem.*, **1989**, *27*, 476-482.
- [33] A. E. Koziol, *J. Cryst. Spec. Res.*, **1992**, *22*, 449-459.
- [34] N. U. Hofsløkken, L. Skattebøl, *Acta Chem. Scand.*, **1999**, *53*, 258-262.
- [35] R. H. Burnell, M. Jean, S. Marceau, *Can. J. Chem.*, **1988**, *66*, 227-230.
- [36] F. Gallinovskiy, P. Knoth, W. Fischer, *Mh. Chem.*, **1955**, *86*, 1014-1023.
- [37] H. Grabowska, W. Miśta, L. Syper, J. Wrzyszc, M. Zawadzki, *Res. Chem. Intermed.*, **1997**, *23*, 135-141.

4. Part II. Cyclobutanes through S_Ni' Ring Closure, a Mechanistic Study

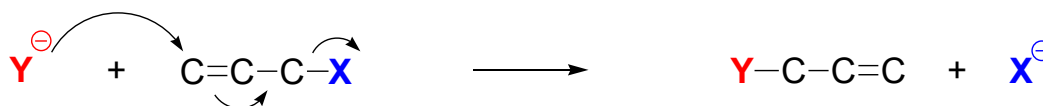
4.1 Introduction

The conventional S_N2 reaction is a one step process in which a nucleophile, for example chloride ion attacks the substrate and a nucleofuge, e.g. halogenide, tosylate or mesylate ion is expelled. The incoming nucleophile approaches from a 180° angle to the leaving group, leading to Walden inversion at a carbon center, *Scheme 25*. The energy for breaking the carbon-leaving group bond is supplied by the energy of the carbon-nucleophile bond being formed [38].



Scheme 25. Mechanism of the S_N2 reaction.

The S_N2' reaction differs from the S_N2 reaction in the sense that nucleophilic attack on an allylic system bearing a leaving group takes place at the γ-carbon, leading to migration of the double bond, *Scheme 26*. Although this reaction is less common than the S_N2 reaction, the variant has been extensively studied and several disputes were fought over the last century. Originally discovered in the late 1930's independently by Hughes and Winstein, the S_N2' reaction was reported to dominate over the S_N2 reaction in a variety of allylic displacement reactions [38][39].

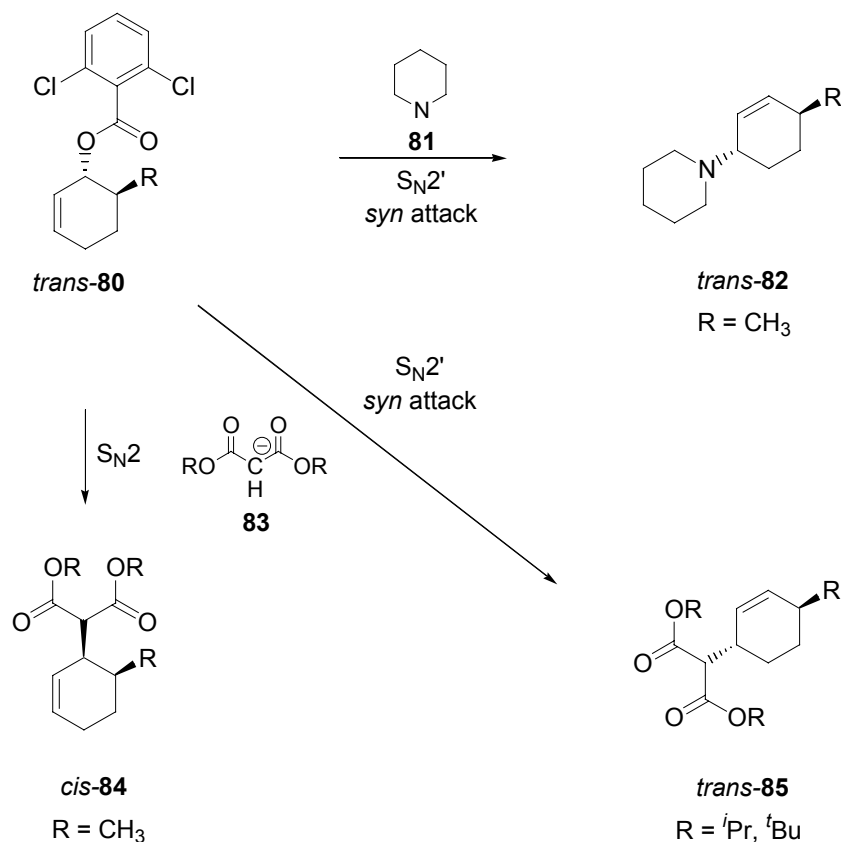


Scheme 26. Mechanism of the S_N2' reaction.

In the comprehensive article, cited above, Hughes called the newly discovered mechanism “nucleophilic substitution in an extended system”. Simultaneously, Winstein reported what he called the “abnormal S_N2 reaction” in his dissertation and later, more detailed, in a publication on the allylic rearrangements of crotyl and methyl vinyl-halides in the presence of sodium ethoxide [39][40].

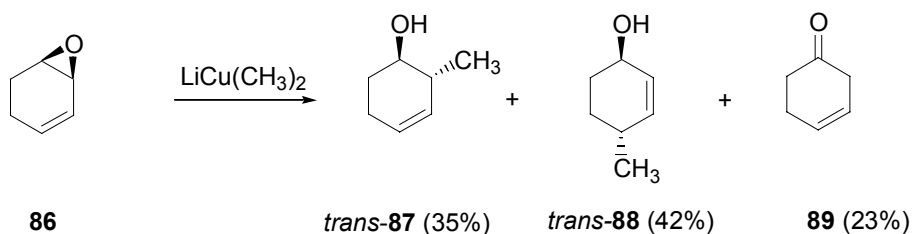
The present dissertation reports results obtained from the investigation of the intramolecular version of the S_N2' reaction, the so called S_Ni' reaction (intramolecular, nucleophilic substitution in an allylic system) [41]. Its mechanism is strongly related to that of the S_N2' reaction and the results from stereochemical analysis of the S_N2' reaction apply to the intramolecular S_Ni' version as well. In the early days of S_N2' chemistry, Stork and White performed extensive research on S_N2 vs. S_N2' reactions [42]. The S_N2' reaction of *trans*-**80** with piperidine **81** led to the *trans*-product *trans*-**82**, resulting from *syn* displacement of the leaving group, *Scheme 27*. The reaction with

malonate ion **83** led to a mixture of the S_N2 product *cis*-**84** and the S_N2' product *trans*-**85**. Based on their experimental results, the authors reported that in all of the observed S_N2' reactions, the nucleophile entered *syn* relative to the departing nucleofuge.



Scheme 27. S_N2 vs. S_N2' reactions by Stork et al.

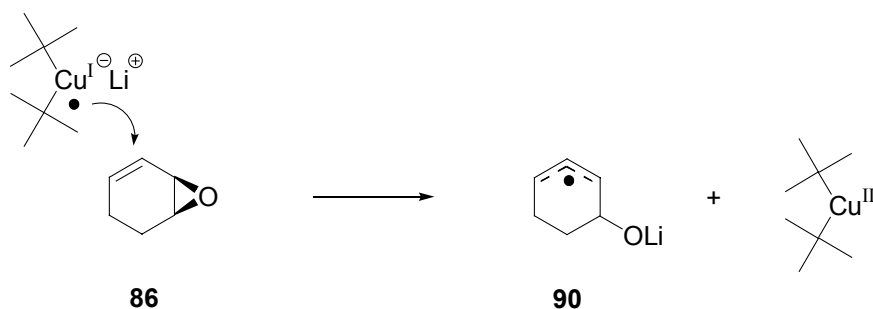
Staroscik and Rickborn provoked a dispute by publishing contradictory results based on the addition of methyl-organometallic reagents to cyclohexene mono-epoxide **86** [43], *Scheme 28*. The authors found that, when organocopper reagents were used, *trans*-**88** was formed with *anti* stereoselectivity, together with the S_N2 product *trans*-**87** and the epoxide rearrangement product **89**.



Scheme 28. S_N2 and S_N2' reaction of 1,3-cyclohexadiene mono-epoxide with organo cuprates, by Rickborn et al.

Simultaneously, Johnson and Wieland published results obtained from a similar reaction [44]. In general the results were in accord with those reported by Rickborn and his co-workers. For the reaction of **86** with (*t*Bu)₂CuLi the authors proposed a mechanism involving an intermediate radical anion **90**, *Scheme 29*. It seems, however, difficult to imagine that the stereochemical

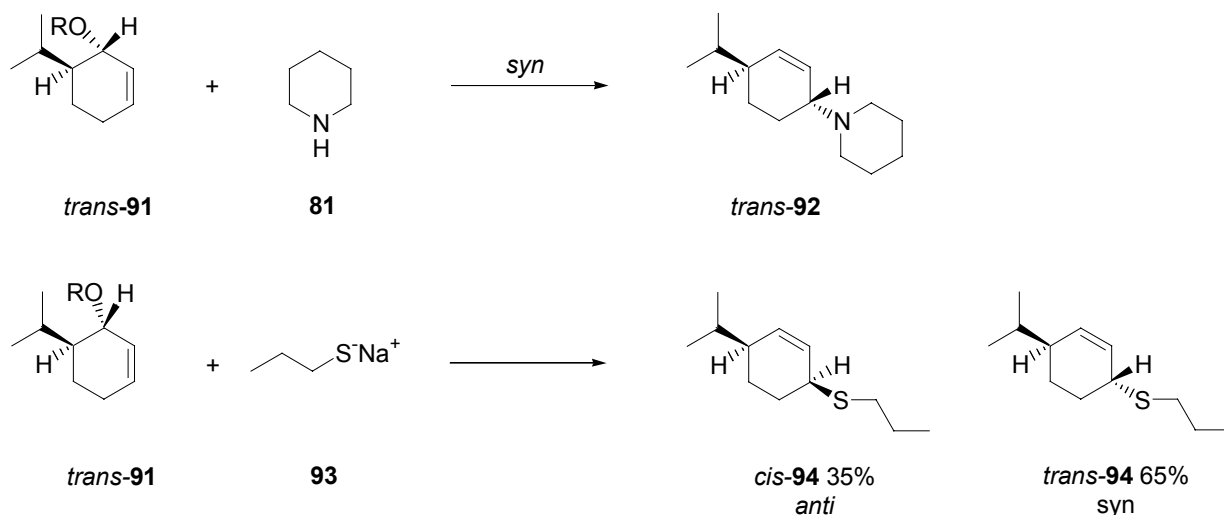
influence of the optically active epoxide would be strong enough to result in predominant *anti* substitution.



Scheme 29. Radical anion mediated mechanism postulated by Johnson et al.

Rickborn et al. speculated that a Lewis acid catalyzed $\text{S}_{\text{N}}1$ mechanism involving an allyl-carbonium ion would also be tenable. The formation of the epoxide rearrangement product **89** in *Scheme 28* offers some evidence for this hypothesis.

Stork and Kreft found evidence that the stereochemical outcome of $\text{S}_{\text{N}}2'$ reactions in cyclic and acyclic systems depends on the nature of the nucleophile and showed that the reaction of *trans*-**91** and piperidine led to the *syn* product *trans*-**92** [45], *Scheme 30*. On the other hand, the reaction with sodium propane-1-thiolate **93** led to the *anti* $\text{S}_{\text{N}}2'$ product *cis*-**94** in 35% yield, accompanied by 65% of the *syn* displacement product *trans*-**94**.

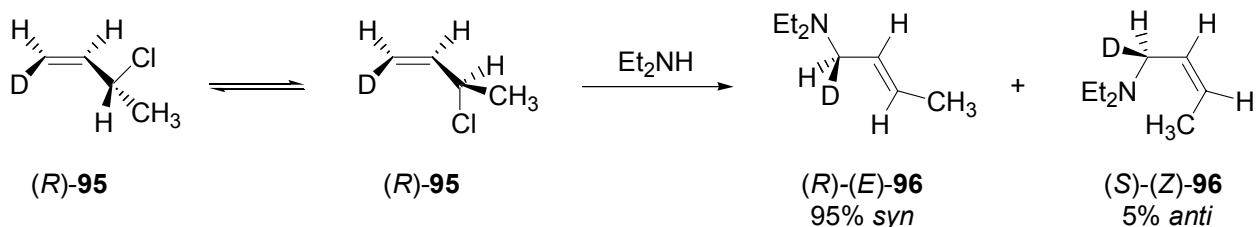


Scheme 30. Evidence for *anti* addition of thiolates by Stork et al.

In a later publication Stork and Kreft reported similar studies on acyclic systems where the evidence for *anti* displacement with thiolate anions in $\text{S}_{\text{N}}2'$ reactions was even more profound [46].

Magid and Fruchey argued, that the cyclohexenyl system may have certain built-in conformational biases that force *syn* attack, regardless of any stereoelectronic requirements of the $\text{S}_{\text{N}}2'$ reaction

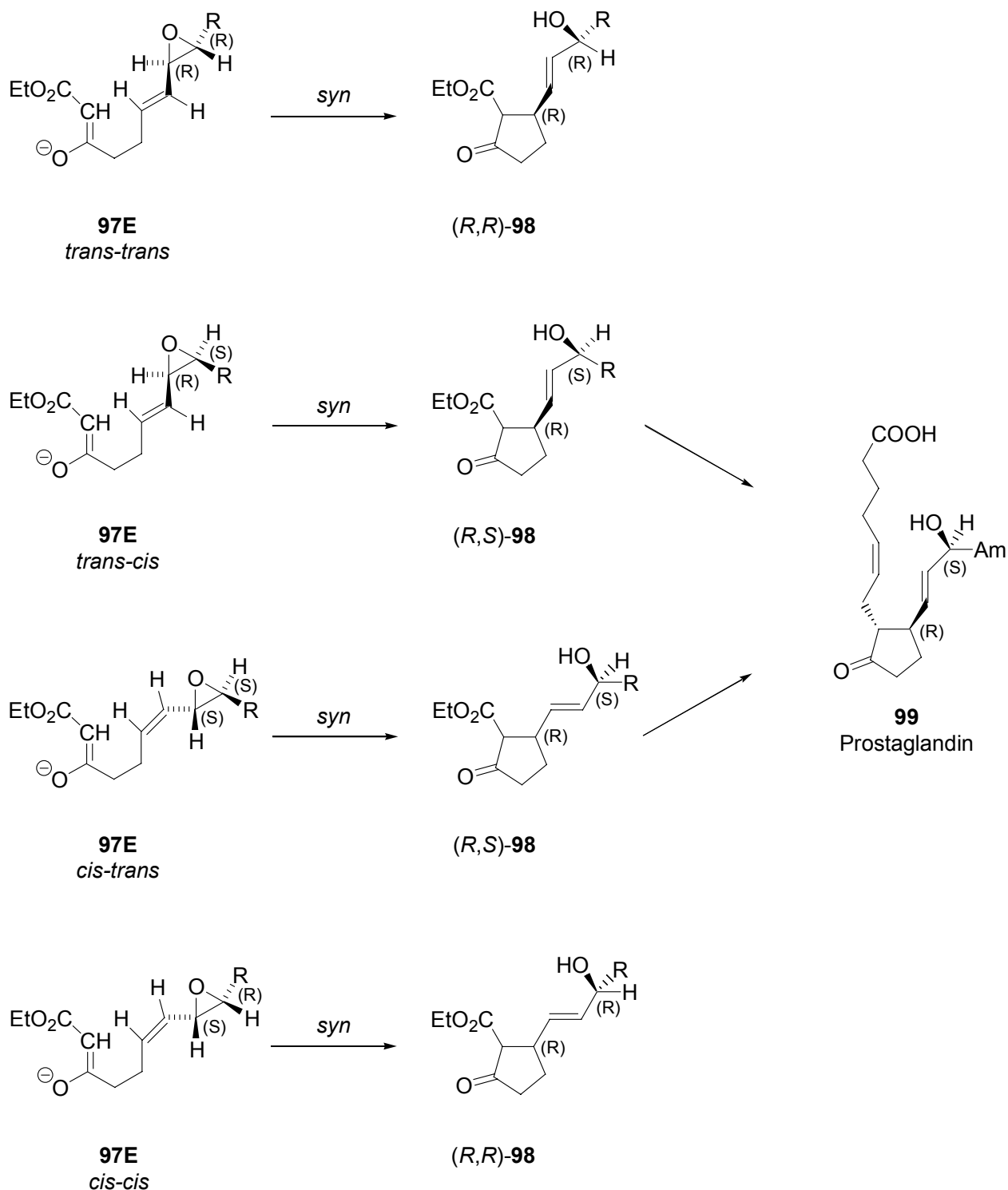
[47].¹⁸ The authors published results from a S_N2' reaction in an acyclic system. Enantiomerically enriched deuterated allylic chloride (*R*)-**95** was prepared and reacted with diethylamine affording the S_N2' product **96**, containing no more than 1% of the corresponding S_N2 product, *Scheme 31*. The (*E*)/(*Z*) ratio in (*R*)-(*E*)-**96** was 95:5. Comparison of the specific rotation of the S_N2' product with pure reference material showed that the reaction had occurred with 95 (+/- 2%) *syn* stereochemistry.



Scheme 31. Evidence for selective *syn* displacement in unbiased S_N2' reactions.

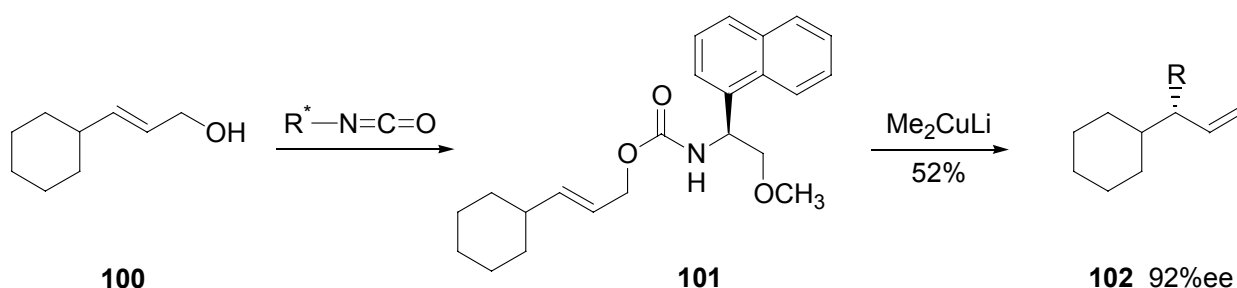
Toromanoff applied the S_Ni' reaction in the total synthesis of prostaglandin **99** [48], *Scheme 32*. Instead of a simple nucleofuge such as chloride, mesylate or tosylate ion, he used an allylic epoxide resulting in a chiral allylic alcohol side chain on the newly formed five member ring. Construction of the stereogenic center in β -position of the cyclopentanone ring was the key step, diastereoselective insertion of the alkyl group at the α -carbon then led to enantiomerically pure prostaglandine. As illustrated in *Scheme 32*, *syn* S_Ni' reaction of *cis-trans*-**97E** and *trans-cis*-**97E** will lead to (*R,S*)-**98** having the same configuration at the chiral centers as the prostaglandin. Toromanoff used *cis-trans*-**97E** for his studies because it was easier to synthesize. The configuration of the resulting secondary alcohol depends on the configuration of the initial epoxide. The four configurational isomers of **97E**, illustrated in *Scheme 32*, lead to (*R*)-configuration at C(3) of the cyclopentane ring in **98**. As predicted, cyclization of *cis-trans*-**97E** led to the formation of (*R,S*)-**98**. The results presented by Toromanoff constitute an example of a clean S_Ni' reaction with *syn*-stereochemistry.

¹⁸ Magid et al. wrote an excellent review on S_N2' reactions organized in three chapters, the first chapter discusses the results from S_N2' reactions in the absence of transition metals and the second chapter covers the transition metal mediated reactions [49]. The latter possibly follow different mechanistic pathways and are therefore not relevant for this research. In the third chapter the authors added a useful collection of methods to access allylic halides from the corresponding alcohols in a stereoselective manner.



Scheme 32. S_Ni' reaction in the prostaglandin synthesis by Toromanoff.

Denmark and Marble performed the S_N2' reaction on prochiral allylic systems bearing an optically active leaving group [50], *Scheme 33*. Optically active allylic phenyl carbamates were alkylated regio- and stereoselectively with alkyl-lithium-copper reagents. The substrate chosen for the study was the allylic alcohol **100**. It was found that reaction of Me_2CuLi with carbamate **101**, derived from **100** and (*S*)- α -naphthylglycine, gave the highest enantioselectivity in **102** (92% ee).



Scheme 33. Enantioselective $\text{S}_{\text{N}}2'$ reaction by Denmark et al.

4.1.1 Summary of different $\text{S}_{\text{N}}2'$ reactions from the literature

Table 4 contains a selection of inter- and intramolecular $\text{S}_{\text{N}}2'$ reactions involving different nucleophile and nucleofuge functionalities. The examples are in systematic order of decreasing $\text{S}_{\text{N}}2'$ selectivity and *syn* preference. From the data it can be seen that secondary amines, carbanions and alcoholates react with high *syn* selectivity, regardless of the nature of the leaving group. When switching from carbon to sulfur nucleophiles the reaction becomes less selective and in some cases the *anti* products prevail. With exception of one intramolecular reaction involving a thiolate anion [45] only metal mediated reactions led to products with preferred *anti* stereoselectivity.

Table 4. Summary of $\text{S}_{\text{N}}2'$ reactions from the literature

Starting material	Nucleophile	Leaving group	Product	$\text{S}_{\text{N}}2/\text{S}_{\text{N}}2'$	$\text{S}_{\text{N}}2'$ product		Lit.
					% <i>syn</i>	% <i>anti</i>	
	$(\text{CH}_3)_2\text{NH}$	CH_3SO_2^-		1 : 100	100	0	[51]
	$(\text{CH}_3)_2\text{NH}$	$(\text{CH}_3)_3\text{N}$		1 : 100	100	0	[51]
	CH_3O^-	Cl^-		1 : 100	100	0	[52]
	Enolate	CH_3O^-		1 : 100	100	0	[53]

				> 90% S _N 2'	100	0	[42]
	(CH ₃ CH ₂) ₂ NH	Cl ⁻		1 : 99	96	4	[47]
				20 : 80	100	0	[45]
				1 : 100	92	2	[45]
				69 : 31	90	10	[45]
				60 : 40	70	30	[45]
				50 : 50	35	65	[45]
	(^t Bu) ₂ CuLi			35 : 65	12	88	[44]
	CH ₃ Li (5 mol% CuI)			75 : 25	12	88	[44]
	R ⁻ CuN(CH ₃)Ph	Bu ₃ PO ⁻		5 : 95	7	88	[54]

	PhLi			+		70 : 28	7	93	[44]			
	S ⁻					1 : 100	< 5	> 95	[46]			
	LiCu(CH ₃) ₂			35%		42%		23%	45 : 55	0	100	[43]
	LiCu(CH ₃) ₂								46 : 54	0	100	[44]
	Ph ₂ CuLi								69 : 31	0	100	[44]
	CH ₃ Li								100 : 1			[44]
									100 : 1			[42]

4.1.2 Stereochemical analysis of the S_N2' reaction by MO considerations

Liotta et al. published a theoretical tool that allows the prediction of the stereochemical course of nucleophilic and electrophilic processes based on the orbital distortion technique [55]. According to this theory, the geometry of nucleophilic displacement in an allylic system is governed by the LUMO of the allylic substrate, *Figure 15*. It is the C-X substituent in 1-position which is primarily responsible for the distortion of the π -system in the molecule. *TS 1* shows the undistorted LUMO in an allylic system and *TS 2* shows the distortion of the molecular orbitals for maximum bonding.

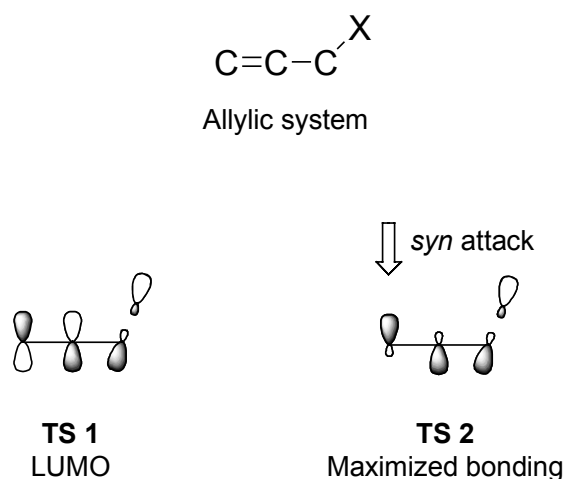


Figure 15. LUMO distortion in allylic systems by Liotta et al.

This orbital symmetry analysis shows that nucleophilic approach is expected to occur *syn* to the C-X substituent. The author concluded that this theory provided profound evidence that the $\text{S}_{\text{N}}2'$ and $\text{S}_{\text{N}}\text{i}'$ reactions can be expected to proceed in a stereoselective “concerted” fashion and that the displacing nucleophile will attack *syn* to the leaving group. The authors suggested, that the *anti* displacement with organo-cuprates, observed by Rickborn and Johnson, most likely proceeded by a single electron transfer step followed by the transfer of an alkyl group [43][44]. In 1975 when Liotta et al. published this work, the authors were not yet aware of the predominant *anti* $\text{S}_{\text{N}}2'$ displacement with thiolate anions, reported by Stork et al in 1977 [46].

A similar approach regarding the non-bonded interactions was published by Stohrer [56]. The author considered the stereoelectronic changes that occur at the central carbon atom of the allylic system during the substitution, *Figure 16*. In the $\text{S}_{\text{N}}2'$ transition state, the central carbon atom C(2) of the allylic system will accumulate more or less negative charge, depending on whether neutral or charged nucleophiles are involved. In the *anti*-transition state **103**, C(2) is sp^2 -hybridized and therefore planar. In contrast, C(2) in the *syn*-transition state **104**, is no longer planar but sp^n -hybridized ($2 < n < 3$) and resembles more transition state **105**. The electron density on the central carbon atom lies on the opposite side of the two nucleophiles.

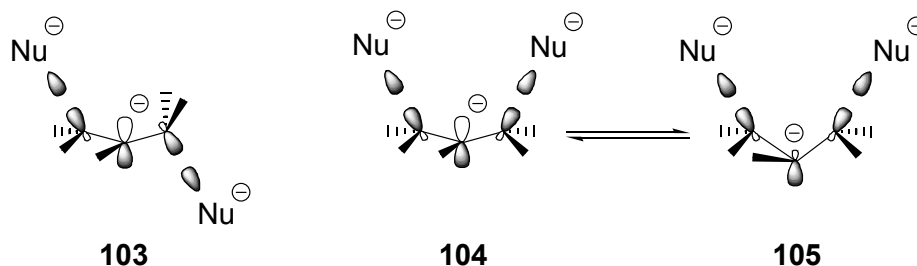


Figure 16. Static distortion in the *syn* and *anti* transition state by Stohrer.

The change in hybridization can be understood by considering the frontier molecular orbital theory, illustrated in *Figure 17*. The approaching nucleophile interacts with the double bond LUMO to establish a σ -bond (a) while the molecular frame gets distorted to minimize antibonding

effects (b) with the molecular orbital of C(2), forcing the electron density to the opposite side of the molecule.

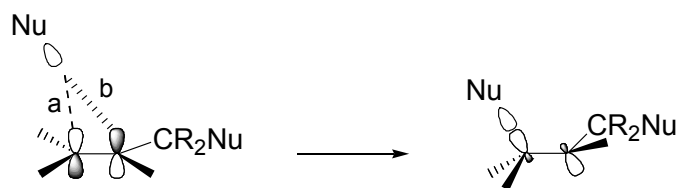


Figure 17. sp^n -Hybridization of the central carbon atom in the allylic system.

a) Bonding interaction with double bond LUMO. b) Antibonding interaction with negative charge on the central atom.

The effect of polarization on the charge density at the central atom C(2) of an allylic system for a *syn* (i) and *anti* (ii) nucleophilic attack is illustrated in *Figure 18*. Stohrer argues that in order for the *anti* reaction (ii) to prevail, the polarized electron density at the sp^n -hybridized central carbon C(2) would have to undergo inversion. Due to this inversion barrier, the *anti* reaction is disfavored.

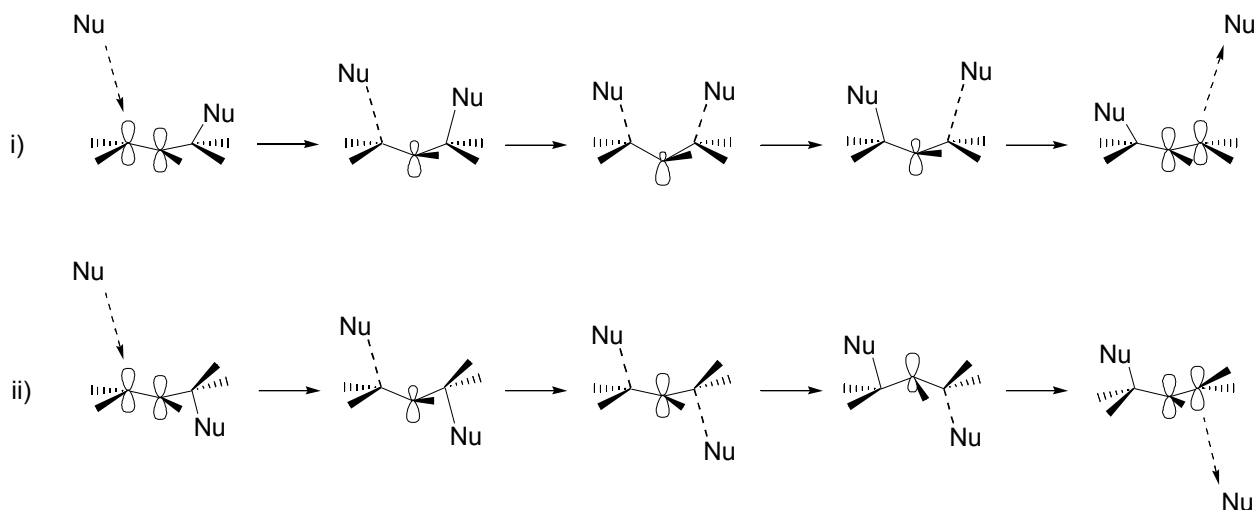


Figure 18. Static distortion of the allylic system in the *syn* and *anti* transition state.

This effect will be more pronounced, the more negative charge is present at C(2). E.g., the larger the electronic difference between the entering and the leaving nucleophile the more negative charge is “stored” at the central carbon atom. Under these considerations a strongly attached leaving group should favor the *syn* reaction and an easily expelled leaving group should lead to the *anti* reaction. The impact of this natural barrier can be influenced by other known factors like steric hindrance and electrostatic effects.

In 1983 Houk et al. publish their theory based on model calculations which confirmed that pyramidalization of C(2) in the allylic system had a strong impact on the stereochemical outcome of the reaction [57].

Epitotis et al. proposed, that nonbonded attraction and electrostatic repulsion are key factors in determining the preferred geometry in the transition state of S_N2' reactions [58]. The allyl framework plus the nucleophile and the leaving group constitute a 6π electron system which is

more stable in a *cis* geometry (Hückel aromatic system) than in a *trans* geometry (extended non-aromatic system), *Figure 19*.

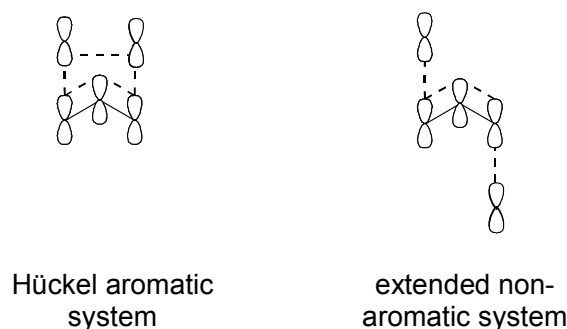


Figure 19. Aromatic transition state in S_N2' reactions proposed by Epiotis et al.

The research led Epiotis et al. to some interesting ideas on the trajectory of the incoming nucleophile in an allylic system, *Figure 20*. A perpendicular approach (a) would have to go through a highly unfavored Möbius antiaromatic configuration. If the nucleophile enters following a path parallel to the nodal plane of the allylic system (b) continuous enhancement of Hückel aromaticity is in effect.

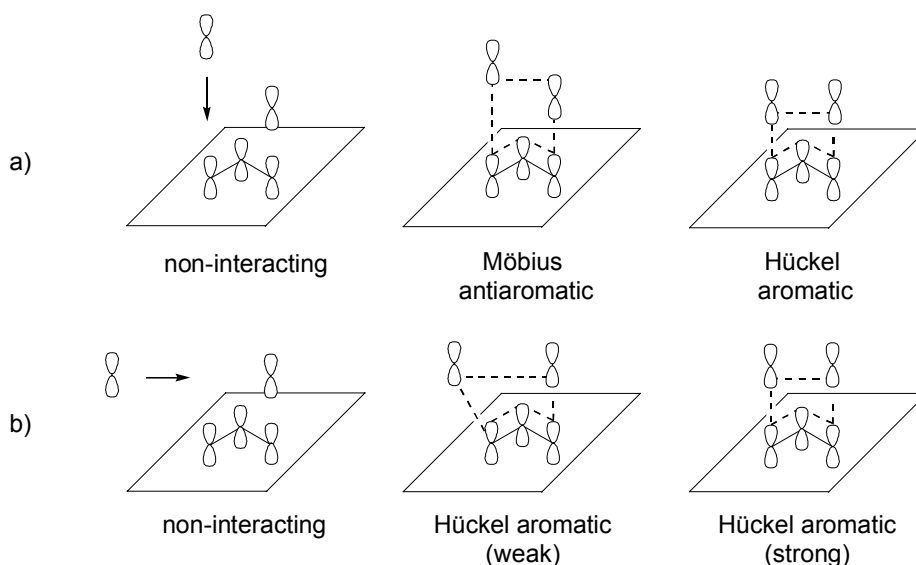


Figure 20. Trajectory for nucleophilic *syn* attack on allylic systems.

a) Disfavoured perpendicular approach passing through a Möbius antiaromatic configuration. b) Favoured parallel approach resulting in continuous enhancement of Hückel aromaticity.

Ab initio calculations showed that the charge on the nucleophile influences the stereochemical course of the reaction, *Figure 21*. If the displacing nucleophile is neutral, the N and X groups are expected to be oppositely charged in the transition state and nonbonded attraction will tend to stabilize the *syn* geometry more than the *anti*. If however, the attacking nucleophile is charged, the N- and X-groups are expected to both be negatively charged and the resulting electrostatic

repulsion will tend to destabilize the aromatic transition state in favor of the *anti* geometry allowing greater distance between the two equally charged centers.

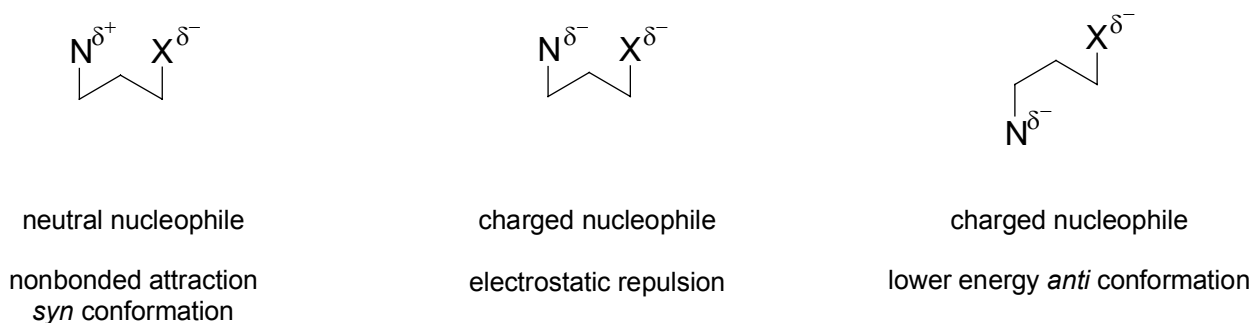


Figure 21. Preferred transition states for charged and neutral nucleophiles.

Epiotis et al. concluded, that even though nonbonded attraction favors *syn* attack, the dominant factor for determining the stereochemistry of a S_N2' reaction, in which the nucleophile is charged, is the electrostatic interaction factor. Table 5 shows the preferred trajectory for neutral and charged nucleophiles in the S_Ni' reaction.

Table 5. Non-bonded vs. electrostatic interactions in S_N2' reactions by Epiotis et al.

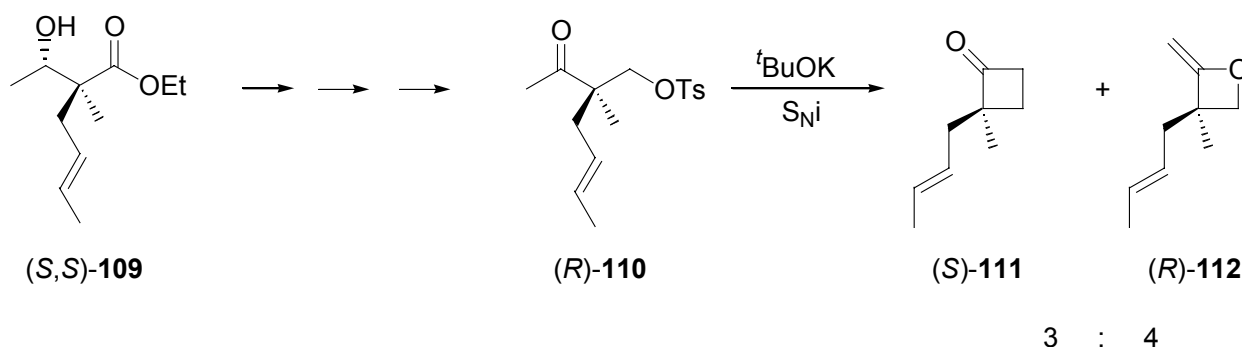
	Neutral nucleophile	Charged nucleophile
Nonbonded interaction	<i>syn</i> > <i>anti</i>	<i>syn</i> > <i>anti</i>
Electrostatic interaction	<i>syn</i> > <i>anti</i>	<i>anti</i> > <i>syn</i>

The generally accepted concerted mechanism of the S_N2' reaction has been questioned repeatedly. Dewar published a interesting study, casting a different light on the S_N2' reaction [59]. The author pointed out, that most reactions can be considered to be of the one-bond type, meaning that one bond after the other is made or broken, step wise. The only reactions that were considered to involve a synchronous multibond mechanism were the pericyclic reactions “allowed” by the Woodward-Hoffmann rules and the S_N2' and E2 reactions. This predominance of one-bond reaction mechanisms is unusual and may be an indicator that there is a factor making synchronous multi-bond reactions unfavorable. Experiments performed in Dewar’s laboratories gave the authors reason to believe that the S_Ni' reaction is actually a stepwise process.

Based on theoretical considerations, Dewar proposed a reaction pathway for the S_N2' reaction of chloride ion on 1-chloro-2-propen and concluded that major weakening of the carbon-nucleofuge bond does not need to precede the addition of the nucleophile to the carbon-carbon double bond.

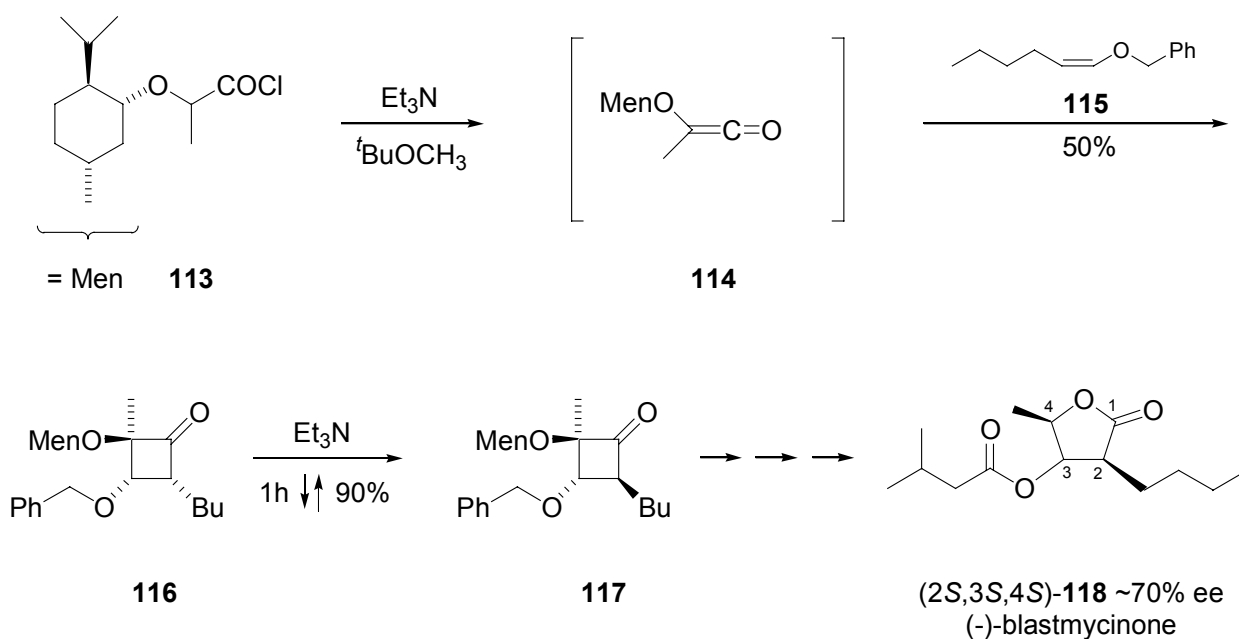
4.1.3 Synthetic routes leading to optically active cyclobutanones

During research on the stereoselective synthesis of chiral α -disubstituted β -hydroxy esters (*S,S*)-**109**, Fráter et al. reported a new stereoselective synthesis of cyclobutanones by an S_Ni reaction (intramolecular, nucleophilic substitution) [60], *Scheme 34*. Compound (*R*)-**110** was converted to cyclobutanone (*S*)-**111** and oxetane (*R*)-**112**. These findings constitute a method to access chiral cyclobutane structures, bearing alkyl substituents.



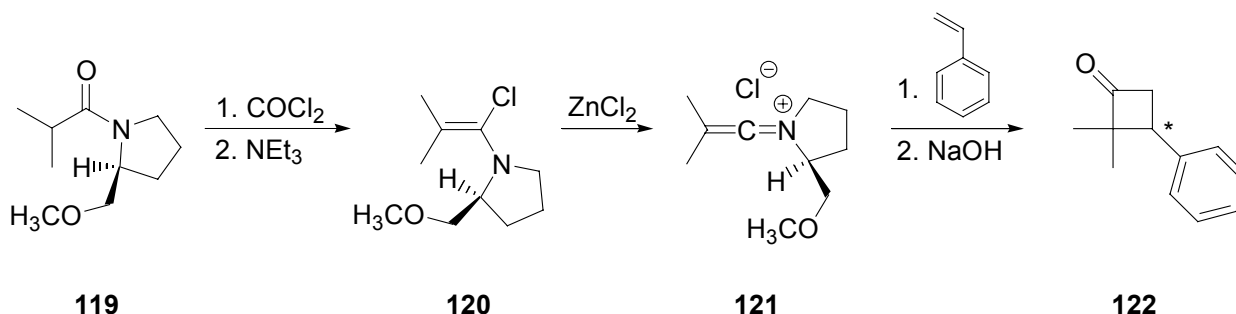
Scheme 34. Cyclobutanone and oxetane through S_Ni ring closure by Fráter et al.

In a later publication Fráter et al. reported a [2+2] addition of optically active ketene **114** to (*Z*)-olefins leading to optically active cyclobutanones [61]. The authors applied this new method in the synthesis of (-)-blastmycinone (*2S,3S,4S*)-**118**, *Scheme 35*. Addition of ketene **114**, derived from the acyl chloride **113**, to (*Z*)-ethyl propenyl ether **115** led to the kinetically controlled product **116**. Refluxing in Et_3N converted **116** to the thermodynamic mixture of **117** and **116** in a 9:1 ratio.



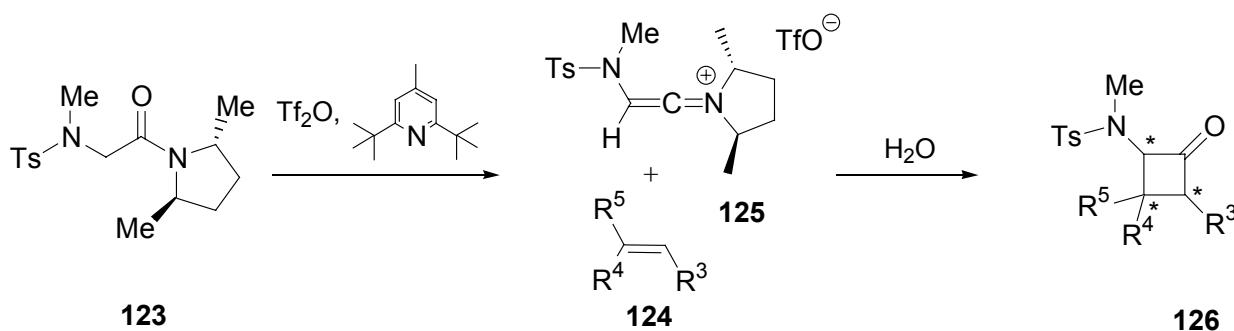
Scheme 35. Diastereoselective cyclobutanone synthesis through [2+2] addition of optically active ketenes to olefins, by Fráter et al.

Another efficient synthesis of cyclobutanones involves the [2+2] addition of keteniminium salts to olefins following a procedure by Ghosez [62], *Scheme 36*. Based on this method, the authors reported preliminary results from an asymmetric cyclobutanone synthesis using keteniminium salts derived from optically active amines [63]. Addition of **121** to styrene led to **122** in 55% yield and 80% ee.



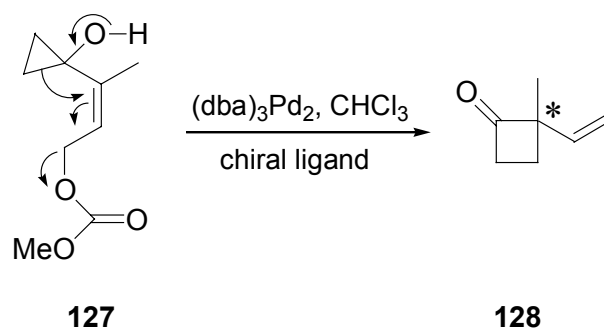
Scheme 36. Diastereoselective cyclobutanone synthesis, by Ghosez et al.

The authors then extended their research to the reaction of olefins **124** with optically active keteniminium salts **125** derived from *N*-tosylsarcosinamide **123**, *Scheme 37*. The electron withdrawing *N*-TsMe group was found to ensure the regioselective Bayer-Villiger oxidation of the resulting cyclobutanone thereby generating a masked aldehyde group in the product. The reaction formally amounts to the regio- and stereoselective attachment of a carboxylic and a carbonyl group to an unactivated olefin. To avoid the formation of diastereomeric mixtures of the keteniminium salt **125**, the authors used the C2-symmetric 2,5-dimethylpyrrolidine instead of methoxy methylpyrrolidine (*Scheme 36*) as the optically active amine [64].



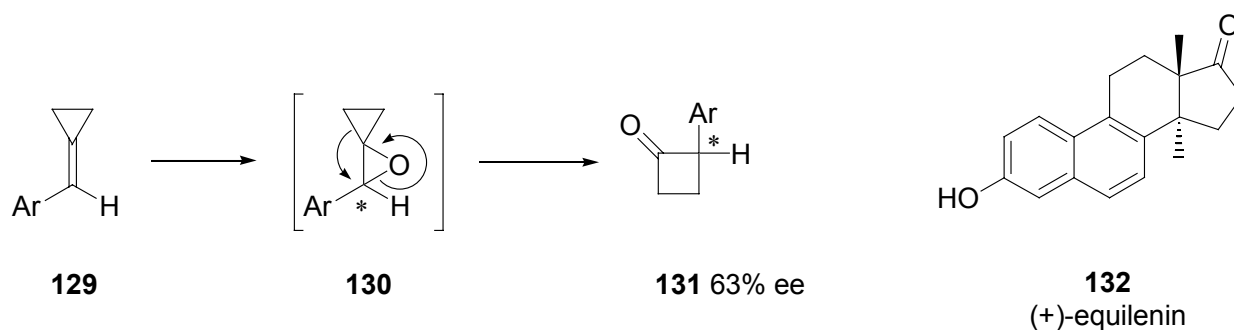
Scheme 37. Synthesis of chiral cyclobutanones by Ghosez et al.

Only a few other methods for the enantioselective preparation of cyclobutanones can be found in the literature. Trost et al. reported a synthesis of chiral cyclobutanones **128**, involving an asymmetric Wagner-Meerwein shift in compounds of type **127** [65], *Scheme 38*.



Scheme 38. Chiral cyclobutanones by Trost et al.

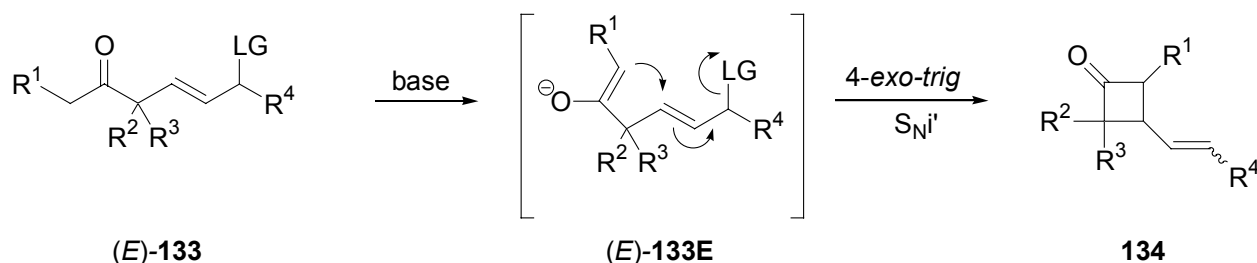
Asymmetric epoxidation of cyclopropylidene derivatives **129**, followed by an in-situ cascade ring expansion of the intermediate **130**, leads to the optically active cyclobutanones **131**, *Scheme 39*. This reaction was reported by Ihara et al. in the total synthesis of (+)-*equilenin* **132** [66].



Scheme 39. Chiral cyclobutanone by Ihara et al.

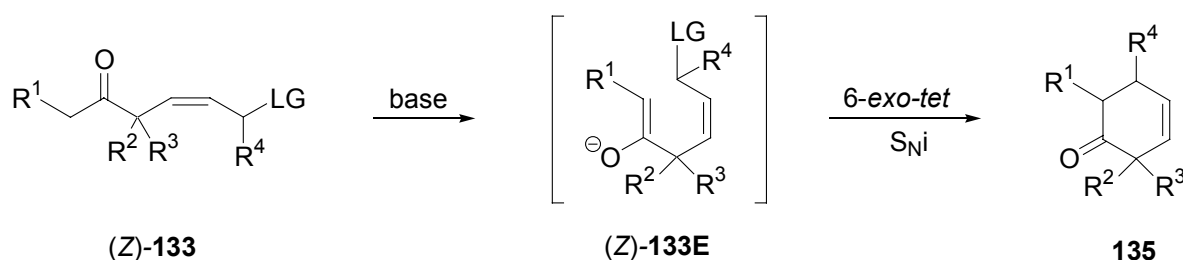
4.2 Objectives

In theory, it is possible to perform the S_{Ni}' reaction, in a system of type (*E*)-**133**, *Scheme 40*. S_{Ni}' ring closure of (*E*)-**133E**¹⁹ will lead to 4-vinyl substituted cyclobutanones **134**. It was the objective of this research to investigate the scopes and limitations of the S_{Ni}' reaction in the synthesis of four member rings.



*Scheme 40. Cyclobutanones by the S_{Ni}' , 4-*exo-trig* ring closure reaction.*

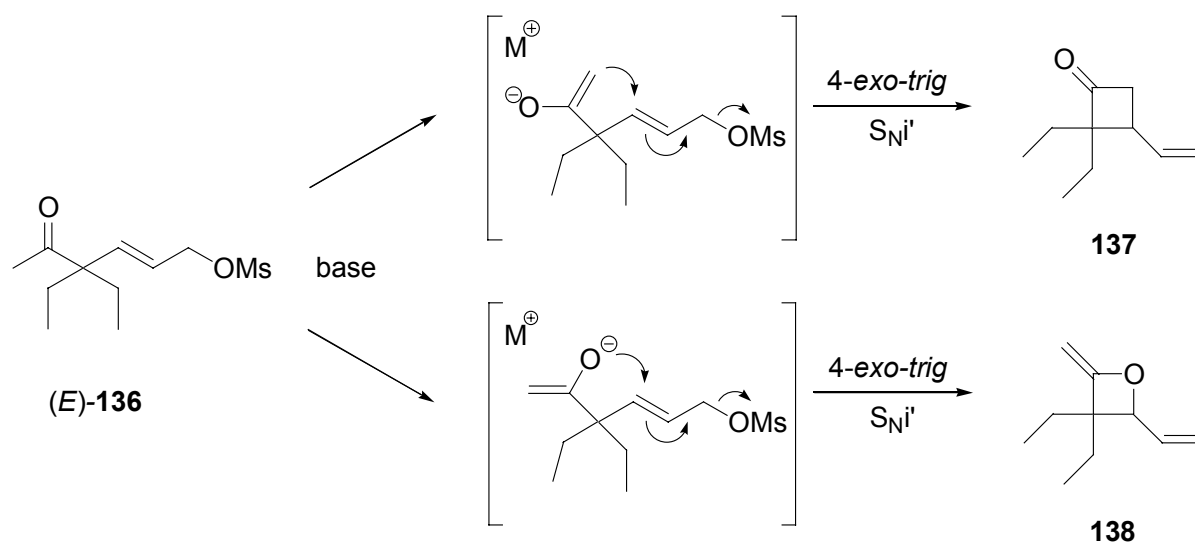
Several requirements must be met for this reaction to proceed. According to the Baldwin rules of ring closure the 4-*exo-trig* mechanism, illustrated in *Scheme 40*, is a favoured process [67]. The double bond in **133** must have (*E*)-configuration, to prevent the reaction from following the allowed 6-*exo-tet* mechanism, leading to six member rings **135**, *Scheme 41*.



*Scheme 41. 6-*Exo-tet* ring closure leading to six member rings.*

The general feasibility and chemoselectivity of the S_{Ni}' cyclobutanone synthesis can be explored by studying compound (*E*)-**136**, leading to cyclobutanone **137** and/or oxetane **138** upon S_{Ni}' ring closure, *Scheme 42*. The introduction of the two ethyl groups in 3-position is advantageous to maintain a sufficiently high molecular weight, facilitating the handling of the products. Two identical substituents in α -position make the formation of diastereomers at this stereogenic center impossible.

¹⁹ Enolates are indicated with the number of the parent compound bearing the appendix E.



Scheme 42. Cyclobutanone vs. oxetane formation in the 4-*exo-trig* S_Ni' reaction.

Apart from the chemoselectivity of the reaction, it was of particular interest to determine whether the nucleophilic attack of the enolate on the allylic system takes place *syn* or *anti* with respect to the leaving group [45][46]. But the analysis of the reaction mechanism and transition state of the S_Ni' reaction leading to cyclobutanones requires more information than can be deduced from the cyclization of (E)-136. The introduction of a leaving group, defined by its absolute configuration as in compound (S)-(E)-139, allows to analyze these parameters by means of the Curtin-Hammett principle and the stereoelectronic characteristics of the S_Ni' reaction. The Curtin-Hammett principle discusses the effects a conformational equilibrium can have on a chemical reaction. First, assuming the enolate attacks the allylic system in *syn* fashion, (S)-(E)-139 can adopt *conformation 1* and *conformation 2*, as illustrated in Figure 22.

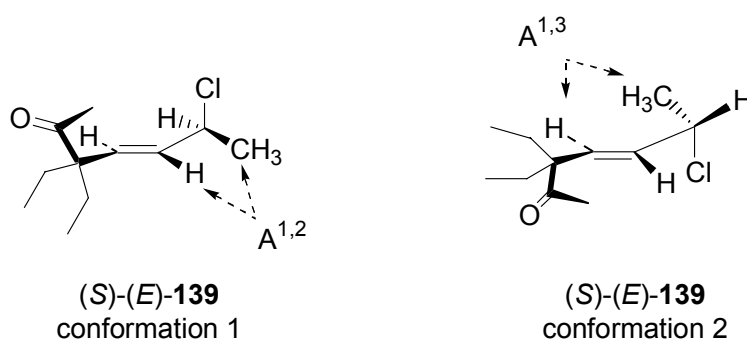


Figure 22. A^{1,2} and A^{1,3} strain in the allylic system of (S)-(E)-139.

Although *conformer 1* is lower in energy, because of a minor A^{1,3} strain, both conformers interchange by a rapid equilibrium, as the energy differences between them are very small (~12 kJ/mol) at reaction temperature, Figure 23. Therefore, the product ratio is not dependent on ΔG_c but rather on the difference between ΔG_a and ΔG_b , regardless of the ratio of the conformers. Performing the ring closure reaction at lower temperatures, should push the product ratio towards the (E)-isomer, requiring a lower activation energy.

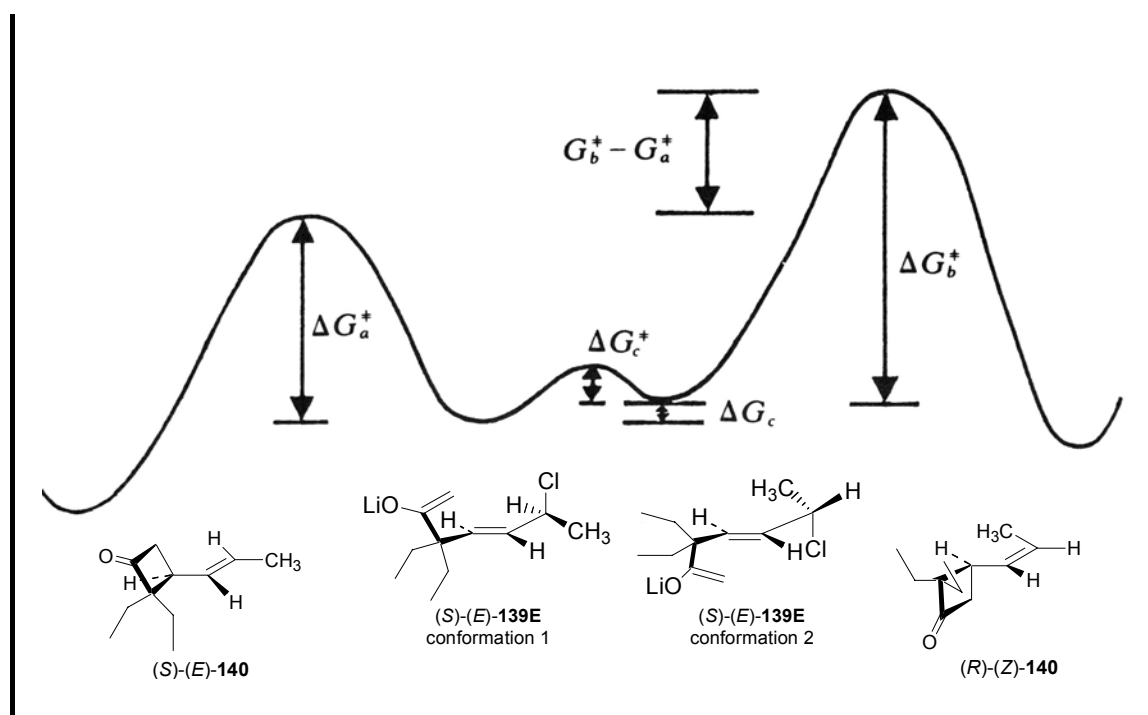
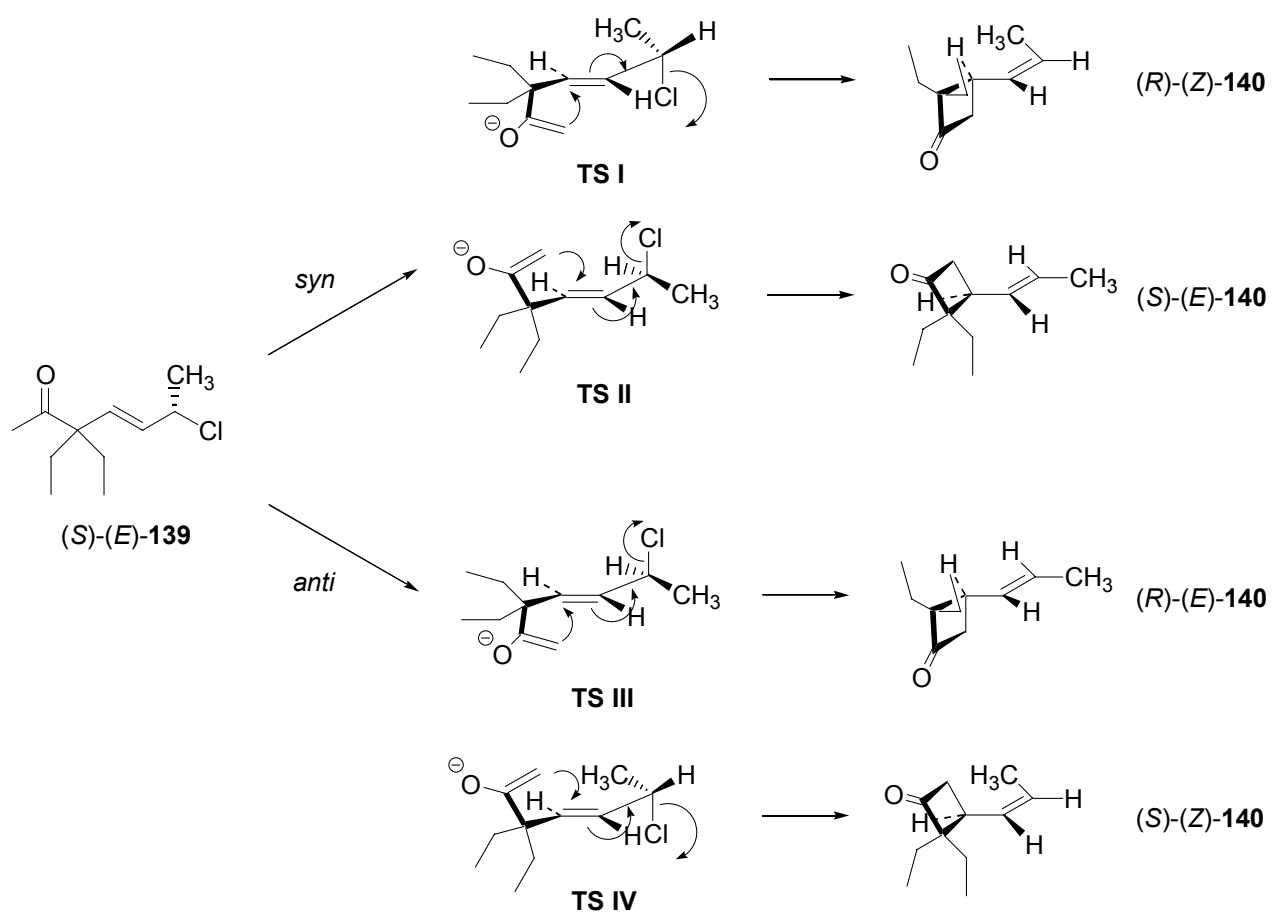


Figure 23. Evans-Polanyi plot for the syn-reactions of conformer 1 and 2 of (S)-(E)-139E.

The S_Ni' displacement may take place with *syn* or *anti* geometry in respect to the leaving group, the overall picture is depicted in *Scheme 43*. If the reaction follows a *syn* reaction path through transition state *TS II*, the energetically more stable *trans*-cyclobutanone (S)-(E)-140 will be formed. In the same way *anti* attack through *TS III* will lead to the *trans*-cyclobutanone (R)-(E)-140 with opposite absolute configuration at C(3) of the cyclobutane ring. The alternative *syn* attack proceeds through transition state *TS I* and will lead to *cis*-cyclobutanone (R)-(Z)-140. Similarly, the alternative *anti* displacement through *TS IV* will lead to *cis*-cyclobutanone (S)-(Z)-140. *Trans*-cyclobutanone (E)-140 resulting from either *syn* or *anti* attack and *cis*-cyclobutanone (Z)-140 formed by either mechanistic route are expected to possess the opposite absolute configuration. Therefore each of the four possible mechanisms will give rise to one distinct stereoisomer of 140. Separation of (E)-140 and (Z)-140, followed by determination of the enantiomeric excess and absolute configuration of the individual products, will provide the conformational information needed to unambiguously determine which of the transition states, illustrated in *Scheme 43*, are in effect during the S_Ni' ring closure of (S)-(E)-139.

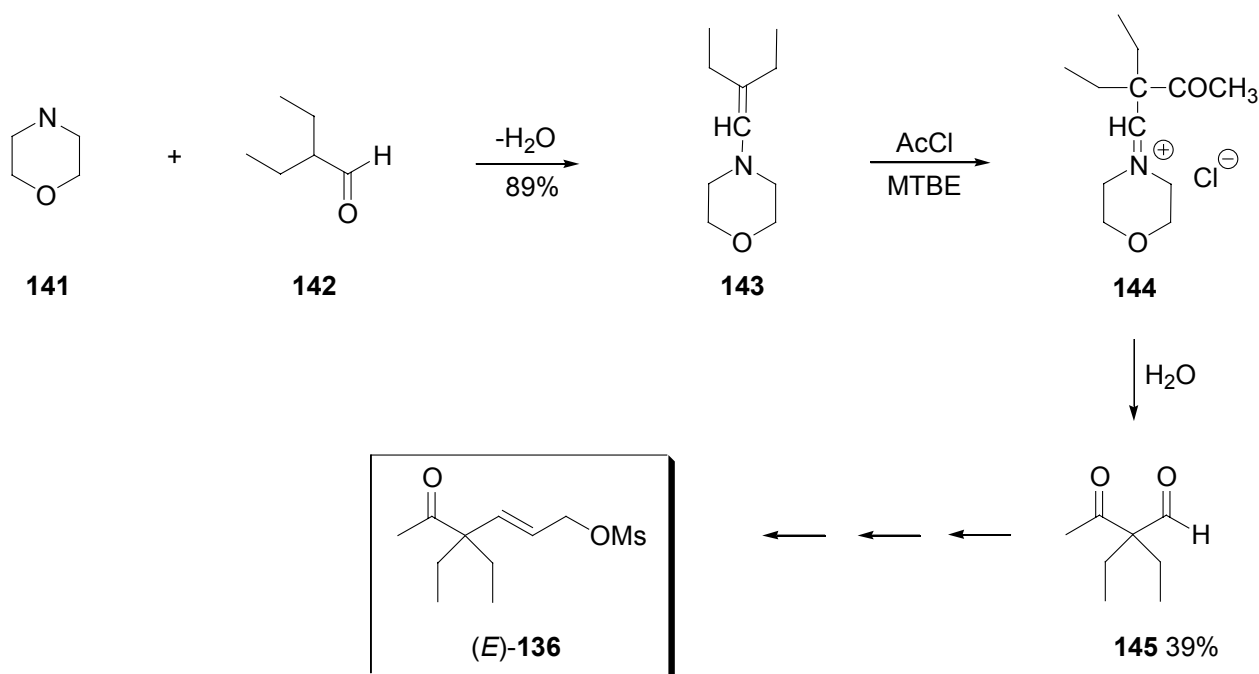


Scheme 43. Mechanistic pathways of the S_Ni' reaction leading to cyclobutanones.

4.3 Results and Discussion

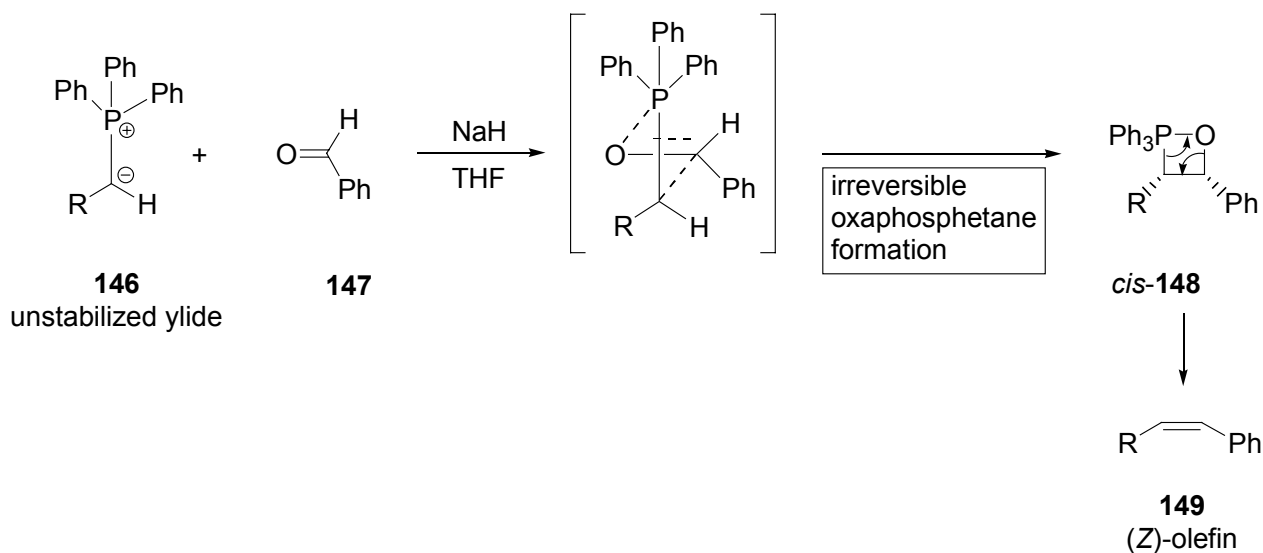
4.3.1 Synthetic intermediates

The key-intermediate in the synthesis of (*E*)-**136** and (*E*)-**139** is the keto-aldehyde **145**, *Scheme 44*. The Stork enamine synthesis of **143** followed by acetylation with acetic anhydride offered a convenient, but low yielding access to **145**. Following a procedure by Benzing, morpholine **141** and 2-ethyl-butyril aldehyde **142** were condensed in refluxing benzene using a Dean-Stark water separator [68]. The resulting enamine **143** was treated with acetyl chloride, followed by hydrolysis [69]. The resulting keto-aldehyde **145** was obtained in 39% over all yield. ^{13}C -NMR (75 MHz, CDCl_3) spectroscopy showed distinct carbonyl signals at 207.4 ppm for the ketone carbonyl carbon and at 202.3 ppm for the aldehyde carbonyl carbon.



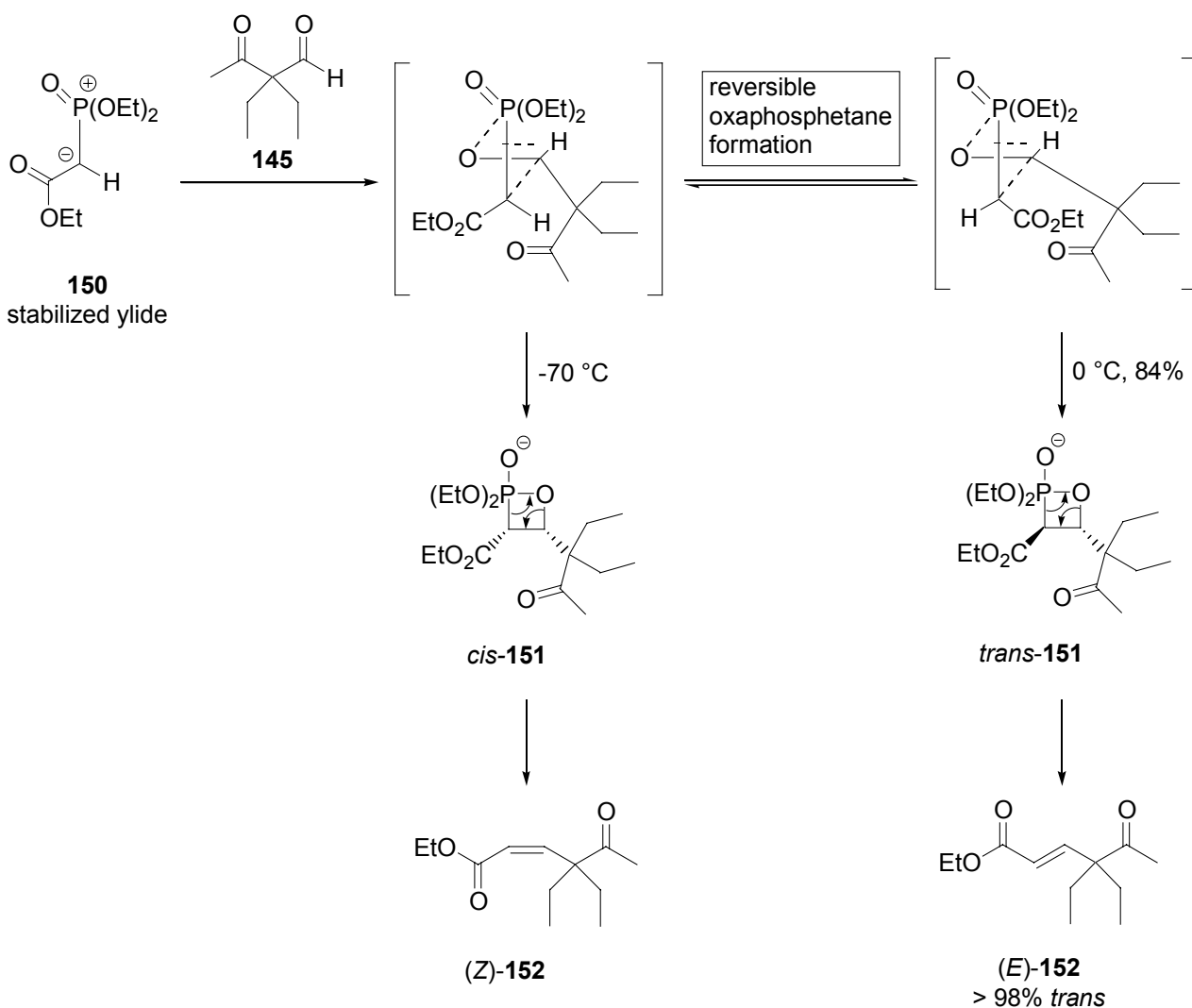
Scheme 44. Synthesis of the key-intermediate **145** by the Stork enamine synthesis.

The (*E*)-double bond in (*E*)-**136** can be constructed by a chemoselective Horner-Emmons reaction on the aldehyde moiety of **145**. In the Wittig and Horner-Emmons reaction a carbonyl compound **147** approaches a phosphonium ylide **146** perpendicular to the carbon-phosphorous double bond in a sense that the larger substituents point away from each other, leading to the oxaphosphetane *cis*-**148** which upon decomposition leads to the *cis*-olefin (*Z*)-**149**, *Scheme 45*.



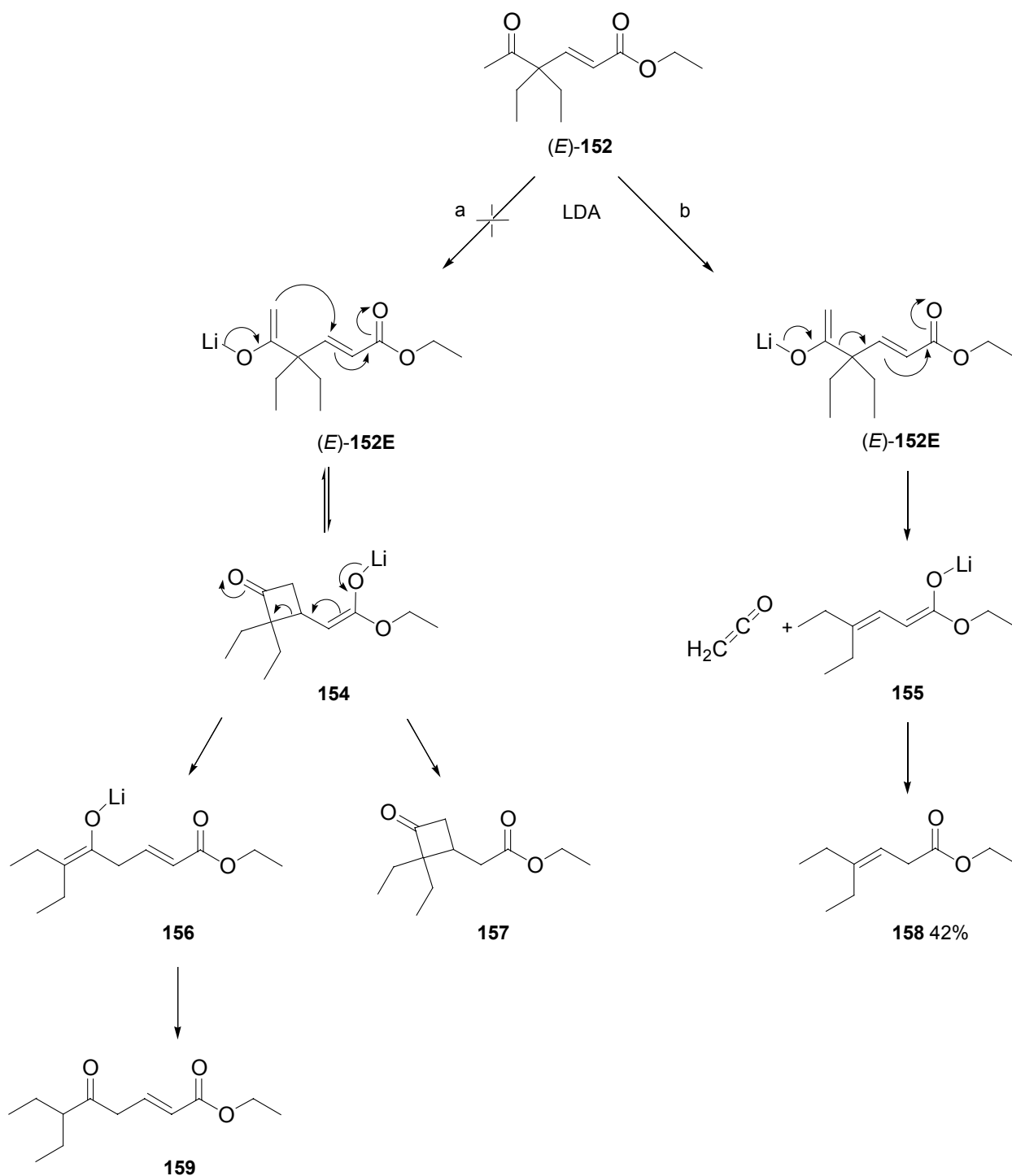
Scheme 45. (Z)- selectivity of unstabilized phosphonium ylides.

Stabilized ylides such as **150**, whose anion is stabilized by conjugation, are less reactive and the formation of the corresponding oxaphosphetanes is reversible, *Scheme 46*.



Scheme 46. (E)- and (Z)-selectivity of stabilized phosphonium ylides.

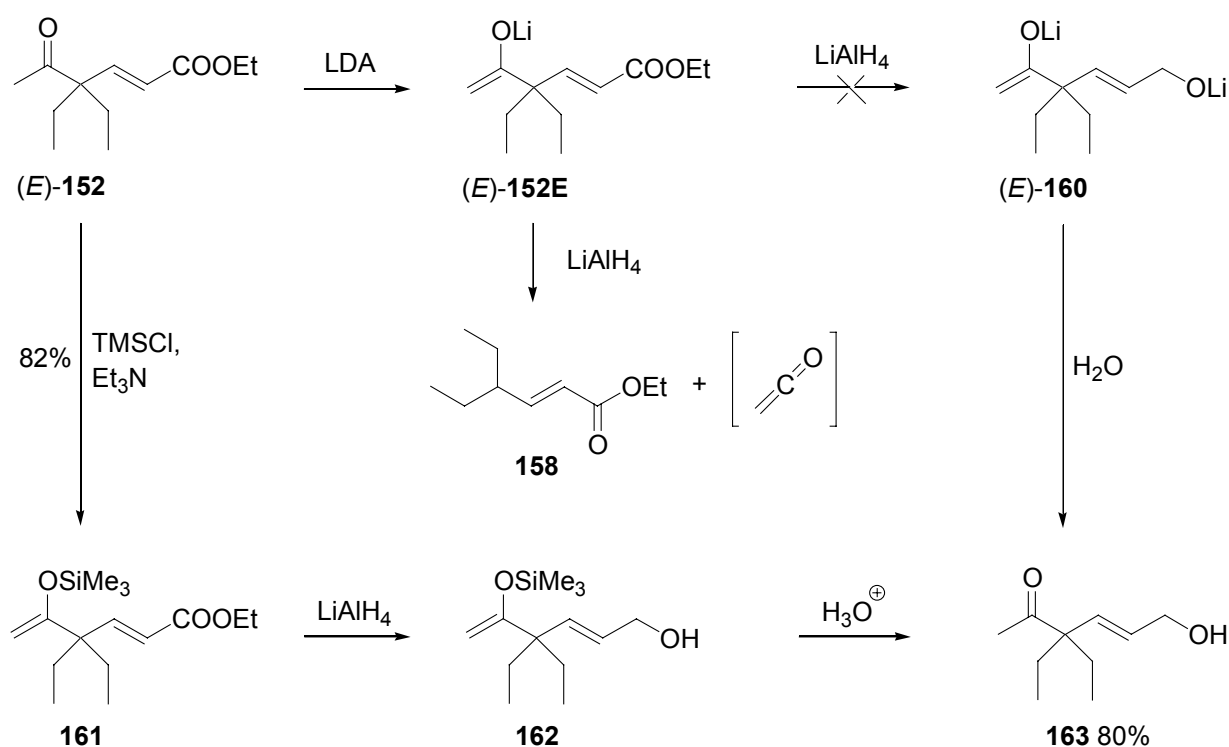
Due to the rapid ring opening and closing, *cis*-**151** will isomerize to the sterically more stable *trans*-**151** under thermodynamic conditions. At -70 °C the interchange between *cis*-**151** and *trans*-**151** is much slower and the formation of (*Z*)-**152** can be expected to be more pronounced. Reaction of **145** with phosphonate ester **150** at 0 °C led to (*E*)-**152** with 84% yield. The ¹H-NMR (300 MHz, CDCl₃) spectrum of (*E*)-**152** showed two clean doublets at 7.02 and 5.89 ppm resulting from the olefinic protons. The *J*-value of 16.4 Hz was a clear indicator of the exclusive (*E*)-configuration of the double bond.



Scheme 47. Possible reaction mechanisms for the cyclization of keto-ester (*E*)-**152**.

It was interesting to investigate whether (*E*)-**152** could undergo intramolecular Michael addition leading to the cyclobutanone **157**, *Scheme 47, path a*. First, the compound was converted to its enolate by deprotonation with LDA. However, the lithium enolate (*E*)-**152E** did not follow the reaction path (a) leading to the desired cyclobutanone, but followed *path b*, i.e. the formation of the intermediate enolate **155** via the tentative cleavage of a ketene. After work-up, the β,γ -unsaturated ester **158** was isolated in 42% yield. $^1\text{H-NMR}$ (300 MHz, CDCl_3) showed a complex signal at 5.24 ppm, resulting from the single vinylic proton, and two singlets at 1.67 and 1.56 ppm resulting from the protons of the terminal methyl groups. The retro-Michael product **159** could not be identified in the crude product mixture, indicating that no cyclobutanone intermediates were formed.

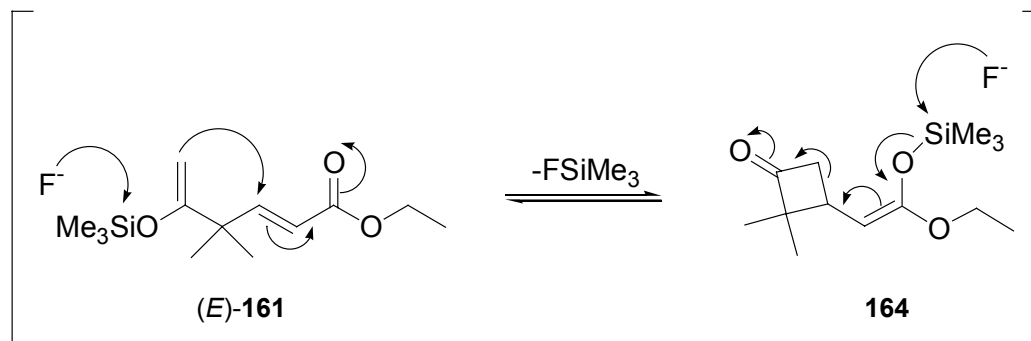
The chemoselective reduction of the ester group in (*E*)-**152** was attempted by protecting the ketone function as lithium enolate, followed by in-situ reduction of the ester group with LiAlH_4 [60], *Scheme 48*. It was found that the intermediate ketone enolate (*E*)-**152E** underwent fragmentation leading to **158** before reacting with LiAlH_4 . Conversion of (*E*)-**152E** to the silyl-enol ether (*E*)-**161**, followed by reduction of the ester group with LiAlH_4 , led to the ketone protected intermediate (*E*)-**162**, under anhydrous work-up conditions. If the reaction mixture was washed with water during the work-up procedure, the deprotected keto-alcohol (*E*)-**163** was obtained directly.



Scheme 48. Chemoselective reduction of the ester function in keto-ester (*E*)-**152**.

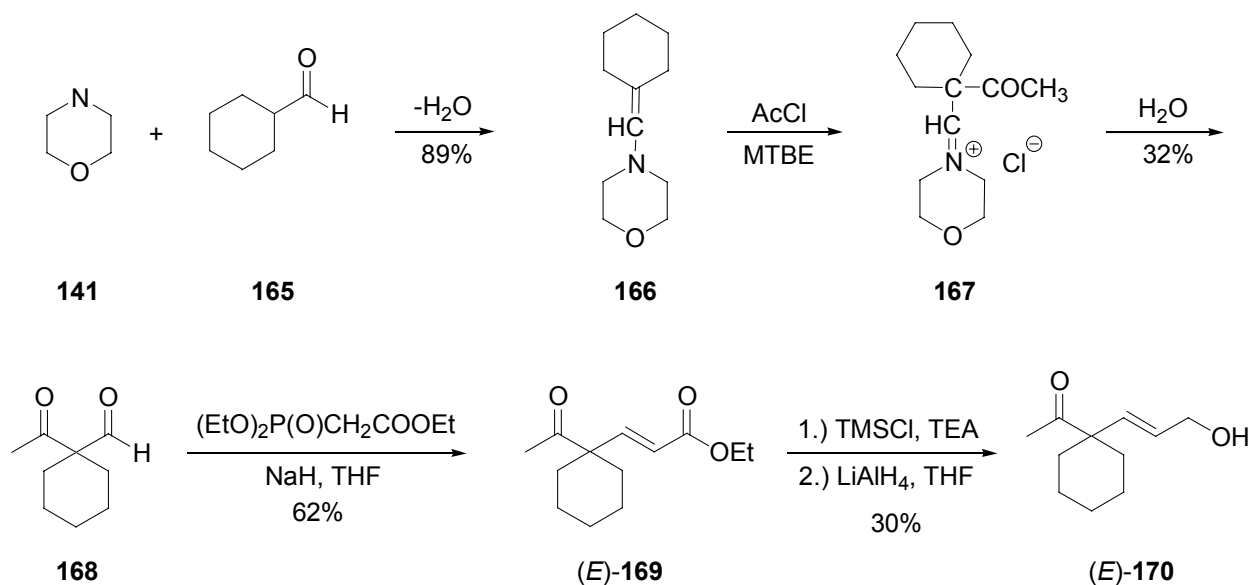
The Mukaiyama-aldoladdition involves the addition of aldehydes to silyl-enol ethers catalyzed by Lewis-acids, usually TiCl_4 [70]. The reaction can also be catalyzed with tetrabutyl-ammonium fluoride, as described by Nakamura [71]. When (*E*)-**161** is treated either way reversible cyclization

could occur to give **164**, *Scheme 49*. Experimental results showed no evidence for this equilibrium. Gradual deprotection of the ketone function by trace amounts of water was the only reaction observed.



Scheme 49. Fluoride ion catalyzed S_Ni' reaction by Nakamura et al.

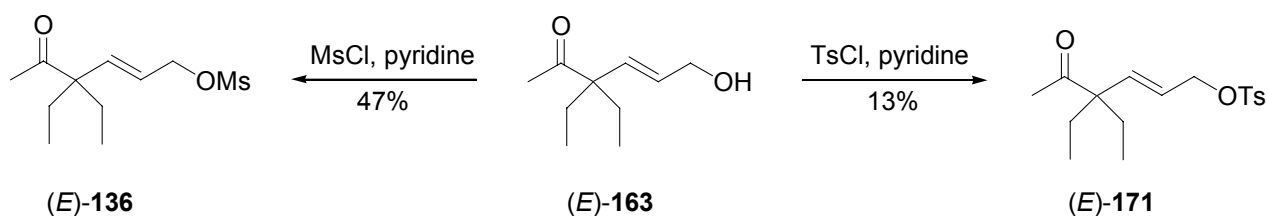
Precursor (*E*)-**170**, containing a cyclohexane ring in place of the geminal diethyl groups in (*E*)-**163**, was prepared in a similar fashion, *Scheme 50*. Stork enamine synthesis with cyclohexane carbaldehyde **165**, followed by acetylation with AcCl, led to the intermediate keto-aldehyde **168**. Horner-Evans-olefination and selective reduction of the ester group afforded (*E*)-**170**.



Scheme 50. Synthesis of (*E*)-**170** containing a cyclohexane ring.

Cyclobutanone formation through S_Ni' ring closure

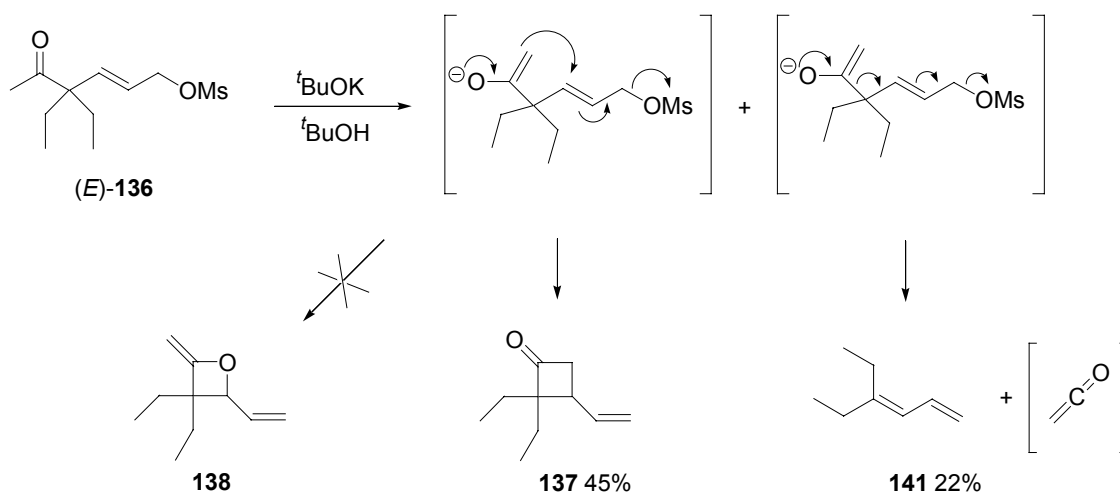
The attempt to convert (*E*)-**163** into the corresponding toluene sulfonate (*E*)-**171** was not satisfactory, *Scheme 51*. Upon treatment with toluenesulfonyl chloride (TsCl) in pyridine, (*E*)-**171** was isolated in low yield (13%).



Scheme 51. Synthesis of methanesulfonyl- and toluenesulfonyl-ester precursors.

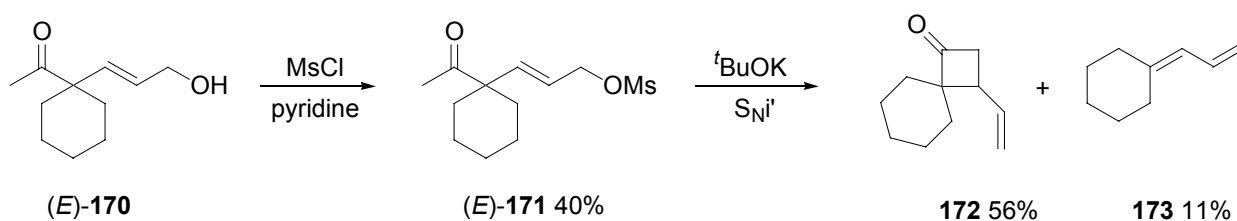
$^1\text{H-NMR}$ (300 MHz, CDCl_3) spectroscopy showed two distinct doublets of doublets at 7.71 ppm ($J = 23.7, 8.4$ Hz) and 6.72 ppm ($J = 11.4, 7.8$ Hz) resulting from each pair of protons across the aromatic ring of the toluene sulfonate group. The toluene sulfonate ion peak was observed at 155 (14%) m/z in the EI-MS spectrum. Treatment of $(E)\text{-163}$ with methanesulfonyl chloride in pyridine led to the mesylate $(E)\text{-136}$ with higher yield (47%), *Scheme 51*. The sharp singlet from the methane sulfonate methyl protons observed at 2.27 ppm in the $^1\text{H-NMR}$ (300 MHz, CDCl_3) spectrum, down field from the singlet resulting from the acetyl-methyl protons at 1.75 ppm, was a clear indicator that $(E)\text{-136}$ had been isolated.

Treatment of $(E)\text{-136}$ with 5% excess $t\text{BuOK}$ in THF led to cyclobutanone **137** in 45% yield, *Scheme 52*. Comparison of the IR-spectrum of **137** with the original IR-spectrum recorded from $(S)\text{-111}$ (*Chapter 4.1.3, Scheme 34*) showed that the strong signal at 1769 cm^{-1} , resulting from the cyclobutanone carbonyl vibrations, is in good agreement with the signal at 1780 cm^{-1} observed in the IR-spectrum of $(S)\text{-111}$ [60]. A spot with an R_f value of 0.6 on TLC, showing activity towards KMnO_4 and no fluorescence under UV-light, indicated the presence of the formal “ketene elimination” product **141**. No oxetane **138** was identified.



Scheme 52. Cyclobutanones through S_{Ni}' reaction of mesylate $(E)\text{-136}$.

In a similar fashion $(E)\text{-170}$ was converted to the mesylate $(E)\text{-171}$ by the same procedure and treated with 1M $t\text{BuOK}$ in $t\text{BuOH}$, *Scheme 53*. The S_{Ni}' reaction took place smoothly leading to a mixture of cyclobutanone **172** and ketene elimination product **173**.



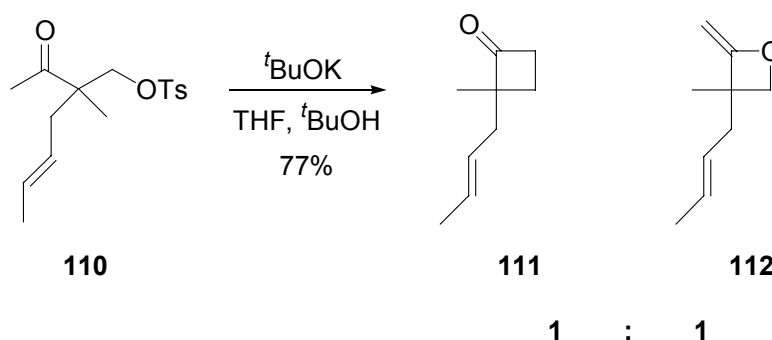
Scheme 53. S_Ni' reaction leading to spiro cyclobutanones.

Cyclobutanone **172** showed a strong signal at 1769 cm^{-1} in the IR-spectrum, indicating the presence of a cyclobutanone carbonyl group. By-product **173** was identified by GC/MS. The molecular ion at m/z 122 (40%) and the $[M-C_3H_4]^+$ peak at m/z 79 (100%) were good indicators for the presence of **173**. Again, no oxetane was identified in the reaction mixture.

The S_Ni' reaction of the two model compounds (E)-**136** and (E)-**171** lead to similar results which allowed the conclusion that cyclobutanones with different substitution patterns can principally be synthesized by this route.

4.3.3 Cyclobutanone vs. oxetane, the HSAB theory

In 1984 Fráter et al. reported, that compound **110** undergoes a S_Ni ring closure upon treatment with base, leading to a 1:1 mixture of the corresponding cyclobutanone **111** and oxetane **112** [60], *Scheme 54* and *Chapter 4.1.3, Scheme 34*.



Scheme 54. O- vs. C-nucleophilicity in the S_Ni reaction.

The S_Ni' model reactions on the other hand, did not lead to any detectable amount of oxetane **138** resulting from nucleophilic attack of the oxygen atom, *Scheme 52*. The observed trend can be rationalized by applying the hard-soft acid base (HSAB) rule, originally proposed by Pearson in 1963 [72]. He stated, that every atom possessing an empty p-orbital, capable of accepting electrons, is to be considered a Lewis acid and every atom possessing a pair of unshared electrons capable of making a covalent bond is a Lewis base. He categorized a series of such acids and bases into groups of comparable “hardness” and “softness” and stated, based on experimental and mathematical evidence, that complexes between acids and bases of comparable hardness are favored. Based on the conclusions drawn by Pearson, Ho published a review in 1985 applying the HSAB theory to different types of organic reactions involving ambident substrates [73]. For the

chemoselectivity of the S_Ni' ring closure of the ambident enolate (*E*)-**136E**, it can be predicted that the oxygen anion is a harder base than the carbanion and therefore will prefer to bind to a hard acid, *Figure 24*.

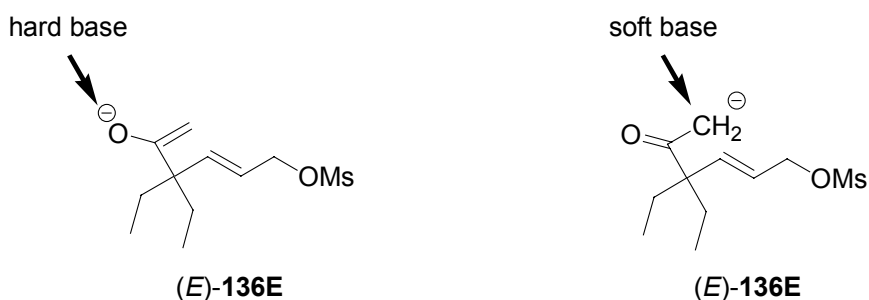


Figure 24. HSAB considerations in the S_Ni' reaction.

As far as the “carbonium-type” acid is concerned, it is not clear whether the olefinic carbon in (*E*)-**136E** or the alkyl carbon in **110E** acts as the harder acid, *Figure 25*. It can be assumed however, that delocalization of charge in the allylic system constitutes softer acid properties and is therefore prone to be attacked by the soft nucleophilic carbon rather than the hard oxygen anion.

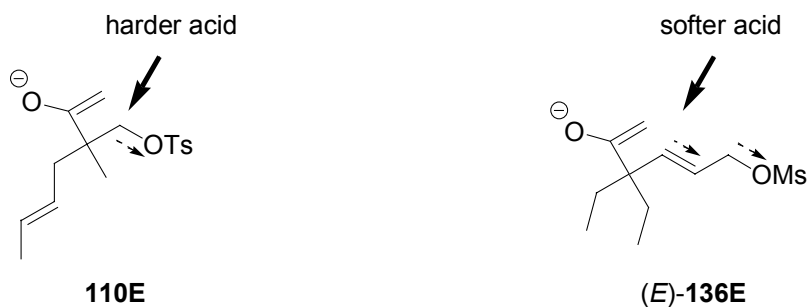
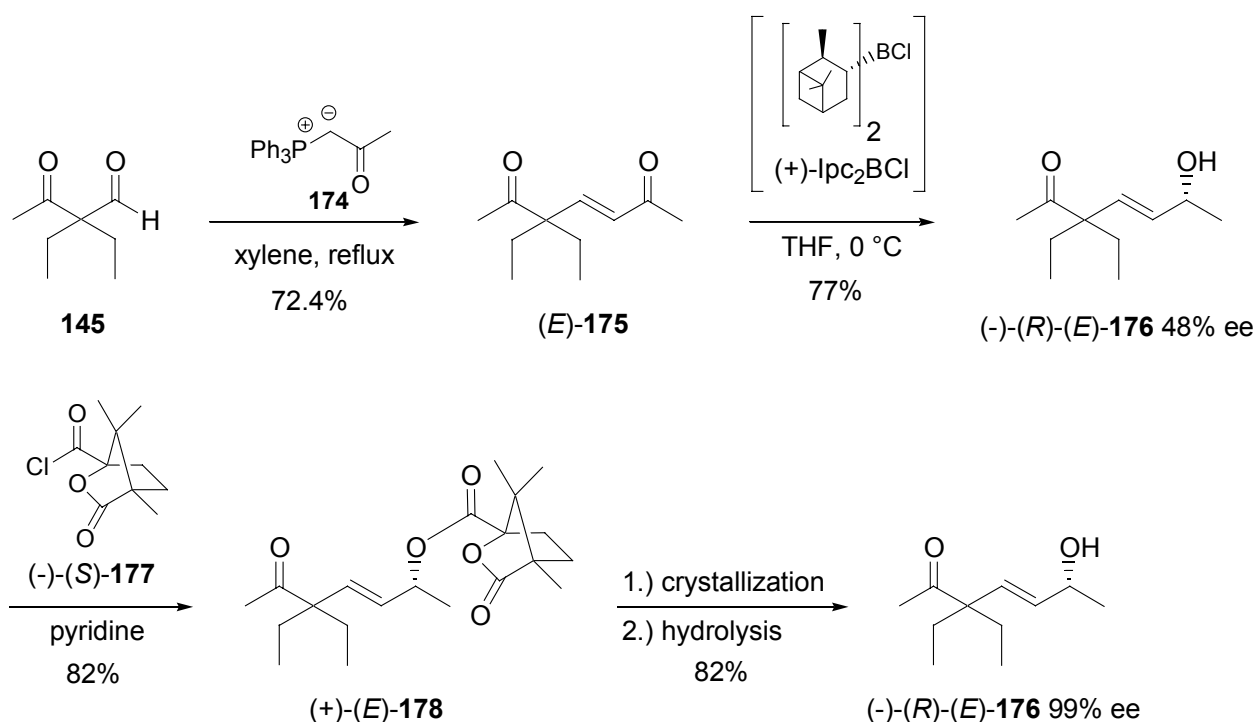


Figure 25. HSAB effects in alkyl vs. allylic systems.

The HSAB theory offers a possible explanation why the formation of the oxetane **138** was not detected in the product of the S_Ni' ring closure reaction of (*E*)-**136**.

4.3.4 Synthesis of the S_{Ni}' precursor (*S*)-(*E*)-139

Diketone (*E*)-**175** was prepared by Wittig reaction of the keto-aldehyde **145** with the stabilized phosphonium ylide **174**, leading selectively to (*E*)-configuration of the double bond in **175** (*Chapter 4.3, Scheme 46*), *Scheme 55*. The α,β -unsaturated ketone function was then reduced chemo- and enantioselectively by a modified Midland procedure using (+)-diisopinocampheylchloroborane ((+)-Ipc₂BCl), derived from (-)- α -pinene and BH₃·SMe₂ [74]. Because (-)-(*E*)-**176**²⁰ could only be obtained in 48% enantiomeric purity, the product was reacted with (-)-camphanoic acid chloride (-)-(*S*)-**177**, to give the solid camphanoate (+)-(*E*)-**178**. Selective crystallization from hexane/ether, led to the pure diastereomer. The presence of a single diastereomer was indicated by the clean doublet at 16.7 ppm $J = 6.6$ Hz in the ¹³C-NMR (100 MHz, CDCl₃) spectrum resulting from the geminal dimethyl group of the camphanoate moiety.



Scheme 55. Enantioselective synthesis of the hydroxy ketone (-)-(R)-(E)-**176**.

4.3.5 X-ray crystallography of the camphanoate derivative of (+)-(*E*)-178

A single crystal of camphanoate (+)-(*E*)-**178** was submitted for X-ray crystallography, *Figure 26*. The structure of (+)-(*E*)-**178** was solved and refined successfully. The crystallographic analysis showed that the sample was enantiomerically pure. Based on the known configuration of the (-)-(*S*)-camphanoate moiety, the quaternary center in (-)-(*E*)-**176** was determined to have (*R*)-configuration.

²⁰ For reasons of clarity and a better overview, the sign of the optical rotation is indicated at the beginning of the compound labels in this dissertation.

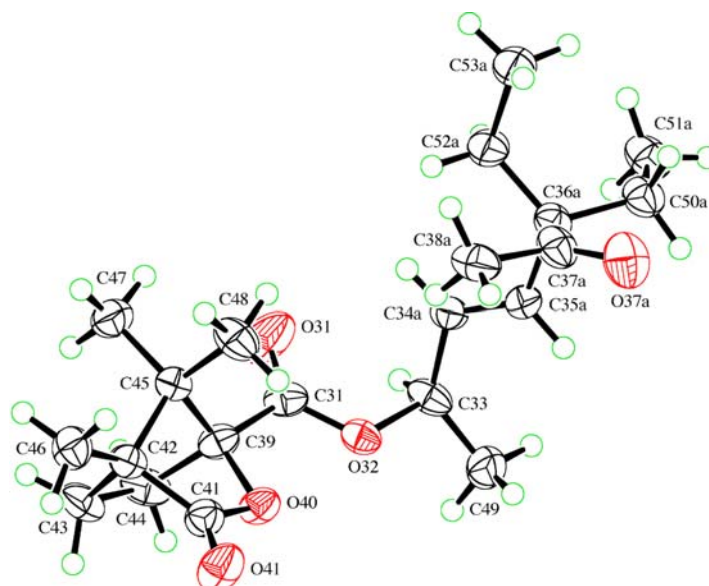
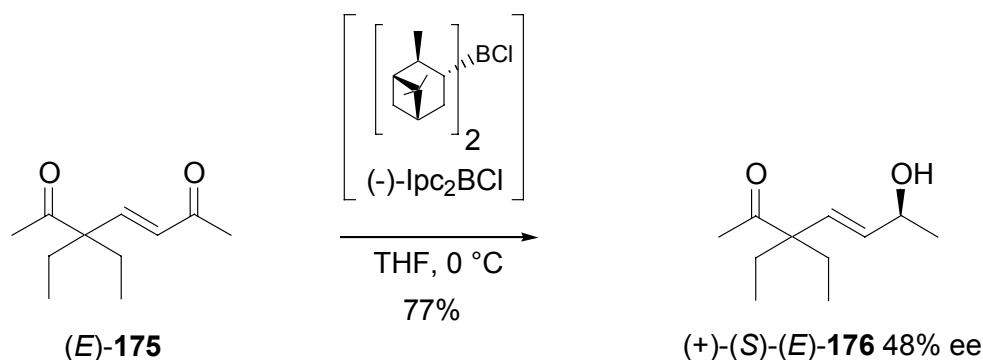


Figure 26. ORTEP plot of the camphanoate derivative of (+)-(E)-178.

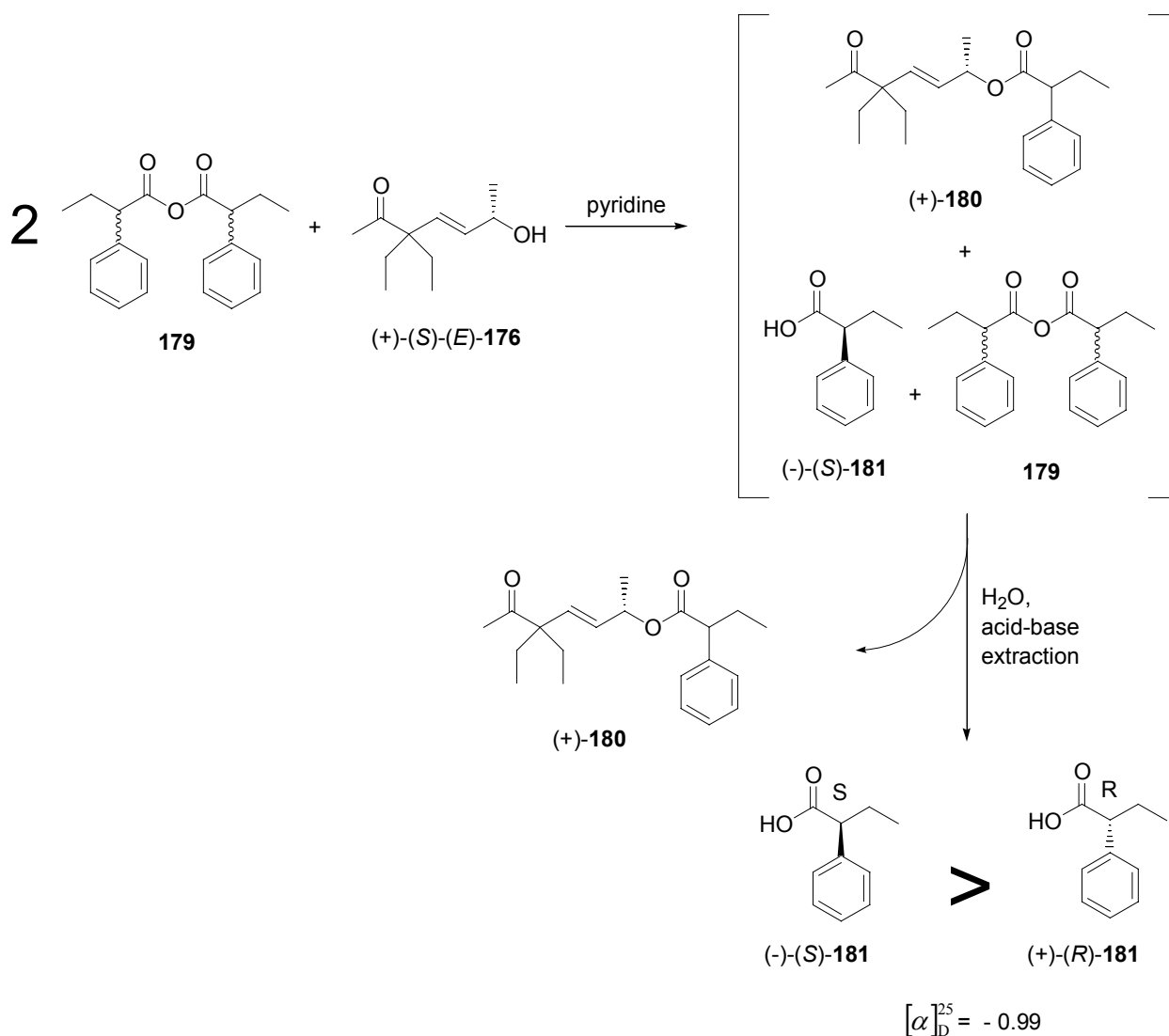
4.3.6 Determination of the absolute configuration of secondary alcohols by Horeau

The modified Midland procedure (*Scheme 55*) can also be performed with (-)-Ipc₂BCl derived from (+)- α -pinene, resulting in the formation of the other enantiomer (+)-(S)-(E)-176, *Scheme 56*.



Scheme 56. Synthesis of (+)-(S)-(E)-176 with (-)-Ipc₂BCl by Midland et al.

In order to confirm the absolute configuration of (-)-(R)-(E)-176, predicted by X-ray crystallography of the corresponding camphanoate (+)-(E)-178 (*Figure 26*), a chemical method was sought to determine the absolute configuration of its enantiomer (+)-(S)-(E)-176. Horeau developed an empirical method to determine the absolute configuration of secondary alcohols, based on the principal of kinetic resolution [75], *Scheme 57*.



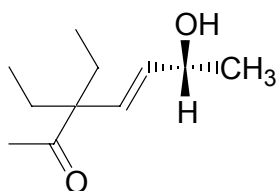
Scheme 57. Determination of the absolute configuration of (+)-(S)-(E)-176 by Horeau's empirical method.

An excess of optically inactive 2-phenylbutyric acid anhydride **179** (505 mg, 3 equiv.) was reacted with the enantiomerically enriched secondary alcohol (+)-(E)-**176** (100 mg, 47% ee) in pyridine. It does not matter that the anhydride is a mixture of (*R,R*)/(*S,S*) and (*R,S*) species: one of the chiral $\text{C}_6\text{H}_5\text{CH}(\text{C}_2\text{H}_5)\text{COO}^-$ moieties will react faster with the enriched enantiomer of the alcohol than its enantiomer. The sign of the optical rotation of the 2-phenylbutyric acid **181**, isolated after the hydrolysis of the excess anhydride **179**, can then be compared to experimental values in the literature allowing the determination of the absolute configuration of the original secondary alcohol with high probability. The reaction was complete after 15 h and measurement of the optical rotation of **181** (340 mg, 76%) gave a negative value of $[\alpha]_{\text{D}}^{25} = -0.99$.

Horeau performed a significant number of experiments with secondary alcohols of known configuration, to test his theory.

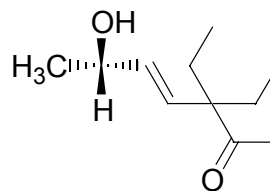
In all of the cases the absolute configuration of the secondary alcohol could be established precisely by his method. These results led Horeau to publish the following empirical rule:

If the resulting 2-phenylbutyric acid (181**) exhibits a *positive* optical rotation, then, if looking at the secondary alcohol in a horizontal Fischer projection, with the hydrogen pointing down and the hydroxyl group pointing up, the larger group is pointing to the left, *Figure 27*.**



(-)-(R)-(E)-176

(*R*)-configuration if optical rotation of 2-phenylbutyric acid **181** is *positive*.



(+)-(S)-(E)-176

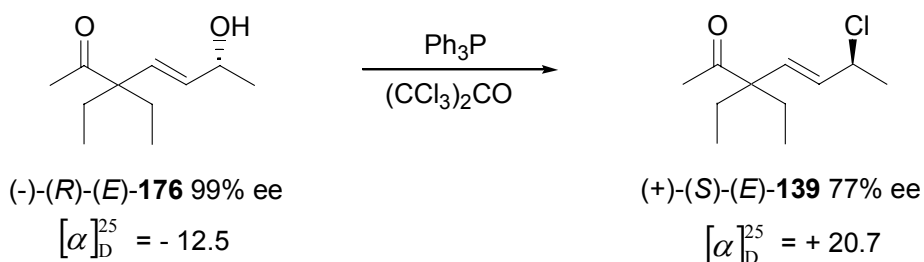
(*S*)-configuration if optical rotation of 2-phenylbutyric acid **181** is *negative*.

Figure 27. Interpretation of the results from Horeau's method.

Since the reaction of (+)-(S)-(E)-**176** with **179** led to 2-phenylbutyric acid with a *negative* optical rotation it can be concluded, according to the rule stated above, that the enriched enantiomer in (+)-(E)-**176** possesses (*S*)-configuration, as expected. The results obtained were comparable in yield, reaction time and intensity of optical rotation to the experiments reported by Horeau.

4.3.7 Searching for suitable leaving groups

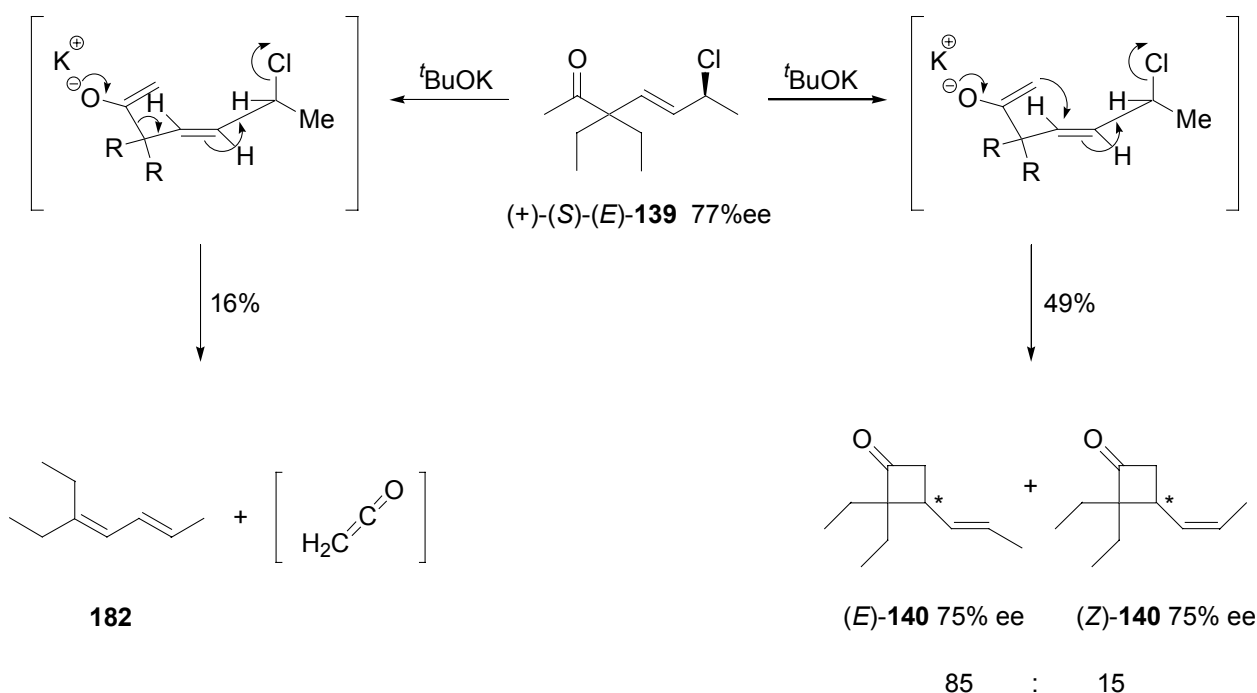
Several attempts to convert the hydroxyl group in (-)-(R)-(E)-**176** into a suitable leaving group failed. Treatment of (-)-(R)-(E)-**176** with methanesulfonic acid chloride in pyridine did not lead to the expected mesylate, but rather to S_N2 substitution of the hydroxyl group with Cl⁻, leading to (+)-(S)-(E)-**139** in low yield (~10%). Preliminary cyclization experiments showed that chloride ion was actually a suitable leaving group for the S_Ni' reaction. The chloro-ketone (+)-(S)-(E)-**139** could also be prepared directly from (-)-(R)-(E)-**176** following a stereoselective procedure by Magid et al. [76], *Scheme 58*. Nevertheless, some loss of enantiomeric purity was observed in product (+)-(S)-(E)-**139**.



Scheme 58. Stereoselective S_N2 displacement by Magid et al.

4.3.8 Chiral cyclobutanones through stereoselective S_Ni' reaction

Chloro-ketone (+)-(*S*)-(*E*)-**139** was cyclized by using 1M t BuOK in t BuOH at 0 °C following the procedure by Fráter et al [60], *Scheme 59*.



Scheme 59. S_Ni' reaction of chiral chloro-ketone (+)-(*S*)-(*E*)-**139**.

The reaction afforded a mixture of 85% (*E*)-**140** and 15% (*Z*)-**140** in 49% isolated yield together with 16% (GC) of the formal ketene elimination product **182**. The strong cyclobutanone carbonyl signal at 1768 cm^{-1} in the IR spectrum of (*E/Z*)-**140** suggested that the product possessed the cyclobutanone structure. Due to the volatility of **182**, it was lost during workup and short path distillation, a strongly UV active spot on TLC, however, was a good indicator that some diene **182** was formed during the reaction.

Chloroketone (+)-(*S*)-(*E*)-**139** and the resulting cyclobutanones (*E*)- and (*Z*)-**140** were analyzed by chiral gas chromatography, *Figure 28*. *Chromatogram a* shows the (*R*)- and (*S*)-enantiomer of (+)-(*E*)-**139** (77% ee) and *chromatogram b* illustrates the enantiomeric distribution of the (*E*)- and (*Z*)-isomers of **140** in a racemic mixture. Racemic (*E*)-**140** was prepared by replacing the modified Midland reduction of the diketone (*E*)-**175** (*Chapter 4.3.4, Scheme 56*) by a non-stereoselective reduction with diisobutylaluminum hydride (DIBAH). *Chromatogram c* represents the enantiomeric distribution of (*E*)- and (*Z*)-**140** in the crude product prepared from (+)-(*S*)-(*E*)-**139** (77% ee). The enantiomeric excess of the (*E*)- and (*Z*)-isomers in the optically active cyclobutanone **140** was found to be 75% for both isomers. This is a good indication, that the S_Ni' reaction proceeded with almost complete stereoselectivity.

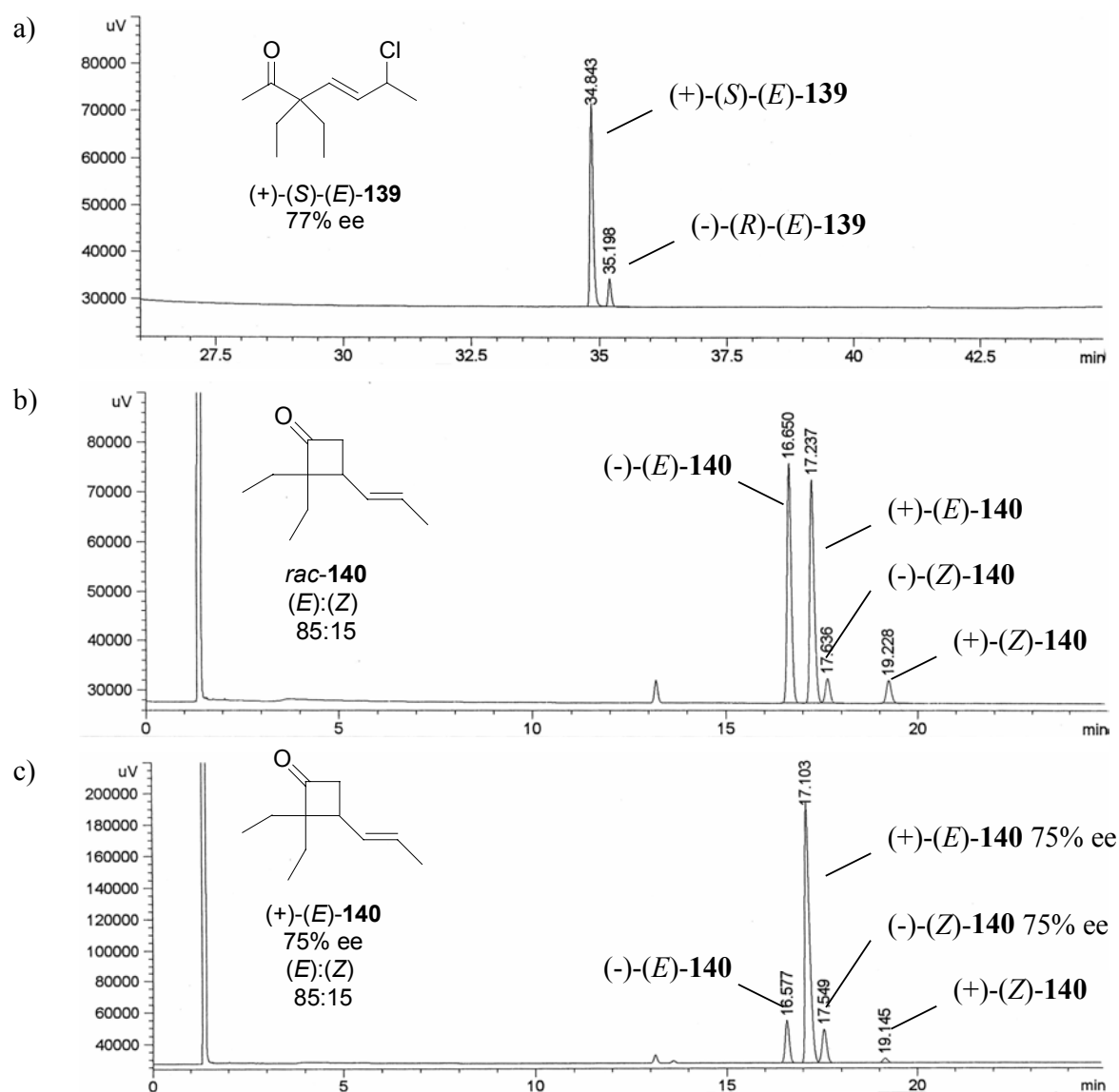
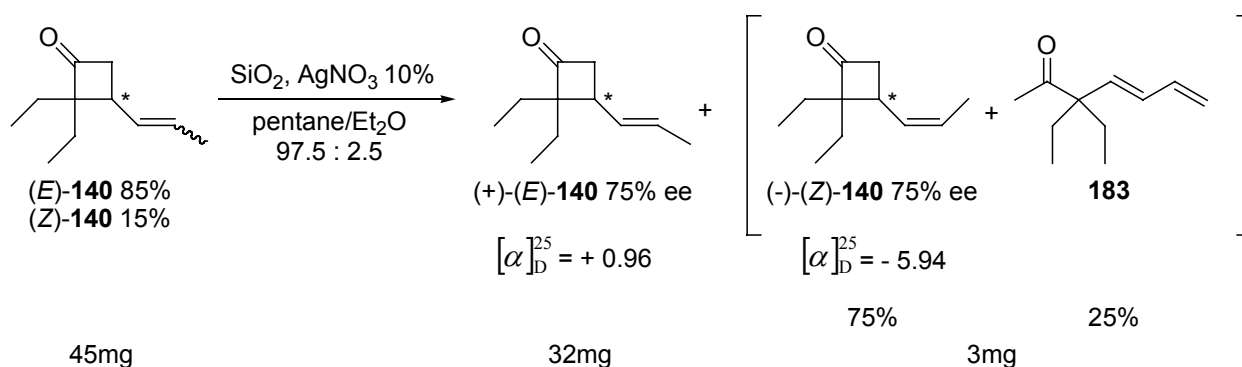


Figure 28. Analysis of the cyclobutanone products by chiral GC.

a) Chiral GC of the chloro-ketone (+)-(S)-(E)-139 (77% ee). b) Racemic cyclobutanone (E)- and (Z)-140. c) Optically active cyclobutanone from (+)-(S)-(E)-139 (77% ee).

To precisely analyze the S_N1' reaction mechanism, it was necessary to separate (+)-(E)-140 and (-)-(Z)-140 and determine the absolute configuration of both products, *Scheme 60*. The separation was accomplished by chromatography over silica gel impregnated $AgNO_3$, pentane/ Et_2O 97.5: 2.5 was used as the eluent. 2D-HSQC NMR spectroscopy of (+)-(E)-140 showed a single signal at 18 ppm, typical for a *trans*-methyl group on a double bond. Similarly, (-)-(Z)-140 showed a single signal at 13 ppm in the 2D-HSQC NMR spectrum, indicating the presence of a *cis*-methyl group on the double bond. Analysis of (-)-(Z)-140 by 1H -NMR (500 MHz, $CDCl_3$) spectroscopy revealed signals from olefinic protons at δ 6.2 (*m*, 1 H); 6.0 (*dd*, $J = 10.5, 16.0$ Hz, 1 H); 5.0 (*d*, $J = 15.0$ Hz, 1 H) and 5.06, 5.03 (*m*, 1H) and 5.1, 5.0 (*m*, 1H) indicating that (-)-(Z)-140 contained 25% of dehydrochlorination product **183**, that had gone undetected so far.



Scheme 60. Separation of $(+)\text{-(E)-}$ and $(-)\text{-(Z)-140}$ over AgNO₃ impregnated silica gel.

4.3.9 Absolute configuration of $(E)\text{-}$ and $(Z)\text{-cyclobutanones}$ with VCD and ROA

Vibrational Circular Dichroism (VCD) and RAMAN Optical Activity (ROA) spectroscopy are reliable tools for determining the absolute configuration of carbonyl compounds. Prof. W. Hug from the University of Fribourg offered to measure samples of $(+)\text{-(E)-140}$ and $(-)\text{-(Z)-140}$ on his RAMAN instrument and to perform the ab initio calculations required to provide profound evidence of the absolute configuration.

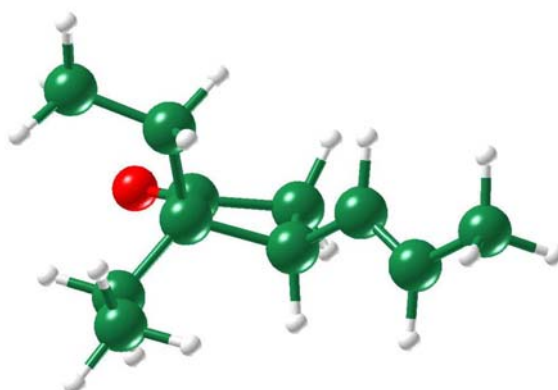


Figure 29. Lowest energy conformer of $(+)\text{-(S)-(E)-140}$.

The mathematical analysis revealed that the lowest energy conformer of $(+)\text{-(S)-(E)-140}$, illustrated in *Figure 29*, contributes 39% to the conformational equilibrium at room temperature. The red curve (a) in *Figure 30* represents the calculated spectrum of $(+)\text{-(S)-(E)-140}$, the five most abundant conformers were calculated separately and contribute to the simulated spectrum according to their percentage in the mixture. By comparing the signs of the peaks in the measured ROA spectrum (b) with those of the calculated spectrum for $(+)\text{-(S)-(E)-140}$ (a), it can be seen that the signals are of identical sign, indicating that S_{Ni}' ring closure of $(+)\text{-(S)-(E)-139}$ leads to $(+)\text{-(S)-(E)-140}$ possessing (S) -configuration at C(3).

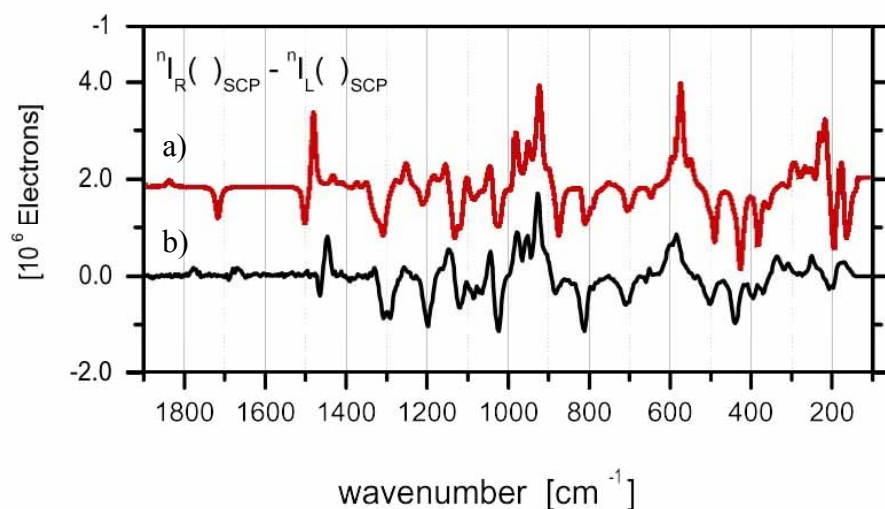


Figure 30. ROA spectra of (+)-(S)-(E)-140.

a) Calculated ROA spectrum for (+)-(S)-(E)-140. b) Experimental ROA spectrum of (+)-(S)-(E)-140.

Based on the mechanistic considerations discussed in *Chapter 4.2, Scheme 43*, the (Z)-cyclobutanone is expected to have the opposite absolute configuration at C(3) of the cyclobutanone ring compared to the (E)-cyclobutanone, assuming that the nucleophilic attack takes place stereoselectively. Superimposing the ROA spectrum of (+)-(S)-(E)-**140** and (-)-(Z)-**140** shows that most of the signals exhibit inversed polarity, indicating the presence of two opposite enantiomers, *Figure 31*. The small discrepancies in the signals are due to the different (E)/(Z)-configuration of the compounds and the strong positive signal at 1600-1700 cm^{-1} in the (-)-(R)-(Z)-**140** spectrum results from the contaminant **183** (*Scheme 60*).

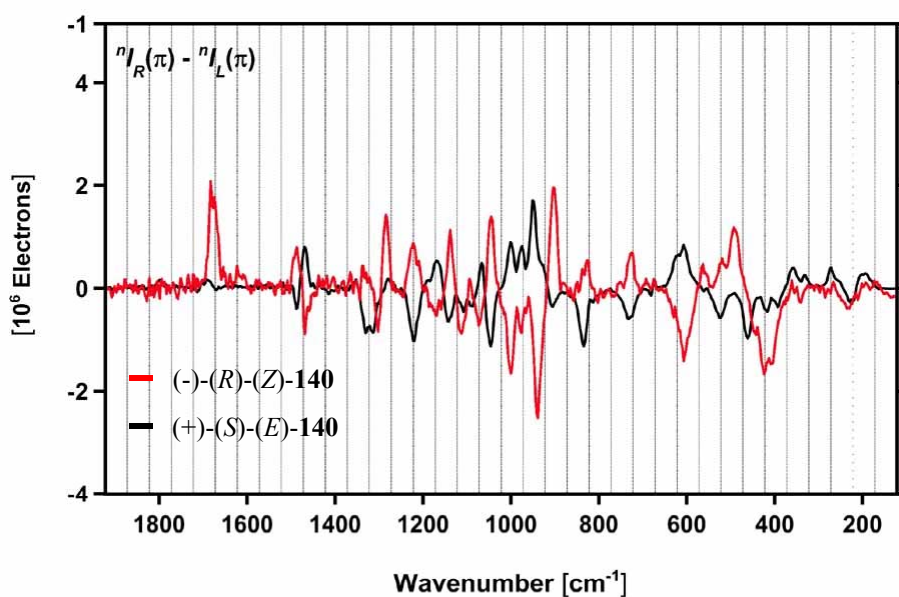


Figure 31. Superimposed experimental ROA spectra of (+)-(S)-(E)- and (-)-(R)-(Z)-140.

A sample of (+)-(*S*)-(*E*)-**140** was sent to Prof. E. Vass at the Eötvös-Loránd University in Budapest to verify the absolute configuration by “Vibrational Circular Dichroism” (VCD) spectroscopy, *Figure 32*. The spectrum was measured as neat liquid film between NaCl windows over a range of 1900-1200 cm^{-1} , with an average of 7200 scans and a resolution of 4 cm^{-1} . Because of the weak VCD effect, the spectrum is of relatively poor quality (low signal-to-noise ratio) and had to be baseline corrected. It is however, good enough to determine the absolute configuration of (+)-(*S*)-(*E*)-**140**.

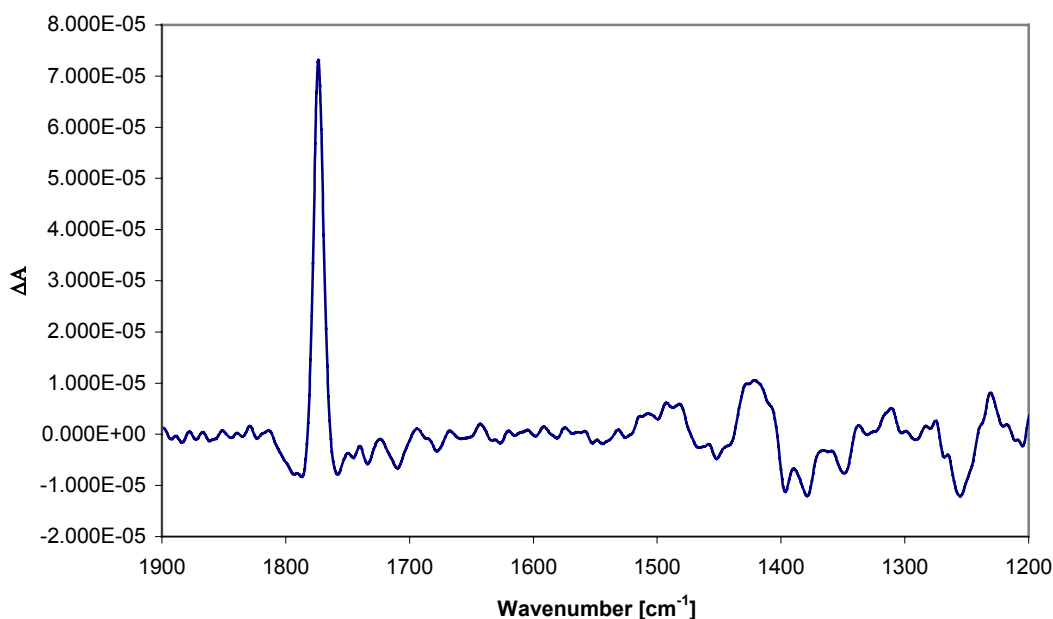


Figure 32. VCD spectrum of (+)-(*S*)-(*E*)-**140**.

Based on quantum chemical calculations, the strong positive carbonyl VCD signal at 1773 cm^{-1} is in agreement with the (*S*)-enantiomer illustrated in *Figure 29*. Unfortunately the C=C stretching vibration is too weak and is buried in the noise (it should be a weak negative band at around 1670 cm^{-1} , according to the quantum chemical calculations).

4.3.10 Mechanism of the S_{Ni}' reaction

Now that the absolute configuration of the chloro-ketone (+)-(*S*)-(*E*)-**139** and the resulting cyclobutanones (+)-(*S*)-(*E*)-**140** and (-)-(*R*)-(*Z*)-**140** had been determined, it was possible to establish the exact mechanistic course of the reaction. The experimental data is summarized in *Figure 33*. Chiral GC analysis showed that the products exhibit almost the same ee as the starting material. This shows that *anti* attack of the nucleophile can not be in effect to more than 3% and provides proof that the S_{Ni}' reaction, leading to cyclobutanones, proceeds with 97% *syn* stereoselectivity.

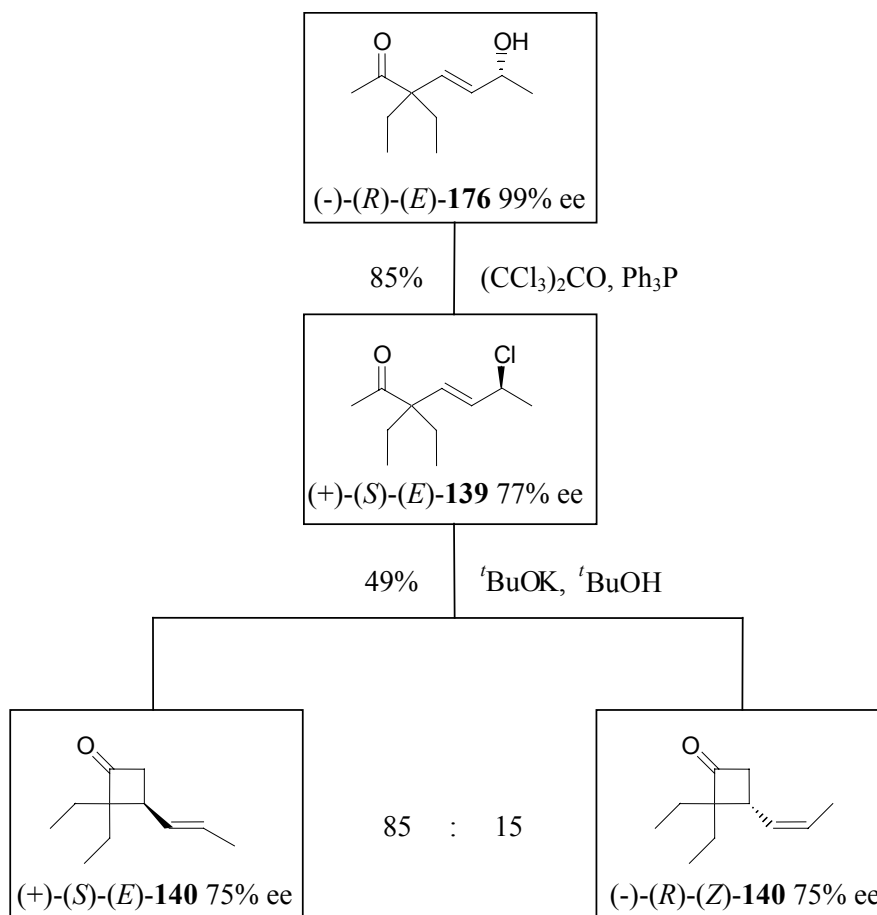
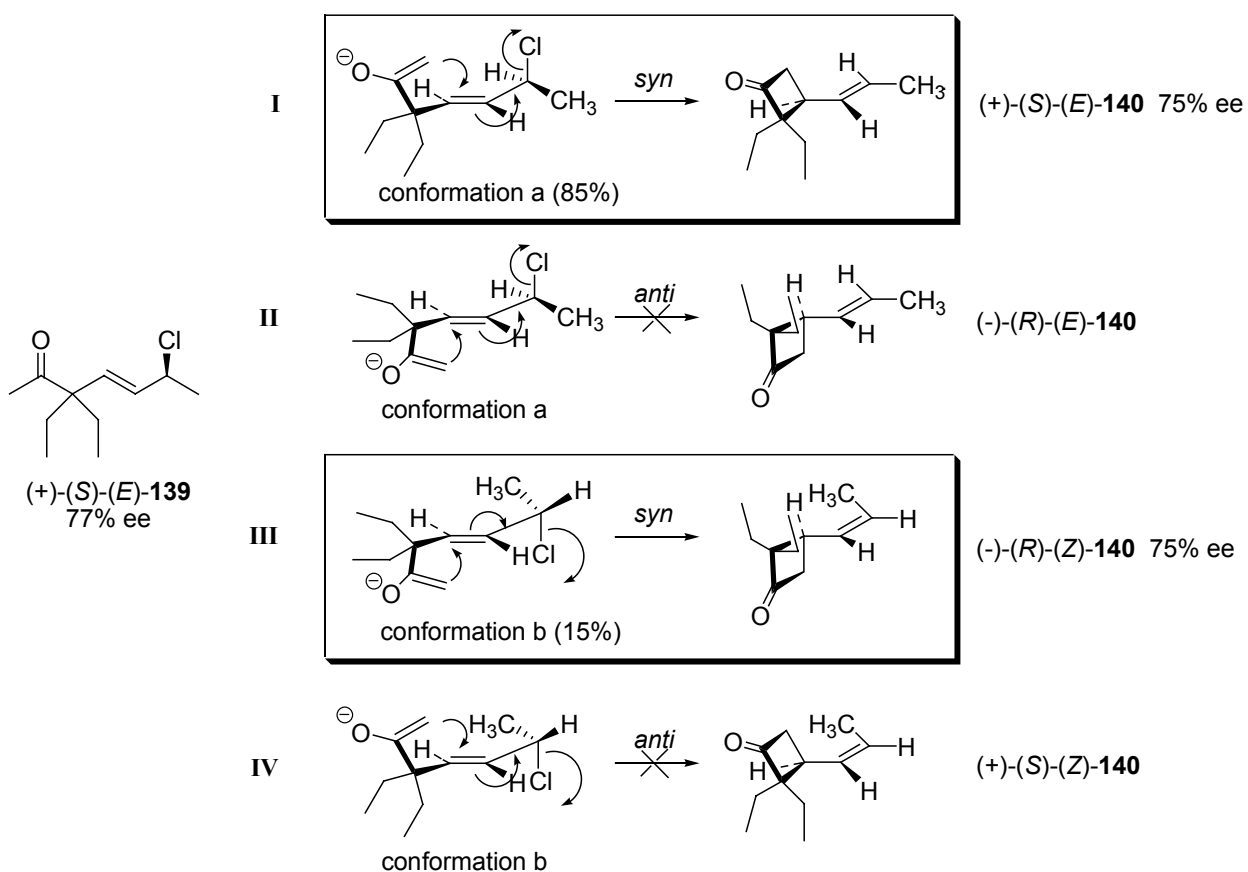


Figure 33. Experimental data from the stereoselective S_Ni' reaction.

The possible mechanistic pathways for the S_Ni' reaction of **(+)-(S)-(E)-139** are illustrated in *Scheme 61*. Transition state **I**, leading to **(+)-(S)-(E)-140**, proceeds with *syn* geometry. Because almost complete preservation of optical activity was observed in the product (*Figure 33*), *anti*-attack of the nucleophile, as depicted in transition state **II**, can be excluded for it will lead to **(-)-(R)-(E)-140**. Formation of the minor product **(-)-(R)-(Z)-140** proceeds through transition state **III**, also with *syn* geometry. Again, the optical activity was preserved to 97%, therefore, transition state **IV** with *anti* geometry could be excluded, for it would lead to the formation of **(+)-(S)-(Z)-140**.



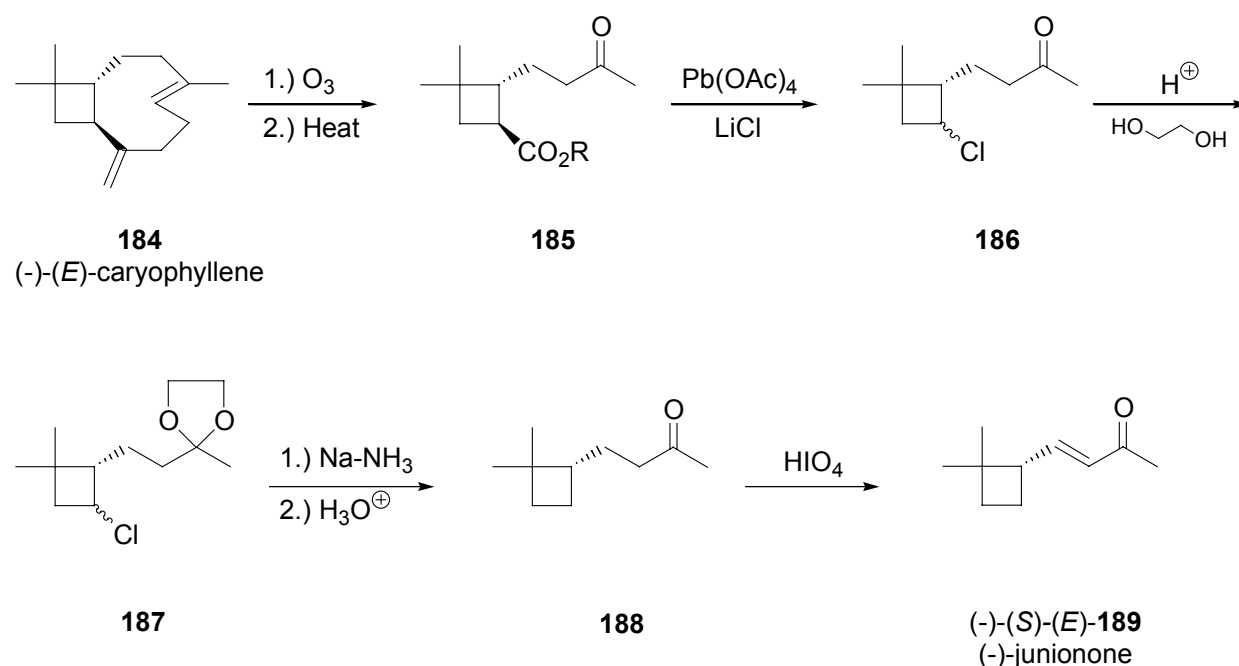
Scheme 61. Reaction mechanism of the 4-*exo-trig* S_{Ni'} reaction.

From the experimental data it can be concluded that (+)-(S)-(E)-139 will adapt *conformation a* to 85% in the transition state, thereby minimizing the unfavorable A^{1,3} strain illustrated in *Chapter 4.2, Figure 22*. *Syn*-attack leads to the major product (+)-(S)-(E)-140, proceeding through transition state **I**, *Scheme 61*. At reaction temperature (+)-(S)-(E)-139 adapts *conformation b* to 15%. This conformer will react passing through transition state **III** resulting in the minor product (-)-(R)-(Z)-140.

4.4 Total Synthesis of Junionone

4.4.1 Introduction

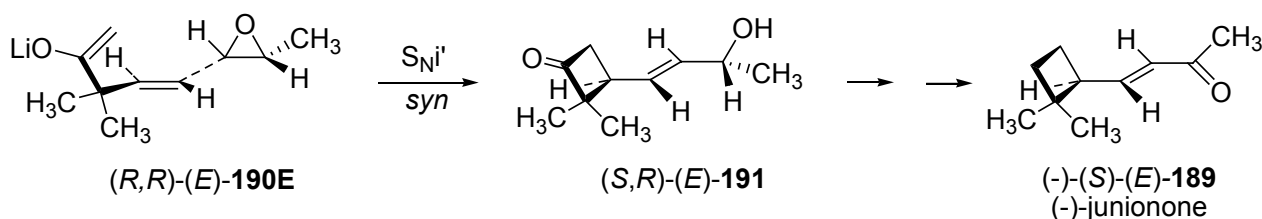
Junionone is a natural cyclobutane monoterpene, first isolated from the oil of the fruit of *juniperus communis*, L. by Thomas et al. in 1973 [77]. During the analysis of juniper berry oil the authors isolated a small amount of a substance with interesting olfactory properties. Structure determination by MS and NMR experiments led to structure (*E*)-**189**. Insufficient natural product was available to be certain about the sign of the optical rotation. To confirm the proposed structure, (-)-(*S*)-(*E*)-**189** was synthesized from caryophyllene (-)-(*E*)-**184**, *Scheme 62*.



Scheme 62. (-)-Junionone from (-)-(*E*)-caryophyllene by Thomas et al.

Although the structure of junionone could be proven by synthesis, the absolute configuration of the natural product was never established. The cyclobutane ring in the junionone structure can be constructed by the S_N1' method. Similar to leaving groups such as methane sulfonate and chloride, used in previous examples, nucleophilic epoxide-opening can also result in a leaving group effect, leading to formation of allylic alcohols. Following the example in Toromanoff's prostaglandin synthesis (*Chapter 4.1, Scheme 32*), it was envisioned that it should be possible to construct the carbon skeleton of the junionone molecule stereoselectively in one step by a *syn* S_N1' reaction of the optically active epoxy ketone (*R,R*)-(*E*)-**190**, *Scheme 63*. Wolff-Kishner reduction of the cyclobutanone (*S,R*)-(*E*)-**191**, followed by oxidation of the allylic alcohol would furnish optically active junionone (-)-(*S*)-(*E*)-**189**. Comparing the sign of the optical rotation with that reported by

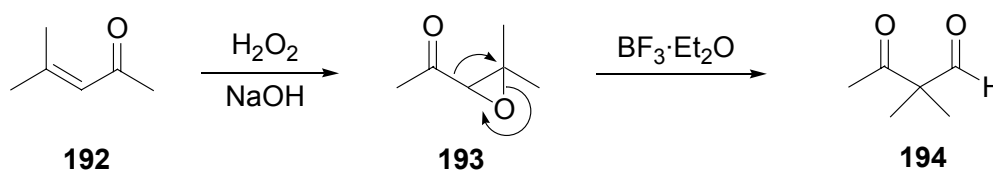
Thomas et al. for (-)-(*S*)-(*E*)-**189**, made from caryophyllene, will allow quick verification of the absolute configuration.



Scheme 63. Synthetic route leading to (-)-junionone.

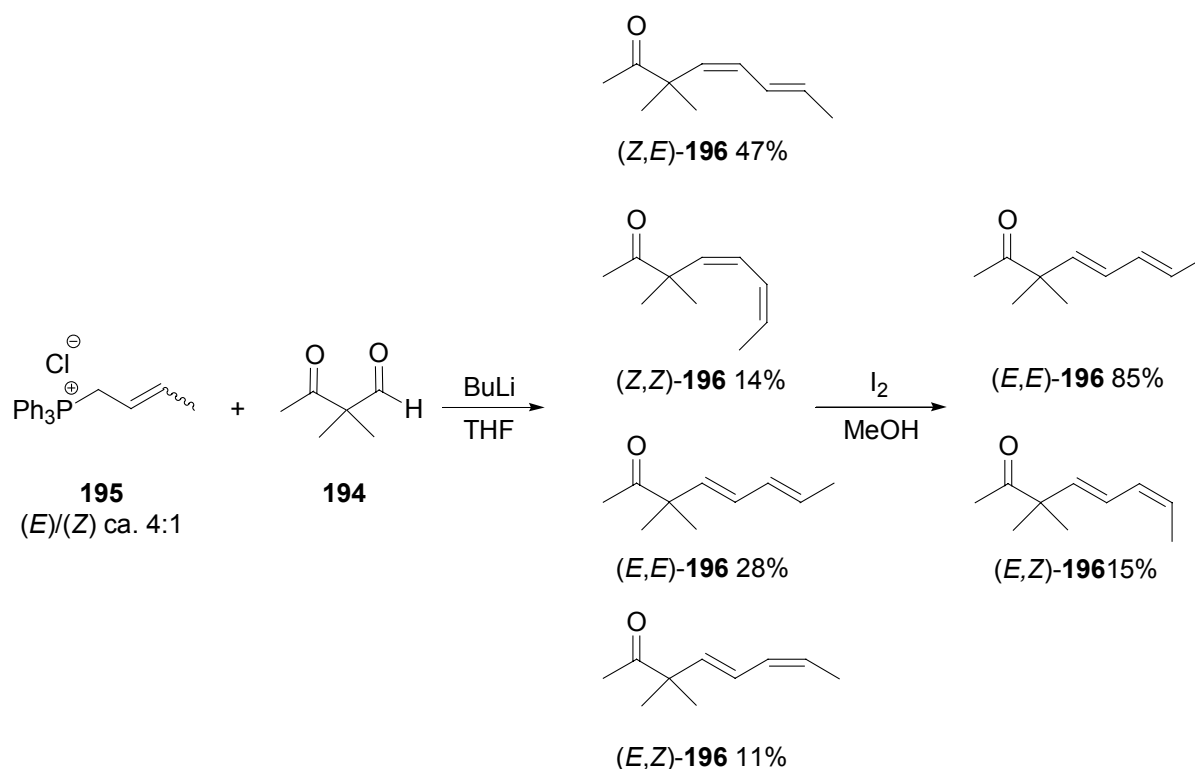
4.4.2 Synthetic intermediates

The optically active starting material (*R,R*)-(*E*)-**190** was prepared by a similar approach as compound (*S*)-(*E*)-**176** described in *Chapter 4.3.4*. The key intermediate **194** can be synthesized by the Stork enamine synthesis. A more convenient and higher yielding preparation involves the $\text{BF}_3 \cdot \text{Et}_2\text{O}$ induced rearrangement of 3,4-epoxy-4-methyl-2-pentanone **193**, reported by House et al. [78], *Scheme 64*. Compound **193** was prepared by action of alkaline hydrogen peroxide on mesityl oxide **192**, following a procedure by Weitz et al. [79].



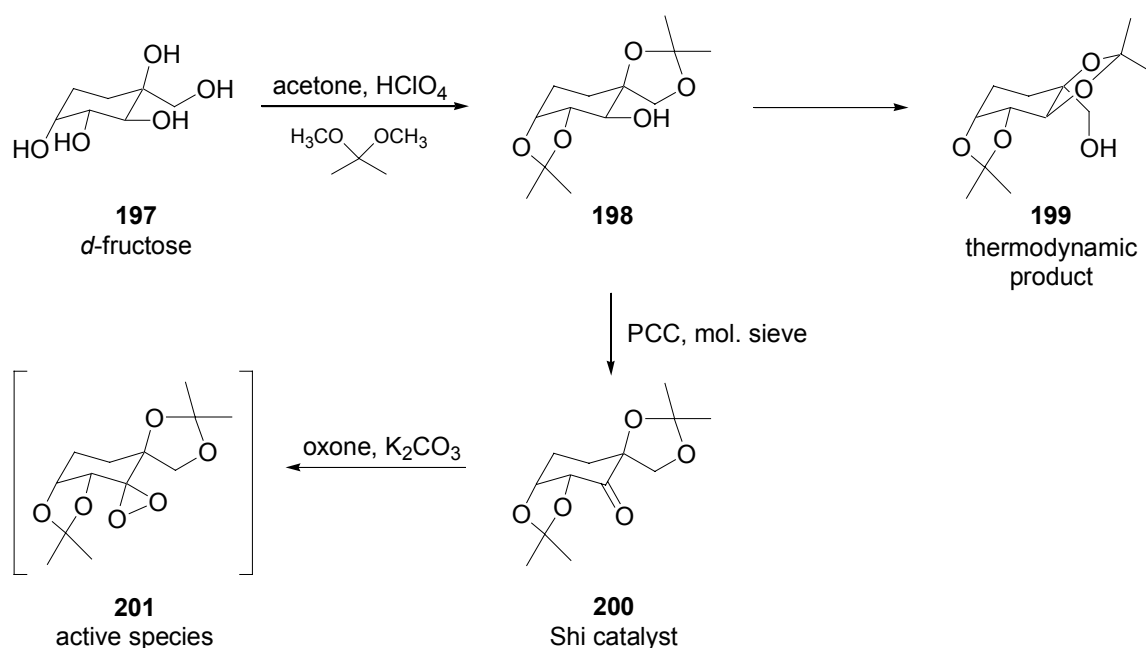
Scheme 64. Keto-aldehyde **194** through epoxide rearrangement by House et al.

Chemoselective reaction of **194** with the Wittig salt **195** led to a mixture of the four possible (*E*)- and (*Z*)-isomers of **196**, *Scheme 65*. Isomerization with I_2 in MeOH at room temperature led to a mixture of 85% (*E,E*)-**196** and 15% of (*E,Z*)-**196**. The (*E*)/(*Z*) configuration of the different isomers was determined by GC analysis and NMR spectroscopy of enriched samples. The spin coupling constant for the (*E*)-protons in (*Z,E*)-**196** in the ^1H -NMR (400 MHz, CDCl_3) is $J = 11.4$ Hz. The (*E*)-protons on the 4,5-double bond of (*E,E*)-**196** give rise to a spin coupling constant of $J = 14.8$ Hz. The configuration at the terminal double bond can easily be determined by examining the ^{13}C -NMR (75 MHz, CDCl_3) spectrum. (*E,E*)-**196** exhibits a peak at 17.9 ppm resulting from the terminal methyl group in (*E*)-position. The (*Z*)-methyl group in (*E,Z*)-**196** gives rise to a signal at 13.2 ppm.



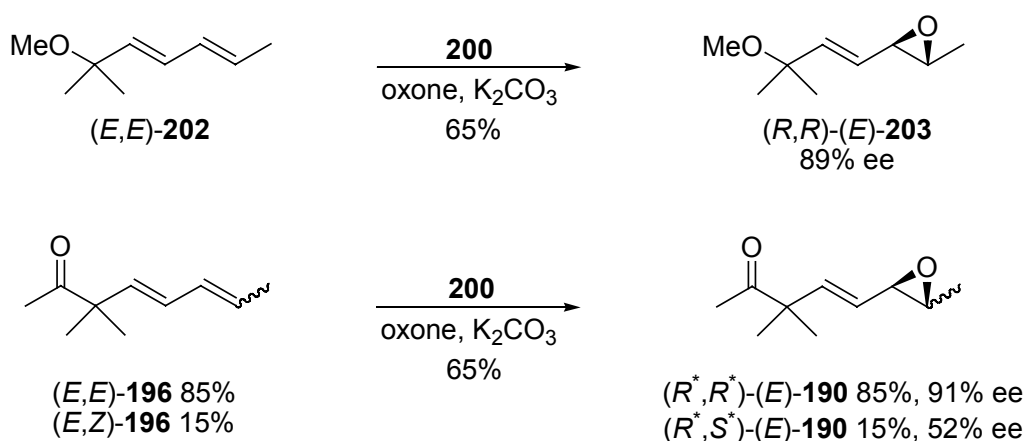
Scheme 65. Construction of (*E,E*)-**196** by the Wittig reaction followed by I_2 catalyzed isomerization.

Shi et al. developed a highly regio- and enantioselective monoepoxidation of conjugated dienes using a catalyst **200** derived from *d*-fructose [80]. The catalyst is not commercially available and has to be prepared by acetalization of *d*-fructose **197** with acetone followed by oxidation of the resulting diacetal **198** with pyridinium chlorochromate (PCC) to ketone **200**, *Scheme 66*. Monitoring the reaction by GC revealed the formation of two products. As the reaction proceeded, the signal at lower retention time diminished in favor of the product peak with higher retention time. It seemed obvious at the time that one signal represents the mono-acetal and the signal with the higher retention time represents the diacetal **198**. When the isolated product was oxidized with PCC, the reaction failed completely and only small amounts of intractable material could be identified after stirring over night. Careful interpretation of the NMR spectrum revealed that not the desired product **198** but rather the thermodynamic rearrangement product **199** had been isolated. Based on these findings it was possible to obtain the desired product **198** by quenching the reaction at lower temperature and after a shorter reaction time. Oxidation of **198** with PCC, leading to the Shi catalyst **200**, was possible only by applying a mixture of PCC and powdered molecular sieve as described by Herscovici et al. [81].



Scheme 66. Preparation of the Shi catalyst 200.

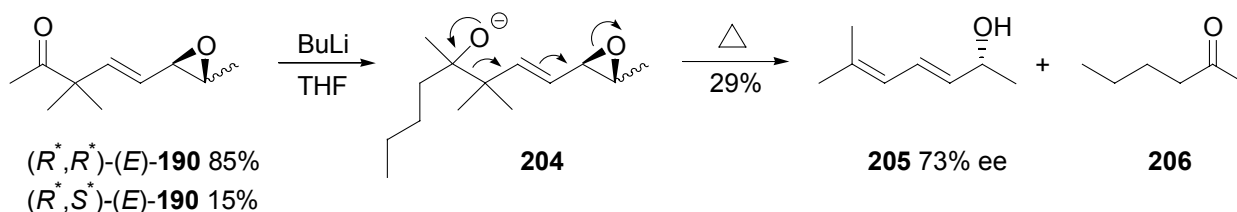
The regio- and enantioselective epoxidation of (*E,E*)-**202** is one of the examples published by Shi et al., *Scheme 67*. Due to its similarity to diene (*E,E*)-**196** it can be estimated, that epoxidation of (*E,E*)-**196** by this method will most likely lead to (*R,R*)-(*E*)-**190**. By performing ^1H -NMR experiments with chiral shift reagents it was possible to determine the enantiomeric excess of the *cis* and *trans* epoxides (*R*^{*},*S*^{*})-(*E*)- and (*R*^{*},*R*^{*})-(*E*)-**190** to be 52% and 91%, respectively. The *cis/trans* ratio of the epoxide can be determined by integrating the signals from the olefinic protons in the ^1H -NMR (300 MHz, CDCl_3) spectrum at 5.29 ppm (*dd*, $J = 7.6$ Hz) and 5.98 ppm (*d*, $J = 15.6$ Hz) for the (*E*)-isomer and 5.44 ppm (*dd*, $J = 7.6$ Hz) and 6.01 ppm (*d*, $J = 15.6$ Hz) for the (*Z*)-isomer.



Scheme 67. Regio- and enantioselective epoxidation by Shi et al.

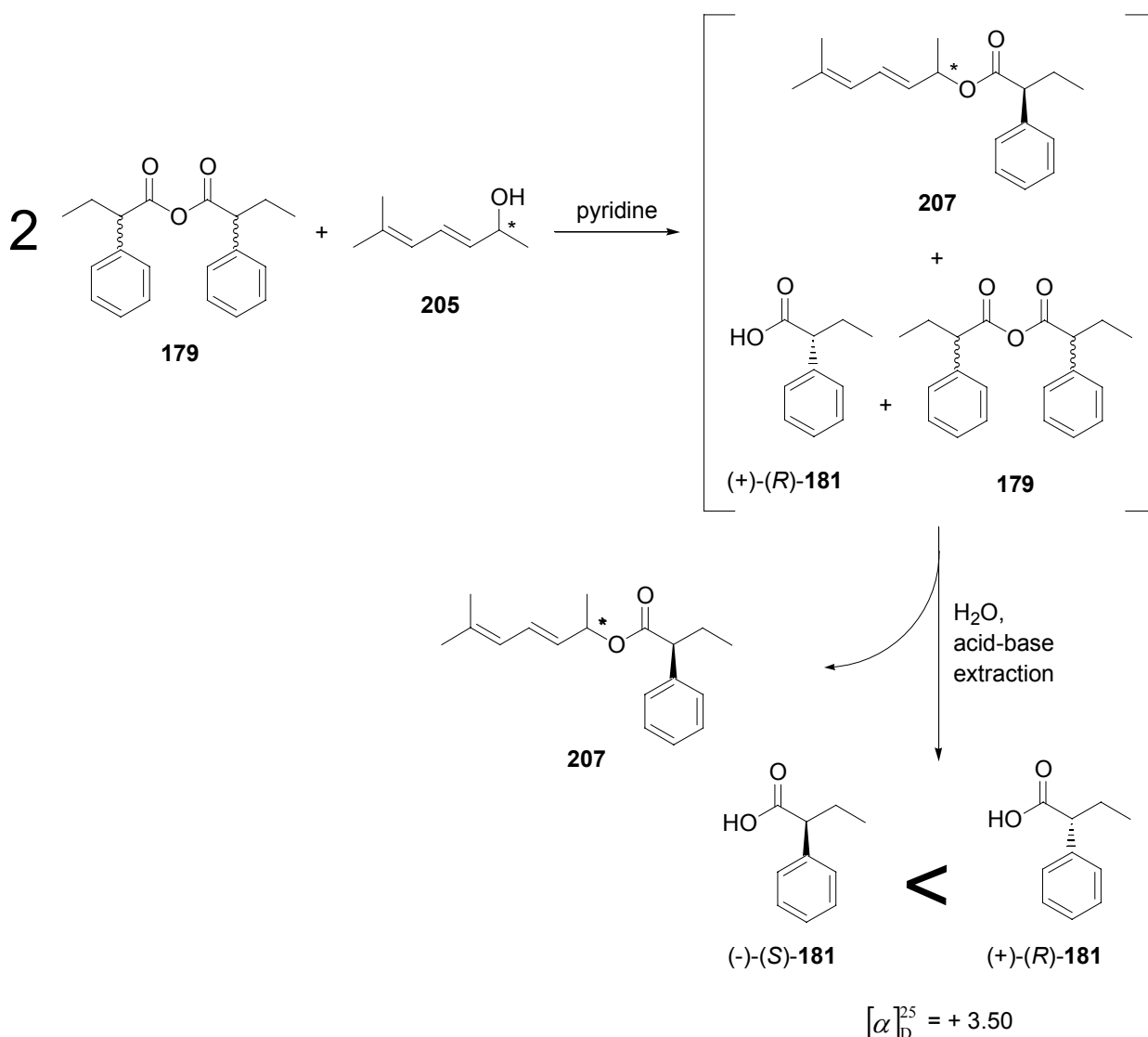
4.4.3 Determination of the absolute configuration of keto-epoxide (*E*)-190

To determine the exact reaction mechanism of the S_N1' cyclization it was essential to be certain about the absolute configuration of the epoxyketone (R^*,R^*)-(*E*)-190. In previous experiments it was observed that fragmentation is a major side reaction, *Chapter 4.3.2*. Initial cyclization experiments with (*E*)-190 revealed that treatment with BuLi and subsequent addition of $\text{BF}_3 \cdot \text{Et}_2\text{O}$ led to selective fragmentation, resulting in the optically active dienol **205**, *Scheme 68*.



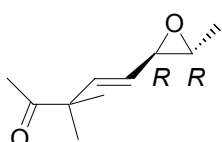
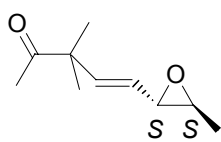
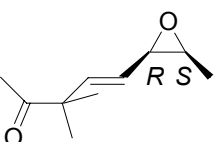
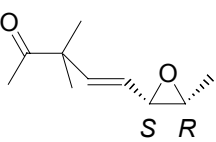


Scheme 68. Fragmentation reaction leading to optically active alcohol **205**.

Determination of the absolute configuration of **205** by Horeau's empirical method provided the necessary information to derive the absolute configuration of the epoxide (*E*)-190, *Scheme 69*.



Scheme 69. Determination of the absolute configuration of **205** by Horeau's method.

The epoxyketone (*R,R*)-(*E*)-**190** contains 15% of *cis*-epoxide (*Z*)-**190** of unknown absolute configuration. The absolute configuration of (*Z*)-**190** can be derived from the enantiomeric excess of **205**, Table 6. In *variation a* (*R,S*)-(*Z*)-**190** is considered to be the more abundant *cis* isomer and in *variation b* (*S,R*)-(*Z*)-**190** is the major enantiomer. Adding the percentage of the enantiomers contributing to the (*R*)-configuration in **205** will result in a theoretical value for the expected enantiomeric excess. The result obtained from *variation a* fits the 73% ee (determined by NMR experiment with chiral shift reagent) of **205** best, whereas *variation b* would lead to a significantly higher ee in dienol **205**. Based on these considerations it was determined, that the absolute configuration of the major enantiomer of the *cis*-epoxyketone corresponds to (*R,S*)-(*Z*)-**190**.

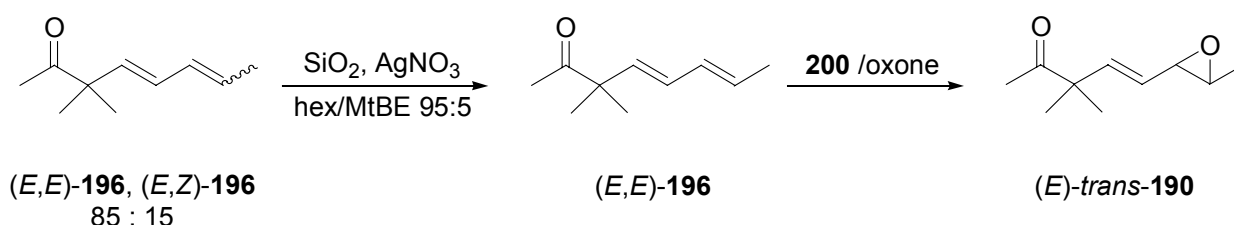
			
(R,R)-(E)-190 95%	(S,S)-(E)-190 5%	(R,S)-(Z)-190	(S,R)-(Z)-190
			
85% (91% ee)		a.) 76% b.) 24% 24% 76%	
		15% (52% ee)	

<i>(E)</i> - 190	contribution to (<i>R</i>)-enantiomer variation a (%)	contribution to (<i>R</i>)-enantiomer variation b (%)
<i>(R,R)</i> - <i>(E)</i> - 190	81	81
<i>(S,R)</i> - <i>(E)</i> - 190	4	11
% (<i>R</i>)- 205 :	85 (70% ee)	92 (84% ee)

After two additional synthetic steps the absolute configuration of the cyclobutanone (*E*)-**191**, resulting from S_Ni' ring closure of (*R,R*)-(*E*)-**190**, can be correlated with the known configuration of junionone (-)-(*S*)-(*E*)-**189**, derived from caryophyllene.

Because of the absolute configuration of epoxyketone (*E*)-**190** was of great importance for determining the reaction mechanism of the S_NI' ring closure reaction, ROA spectroscopy was applied to verify the results obtained from Horeau's empirical method, *Chapter 4.4.3*.

When following the synthesis illustrated in *Chapter 4.4.2*, the epoxyketone (*E*)-**190** was obtained as a mixture of (*E*)-*trans*- and (*E*)-*cis*-**190** in a ratio of 85:15. In order to get a clean ROA spectra, it was necessary to measure a sample of pure (*E*)-*trans*-**190**. In order to obtain pure (*E*)-*trans*-**190**, pure (*E,E*)-**196** had to be subjected to the Shi epoxidation reaction. The (*E/Z*) isomers of **196** were separated by chromatography over silica gel impregnated with AgNO₃, *Scheme 70*. A sample of pure (*E,E*)-**196** was converted to the mono-epoxide (*E*)-*trans*-**190** and then submitted for ROA spectroscopy.



The absolute configuration of (*E*)-*trans*-**190** was determined by comparing the measured ROA spectrum with that of (*R,R*)-2-methyl-3-vinyloxirane **208**. Due to the similar local geometry of the epoxide region the ROA signals are expected to have the same sign. The two most significant signals between 800 cm⁻¹ and 900 cm⁻¹ result from symmetrical deformation vibrations, *Figure 34*. As expected, the signals exhibit identical signs. Based on the spectroscopic data and the empirical determination by Horeau's method it was possible to unambiguously determine that the epoxyketone (*E*)-*trans*-**190**, prepared by the method developed by Shi et al. (*Chapter 4.4.2*), possesses (*R,R*)-configuration.

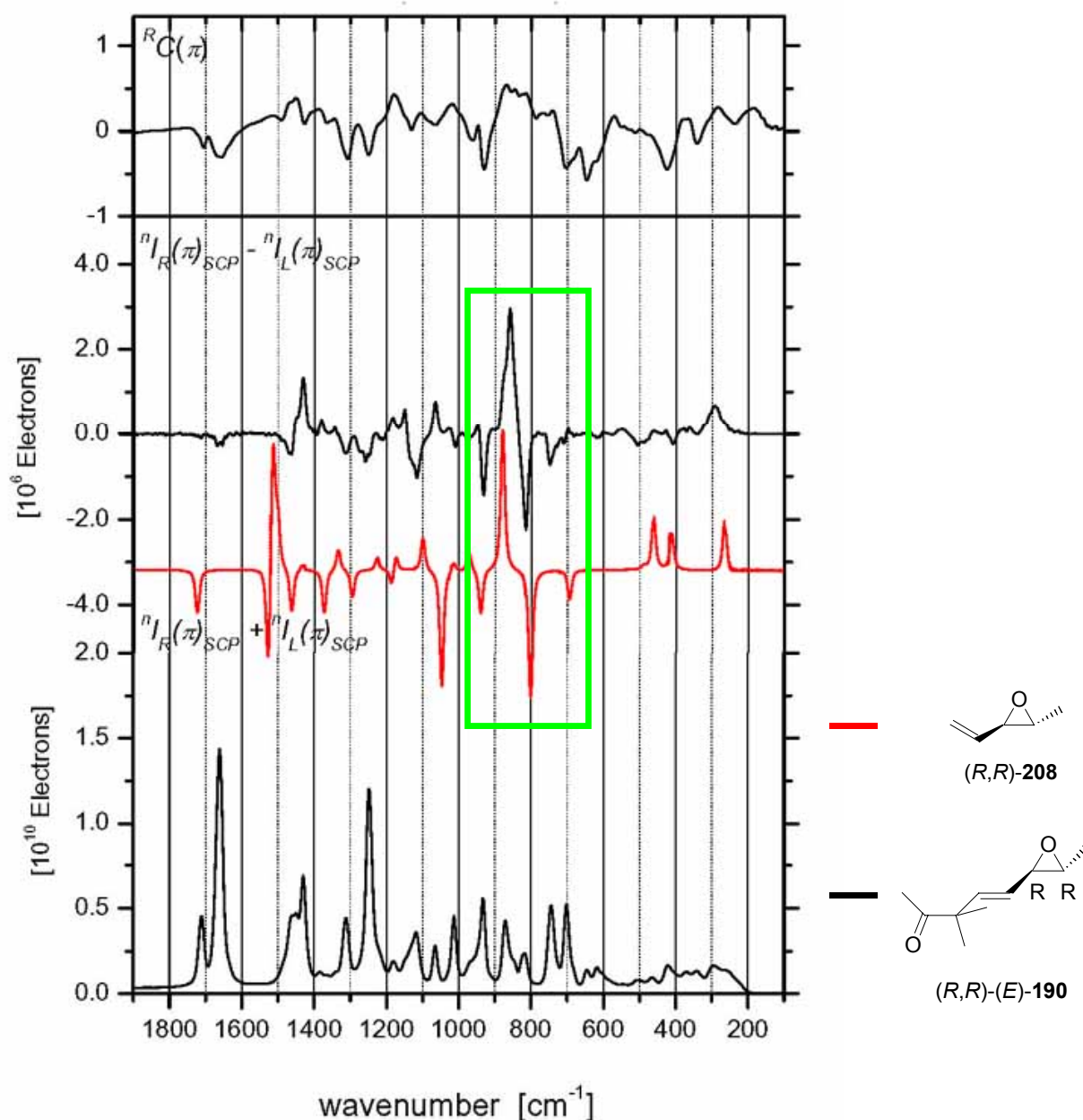
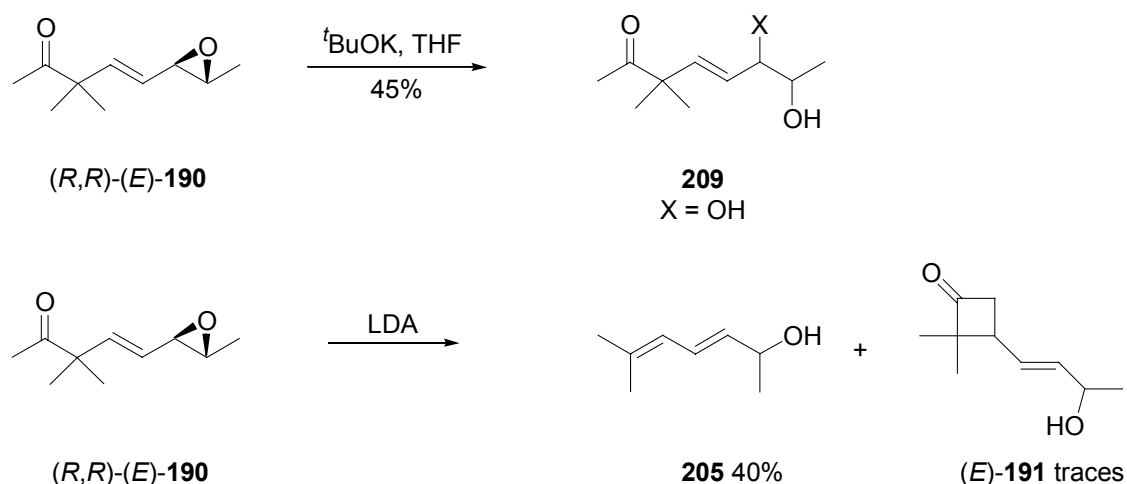


Figure 34. RAMAN/ROA spectrum of (R,R) -(*E*)-190 vs. (R,R) -208.

4.4.5 Cyclization of epoxyketone (R,R) -(*E*)-190

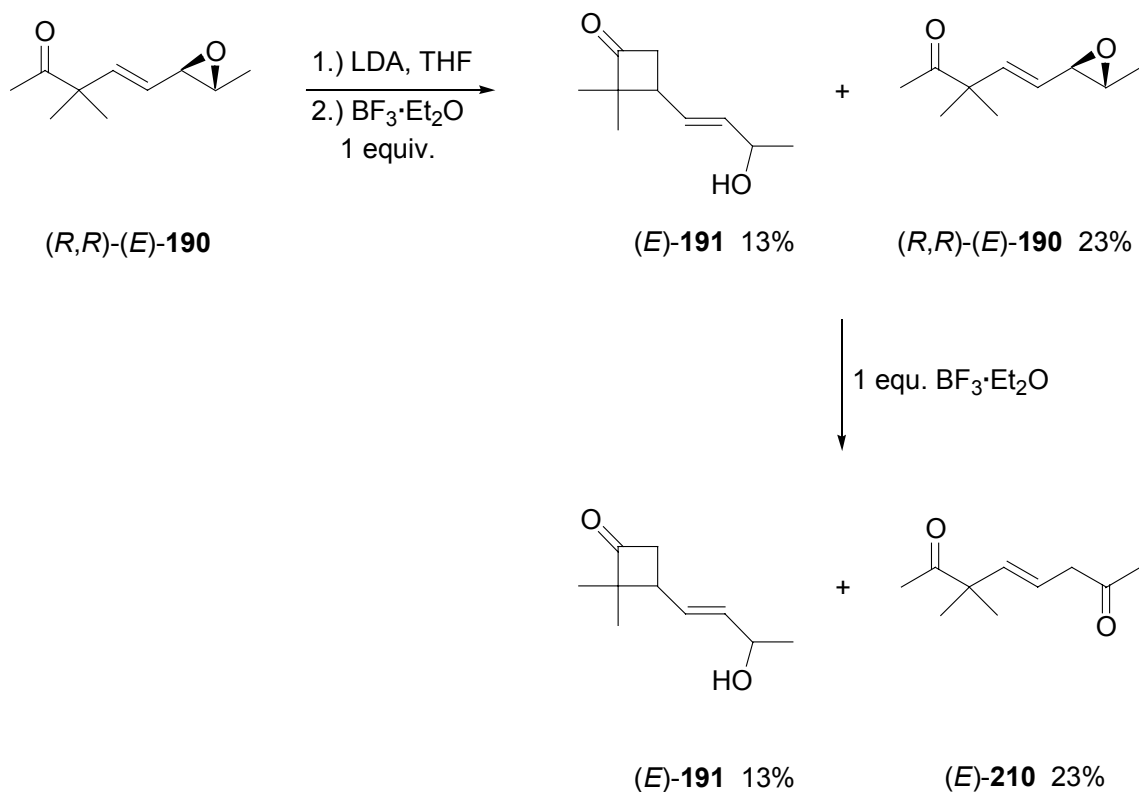
Now that the epoxyketone (R,R) -(*E*)-190 was available, suitable cyclization conditions had to be found. First attempts to perform the S_Ni' reaction on (R,R) -(*E*)-190 with t BuOK in THF resulted in the formation of diol **209** exclusively, *Scheme 71*. This was most likely due to the presence of water, introduced into the reaction mixture with the t BuOK. When the S_Ni' reaction was attempted with LDA at $-68\text{ }^{\circ}\text{C}$, the elimination product **205** was the major product and only traces of the desired product (*E*)-191 could be isolated by preparative TLC. A strong carbonyl band at 1775 cm^{-1} in the IR spectrum was a good indicator for the presence of a cyclobutanone structure.



Scheme 71. Attempted, base induced, S_Ni' reaction of $(R,R)\text{-(}E\text{)-190}$.

These results showed, that the epoxide must be activated to promote the S_Ni' ring closure and to inhibit formal “ketene” elimination. In recent publications, $\text{BF}_3 \cdot \text{Et}_2\text{O}$ was reported to make epoxides more electrophilic. See for example Yamaguchi or Davies [82][83][84].

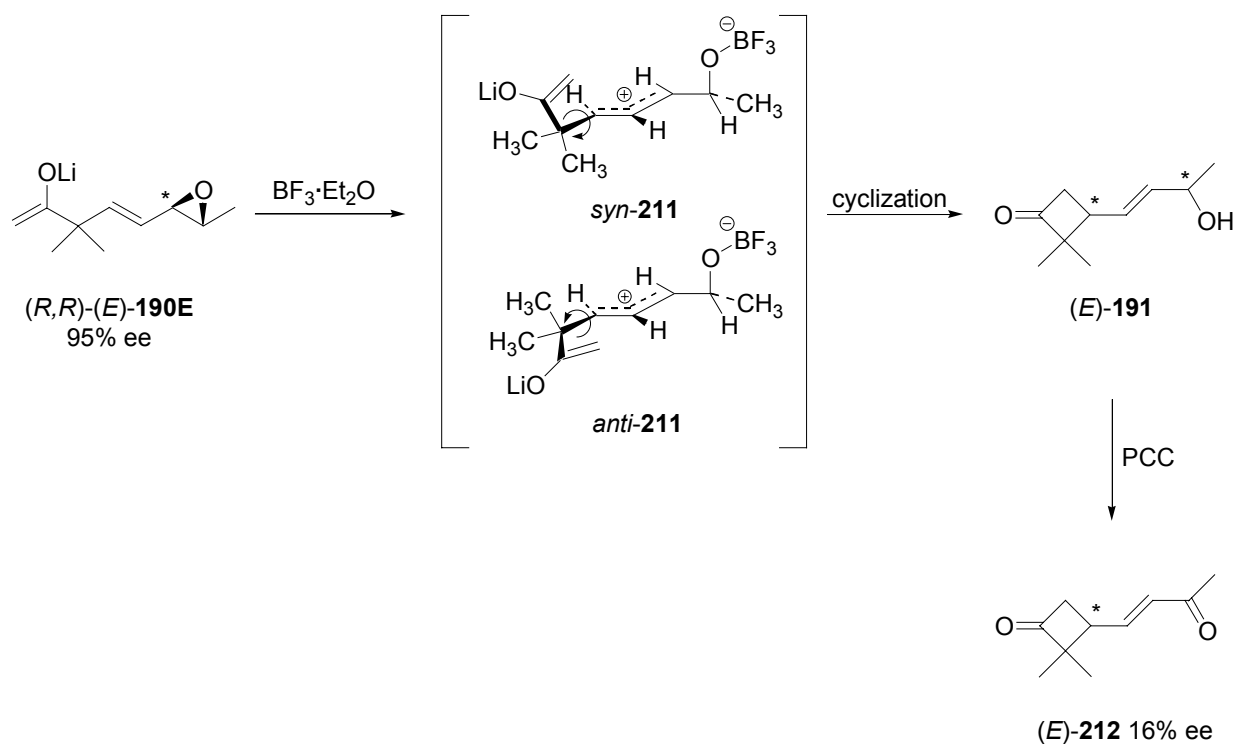
The S_Ni' ring closure reaction was carried out by preparing the ketone enolate with LDA at low temperatures and then adding one equivalent of $\text{BF}_3 \cdot \text{Et}_2\text{O}$ to the reaction mixture, *Scheme 72*. Monitoring the progress of the reaction by TLC analysis revealed that, when one equivalent of $\text{BF}_3 \cdot \text{Et}_2\text{O}$ was added, only half of the starting material $(R,R)\text{-(}E\text{)-190}$ would react to give $(E)\text{-191}$ and the other half would remain unreacted. If more Lewis acid was added, the remaining $(R,R)\text{-(}E\text{)-190}$ would undergo epoxide rearrangement leading to $(E)\text{-210}$.



Scheme 72. S_Ni' reaction of $(R,R)\text{-(}E\text{)-190}$ after epoxide activation with $\text{BF}_3 \cdot \text{Et}_2\text{O}$.

The first assumption was that deprotonation of *(R,R)*-(*E*)-**190** with LDA was incomplete and therefore the reaction did not go to completion. Equimolar amounts of hexamethylphosphoramide (HMPA) and dimethylpropylen urea (DMPU) were added to the reaction mixture, in an attempt to make the anion more reactive. Analysis of the reaction mixtures showed no difference in product distribution than in absence of solvating agent. The use of lithium hexamethyl disilazane (LiHMDS) in place of the LDA resulted in an improvement of the yield from 13% to 50%, *Table 8*.

The (*E*)-configuration of the double bond was determined by measuring the coupling constant of the signals at 5.69 ppm resulting from the olefinic protons in the ^1H -NMR (300 MHz, CDCl_3). The measured values $J = 5.3$ and 2.7 Hz indicate the presence of an (*E*)-configured double bond. NMR analysis of (*E*)-**191** in the presence of Pirkle's reagent gave rise to a complicated spectrum indicating high enantiomeric enrichment for some signals and providing inconclusive results for others. For this reason, samples of (*E*)-**191** were oxidized with PCC on powdered molecular sieve, *Scheme 73*. The resulting diketone **212** was analyzed by NMR and found to possess (*E*)-configuration. Experiments with optically active shift reagent showed that the stereogenic center at C(3) of the cyclobutanone ring possessed an ee of only 10%. Considering the high ee of the starting material, this result indicates that a significant amount of epimerization has taken place during the cyclization reaction. Based on these results, a mechanism involving the allyl cation intermediates *syn*- and *anti*-**211** illustrated in *Scheme 73* was postulated.



Scheme 73. Allyl cation intermediate in the $\text{BF}_3 \cdot \text{Et}_2\text{O}$ cyclization of *(R,R)*-(*E*)-**190E**.

Although the experimental data indicated that cyclobutanone (*E*)-**191** could be synthesized by the reaction illustrated in *Scheme 73*, there were still two major problems to solve. The reaction proceeded with low yield (50%), mostly due to the competing epoxide rearrangement reaction affording (*E*)-**210**, *Scheme 72*. Formation of the intermediate allyl cation **211** results in loss of facial selectivity, leading to significant epimerization at C(3) of the cyclobutanone ring. In an effort to improve the stereoselectivity of the cyclization, it was desirable to find a “softer” Lewis acid that would coordinate with the epoxide oxygen and weaken the carbon-oxygen bond, without actually breaking it, allowing nucleophilic attack at the allylic system, *Figure 35*.

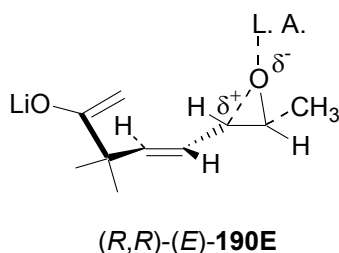
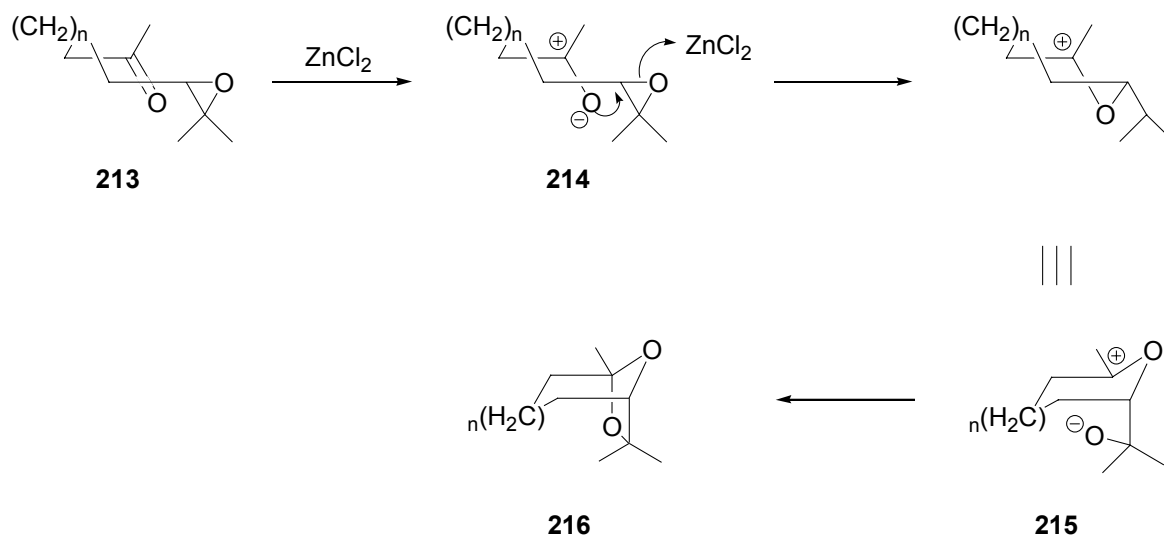


Figure 35. Weakening of the epoxide carbon-oxygen bond by a soft Lewis acid.

A literature search was conducted to find better conditions for the stereoselective, nucleophilic reaction of epoxides with enolates. Wasserman et al. reported the use of anhydrous ZnCl_2 to activate epoxide **213** in the synthesis of the *Musculus* pheromone [85], *Scheme 74*.



Scheme 74. Epoxide activation with ZnCl_2 by Wasserman et al.

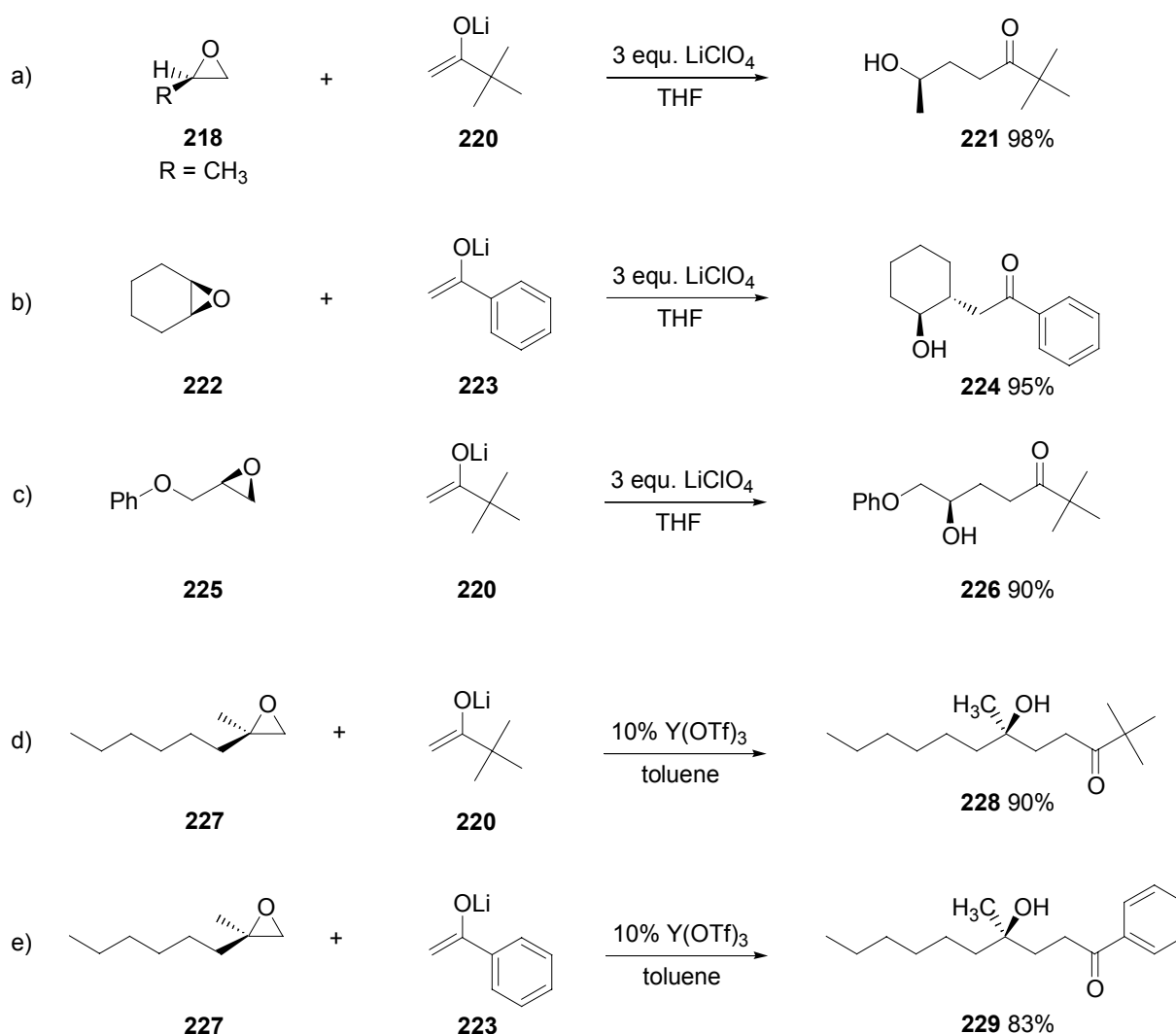
Taylor et al. described the use of aluminum ester enolates to open mono substituted epoxides leading to the corresponding γ -hydroxy-carbonyl compounds [86], *Table 7*. The (*E*)-enolate of **217** was generated by treatment with LDA and then converted to the aluminum enolate by adding Et_2AlCl . The experimental data indicated that the reaction proceeded with high diastereoselectivity and moderate yields.

Table 7. Epoxide activation with aluminum ester enolates by Taylor et al.

R	R'	Yield (%)	<i>syn</i> : <i>anti</i>
Me	Me	56	84 : 16
Me	Et	43	84 : 16
Me	<i>i</i> Pr	56	88 : 12
Me	<i>t</i> Bu	38	95 : 5

Only two years later Crotti et al. published the results from reacting ketone enolates with epoxides in the presence of LiClO₄ [87], *Scheme 75 a-c*. The results from the metal salt catalyzed opening of 1,2-epoxides with amines, azides and cyanide ion, prompted the authors to conduct research on the metal salt catalyzed opening of epoxides with ketone enolates. The enolates were generated in anhydrous THF with LiHMDS from the corresponding ketones. LiHMDS was chosen over LDA to avoid complications due to competitive aminolysis of the epoxide, observed by the authors in other metal salt catalyzed reactions involving epoxides. The reactions proceeded with high stereoselectivity. Asymmetrical epoxides were attacked at the less hindered oxirane carbon leading to the *anti*-Markovnikov type products.

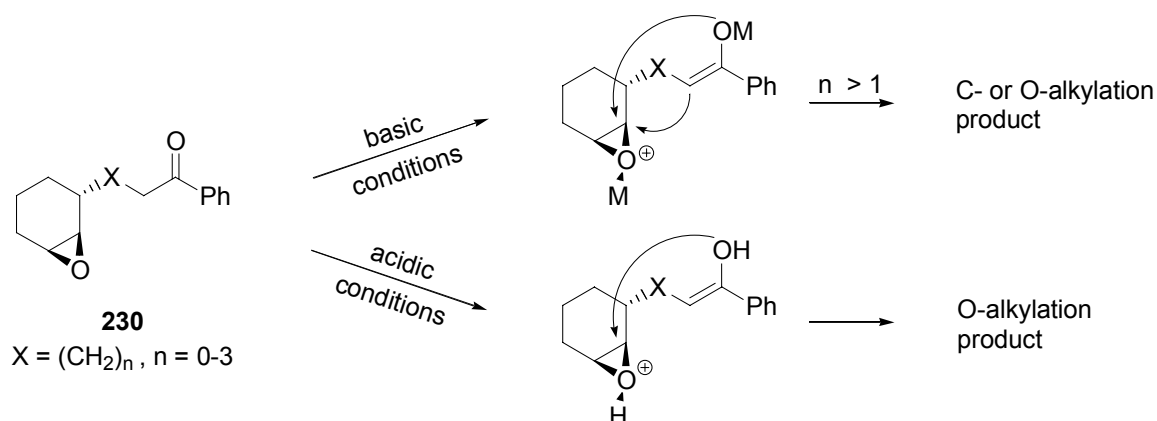
Later the authors reported that the reactions could be carried out with a catalytic amount of yttrium triflate (Y(OTf)₃ 10%) in toluene [88], *Scheme 75 d-e*. The use of the new solvent and catalyst system resulted in improved yields and better quality products. Under the improved reaction conditions, the authors succeeded to perform the reaction with **227** (*Scheme 75*, entries d and e), which had not been possible by the LiClO₄ method.



Scheme 75. Metal salt induced epoxide activation by Crotti et al.

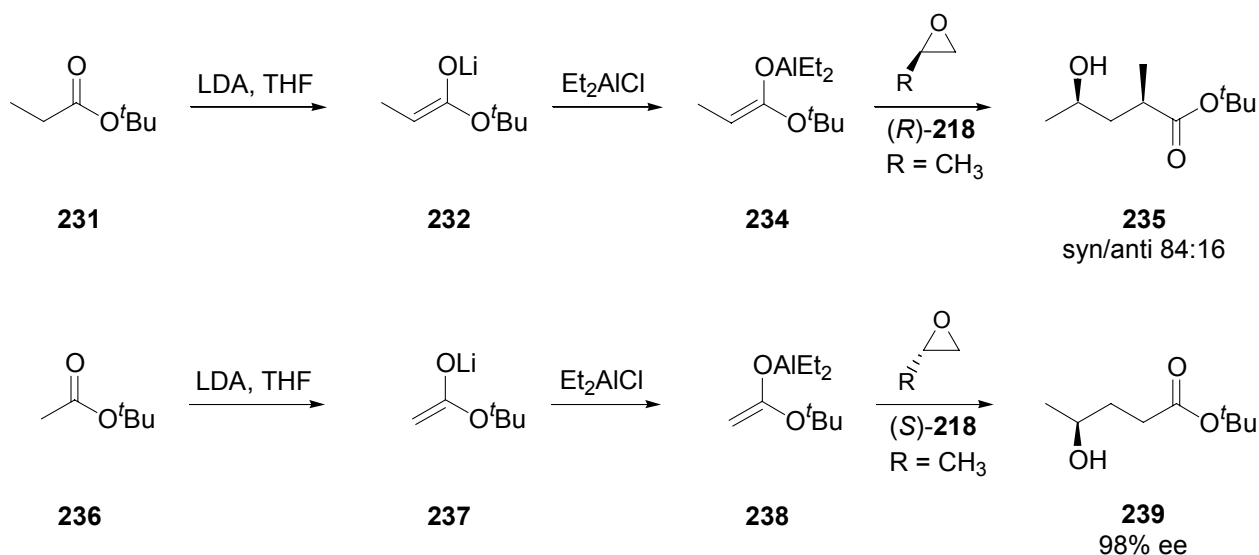
Crotti et al. extended their research in an attempt to improve the reactions with sterically demanding enolates and bicyclic epoxides [89]. They finally found that Sc(OTf)₃ was the most efficient catalyst for the epoxide opening reaction. The products obtained from prochiral enolates resulted in a mixture of diastereoisomers, showing only little preference for the *syn* product. Later Crotti's research group published results obtained from intramolecular reactions [90], *Scheme 76*. A series of epoxy ketones of type **230** were synthesized and cyclized under the Sc(OTf)₃ conditions and also by common EtONa/EtOH conditions which in certain cases rendered the corresponding γ -hydroxy ketones in high yield (without formation of diol, as observed during our research). In addition they also performed the cyclization under acidic conditions with acidic amberlyst in CH₂Cl₂. The outcome of the reaction depends strongly on the length of the alkyl chain and will produce both C- and O-alkylated products under basic conditions and exclusively O-alkylated products under acidic conditions. The authors explained their findings by theoretical analysis of the transition states and by applying the Baldwin rules of ring closure. Interestingly, the

authors concluded that formation of a four member or strained five member transition state is unfavorable and that O-alkylation will dominate instead.



Scheme 76. S_Ni reaction between ketone enolates and epoxides by Crotti et al.

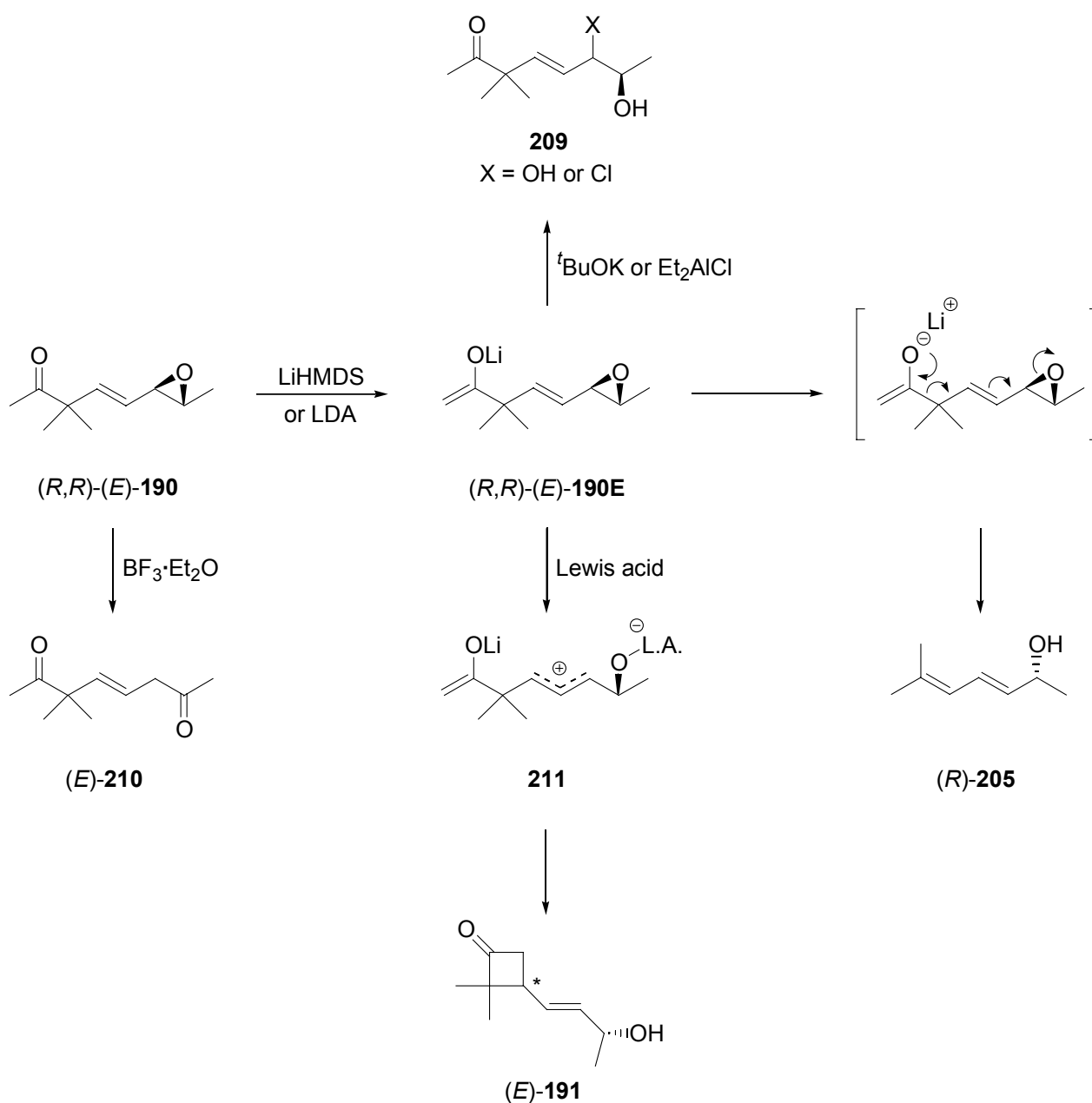
Parallel to the studies performed by Crotti et al., Taylor and his research group continued to work on the aluminum enolate promoted epoxide opening [91]. In this publication the authors show that the reaction takes place in a diastereoselective manner and they report the results obtained when using optically active epoxides, *Scheme 77*. The (*E*)-enolate of *tert*-butyl propionate **231** was prepared by treatment of **231** with LDA. The aluminum enolate **234** was obtained by adding Et₂AlCl and was then reacted with methyl oxirane (*R*)-**218**. The *syn/anti* ratio in the product was reported to be 84:16. In the same manner the reaction of **238** with enantiomerically pure (*S*)-**218** led to **239** with complete retention of optical purity.



Scheme 77. Reaction of aluminum ester enolates with epoxides by Taylor et al.

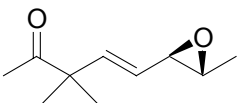
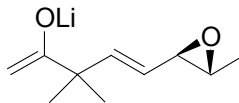
Based on the results by Arbusow, Wassermann, Crotti and Taylor the research on the S_Ni' ring closure reaction of epoxyketone (*R,R*)-(*E*)-**190** was continued. It was found, that if any hydroxy or halogen ions were present in the reaction mixture a significant amount of the S_N2 product **209** was formed. For this reason, the aluminum enolate reaction with Et₂AlCl failed. The use of Et₃Al on

the other hand led to the cyclobutanone (*E*)-**191** with low yield (28%) and high stereoselectivity (43% ee), compared to the $\text{BF}_3 \cdot \text{Et}_2\text{O}$ induced reactions. The $\text{ZnCl}_2 \cdot \text{Et}_2\text{O}$, LiClO_4 , $\text{Sc}(\text{OTf})_3$ and $\text{Y}(\text{OTf})_3$ catalyzed $\text{S}_{\text{N}}\text{I}'$ reactions of (*R,R*)-(*E*)-**190** failed to yield cyclobutanone (*E*)-**191**. It was found that Me_3SiOTf gave the best yield by far (92%), unfortunately, significant epimerization took place resulting in (*E*)-**191** with an ee of 10% [92]. The results from the cyclization experiments of (*E*)-**190** under different conditions are summarized in *Table 8* and in *Scheme 78*.



Scheme 78. Products formed from (*R,R*)-(*E*)-**190** with different Lewis acids.

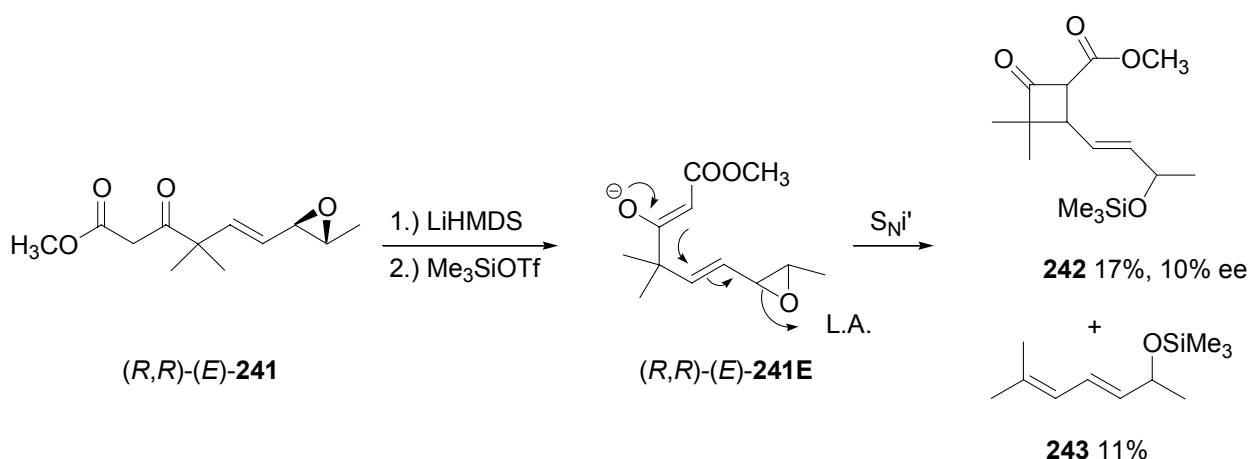
Table 8. Cyclization experiments of *(R,R)*-(*E*)-**190** with different Lewis acids.

<div style="display: flex; align-items: center; justify-content: space-around;"> <div style="text-align: center;">  <p><i>(R,R)</i>-(<i>E</i>)-190</p> </div> <div style="text-align: center;"> $\xrightarrow[\text{or LDA}]{\text{LiHMDS}}$ </div> <div style="text-align: center;">  <p><i>(R,R)</i>-(<i>E</i>)-190E</p> </div> <div style="text-align: center;"> \longrightarrow </div> <div> <p>210, 209, 205, (<i>E</i>)-191</p> </div> </div>						
Solvent	Base	Additive	Major product	%Yield (% ee) ²¹	Minor product	%Yield (% ee)
THF	^t BuOK	-	209 , X = OH	quant.	-	-
THF	BuLi	BF ₃ ·Et ₂ O	(<i>R</i>)- 205	30	(-)-(<i>E</i>)- 191	8 (10)
THF	LDA	-	(<i>R</i>)- 205	80	(-)-(<i>E</i>)- 191	13 (16)
THF	LDA	BF ₃ ·Et ₂ O	(<i>E</i>)- 210	23	(-)-(<i>E</i>)- 191	12 (16)
THF	LDA	ZnCl ₂ ·Et ₂ O	(<i>R</i>)- 205 + SM	~30	-	-
THF	LiHMDS	BF ₃ ·Et ₂ O	(-)-(<i>E</i>)- 191	50 (16)	(<i>R</i>)- 205	~20
THF	LiHMDS	LiClO ₄	(<i>R</i>)- 205 + SM	~50	-	-
toluene	LiHMDS	Sc(OTf) ₃	(<i>R</i>)- 205	~10	intractable mat.-	-
toluene	LiHMDS	Y(OTf) ₃	(<i>R</i>)- 205	quant.	-	-
THF	LiHMDS	Et ₂ AlCl	209 , X = Cl	3	(<i>E</i>)- 190	2
THF	LiHMDS	Et ₃ Al	(+)-(<i>E</i>)- 191	28 (43)	(<i>E</i>)- 210 + (<i>R</i>)- 205	traces
THF	LiHMDS	Me ₃ Al	-	-	intractable mat.	-
THF	LiHMDS	(^t Bu) ₃ Al	-	-	intractable mat.	-
THF	LiHMDS	Me ₃ SiOTf	(-)-(<i>E</i>)- 191	69 (10)	-	-

4.4.6 Cyclization experiments with β -keto-ester *(R,R)*-(*E*)-**241**

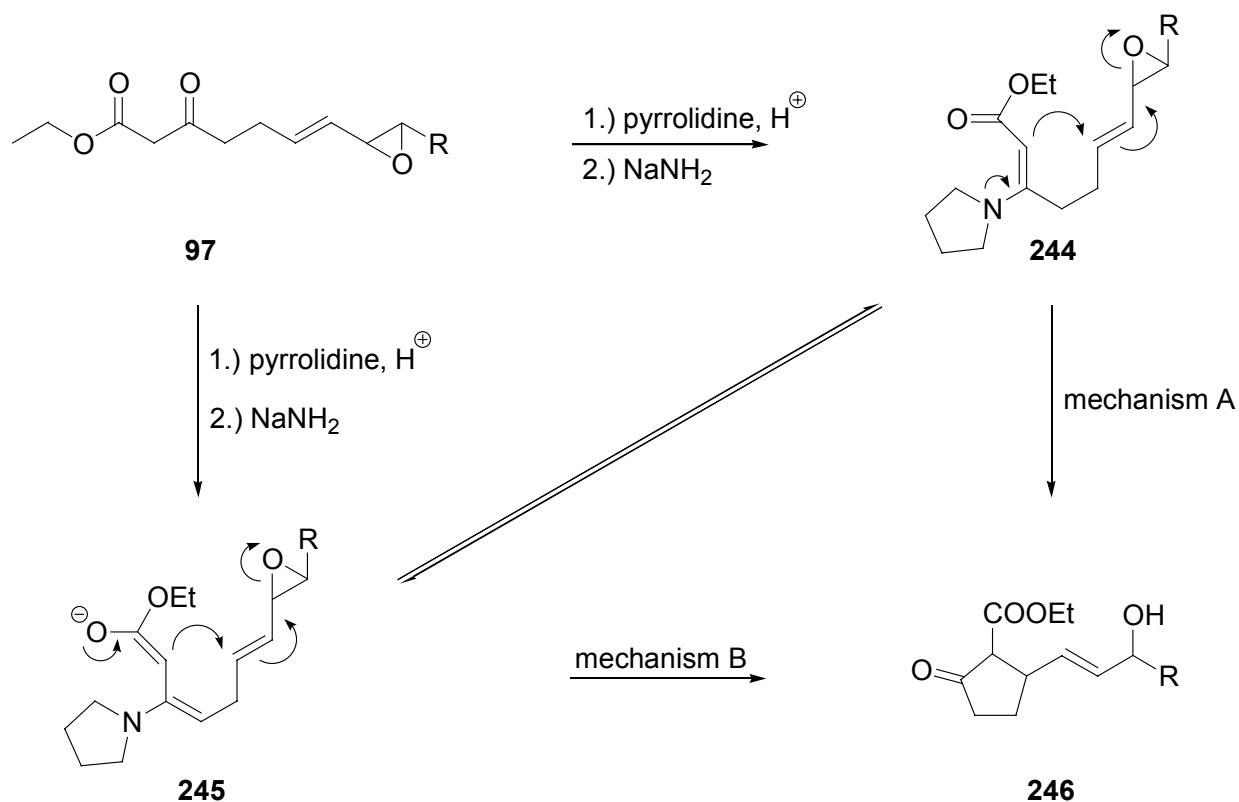
In analogy to the S_Ni' ring closure performed by Toromanoff et al. in the key step of the prostaglandin synthesis, the β -keto-ester *(R,R)*-(*E*)-**241** was prepared from *(R,R)*-(*E*)-**190** and methyl cyanoformate, *Scheme 79*. Deprotonation with LiHMDS and treatment with Me₃SiOTf led to cyclobutanone **242** in 17% yield and approx. 10% ee together with the fragmentation product **243** (11%) and intractable material.

²¹ The indicated ee values refer to C(3) on the cyclobutanone ring.



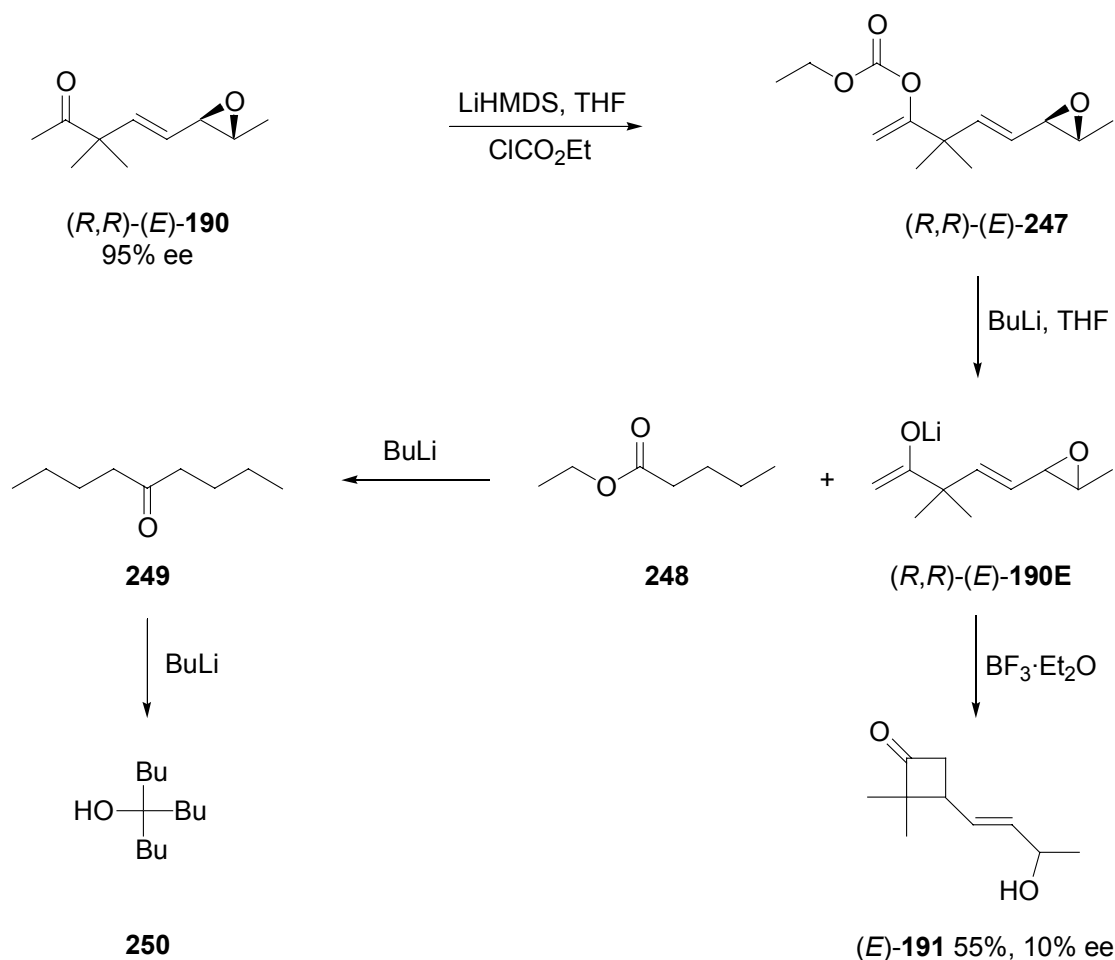
Scheme 79. S_{Ni}' reaction of β -keto ester epoxide (*E*)-241.

Toromanoff and his co-workers did not succeed in performing the S_{Ni}' reaction directly with the β -keto-ester **97**, *Scheme 80*. The authors found, that when the pyrrolidine enamine **244** was treated with NaNH_2 the cyclization would proceed smoothly leading to **246**. Attempts to prepare the pyrrolidine or morpholine enamine of (*R,R*)-(*E*)-**241** failed. The apparent difference between **97** and (*R,R*)-(*E*)-**241** is the fully substituted 4-position in (*R,R*)-(*E*)-**241**. *Mechanisms A + B* illustrate two possible pathways by which the cyclization could have taken place. *Mechanism A* proceeds through enamine **244**, as reported by Toromanoff et al. It is however imaginable that *mechanism B* was actually in effect and that the reaction path proceeded via intermediate **245**. The fully substituted C(4) in (*R,R*)-(*E*)-**241** will inhibit the formation of such an intermediate.



Scheme 80. Possible mechanisms for the S_{Ni}' reaction performed in the prostaglandin synthesis by Toromanoff et al.

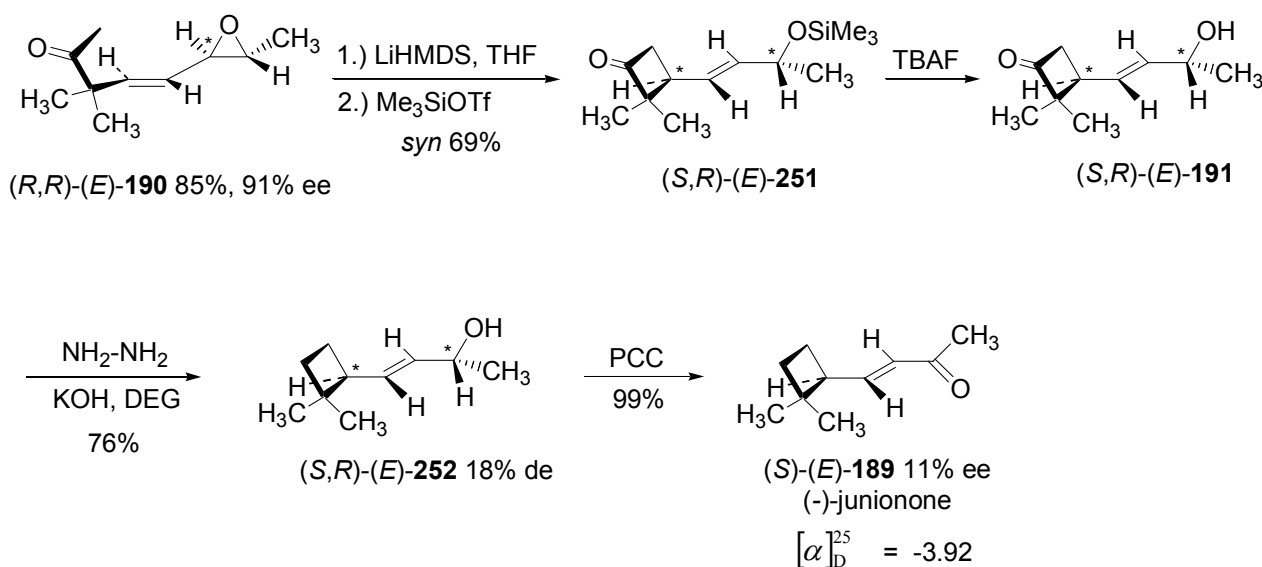
The epoxycarbonate *(R,R)*-(*E*)-**247** was prepared from *(R,R)*-(*E*)-**190** and ethyl chloroformate. It was interesting to observe that when *(R,R)*-(*E*)-**247** was treated with excess BuLi followed by one molar equivalent of $\text{BF}_3 \cdot \text{Et}_2\text{O}$ the desired cyclobutanone (*E*)-**191** was formed in acceptable yield (55%). The enantiomeric excess was 10%, being equal to the ee obtained when performing the cyclization with the original epoxyketone *(R,R)*-(*E*)-**190**, LiHMDS and $\text{BF}_3 \cdot \text{Et}_2\text{O}$. The mechanism illustrated in *Scheme 81* is believed to be in effect. Grignard-style attack on the carbonate by the organo-lithium reagent leads to *(R,R)*-(*E*)-**190E** and one molar equivalent of the ester **248**. Reaction of **248** with an other equivalent of BuLi leads to ketone **249** which will react with another equivalent of BuLi leading to tributyl carbinol **250**. Upon addition of $\text{BF}_3 \cdot \text{Et}_2\text{O}$, *(R,R)*-(*E*)-**190E** will undergo cyclization in the usual manner leading to cyclobutanone (*E*)-**191**. In contrast to previous cyclization experiments starting from *(R,R)*-(*E*)-**190**, the cyclization by this route takes place at lower temperatures and with higher yield. The large amount of BuLi in the reaction mixture will exclude any traces of water, this may be one factor contributing to the higher yield and reactivity. It is conceivable that the lithium alcoholate of **250** is acting as a non-hydrophilic base or has the ability to stabilize the ketoneenolate. **250** was synthesized by an independent route and identified by GC/MS and TLC.



Scheme 81. Cyclobutanone synthesis from β -keto-ester *(R,R)*-(*E*)-**247** with BuLi.

4.4.7 Total synthesis of (-)-(*S*)-junionone

A mixture of (*R,R*)-(*E*)-**190** (85%) and (*R,S*)-(*E*)-**190** (15%) in THF was deprotonated with LiHMDS, *Scheme 82*. One molar equivalent of Me₃SiOTf was added at -70 °C to activate the epoxide moiety. (*S,R*)-(*E*)-**251** was obtained in good yield (69%). Hydrolysis in the presence of fluoride ion led to the allylic alcohol (*S,R*)-(*E*)-**191**. Wolff-Kishner reduction of the cyclobutanone carbonyl group led to cyclobutane (*S,R*)-(*E*)-**252** which, upon oxidation with pyridine chlorochromate afforded (-)-junionone (*S*)-(*E*)-**189** in quantitative yield. The presence of the cyclobutanone ring was clearly indicated by the strong characteristic carbonyl band at 1671 cm⁻¹ in the IR spectrum. The olefinic protons showed a coupling constant of 15.0 Hz in the ¹H-NMR (500 MHz, CDCl₃) spectrum indicating the presence of a (*E*)-configured double bond. Unfortunately, severe epimerization takes place during the cyclization of (*R,R*)-(*E*)-**190** leading to only 11% ee at C(3) of the cyclobutane ring of the final product (*S*)-(*E*)-**189**, *Chapter 4.4.5, Scheme 73*. The enantiomeric enrichment of (-)-junionone (-)-(*S*)-(*E*)-**189** is an indicator that the reaction proceeds with a slight preference for *syn* geometry in the transition state.

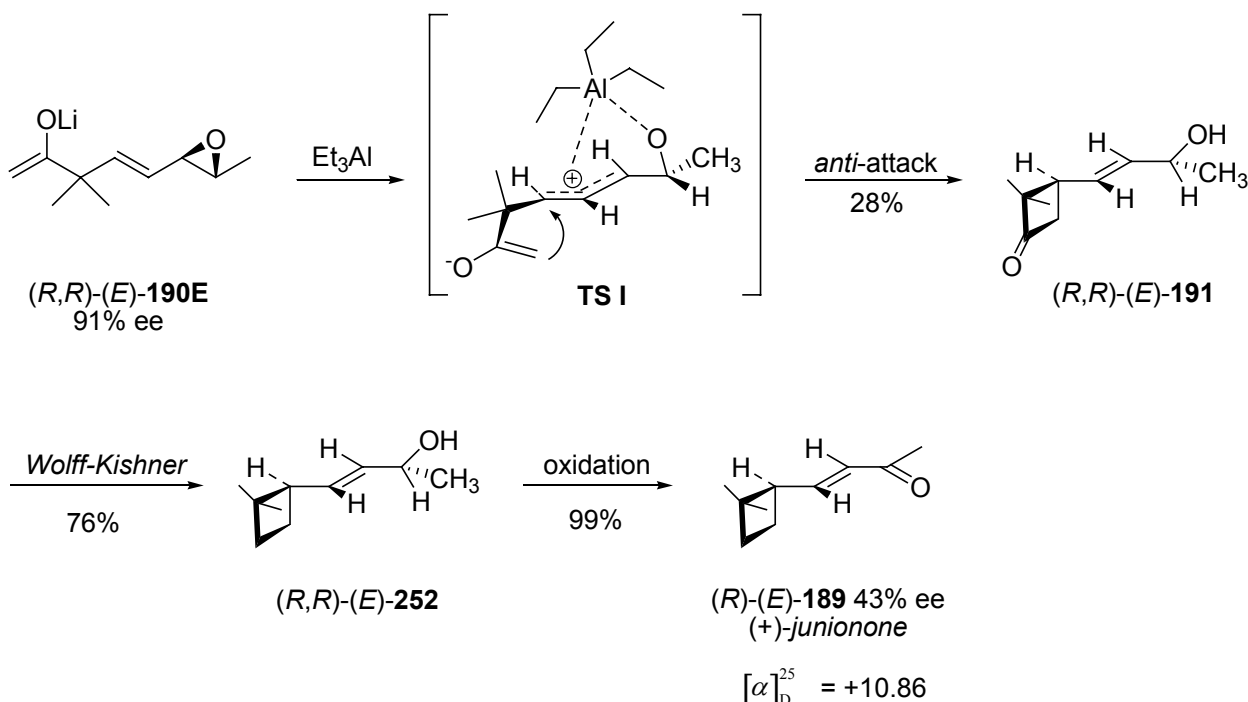


Scheme 82. Synthesis of (-)-junionone using Me₃SiOTf as the Lewis acid.

4.4.8 Total synthesis of (+)-(*R*)-junionone

During the cyclization experiments with different Lewis acids it was found that Et₃Al led to the highest enantiomeric enrichment at C(3) of the cyclobutanone ring in (*E*)-**251**, *Chapter 4.4.5, Table 8*. (*R,R*)-(*E*)-**190E** was treated with one molar equivalent of Et₃Al at -70 °C, *Scheme 83*. Wolff-Kishner reduction of the cyclobutanone carbonyl group followed by oxidation afforded junionone in 21% overall yield. The sign of the optical rotation ($[\alpha]_D^{25} = +10.86$) showed that (+)-junionone (*R*)-(*E*)-**189** was obtained, clearly resulting from *anti* attack of the enolate. Because the cyclization of (*R,R*)-(*E*)-**190** most likely proceeds by a allyl cation intermediate, the reaction no

longer follows the rules of an S_N1 reaction. It is imaginable that Et_3Al coordinates to the epoxide oxygen and to the allyl cation, thereby shielding one enantiotopic face of the molecule against nucleophilic attack from the enolate. Do to the occupation of the *syn* face by the Et_3Al the nucleophile is forced to attack with *anti* geometry leading to the observed product (+)-junionone (*R*)-(*E*)-**189**. The selective formation of (*E*)-configured (+)-junionone indicates that transition state **TS I** is in effect, thereby minimizing the unfavorable $A^{1,3}$ strain, Chapter 4.2, Figure 22.



Scheme 83. Synthesis of (+)-junionone with Et_3Al as Lewis acid.

4.4.9 Isolation of natural junionone from *juniperus communis* L.

The structure of natural junionone was first reported by Thomas et al. in 1973 [77], Chapter 4.4.1. The authors isolated a small amount of junionone from the oil of the berrys of the juniper tree, *juniperus communis* L. Due to the small amount of sample, the authors were not able to verify the sign of the optical rotation and therefore the absolute configuration of the natural product was never determined. Modern capillary GC methods with optically active stationary phases will allow the determination of the absolute configuration of natural junionone by co-injection with synthetic (-)-(*E*)-**189** of known configuration. GC/MS analysis revealed that natural juniper berry oil contains approx. 0.01% (*E*)-**189**. In order to obtain credible results, an enriched sample of natural junionone had to be isolated from juniper berry oil. GC analysis of natural juniper oil revealed as many as 224 different compounds. Terpenes and more complex polycyclic hydrocarbons constitute the bulk of the compounds (~90%) in the mixture. Starting from 1 kg of natural juniper berry oil, the hydrocarbons were removed by column chromatography over silica gel with hexane as the eluent. The more polar compounds were retained on the surface of the silica gel. The polarity of the solvent was increased by adding MtBE and the eluent was collected in fractions and

analyzed by GC and GC/MS. A colorless oil (250 mg) containing 7% of natural junionone was isolated and further purified by preparative HPLC, leading to 32mg of colorless oil with a junionone concentration of 55%. Examination by chiral GC revealed an enantiomeric excess of 43%, *Figure 36*.

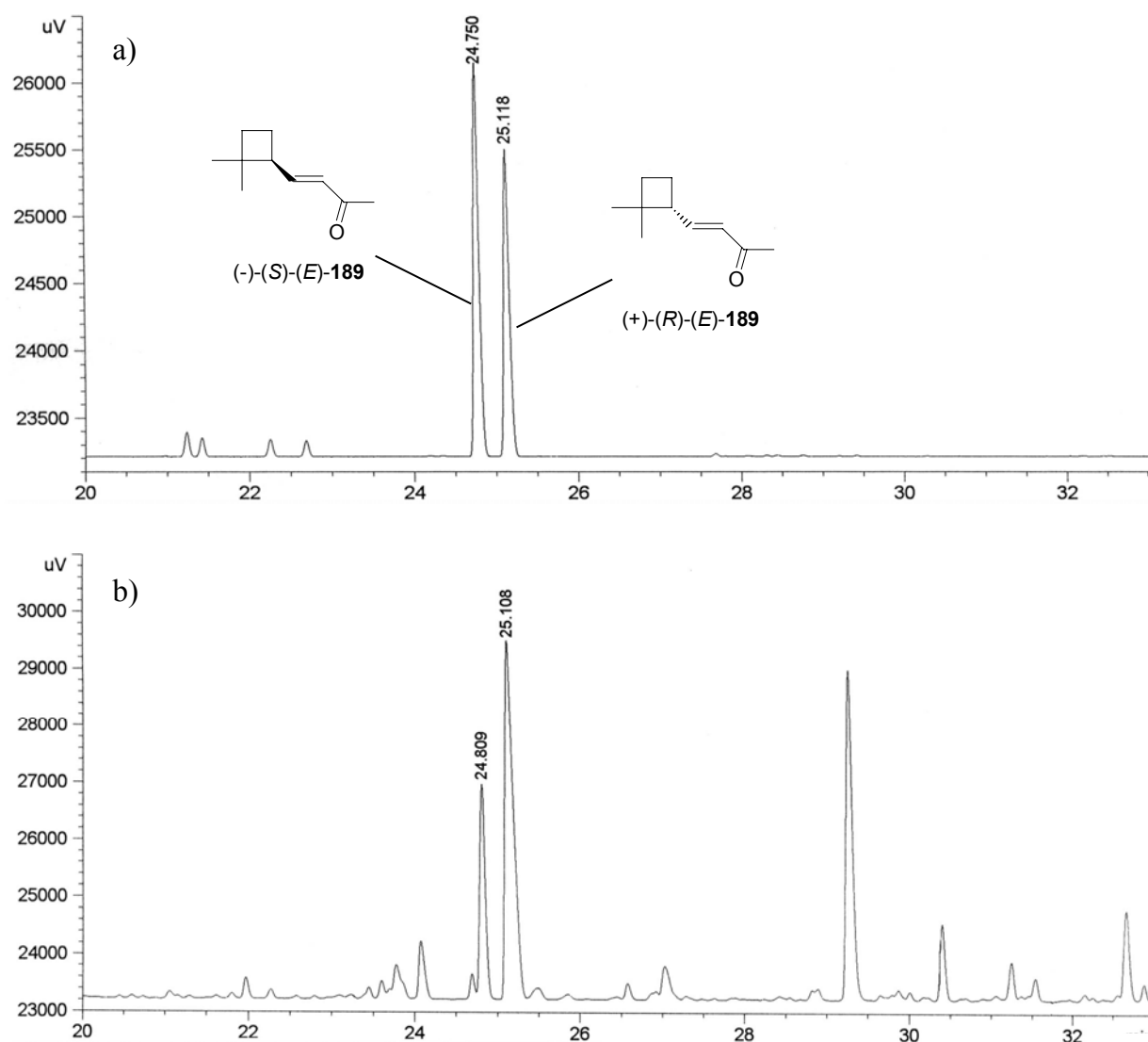


Figure 36. Analysis of junionone with chiral GC.

a) $(-)$ -junionone $(-)-(S)-(E)$ -189. b) Enriched natural junionone from *juniperus communis* L.

Chromatogram (a) shows the GC of synthetic $(-)-(S)-(E)$ -189 (10% ee), on an optically active stationary phase. Chromatogram (b) shows the enantiomeric distribution of natural junionone in the enriched sample. Comparison of the two chromatograms clearly shows the opposite enantiomeric enrichment of the two samples.

During the isolation process from natural juniper berry oil the compounds were adsorbed on silica gel for extended periods of time. It was therefore imaginable that epimerization of the natural junionone $(+)-(R)-(E)$ -189 occurred, falsifying the results. A sample of the enriched natural

junionone (55%, 43% ee) was stored at room temperature in a suspension of silica gel and hexane/MtBE for several weeks. The enantiomeric distribution of (*E*)-**189** was monitored by GC with an optically active stationary phase. No significant change of the enantiomeric excess was observed over a period of four weeks. It can therefore be concluded, that natural junionone does not occur as a single enantiomer, but rather as an approximately 7:3 mixture of (+)-(*R*)-junionone and (-)-(*S*)-junionone. Synthetic (+)-junionone (+)-(*R*)-(*E*)-**189**, prepared by using Et₃Al as the epoxide activating Lewis acid, was analyzed by chiral GC as well, *Figure 37*. Coincidentally the enantiomeric enrichment of the synthetic (+)-junionone (43%) corresponded precisely to that of the (+)-junionone isolated from nature.

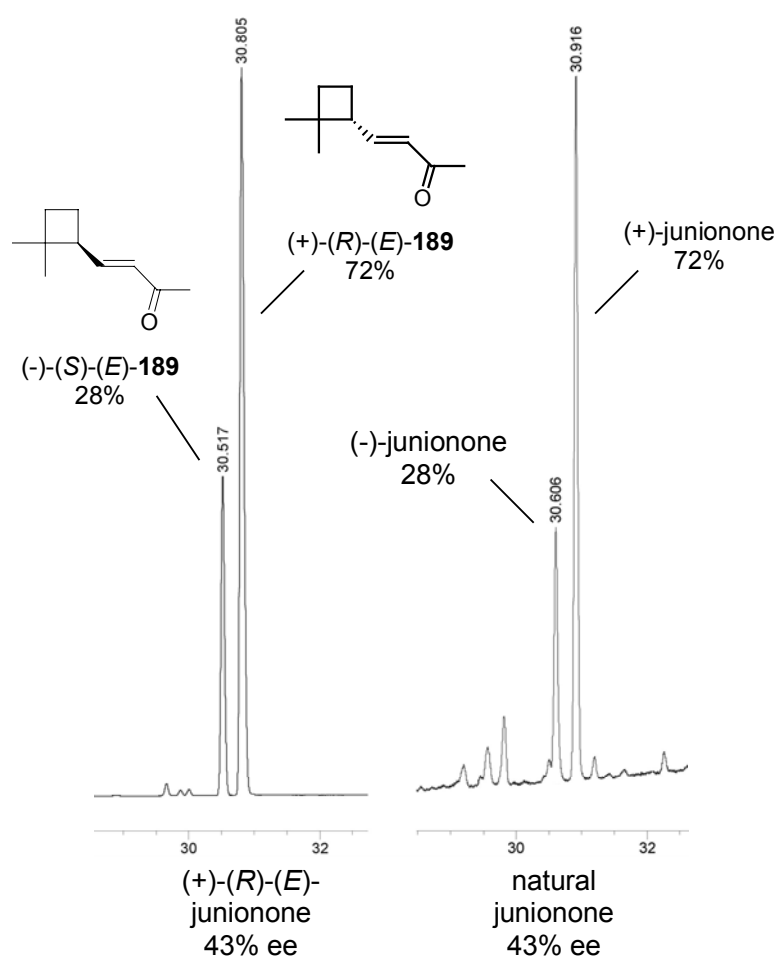
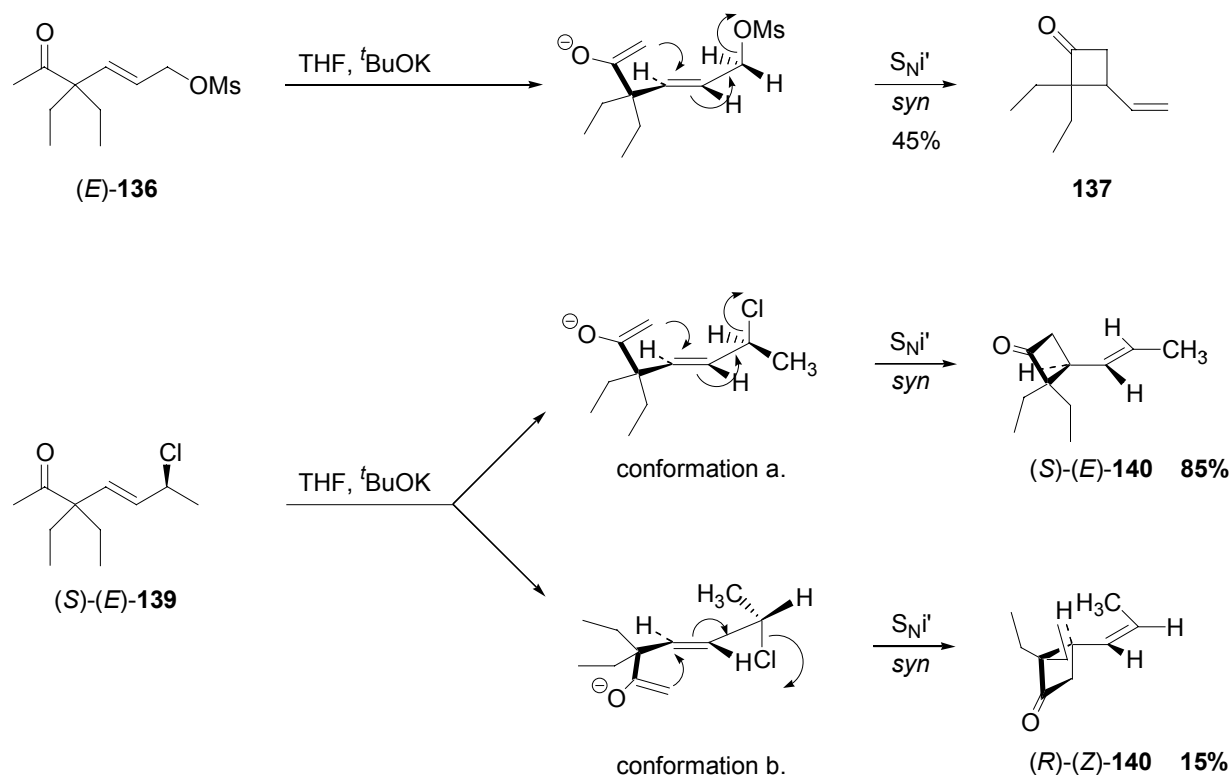


Figure 37. Chiral GC of synthetic (+)-junionone vs. natural junionone.

Based on these results and those obtained by Thomas et al. [77] it has now been found that natural junionone, isolated from the oil of the berries of *juniperus communis* L., occurs as the (+)-(*R*)-(*E*)-enantiomer with 43% enantiomeric excess.

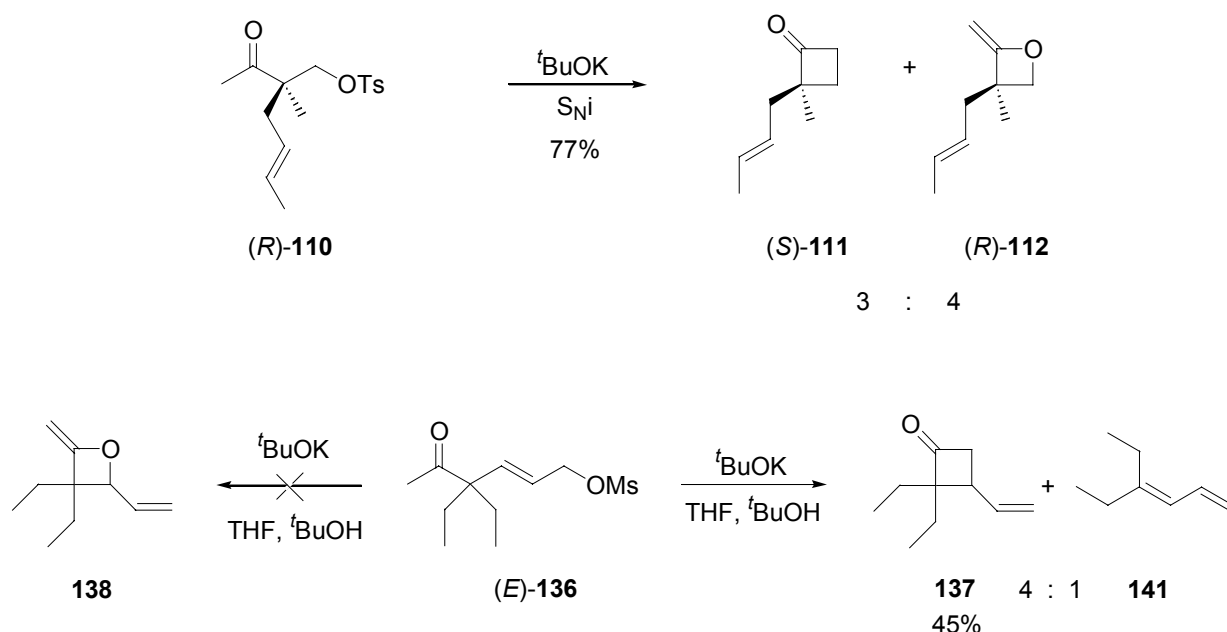
4.5 Conclusions

The current research has shown that substituted cyclobutanones (e.g. **137**) can be prepared by a S_Ni' reaction of β,γ -unsaturated ketones (e.g. **136**), *Scheme 84*. Mechanistic studies with chloro-ketone (*S*)-(*E*)-**139** led to the conclusion that the nucleophilic displacement of the chloride ion by the ketone enolate proceeded exclusively with *syn*-stereochemistry leading to (*E*)- and (*Z*)-**140** of opposite absolute configuration at C(3) of the cyclobutanone ring. These findings were in accord with the results from Stork and White, who found that nucleophilic S_Ni' displacement with enolates in sterically unbiased systems will take place *syn* to the leaving group [42]. The ratio of (*E*)- and (*Z*)-**140** (85:15) reflects the conformational equilibrium of (*S*)-(*E*)-**139** in the transition state.



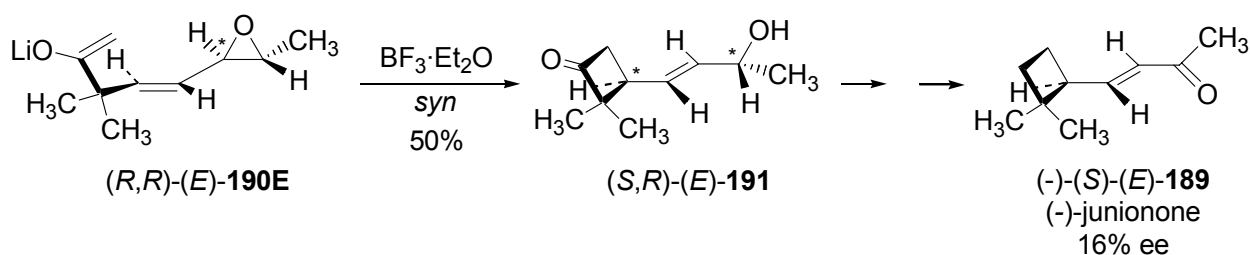
Scheme 84. Mechanism of the S_Ni' reaction leading to cyclobutanones.

In contrast to the synthesis of cyclobutanone (*S*)-**111** and oxetane (*R*)-**112** by the S_Ni reaction reported by Fráter et al. (*Chapter 4.1.3, Scheme 34*) the current S_Ni' pathway did not lead to the formation of O-alkylation product **138**, *Scheme 85*. The preference for C-alkylation in the 4-*exo-trig* S_Ni' reaction can result from a HSAB effect. The carbanion in the ambident ketone enolate acts as a softer base than the oxygen anion and can therefore be expected to favour nucleophilic attack at a soft acid. Due to the more pronounced electron distribution in the allylic system, the olefinic C(4) in (*E*)-**136** constitutes a softer acid than the quaternary C(3) in (*R*)-**110**. On the other hand, fragmentation leading to **141**, being the major side reaction in the 4-*exo-trig* S_Ni' reaction, was not observed by Fráter et al. in the S_Ni reaction.



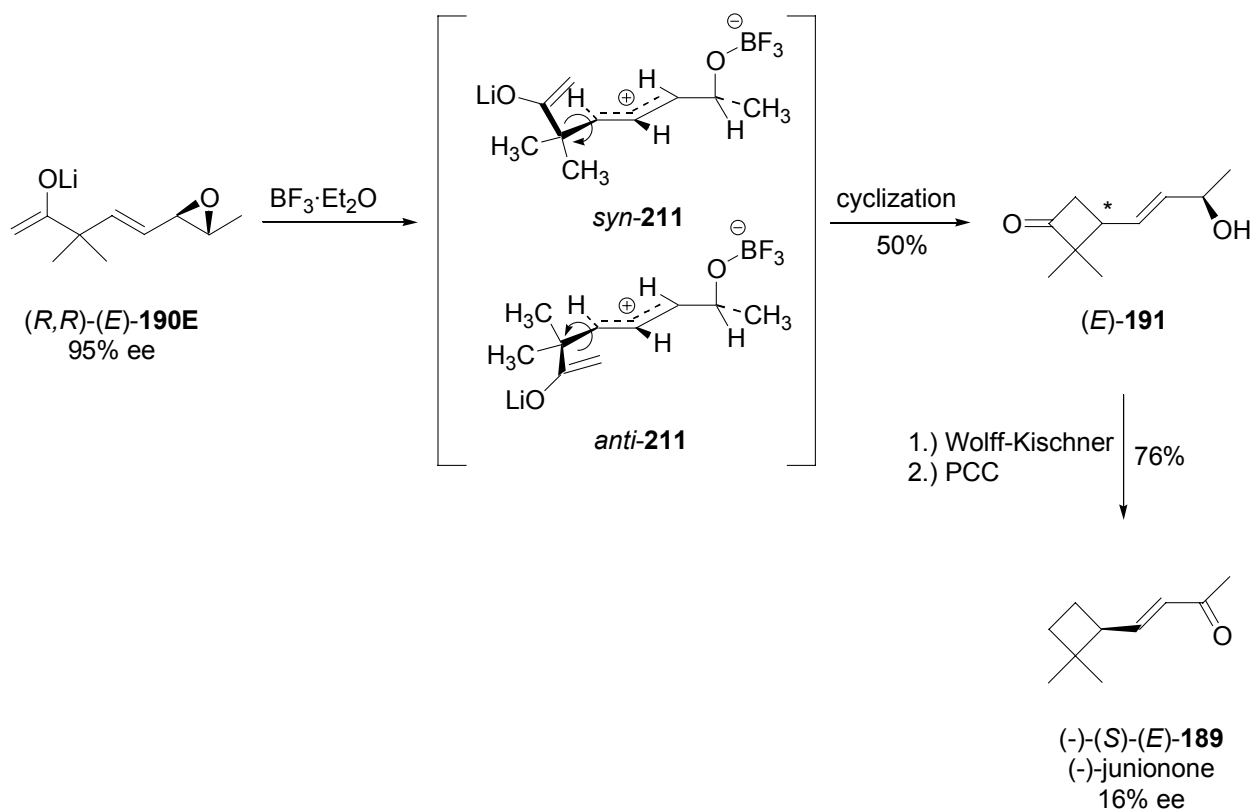
Scheme 85. Cyclobutanone vs. oxetane formation in the S_{Ni} and S_{Ni}' reaction.

The findings offered a new stereoselective route to (+)-(R)- and (-)-(S)-junione, an olfactorily interesting natural cyclobutane mono-terpenoid isolated from *juniperus communis* L., Scheme 86. Based on the S_{Ni}' displacement reaction of an epoxy ketone, applied by Toromanoff in the total synthesis of prostaglandin **99** (Chapter 4.1, Scheme 32) (-)-(S)-(E)-**189** was prepared by allylic epoxide displacement of (R,R)-(E)-**190E** by the ketone enolate followed by reduction of the cyclobutanone (S,R)-(E)-**191** and oxidation of the allylic alcohol. The epoxide moiety in (R,R)-(E)-**190E** was not reactive enough to enable nucleophilic attack of the ketone enolate and had to be activated with a Lewis acid. $\text{BF}_3 \cdot \text{Et}_2\text{O}$ and $(\text{CH}_3)_3\text{SiOTf}$ were suited well leading to the desired cyclobutanone (E)-**191** in 50% and 69% yield, respectively.



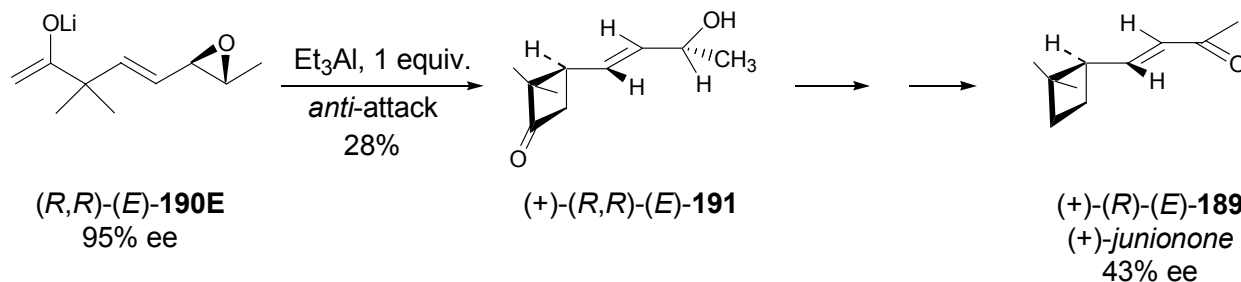
Scheme 86. Total synthesis of (-)-junione (-)-(S)-(E)-**189**.

Under these reaction conditions significant epimerization was observed at the C(3) ring carbon of the cyclobutanone (S,R)-(E)-**191**. A reaction mechanism involving the allyl cation intermediate **211** was considered to be in effect, Scheme 87. The value of the coupling constant of the olefinic proton at C(2') in the ^1H -NMR spectrum ($J = 15$ Hz) indicated that the double bond in **191** possesses (E)-configuration. Therefore (R,R)-(E)-**190E** must adapt a *trans*-conformation in the transition state and loss of stereoselectivity results from the lack of *syn/anti* preference of the allyl cation.



Scheme 87. Allyl cation intermediate in the cyclization of **(R,R)-(E)-190E**.

Extensive experimental research on the effect of different Lewis acids on the yield and stereoselective outcome of the reaction showed that epoxide activation with Et_3Al results in enrichment of the opposite enantiomer **(+)-(R)-(E)-189** in 43% excess, *Scheme 88*.



Scheme 88. Stereoselective cyclization of **(R,R)-(E)-190** with Et_3Al .

The absolute configuration of natural junione has not been reported so far. A sample of enriched natural junione was isolated from the oil of the berries of the juniper tree and compared to the synthetic junione of known configuration by chiral GC. It was found, for the first time, that natural junione occurs predominantly as the **(+)-(R)-**enantiomer with 43% enantiomeric excess.

4.6 Experimental

Abbreviations

abs.	absolut
aq.	aqueous
DEG	diethylenglycol
dil.	diluted
DMF	dimethylformamide
hex	hexane
M	mol/liter
min.	minutes
MS	mass spectrometry
MtBE	<i>tert</i> -butylmethyl ether
r.t.	room temperature
TEA	triethylamine
THF	tetrahydrofuran
TLC	thin layer chromatography

General procedures.

¹H-NMR-Spectra: Routine NMR-spectra were measured on *Bruker AC300* and *Bruker ARX300* (both 300 MHz) spectrometers. Experiments using chiral shift reagents were carried out on *Bruker DPX-400* and *Bruker AVANCE 500* instruments. Deuterated chloroform and benzene were used as solvent with tetramethylsilane as an internal standard. The chemical shifts are indicated in ppm and the values of the J_{HH} -coupling constants are given in Hz. Multiplicities are specified by abbreviations, *s* = singlet, *d* = doublet, *t* = triplet, *m* = multiplet and *td* = triplet of doublets.

¹³C-NMR-Spectra: *Bruker AC300*, *Bruker DPX-400* and *Bruker AVANCE 500*. The solvent itself served as the internal standard: CDCl_3 ($\delta(\text{C}) = 77.00$ ppm, *t*, $J_{\text{CD}} = 31.5$ Hz). DEPT (Distortionless Enhancement by Polarization Transfer) experiments were performed to determine the multiplicity of the carbon nuclei. The multiplicity is designated *q* (quartet) for CH_3 , *t* (triplet) for CH_2 , *d* (doublet) for CH and *s* (singlet) for fully substituted carbon atoms.

Mass Spectrometry: GC/MS was measured routinely on a *HP MSD 5973* instrument with a 30m *HP5/MS* or *Varian VF5ms* column. High resolution mass spectrometry was performed on a *Finnigan MAT 95* (*Finnigan MAT95*, San Jose, CA; USA) double-focusing magnetic sector mass spectrometer (geometry BE). Mass spectra were measured in electron impact (EI) mode at 70 eV,

with a source temperature of 200°C, an acceleration voltage of 5 kV, and a resolution of 10'000. The instrument was scanned between m/z 30 und 900 at 2 scan min.⁻¹. Perfluorokerosene (PFK, ICN Pharmaceutical Inc, Plainview, NY, USA) served for calibration.

Infrared Spectrometry: *Spectrum One FT-IR-* and *Bruker Vector 22 FT-IR*-spectrometers. Liquids were measured 5% in chloroform (0.05 mm cell) and solids were measured as KBr pellets (1mg substance/100mg KBr). The background spectrum was recorded either from the pure solvent or the empty sample path. The relative intensities of the absorption bands are indicated as vs = very strong (> 90%), s = strong (70-90%), m = medium (40-70%), w = weak (< 40%), br = broad.

Thin Layer Chromatography: Silica gel pre-coated plastic sheets *Macherey-Nagel Polygram SIL G/UV₂₅₄* or aluminum oxide pre-coated plastic sheets *Macherey-Nagel Polygram N/UV₂₅₄*. Substances were made visible under UV-light (254 nm or 366 nm) or with staining reagents. $KMnO_4$ reagent was prepared by dissolving 5g of $KMnO_4$ and 15g of K_2CO_3 in 250.0 mL of water. Cesium reagent contained 25g phosphorous molybdenum acid, 13g $Ce(SO_4)_2 \cdot 4 H_2O$ and 60.0 mL H_2SO_4 98% per liter of aqueous solution

Column Chromatography: Silica gel *Chemie Uetikon ZEOCHEM C-Gel C-560*, particle size 40-63 μm or aluminum oxide *Fluka type 5016 basic*, particle size 50-150 μm ; pH 9.5 +/- 0.5 Act. III (*Brockmann*).

Short Path Distillation: Most products were short path distilled by the „kugelrohr“-method. A modified rotary evaporator motor was utilized and the bulb was heated by means of a *Büchi* kugelrohr oven or a hot air gun for micro scale amounts. The vacuum was provided either by a rotary slide pump (0.05 mbar) or by a water-jet vacuum pump (10 mbar).

Gas Chromatography: Standard GC analysis was performed on a *HP 5890* instrument with *HP 3396A* integrator, column DB5 30m, 0.53 mm. Split ratio 1:100, initial temperature 80 °C, rate 10 °C/min. GC/MS was performed on a *CE-Instruments GC 8000 Top* equipped with a *Thermo Quest Voyager* quadrupol MS.

4.6.1 Mechanistic studies on the S_Ni' reaction.

4-(2-Ethylbut-1-enyl) morpholine (143).

2-Ethylbutyric aldehyde **142** (103.85 g, 1.04 mol) was mixed with 200.0 mL of benzene and morpholine (90.00 g, 1.04 mol) was added. The mixture was refluxed over a Dean-Stark water separator for 3 1/2 h. During the course of the reaction the theoretical amount of water (18.7 mL, 1.04 mol) was separated. The mixture was cooled to room temperature and the solvent was removed in vacuo. Distillation of the residue over a 20 cm Vigreux column (48 °C, 0.05 mbar) gave **143** (151.63 g, 86%) as a clear liquid.

IR (neat): 2961m, 2852m, 2806w, 1664w, 1452m, 1360w, 1260m, 1170m, 1115s, 1014m, 866m, 849m.

¹H-NMR (300 MHz, CDCl₃): 5.27 (s, 1 H); 3.71 (m, 4 H); 2.55 (m, 4 H); 2.19 (q = 7.6 Hz, 2 H); 1.96 (m, 2 H); 0.98 (t, 7.6 Hz, 6 H).

¹³C-NMR (75 MHz, CDCl₃): 135.1 (s); 134.2 (d); 66.7 (2 t); 53.4 (2 t); 25.8, 20.7 (2 t); 12.9, 12.4 (2 q).

EI-MS (GC/MS): 169 (6, M^+), 168 (60, $[M-H]^+$), 155 (20), 153 (100), 139 (37), 125 (11), 109 (14), 95 (55).

High res. EI-MS calculated for C₁₀H₁₉ON: 169.1467; *found:* 169.1468.

4-Cyclohexylidenemethylmorpholine (166).

Cyclohexanecarbaldehyde **165** (93.00 g, 0.83 mol) was mixed with 200.0 mL of benzene and morpholine (72.00 g, 0.83 mol) was added. The temperature of the mixture rose to 65 °C, the reactor was equipped with a Dean-Stark H₂O-separator and the contents were heated to reflux. After 3 h at reflux the theoretical amount of water (15.00 mL, 0.83 mmol) had separated and the mixture was cooled to room temperature. Since no acid catalyst was necessary for the reaction to proceed, the mixture was concentrated in vacuo and the product was purified by distillation over a 20 cm Vigreux column (10 mbar, 119 °C). **166** (134.00 g, 89%) was obtained as colorless oil.

IR (neat): 2921s, 2850s, 2806m, 1673w, 1447m, 1364w, 1265w, 1162m, 1115s, 1014m, 865m, 838m.

¹H-NMR (300 MHz, CDCl₃): 5.29 (m, 1 H); 3.70 (m, 4 H); 2.56 (m, 4 H); 2.22 (m, 2 H); 1.99 (m, 2 H); 1.52 (m, 6 H).

¹³C-NMR (75 MHz, CDCl₃): 132.4 (d); 131.0 (s); 66.7 (2 t); 53.3 (2 t); 33.2, 28.3, 27.8, 27.15, 26.7 (5 t).

EI-MS (GC/MS): 181 (28, M^+), 180 (100, $[M-H]^+$), 179 (75), 165 (29), 151 (95), 137 (44), 125 (74), 122 (74), 121 (81), 111 (67), 107 (75), 99 (35), 94 (64), 93 (77), 85 (55), 79 (68), 66 (65).

High res. EI-MS calculated for C₁₁H₁₉ON: 181.1467; *found:* 181.1466.

2,2-Diethyl-3-oxobutylaldehyde (145).

4-(2-Ethylbut-1-enyl)morpholine **143** (169.00 g, 1.00 mol) was placed in a reactor with a strong mechanical stirrer. MtBE was added (250.0 mL) and the solution was stirred at room temperature. Acetyl chloride (157.00 g, 2.00 mol) was added at once. The reaction mixture was stirred at reflux for 4 h. A white solid precipitated and the mixture became pasty. After cooling to room temperature, the solid was removed by filtration and washed with MtBE. The white solid was dissolved in 200.0 mL of water and the heterogeneous mixture was stirred over night. After extraction with MtBE the organic layers were washed with saturated aq. NaHCO₃, water and brine. The organic layers were dried over MgSO₄ and concentrated. Distillation of the residue over a 20 cm Vigreux column (78 °C, 20 mbar) afforded **145** (55.50 g, 39%) as a colorless liquid.

IR (CCl₄): 2972w, 2883w, 1725m, 1698s, 1460w, 1359m, 1219w, 1121w, 771w.

¹H-NMR (300 MHz, CDCl₃): 9.74 (s, 1 H); 2.17 (s, 3 H); 2.01-1.80 (m, 4 H); 0.83 (t = 7.6 Hz, 6 H).

¹³C-NMR (75 MHz, CDCl₃): 207.4 (s); 202.3 (d); 67.8 (s); 27.0 (q); 23.8 (2 t); 8.2 (2 q).

EI-MS (GC/MS): 142 (1, M⁺), 114 (18), 100 (23), 99 (15), 85 (38), 71 (38), 43 (100), 41 (18).

1-Acetylcyclohexanecarbaldehyde (168).

4-Cyclohexylidenemethylmorpholine **166** (45.00 g, 0.25 mol) was added at once to a mixture of AcOCl (19.50 g, 0.25 mol) and 160.0 mL of CH₂Cl₂. The mixture was heated to reflux (45 °C) and stirring was continued for 3 h. The reaction mixture turned deep red. GC analysis showed that some starting material remained in the mixture. Another molar equivalent of AcOCl (19.50 g, 0.25 mol) was added and stirring at reflux was continued for another hour. The reaction mixture was concentrated and mixed with MtBE and water. After stirring at room temperature for 15 h the mixture had decolorized significantly resulting in an orange biphasic mixture. The layers were separated and the aq. layer was extracted with MtBE. The combined organic layers were washed with water and brine, dried and concentrated. The crude product **168** (12.26 g, 32%) was purified by distillation over a 20 cm Vigreux column (0.06 mbar, 62 °C).

IR (CCl₄): 2934m, 2856w, 1727m, 1697s, 1450m, 1356m, 1213w, 1182m, 900w, 830w, 689w.

¹H-NMR (300 MHz, CDCl₃): 5.29 (s, 1 H); 3.70 (m, 4 H); 2.56 (m, 4 H); 2.22 (m 2 H); 1.99 (m 2 H); 1.52 (m 6 H).

¹³C-NMR (75 MHz, CDCl₃): 132.4 (d); 131.0 (s); 66.7, 53.3 (4 t); 33.2, 28.3, 27.8, 27.2, 26.7 (5 t).

EI-MS (GC/MS): 125 (60, [M-CHO]⁺); 110 (100, [M-CH₃CO]⁺); 96 (50); 93 (49); 83 (47); 80 (53); 78 (54); 66 (44); 54 (43).

Anal. calc. for C₉H₁₄O₂ (154): C 70.10, H 9.15; found: C 70.18, H 9.15.

(E)-4,4-Diethyl-5-oxohex-2-enoic acid ethyl ester ((*E*)-**152**).

Sodium hydride 60% in paraffin oil (1.70 g, 42.30 mmol) was suspended in 40.0 mL of THF. Triethyl phosphonoacetate **150** (7.57 g, 33.80 mmol) was added dropwise. The mixture slowly became homogeneous and the temperature rose to 35 °C. After stirring for 20 min. the mixture was cooled to 0-5 °C using an ice/NaCl bath. 2,2-Diethyl-3-oxobutyraldehyde **145** (4.00 g, 28.20 mmol) was added slowly while maintaining the temperature at 0 °C. After the addition the cooling bath was removed and the reaction mixture stirred for additional 30 min. TLC analysis on silica gel plates using hex/MtBE 8:2 as the eluent showed a UV-active product spot with an R_f -value of 0.3. The reaction mixture was poured onto ice/water and extracted with hexane. The hexane layers were combined and washed with aq. NaHCO_3 , dried and concentrated. Short path distillation (90 °C, 0.05 mbar) afforded (*E*)-**152** (5.04 g, 84%) as a colorless oil.

IR (CCl_4): 2971 w , 1708 s , 1646 w , 1461 w , 1366 w , 1301 m , 1270 m , 1168 s , 1038 m , 992 m .

$^1\text{H-NMR}$ (300 MHz, CDCl_3): 11.36 (d , $J = 16.4$ Hz, 1 H); 10.22 (d , $J = 16.4$ Hz, 1 H); 8.56 (m , 2 H); 6.45 (s , 3 H); 6.13 (m , 4 H); 5.65 (t , $J = 7.2$ Hz, 3 H); 5.12 (t , $J = 7.6$ Hz, 6 H).

$^{13}\text{C-NMR}$ (75 MHz, CDCl_3): 208.6, 166.1 (2 s); 149.5, 122.0 (2 d); 60.3 (t); 58.3 (s); 26.4 (2 t); 26.1, 14.1 (2 q); 8.2 (2 q).

EI-MS (GC/MS): 170 (100, $[\text{M}-\text{C}_2\text{H}_4]^+$), 155 (11), 142 (11), 124 (28), 109 (24), 95 (48), 81 (17), 67 (17), 55 (26), 43 (80), 29 (18).

Anal. calc. for $\text{C}_{12}\text{H}_{20}\text{O}_3$: C 67.89, H 9.50; *found*: C 67.64, H 9.31.

(E)-3-(1-Acetylcyclohexyl)acrylic acid ethyl ester ((*E*)-**169**).

Sodium hydride 65% in paraffin oil (4.48 g, 112.00 mmol) was suspended in 250.0 mL of THF. A solution of triethyl phosphonoacetate **150** (20.00 g, 89.60 mmol) in 100.0 mL of THF was added in portions. The temperature was kept below 35 °C by means of an ice/ H_2O bath. After stirring at room temperature for 30 min. the mixture was cooled to -5 °C with an ice/NaCl bath. 1-Acetylcyclohexanecarbaldehyde **168** (11.50 g, 74.70 mmol) was added as a solution in 80.0 mL of THF over 30 min. After the addition was complete the mixture was stirred at room temperature for 30 min. The reaction was monitored by GC.

The mixture was poured onto ice/ H_2O and extracted with hexane. The combined organic layers were washed with aq. NaHCO_3 , brine and water. The hexane solution was dried over MgSO_4 and concentrated. The crude product was purified by distillation over a 15 cm Vigreux column (0.05 mbar, 112 °C) to give (*E*)-**169** (10.45 g, 62%) as a colorless oil.

IR (CCl_4): 2935 m , 2857 w , 1707 vs , 1643 m , 1448 w , 1365 w , 1308 m , 1266 m , 1166 s , 1037 m , 987 m .

$^1\text{H-NMR}$ (300 MHz, CDCl_3): 6.84 (d , $J = 16.0$ Hz, 1 H); 5.87 (d , $J = 16.0$ Hz, 1 H); 4.2 (m , 2 H); 2.11 (s , 3 H); 2.04-1.94 (m , 2 H); 1.72-1.61 (m , 2 H); 1.60-1.36 (m , 6 H); 1.30 (m , 3 H).

$^{13}\text{C-NMR}$ (75 MHz, CDCl_3): 208.0, 166.0 (2 s); 150.2, 122.3 (2 d); 60.3 (t); 55.0 (s); 32.4 (2 t); 25.8 (1 q); 25.4, 22.4 (2 t); 14.0 (q).

EI-MS (GC/MS): 206 (1, $[\text{M-H}_2\text{O}]^+$), 182 (100, $[\text{M-CH}_2\text{CO}]^+$), 154 (10), 136 (15), 107 (44), 94 (16), 79 (31), 67 (28), 55 (18), 43 (65), 29 (18).

(E)-4,4-Diethyl-5-(trimethylsilyloxy)hexa-2,5-dienoic acid ethyl ester ((*E*)-**161**).

(*E*)-4,4-Diethyl-5-oxohex-2-enoic acid ethyl ester (*E*)-**152** (26.46 g, 125.00 mmol) was placed in the reactor and 50.0 mL of CH_3CN were added. Triethylamine (17.67 g, 175.00 mmol) and chlorotrimethylsilane (18.90 g, 175.00 mmol) was added to the stirred solution. A solution of NaI (26.26 g, 175.00 mmol) in 140.0 mL of CH_3CN was prepared and added dropwise at room temperature. The temperature slowly rose to 36 °C. After the addition the mixture was heated to 50-60 °C and stirred for 3 h. GC analysis of the reaction mixture showed that the reaction had only proceeded to 50%. Several tests showed, that if the GC sample was treated with water prior to injection, the silyl ether will decompose leading back to the starting material. Finally, GC analysis of the untreated reaction mixture showed that the reaction had gone to completion. The reaction mixture was poured onto dil. NaHCO_3 /ice and was extracted with MtBE. The organic layers were washed with water and brine. After concentration the product was distilled over a 15 cm Vigreux column (97 °C, 0.05 mbar). (*E*)-**161** (29.00 g, 82%) was obtained as a colorless oil.

IR (CCl_4): 2968w, 1720m, 1620w, 1248s, 1176m, 1144m, 1016s, 842vs.

$^1\text{H-NMR}$ (300 MHz, CDCl_3): 6.73 (d, $J = 16.2$ Hz, 1 H); 5.59 (d, $J = 16.2$ Hz, 1 H); 4.01 (dd, $J = 7.1, 14.1$ Hz, 2 H); 3.93 (dd, $J = 2.0, 29.6$ Hz, 2 H); 1.39 (m, 4 H); 1.11 (m, 3 H); 1.11 (t, $J = 7.1$ Hz, 3 H); 0.59 (m, 6 H); 0.00 (s, 9 H).

$^{13}\text{C-NMR}$ (75 MHz, CDCl_3): 167.0, 160.1 (2 s); 153.5, 120.0 (2 d); 90.4, 60.1 (2 t); 50.0 (s); 26.7 (2 t); 14.2, 8.4, 0.0 (6 q).

EI-MS (GC/MS): 284 (5, M^+), 269 (7, $[\text{M-CH}_3]^+$), 255 (19, $[\text{M-C}_2\text{H}_5]^+$), 213 (15), 181 (15), 151 (8), 137 (10), 109 (13), 95 (11), 83 (20), 75 (31), 73 (100), 45 (18), 29 (12).

(E)-3,3-Diethyl-6-hydroxyhex-4-en-2-one ((*E*)-**163**).

(*E*)-4,4-Diethyl-5-(trimethylsilyloxy)-hexa-2,5-dienoic acid ethyl ester (*E*)-**161** (250 mg, 0.88 mmol) was dissolved in 5.0 mL of THF and cooled to -10 °C by means of an ice/NaCl bath. Lithium aluminum hydride (21 mg, 0.55 mmol) was added in portions keeping the temperature at -10 °C. Cooling was removed and the mixture stirred for 1 h. Analysis of the crude mixture by TLC clearly showed that the reaction had gone to completion. The reaction was quenched by carefully adding water, then the mixture was extracted with MtBE. The organic layers were combined, washed with water and brine, and concentrated. Column chromatography over silica gel with

hex/MtBE 3:7 gave (*E*)-**163** (120 mg, 80%) as a colorless viscous oil after short path distillation (0.05 mbar, 130°C).

IR (CCl_4): 3402s,br, 2967m, 2940m, 2880w, 1702s, 1459m, 1382m, 1355m, 1206m, 1117m, 1089m, 1017m, 977s.

$^1\text{H-NMR}$ (300 MHz, CDCl_3): 5.70 (m, 2 H); 4.18 (m, 2 H); 2.28 (s, 1 H); 2.09 (s, 3 H); 1.85-1.60 (m, 4H); 0.76 (t, $J = 7.6$ Hz, 6 H).

$^{13}\text{C-NMR}$ (75 MHz, CDCl_3): 211.2 (s); 133.2, 130.3 (2 d); 63.4 (t); 57.4 (s); 26.0 (2 t); 25.7 (q); 8.1 (2 q).

EI-MS (GC/MS): 141 (4, $[\text{M}-\text{C}_2\text{H}_4]^+$), 110 (52), 95 (26), 81 (64), 67 (33), 55 (73), 43 (100), 41 (46), 29 (18).

(*E*)-4,4-Diethyl-5-(trimethylsilyloxy)hexa-2,5-dien-1-ol ((*E*)-**162**).

(*E*)-4,4-Diethyl-5-(trimethylsilyloxy)-hexa-2,5-dienoic acid ethyl ester (*E*)-**161** (5.00 g, 17.60 mmol) was placed in a reactor and 100.0 mL of THF were added. The solution was cooled to -10 °C by means of an ice/NaCl bath. Lithium aluminum hydride (669 mg, 17.60 mmol) was added in portions keeping the temperature below 0 °C. The reaction was monitored by TLC. Cooling was removed and the mixture stirred for 1 h. Instead of the usual work-up procedure with water, acetone was added to destroy excess LiAlH_4 and the solids were removed by filtration over silica gel with hex/MtBE 1:1. The filtrate was concentrated and the residue purified by chromatography over silica gel with hex/MtBE 95:5. Short path distillation (0.05 mbar, 80°C) afforded (*E*)-**162** (1.36 g, 32%) as a colorless oil.

IR (CCl_4): 2965w, 2879w, 1616w, 1249s, 1016s, 987m, 841s, 753w, 691w.

$^1\text{H-NMR}$ (300 MHz, C_6D_6): 5.68-5.49 (m, 2 H); 4.23 (dd, $J = 1.5, 2.7$ Hz, 2 H); 3.92 (m, 2 H); 1.60 (m, 4 H); 0.86 (t, $J = 7.4$ Hz, 6 H); 0.17 (s, 9 H).

$^{13}\text{C-NMR}$ (100 MHz, CDCl_3): 162.0 (s); 135.8, 128.6 (2 d); 90.1, 63.6 (2 d); 49.0 (s); 27.4 (2 t); 8.5 (2 q); 0.1 (3 q).

EI-MS (GC/MS): 242 (2, M^+), 227 (4, $[\text{M}-\text{CH}_3]^+$), 213 (48, $[\text{M}-\text{C}_2\text{H}_4]^+$), 171 (14), 95 (12), 81 (16), 75 (35), 73 (100), 55 (15), 45 (18).

High res. EI-MS calculated for $\text{C}_{15}\text{H}_{28}\text{O}_3\text{Si}$: 284.1808; *found*: 284.1798.

1-[1-(*E*)-3-Hydroxypropenyl]cyclohexyl]ethanone ((*E*)-**170**).

Trimethylchlorosilane (1.20 g, 11.16 mmol) and triethylamine (1.13 g, 11.16 mmol) were placed in a reactor and (*E*)-**169** (2.00 g, 8.93 mmol) was added. The mixture was cooled to 0 °C in an ice/ H_2O bath. NaI (1.67 g, 11.16 mmol) was dissolved in 11.0 mL of CH_3CN and added dropwise over a period of 20 min. The ice bath was removed and the white suspension was stirred at room temperature for 1 h. The mixture was heated to 50 °C and stirring was continued for 5 h. GC

analysis showed the formation of the silyl enol ether and the consumption of (*E*)-**169**. The reaction was quenched with water and extracted with MtBE. The organic layers were washed with water and brine, dried over MgSO₄ and concentrated. Purification of the residue by chromatography over silica gel with hex/MtBE 95:5 afforded (*E*)-3-{1-[1-(trimethylsilyloxy)-vinyl]cyclohexyl}acrylic acid ethyl ester (1.75 g, 66%) as a colorless liquid.

IR (CCl₄): 2935*m*, 2860*w*, 1719*m*, 1620*w*, 1265*s*, 1167*s*, 1012*s*, 842*vs*.

¹*H*-NMR (300 MHz, C₆D₆): 6.64 (*d*, *J* = 16.0 Hz 1 H); 5.62 (*d*, *J* = 16.0 Hz, 1 H); 3.99 (*m*, 4 H); 1.61-1.17 (*m*, 10 H); 1.10 (*m* 3 H); 0.17 (*s*, 9 H).

¹³*C*-NMR (100 MHz, CDCl₃): 167.0, 161.3 (2 *s*); 120.2 (*d*); 89.5, 60.0 (2 *t*); 46.3 (*s*); 33.3, 26.0, 22.3 (5 *t*); 14.2 (*q*); -0.39 (3 *q*).

EI-MS (GC/MS): 296 (6, *M*⁺), 223 (17), 208 (19); 196 (15), 183 (19), 161 (10), 133 (10), 107 (11), 91 (15), 75 (32), 73 (100), 45 (19).

High res. EI-MS calculated for C₁₆H₂₈O₃Si: 296.1808; *found*: 296.1797.

A solution of (*E*)-3-{1-[1-(Trimethylsilyloxy)vinyl]cyclohexyl}acrylic acid ethyl ester (1.00 g, 3.38 mmol) in 20.0 mL of THF was cooled to -60 °C with a CO₂/acetone bath. LiAlH₄ (128 mg, 3.38 mmol) was added in portions to the stirred solution. The reaction was monitored by TLC. Acetone was added to the stirred reaction mixture until a fine white suspension was formed. The solids were removed by filtration over a pad of silica gel with hex/MtBE 1:1. The filtrate was mixed with water and extracted with MtBE. The ether solutions were combined and washed with water and brine. The organic solution was dried over MgSO₄ and concentrated. Chromatography over silica gel with hex/MtBE 1:1 afforded the deprotected 1-[1-((*E*)-3-hydroxypropenyl)cyclohexyl]ethanone (*E*)-**170** (279 mg, 45%) as a colorless oil after drying in vacuo.

IR (CCl₄): 3420*m*, 2932*s*, 2856*m*, 1702*vs*, 1448*m*, 1353*m*, 1206*w*, 1181*w*, 1098*w*, 1017*m*, 974*s*.

¹*H*-NMR (300 MHz, C₆D₆): 5.75-5.54 (*m*, 2 H); 4.15 (*dd*, *J* = 1.3, 5.3 Hz, 2 H); 2.53 (*s* 1 H); 2.10 (*s*, 3 H); 1.95 (*m*, 2 H); 1.55 (*m*, 4 H); 1.38 (*m*, 4 H).

¹³*C*-NMR (100 MHz, CDCl₃): 210.9 (*s*); 134.4, 130.7 (2 *d*); 63.2 (*t*); 54.2 (*s*); 32.9, 25.7 (3*t*); 25.5 (*q*); 22.6 (2 *t*).

EI-MS (GC/MS): 164 (3, [*M*-H₂O]⁺), 151 (5, [*M*-CH₂OH]⁺), 122 (100), 121 (52), 107 (41), 95 (73), 93 (73), 81 (40), 79 (85), 67 (59), 55 (48), 43 (90), 41 (53), 39 (27).

Methanesulfonic acid (*E*)-4,4-diethyl-5-oxohex-2-enyl ester ((*E*)-**136**).

Pyridine (12.0 mL) was placed in a reactor and (*E*)-3,3-Diethyl-6-hydroxyhex-4-en-2-one (*E*)-**163** (1.00 g, 6.50 mmol) was added. The solution was cooled to -10 °C by means of a ice/NaCl bath. Methanesulfonic acid chloride (0.55 mL, 7.15 mmol) was added dropwise and the mixture was stirred at -10 °C for a total of 1.5 h. TLC analysis on silica gel with hex/MtBE 95:5 showed the

slow disappearance of (*E*)-**163** ($R_f = 0.15$) in favor of the mesylate at $R_f = 0.5$. The mixture was poured onto saturated aq. CuSO_4 and extracted with MtBE. The organic layers were washed with aq. CuSO_4 solution until no more darkening of the solution occurred, indication that all of the pyridine had been removed. The organic solutions were combined, washed with water and brine and concentrated. Chromatography over silica gel with hex/MtBE 95:5 gave (*E*)-**136** (750 mg, 47%) as a colorless oil. The product was irritant and sensitive to air and humidity.

IR (CCl_4): 2969w, 1703m, 1351s, 1171s, 974m, 920s, 843m, 801m.

$^1\text{H-NMR}$ (300 MHz, CDCl_3): 5.63 (m, 1 H); 5.33 (m, 1 H); 4.30 (m, 2 H); 2.27 (s, 3 H); 1.75 (s, 3 H); 1.46 (m, 4 H); 0.59 (m, 6 H).

$^{13}\text{C-NMR}$ (75 MHz, CDCl_3): 207.7 (s); 139.3, 123.8 (2 d); 69.8 (t); 57.6 (s); 37.1 (q); 26.3 (2 t); 25.3, 8.1 (3 q).

EI-MS: 219 (1, $[\text{M}-\text{C}_2\text{H}_5]^+$), 135 (15), 110 (87), 109 (22), 95 (46), 81 (100), 79 (18), 67 (33), 55 (18), 43 (59), 41 (17).

Methanesulfonic acid (*E*)-3-(1-acetylcyclohexyl)allyl ester ((*E*)-**171**).

Hydroxyketone (*E*)-**170** (1.50 g, 8.24 mmol) was mixed with 11.0 mL of pyridine and the solution was cooled to $-10\text{ }^\circ\text{C}$ by means of an ice/ NaCl bath. Methanesulfonic acid chloride (0.70 mL, 9.06 mmol) was added dropwise. After stirring for 30 min. a precipitate started to form, stirring was continued for 1 h at $-10\text{ }^\circ\text{C}$. TLC analysis showed that complete conversion of the starting material had taken place. The reaction mixture was poured onto aq. CuSO_4 and extracted with MtBE. The combined ether extracts were washed with aq. CuSO_4 to eliminate residual pyridine and then with water and brine. The organic solution was dried over MgSO_4 and concentrated. Chromatography over silica gel with hex/MtBE 95:5 afforded (*E*)-**171** (850 mg, 40%) after drying in vacuo.

IR (CCl_4): 2936w, 2857w, 1703m, 1350s, 1171s, 972m, 921vs, 814m.

$^1\text{H-NMR}$ (300 MHz, CDCl_3): 5.83-5.65 (m, 2 H); 4.72 (dd, $J = 1.0, 6.3\text{ Hz}$, 2 H); 3.02 (s, 3 H); 2.11 (s, 3 H); 1.97 (m, 2 H); 1.56 (m, 4 H); 1.41 (m, 4 H).

$^{13}\text{C-NMR}$ (75 MHz, CDCl_3): 209.4 (s); 140.8, 123.8 (2 d); 70.0 (t); 54.6 (s); 38.1 (q); 32.7 (2 t); 25.7 (q); 25.6, 22.6 (3 t).

EI-MS: 164 (1), 147 (6), 122 (82), 107 (58), 93 (58), 79 (100), 67 (40), 55 (17), 43 (73).

2,2-Diethyl-3-vinylcyclobutanone (**137**).

The reactor was dried with hot air and purged with inert gas. Methanesulfonic acid (*E*)-4,4-diethyl-5-oxohex-2-enyl ester (*E*)-**136** (180 mg, 0.73 mmol) was placed in a reactor and 1.5 mL of THF were added. The solution was cooled to $0\text{--}5\text{ }^\circ\text{C}$ by means of an ice/ H_2O bath and 1 M potassium *tert*-butoxide in *tert*-butanol (0.75 mL, 0.75 mmol) were added dropwise. The yellow solution was stirred at $0\text{ }^\circ\text{C}$ for 30 min. TLC analysis showed that all of the mesylate (*E*)-**136** had been

consumed in favor of a product having a slightly higher R_f -value. The mixture was poured onto water and extracted with MtBE. The ether layers were washed with water and brine, dried and concentrated. The crude product was purified by column chromatography over silica gel with pentene/ Et₂O 9:1 as the eluent. Cyclobutanone **137** (50 mg, 45%) was obtained as a colorless, volatile liquid after short path distillation (100 mbar, 80 °C).

IR (CCl₄): 2972 m , 2941 m , 1769 s , 1460 w , 1076 w .

¹*H-NMR* (300 MHz, CDCl₃): 5.96 (m , 1 H); 5.20-5.09 (m , 2 H); 3.11-2.92 (m , 2 H); 2.87-2.76 (m , 1 H); 1.75-1.46 (m , 4 H); 0.93-0.85 (m , 6 H).

EI-MS (GC/MS): 110 (21, [M-CH₂CO]⁺), 108 (21), 79 (67), 78 (49), 72 (60), 56 (47), 55 (100).

3-Vinylspiro[3.5]nonan-1-one (172).

A solution of (*E*)-**171** (800 mg, 3.07 mmol) in 6.0 mL of THF was cooled to 0 °C in an ice/H₂O bath. A solution of ^tBuOK 1M in ^tBuOH (3.07 mL, 3.07 mmol) was added dropwise. TLC analysis of the bright yellow solution after 30 min. showed that the reaction had gone to completion and that two products had been formed. The mixture was poured onto water and extracted with Et₂O. The ether layers were combined, washed with water and brine, dried and concentrated. The products were separated by chromatography over silica gel with hex/Et₂O 8:2. Cyclobutanone **172** (280 mg, 56%) and the fragmentation product **173** (60 mg, 11%) were isolated and dried in vacuo.

Spectroscopic data for **172**:

IR (CCl₄): 2928 m , 2853 w , 1769 vs , 1449 w , 1042 w , 995 w , 912 m .

¹*H-NMR* (300 MHz, CDCl₃): 5.94 (m , 1 H); 5.17 (d , J = 1.1 Hz, 1 H); 5.12 (m , 1 H); 3.14 (dd , J = 17.5, 9.155 Hz, 1 H); 2.89 (m , 1 H); 2.68 (m , 1 H); 1.83-1.23 (m , 10 H).

¹³*C-NMR* (75 MHz, CDCl₃): 214 (s); 137.2 (d); 116.2 (t); 67.6 (s); 46.5 (t); 39.7 (d); 33.7, 27.9, 25.4, 22.7, 22.4 (5 t).

EI-MS: 164 (1, M^+), 122 (71), 110 (39), 107 (38), 93 (27), 81 (40), 79 (58), 67 (100), 54 (46), 41 (32), 39 (33), 27 (17).

MS data for **173**:

EI-MS: 122 (40, M^+), 107 (45, [M-CH₃]⁺), 93 (36, [M-C₂H₅]⁺), 79 (100), 67 (30), 53 (17), 39 (18), 27 (8).

(2-Oxopropyl)triphenylphosphonium chloride.

Triphenylphosphine (131.00g, 0.50 mol) was dissolved in 600.0 mL of toluene and placed in a reactor equipped with a mechanical stirrer. Chloroacetone (46.00g, 0.50 mol) was added in portions. The temperature of the mixture slowly rose to 35 °C. The clear solution was then heated to 110 °C and boiled at reflux for 12 h. A suspension of white solids was formed. The suspension was cooled to room temperature and the product was removed by filtration. The solids were

washed with MtBE and dried in vacuo. The (2-Oxopropyl)triphenylphosphonium chloride (162.00 g, 92%) was obtained as a fine white powder. M.p. 239-243 °C. Due to rapid interchange between the phosphonium salt and its stabilized ylid form, the NMR spectrum showed to sets of signals, resulting from the two tautomeric forms.

IR (CCl_4): 2767 m , 1700 m , 1485 w , 1436 m , 1355 m , 1312 m , 1205 w , 1156 w , 1170 s , 996 m , 857 w , 746 s , 715 s , 688 s .

$^1\text{H-NMR}$ (300 MHz, CDCl_3): 7.93-7.53 (m , 15 H); 6.14 and 4.59 (d , $J = 11.4$ and 19.5 Hz, 2 H); 2.54 (m , 3 H).

$^{13}\text{C-NMR}$ (75 MHz, CDCl_3): 201.0, 181.0 (1 s); 134.5-129.6 (15 d); 122.2, 121.0, 119.2, 118.0 (3 s); 70.9, 69.5 (0.5 d); 40.5, 39.7 (0.5 t); 32.2, 23.8, 23.6 (1 q).

1-(Triphenyl- λ^5 -phosphanylidene)propan-2-one (174).

(2-Oxopropyl)triphenylphosphonium chloride (50.00 g, 0.14 mol) was dissolved in 100.0 mL of water. Sodium carbonate (93.00 g, 0.75 mol) was dissolved in 500.0 mL of water and added dropwise, at room temperature in 1 h, to the vigorously stirred solution. A fine white suspension was formed. The suspension was stirred for 2 h and the solid separated by suction filtration. The pasty solid was dried in vacuo. The dried lumps of product were ground in a mortar giving **174** (44.30 g, 99%) as a fine white powder. M.p. 197-198 °C.

IR (CCl_4): 3047 w , 1534 s , 1478 m , 1434 m , 1384 s , 1150 m , 1106 s , 977 m , 868 m , 763 m , 750 m , 716 s , 694 s .

$^1\text{H-NMR}$ (300 MHz, CDCl_3): 7.72-7.39 (m , 15 H); 3.91-3.29 (s , 1 H); 2.09 (d , $J = 1.5$ Hz, 3 H).

$^{13}\text{C-NMR}$ (75 MHz, CDCl_3): 190.8 (s); 133.0, 132.9, 131.8, 128.8, 128.6 (15 d); 127.8, 126.6 (3 s); 52.1, 50.7 (1 d); 28.5, 28.2 (1 q).

EI-MS: 318 (50, M^+), 317 (53), 304 (44), 303 (100, $[M-\text{CH}_3]^+$), 277 (9), 241 (3, $[M-\text{C}_6\text{H}_5]^+$), 201 (9), 183 (26), 165 (14), 152 (7).

(E)-5,5-Diethylhept-3-ene-2,6-dione ((E)-175).

2,2-Diethyl-3-oxo-butylaldehyde **145** (24.43 g, 0.17 mol) was placed in a reactor containing 250.0 mL of xylene. 1-(Triphenyl- λ^5 -phosphanylidene)propan-2-one **174** (60.42 g, 0.19 mol) was added and the solution was heated to reflux. After 24 h the mixture was cooled to room temperature, diluted with MtBE and washed with water and brine. The organic solution was concentrated and the residue distilled over a 20 cm Vigreux column (68 °C, 0.05 mbar). The product (*E*)-**175** (23.00 g, 74%) was obtained as a colorless oil. The typical (*E*)-alkene absorption peaks at 1674 and 988 cm^{-1} in the IR spectrum as well as the vinylic proton spin-coupling constant of $J = 17$ Hz in the $^1\text{H-NMR}$ spectrum are good indicators that the product possesses (*E*)-configuration.

IR (CCl_4): 2969_w, 2881_w, 1703_s, 1674_s, 1619_m, 1459_w, 1425_w, 1357_m, 1255_m, 1200_m, 1118_w, 988_m.

$^1\text{H-NMR}$ (300 MHz, CDCl_3): 6.94 (*d*, $J = 16.8$ Hz, 1 H); 6.12 (*d*, $J = 16.8$ Hz, 1 H); 2.30 (*s*, 3 H); 2.13 (*s*, 3 H); 1.81 (*m*, 4 H); 0.78 (*t*, $J = 7.6$ Hz, 6 H).

$^{13}\text{C-NMR}$ (75 MHz, CDCl_3): 208.7, 198.0 (2 *s*); 148.4, 131.0 (2 *d*); 58.5 (1 *s*); 27.1 (2 *t*); 26.9, 25.8 (2 *q*); 8.3 (2 *q*).

EI-MS (*GC/MS*): 153 (1, $[\text{M}-\text{C}_2\text{H}_5]^+$), 140 (37), 125 (15), 111 (46), 97 (13), 82 (10), 67 (9), 55 (21), 43 (100).

Anal. calc. for $\text{C}_{11}\text{H}_{18}\text{O}_2$ (182): C 72.49, H 9.95; *found*: C 72.36, H 9.72.

Diisopinocampheylborane (+)- Ipc_2BH .

(-)- α -Pinene (20.00 g, 0.15 mol) was placed in a reactor, 50.0 mL of THF were added and the solution was cooled to 0 °C. $\text{BH}_3\cdot\text{Me}_2\text{S}$ (6.33 mL, 75.00 mmol) was added dropwise keeping the temperature at 0 °C. The mixture was stirred at the same temperature for 30 min. and then placed in a refrigerator for 24 h. Large, colorless crystals formed at the bottom of the vessel. The liquid was removed by decantation and the solids were washed three times with dry Et_2O , carefully avoiding the introduction of moisture. After drying in vacuo for 24 h the (+)- Ipc_2BH (13.65 g, 64%) was used without further purification. M.p. 85-90 °C.

(-)-(R)-(E)-3,3-Diethyl-6-hydroxyhept-4-en-2-one ((-)-(R)-(E)-**176**).

(+)- Ipc_2BH (5.00 g, 27.50 mmol) was dissolved in 25.0 mL of Et_2O and cooled to -60 °C. HCl in Et_2O (7.40 mL, 30.00 mmol) was added dropwise over 30 min. After stirring at 0 °C for 1 h the solution was concentrated and dried in vacuo. A colorless, viscous liquid was obtained that was used without further purification. The crude (+)- Ipc_2BCl was dissolved in 25.0 mL of THF and the mixture was cooled to -60 °C. (E)-5,5-Diethylhept-3-ene-2,6-dione (E)-**175** (8.58 g, 30.00 mmol) in 10.0 mL of THF was added dropwise and the mixture was stirred at -60 °C for 1 h. The mixture was left to reach room temperature and stirred for 16 h. The resulting dark purple mixture was treated with diethanol amine (7.00 g, 66.60 mmol). Solids precipitated and the mixture turned bright orange. The solids were removed by filtration and the orange liquid was diluted with MtBE, washed with water and brine and concentrated. After chromatography over silica gel with hex/MtBE 1:1 and drying in vacuo, the hydroxy ketone (R)-(E)-**176** (3.87 g, 77%) was obtained as colorless oil. The product is sensitive to heat and can not be distilled without decomposition.

Opt. rot.: $[\alpha]_{\text{D}}^{25}$ - 6.45 (*c* 0.945, MeOH).

Enantiomeric excess ($^1\text{H-NMR}$ with Pirkel reagent): 48%

IR (CCl_4): 3430_s, 2968_m, 2940_w, 2880_w, 1703_{vs}, 1458_w, 1354_m, 1207_w, 1117_m, 1059_m, 977_m.

$^1\text{H-NMR}$ (300 MHz, CDCl_3): 5.56-5.34 (*m*, 2 H); 4.03 (*m*, 1 H); 1.80 (*s*, 3 H); 1.69-1.44 (*m*, 4 H); 1.26 (*d*, $J = 3.4$ Hz, 1 H); 1.09 (*d*, $J = 6.5$ Hz, 3 H); 0.66 (*dt*, $J = 11.2, 3.6$, 6 H).

$^{13}\text{C-NMR}$ (75 MHz, CDCl_3): 211.1 (*s*); 135.4, 131.5, 68.7 (3 *d*); 57.2 (*s*); 26.0, 25.9 (2 *t*); 25.7, 23.4 (2 *q*); 8.1 (2 *q*).

EI-MS (GC/MS): 169 (1, $[\text{M-CH}_3]^+$), 155 (1, $[\text{M-C}_2\text{H}_5]^+$), 140 (9), 124 (40), 95 (59), 83 (21), 67 (17), 55 (41), 43 (100).

Anal. calc. for $\text{C}_{11}\text{H}_{20}\text{O}_2$ (184): C 71.70, H 10.94; *found*: C 71.56, H 11.29

Absolute configuration of (+)-(E)-3,3-Diethyl-6-hydroxyhept-4-en-2-one ((+)-(E)-176) by Horeau's method.

3,3-Diethyl-6-hydroxyhept-4-en-2-one (+)-(E)-**176** (100 mg, 0.54 mmol), prepared with (-)- Ipc_2BCl , was mixed with 1.5 mL of pyridine and 2-phenylbutyric anhydride **179** (505 mg, 1.63 mmol) was added. The mixture was stirred at room temperature and monitored by GC. After 12 h the reaction had gone to completion. Water and a trace of phenolphthalein was added to the stirred solution and NaOH 33% was added until the color of the mixture turned blue, indicating that all of the acid anhydride had been neutralized. The aq. mixture was extracted with MtBE and then acidified with AcOH. The carboxylic acid was extracted from the water layer with MtBE and isolated. The optical rotation of the resulting 2-phenylbutyric acid **181** (340 mg, 76%) was measured in EtOH in a 1 dm cell. The measured optical rotation of $[\alpha]_{\text{D}}^{25} - 6.45$ (c 0.945) indicated that, according to Horeau's rule, (+)-(E)-**176** prepared with (-)- Ipc_2BCl , possesses (*S*)-configuration, Chapter 4.3.6.

The neutral ether extract containing the 2-phenylbutyrate (+)-**180** was washed with water and brine and concentrated. After drying in vacuo (+)-**180** (180 mg, quant.) was obtained as a colorless oil. $[\alpha]_{\text{D}}^{25} + 1.35$ (c 1.11, EtOH).

1-((E)-4,4-Diethyl-1-methyl-5-oxohex-2-enyloxymethyl)-4,7,7-trimethyl-2-oxabicyclo[2.2.1]heptan-3-one ((+)-(E)-178).

(-)-(E)-3,3-Diethyl-6-hydroxyhept-4-en-2-one (-)-(E)-**176** (500 mg, 2.70 mmol) was mixed with 5.0 mL pyridine and cooled to 0 °C. (-)-(S)-Camphanic acid chloride (-)-(S)-**177** (1.00 g, 4.63 mmol) was added and the mixture was stirred at 0 °C for 1 h. The mixture was warmed to room temperature and stirred for an additional 3 h. TLC analysis showed that all of the hydroxy-ketone (-)-(E)-**176** had been consumed. The reaction was quenched with H_2O /ice and acidified to pH 2 with dilute HCl. The aqueous layer was extracted with MtBE and the organic layers were washed with water and dried. Chromatography over silica gel with hex/MtBE 8:2 afforded (+)-(E)-**178** (810 mg, 82%) as a colorless solid. The product was dissolved in hex/MtBE and left at room

temperature for 24 h. Long, colorless needles of (+)-(*E*)-**178** formed. The liquid was removed and the crystals were washed with hexane. The crystallization sequence was repeated three times until the value of the optical rotation remained constant. The crystals were dried in vacuo. M.p. 67-69 °C. A single crystal was submitted for X-ray crystallography and was determined to possess (*R*)-configuration at the carbon bearing the original allylic hydroxy group. The diastereomeric purity of the product can be determined by examining the ^{13}C -NMR signal resulting from the methyl protons at the carbon bearing the camphanonate at 16.7 ppm $J = 6.6$ Hz, resulting from the methyl group at the stereogenic centre bearing the camphanoate. By this method the de was determined to be >95%.

Opt. rot.: $[\alpha]_{\text{D}}^{25} + 9.75$ (c 1.005, CH_2Cl_2).

IR (neat): 2968 m , 1781 s , 1715 s , 1703 s , 1453 m , 1355 m , 1268 s , 1171 s , 1099 s , 1027 s , 993 m , 982 m , 931 m , 848 w , 797 w .

^1H -NMR (300 MHz, CDCl_3): 5.82 (d , $J = 15.2$ Hz, 1 H); 5.56 (d , $J = 7.1$ Hz, 1 H); 2.41 (m , 1 H); 2.06 (s , 3 H); 2.02 (m , 1 H); 1.92 (m , 1 H); 1.80-1.60 (m , 6 H); 1.40 (d , $J = 6.3$ Hz, 3 H); 1.11 (s , 3 H); 1.04 (s , 3 H); 0.94 (s , 3 H); 0.73 (t , $J = 7.6$ Hz, 6 H).

^{13}C -NMR (100 MHz, CDCl_3): 210.5, 178.2, 166.7 (3 s); 135.8, 130.1 (2 d); 91.0 (s); 72.9 (d); 57.5, 54.8, 54.1 (3 s); 30.5, 28.9, 26.2, 26.0 (4 t); 25.9, 20.5, 16.7, 16.6, 9.6, 8.2 (7 q).

EI-MS: 335 (10, $[\text{M}-\text{C}_2\text{H}_5]^+$), 321 (15), 275 (8), 137 (33), 125 (63), 124 (100), 123 (75), 109 (40), 97 (26), 95 (83), 83 (42), 81 (24), 67 (22), 55 (33), 43 (83), 41 (27).

Anal. calc. for $\text{C}_{21}\text{H}_{32}\text{O}_5$ (364): C 69.20, H 8.85; *found*: C 69.29, H 8.88.

Hydrolysis of 1-((E)-4,4-Diethyl-1-methyl-5-oxohex-2-enyloxymethyl)-4,7,7-trimethyl-2-oxabicyclo[2.2.1]heptan-3-one ((+)-(*E*)-**178**).

Camphanoate (+)-(*E*)-**178** (600 mg, 1.65 mmol) was dissolved in 10.0 mL of EtOH and cooled to 0 °C. Potassium hydroxide (0.50 g, 9.00 mmol) was dissolved in 3.0 mL of H_2O and added at once. The mixture was slowly warmed to room temperature and stirred for 15 h. Water was added and (-)-(*E*)-**176** was extracted with MtBE. The organic layers were washed with water, dried and concentrated. Chromatography over silica gel with hexane/MtBE 7:3 gave (-)-(*E*)-**176** (280 mg, 92%) as a colorless oil after drying in vacuo.

Opt. rot.: $[\alpha]_{\text{D}}^{25} - 12.48$ (c 1.370, CH_2Cl_2).

In order to exclude the possibility of epimerization during the esterification of (-)-(*E*)-**176** with (-)-(*S*)-camphanic acid chloride (-)-(*S*)-**177** and during the subsequent hydrolysis, a sample of the resolved (-)-(*E*)-**176** was reacted with (-)-camphanic acid chloride and the diastereomeric excess was determined by ^{13}C -NMR (300 MHz, CDCl_3). The presence of a single diastereomer was

indicated by the clean doublet at 16.7 ppm $J = 6.6$ Hz in the ^{13}C -NMR (100 MHz, CDCl_3) spectrum resulting from the geminal dimethyl group of the camphanoate moiety.

(S,E)-6-Chloro-3,3-diethylhept-4-en-2-one ((+)-*(S)*-(*E*)-**139**).

(R,E)-3,3-Diethyl-6-hydroxyhept-4-en-2-one (-)-*(R)*-(*E*)-**176** (280 mg, 1.52 mmol, 98% ee) was placed in a reactor and hexachloroacetone (0.51 mL, 3.34 mmol) was added. The solution was cooled to 0 °C and triphenylphosphine (420 mg, 1.60 mmol) was added at once. The mixture was stirred at 0 °C for 1 h and then at room temperature for 15 h. TLC analysis showed that all of the (-)-*(R)*-(*E*)-**176** had been consumed. The mixture was diluted with MtBE and washed with water, sat. NaHCO_3 solution and brine. After drying and concentration the crude product was purified by chromatography over silica gel with hex/MtBE 95:5. Short path distillation (80 °C, 0.05 mbar) yielded (+)-*(S)*-(*E*)-**139** (260 mg, 85%) as a colorless oil. Chiral GC revealed an enantiomeric excess of 77%.

Opt. rot.: $[\alpha]_{\text{D}}^{25} + 20.70$ (c 1.145, CH_2Cl_2).

Enantiomeric excess (^1H -NMR with Pirkel reagent): 77%

IR (CCl_4): 2969 m , 2881 w , 1706 vs , 1458 m , 1380 w , 1353 m , 1205 m , 1116 m , 1013 m , 974 m , 705 w , 640 m .

^1H -NMR (300 MHz, CDCl_3): 5.68 (m , 2 H); 4.58 (m , 1 H); 2.09 (s , 3 H); 1.84-1.62 (m , 4 H); 1.61 (d , $J = 6.6$ Hz, 3 H); 0.75 (m , 6 H).

^{13}C -NMR (75 MHz, CDCl_3): 210.2 (s); 133.5, 133.3, 57.9 (3 d); 57.3 (1 s); 26.2, 26.0 (2 t); 25.7, 25.2 (2 q); 8.1 (2 q).

EI-MS (*GC/MS*): 173 (3, $[\text{M}-\text{C}_2\text{H}_5]^+$), 167 (2, $[\text{M}-\text{Cl}]^+$), 159 (2, $[\text{M}-\text{CH}_3\text{CO}]^+$), 124 (75), 109 (21), 95 (100), 67 (48), 55 (33), 43 (68).

2,2-Diethyl-3-((*E/Z*)-propenyl)cyclobutanone ((*E/Z*)-**140**).

(+)-*(S)*-(*E*)-6-Chloro-3,3-diethylhept-4-en-2-one (+)-*(S)*-(*E*)-**139** (1.00 g, 4.95 mmol, 77% ee) was dissolved in 22.0 mL of THF and cooled to 0 °C. $t\text{BuOK}$ 1M in $t\text{BuOH}$ (5.00 mL, 5.00 mmol) was added dropwise. The yellow solution was stirred at 0 °C for 1 h and was then warmed to room temperature and stirred for additional 4 h. Analysis of the reaction mixture with GC and TLC showed that the reaction had gone to completion. The reaction was quenched with water and extracted with MtBE. The organic layers were washed with water and brine, dried and concentrated. The crude product mixture was purified by chromatography over silica gel with hexane/MtBE 9:1. (*E/Z*)-**140** (402 mg, 49%) was obtained as a colorless oil after short path distillation (10 mbar, 80 °C).

Opt. rot.: $[\alpha]_{\text{D}}^{25} - 5.42$ (c 0.720, CH_2Cl_2).

% ee ($^1\text{H-NMR}$ with Pirkel reagent): 77%

IR (CCl_4): 2967m, 2921w, 1771vs, 1458m, 1380w, 11074m, 967m.

$^1\text{H-NMR}$ (300 MHz, CDCl_3): 5.56 (m, 2 H); 3.03 (dd, $J = 9.1, 17.4$ Hz, 1 H); 2.91 (dd, $J = 7.8, 17.4$ Hz, 1 H); 2.76 (m, 1 H); 1.72 (m, 3 H); 1.70-1.47 (m, 4 H); 0.87 (m, 6 H).

$^{13}\text{C-NMR}$ (75 MHz, CDCl_3): 214.1 (s); 130.0, 127.1 (2 d); 70.6 (s); 47.5 (t); 36.9 (d); 25.0, 21.7 (2 t); 17.8, 8.4, 7.7 (3 q).

EI-MS (GC/MS): 166 (2, M^+), 138 (5, $[\text{M}-\text{C}_2\text{H}_4]^+$), 124 (40), 109 (18), 109 (21), 98 (57), 95 (68), 83 (100), 67 (46), 55 (61), 41 (39).

Anal. calc. for $\text{C}_{11}\text{H}_{18}\text{O}$ (166): C 79.46, H 10.91; found: C 79.44, H 10.72.

High res. EI-MS calculated for $\text{C}_{11}\text{H}_{18}\text{O}$: 166.1358; found: 166.1356.

Separation of 2,2-Diethyl-3-((E)-propenyl)cyclobutanone ((E)-140) and 2,2-Diethyl-3-((Z)-propenyl)cyclobutanone ((Z)-140).

AgNO_3 (6.00 g, 35.00 mmol) was dissolved in 100.0 mL of acetonitrile and silica gel (50.00 g) was added. The acetonitrile was removed on the rotary evaporator at 200 mbar and the AgNO_3 impregnated silica gel was dried at 0.05 mbar for 24 h. A chromatography column (12 \times 1 cm) was filled with the treated silica gel and a mixture of (E)-140 and (Z)-140 85:15 (45 mg, 0.27 mmol) was separated over 48 fractions using hex/MtBE 97.5 : 2.5 as the eluent. The R_f values for (E)-140 and (Z)-140 on AgNO_3 impregnated silica gel TLC plates, with hex/MtBE 95:5 were 0.33 and 0.17 respectively.

The fractions containing the individual (E)- and (Z)-isomers were concentrated separately and purified by microscale distillation (0.05 mbar, 40 °C) under dust free conditions. (E)-140 (32 mg, 79%, 75% ee) and (Z)-140 (3mg, 67%, 75% ee) were submitted for RAMAN and ROA spectroscopy. 2D $^1\text{H-NMR}$ (500 MHz, CDCl_3) experiments showed a distinct signal at 13 ppm for the (Z)-140 and one at 17 ppm for (E)-140. $^1\text{H-NMR}$ signals (500 MHz, CDCl_3) resulting from vinylic protons at 6.2 (m, 1H), 6.0 (m, 1H), 5.55 (dd, $J = 16.0, 0.5$ Hz, 1 H), 5.05 (m, 1H) and 4.95 (m, 1H) indicated that (Z)-140 contained 25% of the dehydrochlorination product 183.

Opt. rot. (+)-(E)-140: $[\alpha]_{\text{D}}^{25} + 0.96$ (c 1.040, CH_2Cl_2).

Enantiomeric excess (+)-(E)-140 (chiral GC): 75%

Opt. rot. (-)-(Z)-140: $[\alpha]_{\text{D}}^{25} - 5.94$ (c 0.690, CH_2Cl_2).

Enantiomeric excess (-)-(Z)-140 (chiral GC): 75%

4.6.2 Synthesis of (-)- and (+)-junionone (*E*)-189

1-(3,3-Dimethyloxiranyl)ethanone (193).

Mesityl oxide (100.00 g, 1.00 mol) was mixed with H₂O₂ 30% (140.00 mL, 1.23 mol) and cooled to 5 °C. NaOH (16.00 g, 0.40 mol) was dissolved in a minimum amount of water and added in small portions over 2 h keeping the temperature below 10 °C. Acetone (100.0 mL) was added to the reaction mixture in small portions during the NaOH addition to speed up the reaction. After the addition was complete, the mixture was stirred at 10-20 °C in an ice bath for 4 h. Shortly after the addition of the NaOH the heat evolution diminished, indicating that the hydroperoxide intermediate was formed. Decomposition of the hydroperoxide leading to **193** then requires significant time. The reaction will become uncontrollable if the temperature rises above 30 °C. Cooling must be continued until no more heat evolution is noticeable, indicating that the reaction has gone to completion.

Acetone (1.0 l) was added to the reaction mixture and the aqueous layer was separated. The acetone solution was washed with brine and concentrated. The residue was distilled over a 20 cm Vigreux column (58 °C, 10 mbar). **193** (66.72 g, 59%) was obtained as a colorless liquid.

IR (CCl₄): 2970, 1718_s, 1455_w, 1380_s, 1356_m, 1243_w, 1185_m, 1118_m, 1053_w, 920_m, 875_w, 834_w, 784_m.

¹H-NMR (300 MHz, CDCl₃): 3.42 (s 1H); 2.23 (s 3H); 1.44 (s 3H); 1.28 (s 3H).

¹³C-NMR (75 MHz, CDCl₃): 207.6 (s); 65.3 (d); 60.6 (s); 27.8, 24.4, 18.1 (3 q).

EI-MS (GC/MS): 114 (3, *M*⁺); 99 (19); 98 (100); 73 (73); 72 (23); 71 (79); 70 (28); 56 (71); 55 (36); 54 (32).

2,2-Dimethyl-3-oxobutyraldehyde (194).

1-(3,3-Dimethyloxiranyl)ethanone **193** (67.50 g, 0.59 mol) was mixed with 800.0 mL of CH₂Cl₂ and the solution was heated to reflux (40 °C). BF₃·Et₂O (15.00 mL, 0.12 mol) was added dropwise over 1 h until the reaction mixture turned dark. The brown solution was poured onto water immediately and shaken vigorously. The layers were separated and the aq. layers were washed with CH₂Cl₂. The organic layers were washed with water and brine, dried and concentrated. Distillation over a 40 cm Vigreux column (10 mbar, 56 °C) afforded **194** (30.16 g, 45%) as a colorless liquid.

IR (CCl₄): 2981_w, 1725_m, 1699_s, 1465_w, 1357_m, 1256_w, 1128_m, 955_w, 910_w, 825_m.

¹H-NMR (300 MHz, CDCl₃): 9.80 (s 1H); 2.37 (s 3H); 1.53 (s 6H).

¹³C-NMR (75 MHz, CDCl₃): 207.1 (s); 200.8 (d); 60.0 (s); 26.3, 18.9 (3 q).

EI-MS (GC/MS): 114 (2, *M*⁺); 85 (51), 72 (17), 70 (100), 57 (12), 56 (60).

High res. HR-CI MS calculated for C₆H₁₁O₂: 115.0759; found: 115.0752.

((E)-But-2-enyl)triphenylphosphonium chloride ((E)-195).

A sealed reactor with magnetic stirring was equipped with a reflux condenser and charged with triphenylphosphine (262.00 g, 1.00 mol) and 1.0 L of toluene. (*E*)-1-Chloro-2-butene (100.00 g, 1.10 mol, (*E*)/(*Z*) = 4:1) was added and the mixture was refluxed for 48 h. The suspension was cooled in a ice bath and the solid was removed by filtration. After washing the phosphonium salt with toluene and drying in vacuo, (*E*)-**195** (246.50 g, 67%) was obtained as a white powder. M.p. 219 – 222 °C.

(E,E/Z)- 3,3-Dimethylocta-4,6-dien-2-one ((E,E/Z)-196).

((E)-But-2-enyl)triphenylphosphonium chloride 195 (11.00 g, 30.00 mmol, (*E*)/(*Z*) = 4:1) was placed in 40.0 mL of benzene and the suspension was cooled to 5 °C. BuLi 1.6 M in hexane (18.75 mL, 30.00 mmol) was added dropwise to the stirred suspension over 20 min. The deep red and homogenous mixture was stirred at 5 °C for 30 min. and then 2,2-dimethyl-3-oxo-butyraldehyde **194** (3.42 g, 30.00 mmol) was added dropwise as a solution in 10.0 mL of benzene. The resulting orange mixture was stirred for 30 min. GC analysis showed the disappearance of **194**, indicating that the reaction had gone to completion. The mixture was diluted with 100.0 mL of hexane and filtered over a pad of silica gel using hex/MtBE 8:2 to wash the solids and the filter pad. The filtrate was concentrated and the residue was short path distilled (0.05 mbar, 70 °C). The distilled 3,3-dimethylocta-4,6-dien-2-one **196** (3.45 g, 76%) consisted of a mixture of (*Z,E*)-**196** (47%), (*Z,Z*)-**196** (14%), (*E,E*)-**196** (28%) and (*E,Z*)-**196** (11%), as determined by GC and NMR.

The mixture of double bond isomers of **196** (3.45 g, 22.70 mmol) was dissolved in 100.0 mL of MeOH and I₂ (0.50 g, 4.00 mmol) was added in several small portions over a total of 48 h. The progress of the isomerization was monitored by GC analysis. The samples were treated with one drop of NaOH 30% prior to injection to prevent uncontrolled isomerization in the hot GC-injector. When no more change of the isomeric distribution was observed, the black reaction mixture was treated with several drops of NaOH 30% until the solution discoloured to a pale yellow liquid. The reaction mixture was poured onto 200.0 mL of water and extracted with MtBE. The ether layers were washed with water and brine and concentrated. Purification of the residue over silica gel with hex/MtBE 9:1 followed by short path distillation (0.05 mbar, 70 °C) furnished **196** (2.14 g, 62%) as a colorless oil. The *E/Z*-ratio of 85:15, at the terminal double bond was determined by integrating the ¹³C-NMR signals of the methyl C(8) carbon at 17.9 ppm for (*E,E*)-**196** and at 13.2 ppm for (*E,Z*)-**196**.

IR (neat): 2973*m*, 1707*vs*, 1466*w*, 1353*m*, 1232*w*, 1123*m*, 989*s*, 953*w*, 925*w*.

¹H-NMR (300 MHz, CDCl₃): 6.15-5.94 (*m*, 2 H); 5.77-5.44 (*m*, 2 H); 2.12(15%), 2.10(85%) (*s* 3 H); 1.76(*m*, 3 H); 1.26(15%), 1.23(85%) (*s*, 6 H).

$^{13}\text{C-NMR}$ (75 MHz, CDCl_3): 211.0 (s); 137.2(15%), 134.8(85%), 131.1(85%), 129.7(85%), 129.3(85%), 128.9(15%), 126.2(15%), 124.5(15%) (4 d); 50.1 (1 s); 25.3 (1 q); 23.9 (2 q); 17.9(85%), 13.3(15%) (1 q).

EI-MS (GC/MS): 152 (9, M^+); 109 (100); 91 (15); 81 (39); 79 (23); 77 (21); 67 (88); 55 (23); 43 (48).

Anal. calc. for $\text{C}_{11}\text{H}_{20}\text{O}_2$ (184): C 78.21, H 10.21; found: C 78.13, H 10.06.

(*E,E*)-3,3-Dimethylocta-4,6-dien-2-one ((*E,E*)-**196**).

Pure (*E,E*)-**196** was isolated out of a mixture of (*E,E*)-**196** and (*E,Z*)-**196** 85:15 (11.50 g, 75.66 mmol) by chromatography over silica gel, impregnated with 10% AgNO_3 with hex/MtBE 95:5. The eluent was collected in 17 fractions and analyzed by GC. Only a weak separation of the (*Z*)- and (*E*)-isomers was achieved. It was however possible to isolate a sample of pure (*E,E*)-**196** (0.50 g, 4%) from the last fractions of the chromatography, this was indicated by the missing signal at 13 ppm in the $^{13}\text{C-NMR}$ spectrum, resulting from the (6*Z*)-methyl group of (*E,Z*)-**196**.

$^1\text{H-NMR}$ (300 MHz, CDCl_3): 6.13-5.98 (m, 2 H); 5.76-5.54 (m, 2 H); 2.09 (s, 3 H); 1.75(m, 3 H); 1.23 (s, 6 H).

$^{13}\text{C-NMR}$ (75 MHz, CDCl_3): 211.0 (s); 134.7, 131.1, 129.7, 129.1 (4 d); 50.0 (1 s); 25.2 (1 q); 23.8 (2 q); 17.8 (1 q).

D-Fructose diacetal 198 by Shi et al.

D-Fructose (140.00 g, 0.78 mol) was suspended in 2.5 L of acetone. Acetone dimethylacetal (56.36 g, 0.54 mol) was added and the solution was cooled to $-10\text{ }^\circ\text{C}$ by means of an ice/ NaCl bath. Perchloric acid 70% (33.00 mL, 0.39 mol) was added in portions. The mixture was stirred at $-10\text{ }^\circ\text{C}$ for 5 h. GC analysis showed a mixture of 85% **198** and 11% **199** accompanied by small amounts of impurities. **198** is water soluble therefore the mixture was neutralized by adding aq. NH_3 and washed once with brine. The acetone solution was dried over MgSO_4 and concentrated. Crystallization from hex/MtBE afforded **198** (112.70 g, 55%) as a white powder. M.p. $115\text{--}116\text{ }^\circ\text{C}$ (lit. $117\text{--}118\text{ }^\circ\text{C}$) [80].

Opt. rot.: $[\alpha]_{\text{D}}^{25}$ - 140.95 (*c* 1.260, MeOH), lit. - 144.20 [80].

IR (neat): 3452s, 2954w, 1367m, 1246m, 1217m, 1112m, 1067s, 1043s, 1016m, 973m, 884s, 849s, 833s, 805m, 725m.

$^1\text{H-NMR}$ (300 MHz, CDCl_3): 4.23-4.08 (m, 2 H); 4.08 (dd, $J = 8.8, 61.4\text{ Hz}$, 2 H); 4.07 (dd, $J = 13.0, 41.0\text{ Hz}$, 2 H); 3.67 (d, $J = 6.5\text{ Hz}$, 1H); 2.14 (br.s, 1H); 1.51 (s, 3 H); 1.44 (s, 3 H); 1.37 (s, 3 H).

$^{13}\text{C-NMR}$ (75 MHz, CDCl_3): 111.7, 109.2, 104.4 (3 s); 77.1, 73.2 (2 d); 72.1 (t); 70.2 (d); 60.5 (t); 27.8, 26.2, 25.8 (4 q).

EI-MS (GC/MS): 245 (71, $[M-OH]^+$), 185 (38), 143 (66), 126 (65), 116 (100), 114 (35), 100 (63), 99 (71), 98 (49), 85 (59), 84 (96), 72 (64), 71(71), 68 (73), 58 (88).

Anal. calc. for $C_{12}H_{20}O_6$ (260): C 55.37, H 7.74; found: C 55.16, H 7.66.

D-Fructose catalyst 200 by Shi et al.

Powdered molecular sieve 3 Å (20.00 g) was suspended in 100.0 mL of CH_2Cl_2 . Pyridine chlorochromate (16.55 g, 76.80 mmol) was added and the mixture was stirred for 30 min. at room temperature. *D*-Fructose diacetal **198** (5.00 g, 19.20 mmol) was added at once. The reaction mixture was stirred at room temperature for 2½ h. GC analysis showed that all of the starting material **198** had been consumed. Hexane was added to the vigorously stirred reaction mixture. A black granular solid formed that quickly settled to the bottom of the reactor when the stirring was stopped, the supernatant was clear and colorless. The suspension was filtered over a pad of silica gel and the filter pad was washed with hex/MtBE 8:2. The organic solution was concentrated and **200** was crystallized from hex/MtBE (3.01 g, 61%). M.p. 95-96 °C.

Opt. rot.: $[\alpha]_D^{25}$ - 119.45 (*c* 1.090, MeOH), lit. - 126.4 [80].

IR (neat): 2992w, 2938w, 1742m, 1455w, 1375m, 1224s, 1095s, 1065s, 989s, 965m, 841s, 781m.

1H -NMR (300 MHz, $CDCl_3$): 4.73 (*d*, *J* = 5.7 Hz, 1 H); 4.61 (*d*, *J* = 9.5 Hz, 1 H); 4.55 (*m* 1 H); 4.39 (*dd*, *J* = 13.73, 2.3 Hz, 1 H); 4.12 (*d*, *J* = 13.4 Hz, 1 H); 3.99 (*d*, *J* = 9.5 Hz, 1 H); 1.55 (*s* 3 H), 1.46 (*s* 3 H); 1.40 (*s* 6 H).

^{13}C -NMR (75 MHz, $CDCl_3$): 196.8, 113.7, 110.5, 104.0 (4 *s*); 77.8, 75.75 (2 *d*); 69.9, 60.0 (2 *t*); 27.0, 26.4, 25.9 (4 *q*).

EI-MS (GC/MS): 243 (42, $[M-CH_3]^+$), 201 (42), 184 (17), 142 (69), 116 (85), 113 (100), 85 (42), 84 (80), 71 (54), 58 (84).

Anal. calc. for $C_{12}H_{18}O_6$ (258): C 55.81, H 7.02; found: C 55.69, H 7.09.

(E)-3,3-Dimethyl-5-(3-methyloxiranyl)pent-4-en-2-one ((+)-*(E)*-trans-**190**).

A mixture of 130.0 mL dimethoxymethane and 70.0 mL of acetonitrile was placed in a reactor and *(E,E)*-**196** (2.00 g, 13.16 mmol) was added. Bu_4NHSO_4 (380 mg, 1.00 mmol), 250.0 mL of buffer solution (0.05 M $Na_2B_2O_4 \cdot 10H_2O$ in $4 \cdot 10^{-4}$ M EDTA) and ketone **200** (1.60 g, 6.27 mmol) were added and the solution was cooled to -10 °C by means of an ice/NaCl bath. A solution of Oxone (17.25 g, 28.25 mmol) in 152.0 mL of aq. $4 \cdot 10^{-4}$ M EDTA and a solution of K_2CO_3 (17.25 g, 124.73 mmol) in 152.0 mL of aq. $4 \cdot 10^{-4}$ M EDTA was added simultaneously in two dropping funnels over 1½ h. The reaction progress was monitored by GC. After the addition of the Oxone and K_2CO_3 solutions the reaction mixture was stirred for 1 h at -10 °C. The reaction was quenched by addition of 1.0 L of hexane. The layers were separated and the aq. layer was extracted with

hexane. The combined organic layers were washed with water and brine, dried and concentrated. Chromatography over silica gel with hex/MtBE 8:2 followed by short path distillation (0.05 mbar, 110 °C) afforded (+)-(*E*)-*trans*-**190** (1.17 g, 53%) as a colorless oil.

Opt. rot.: $[\alpha]_{\text{D}}^{25} + 44.88$ (*c* 1.050, MeOH).

IR (neat): 2972*m*, 1707*s*, 1446*m*, 1354*m*, 1239*w*, 1123*m*, 1010*m*, 971*m*, 929*m*, 867*m*, 812*m*, 740*m*.

¹*H*-NMR (300 MHz, CDCl₃): 5.99 (*d*, *J* = 15.6 Hz, 1 H); 5.29 (*m*, 1 H); 3.07 (*dd*, *J* = 2.3, 8.0 Hz, 1 H); 2.92 (*m*, 1 H); 2.12 (*s*, 3 H); 1.35 (*d*, *J* = 5.0 Hz, 3 H); 1.23 (*d*, *J* = 3.1 Hz, 6 H).

¹³*C*-NMR (75 MHz, CDCl₃): 210.5 (*s*); 139.2, 127.4 (2 *d*); 59.2, 56.3 (2 *d*); 50.1 (*s*); 25.4, 23.8, 23.5, 17.4 (4 *q*).

EI-MS (GC/MS): 168 (11, *M*⁺), 150 (13), 125 (33), 124 (57), 110 (43), 108 (100), 92 (53), 90 (51), 80 (48), 78 (54), 76 (54), 66 (67), 64 (64), 54 (76).

Anal. calc. for C₁₀H₁₆O₂ (168): C 71.39, H 9.59; found: C 71.44, H 9.47.

*Determination of the absolute configuration of (+)-(*E*)-*trans*-**190** by Horeau's method.*

A solution of epoxyketone (+)-(*E*)-*trans*-**190** (2.00 g, 11.90 mmol) in 10.0 mL of THF was cooled to -60 °C by means of a CO₂/acetone bath. BuLi 1.6 M in hexane (9.30 mL, 14.87 mmol) was added dropwise to the well stirred solution. The reaction mixture was warmed to -20 °C, stirred for 15 min. and then cooled to -60 °C again. BF₃·Et₂O (1.85 mL, 14.87 mmol) was added dropwise over 5 min. After stirring for 15 min. at -60 °C TLC analysis showed the complete disappearance of the epoxyketone (+)-(*E*)-*trans*-**190**. The reaction was quenched with water and extracted with MtBE. The ether layers were washed with water and brine, dried and concentrated. TLC analysis showed that a mixture of diketone (*E*)-**210** and the desired dienol (-)-**205** was formed, the major product being (*E*)-**210**. Dienol (-)-**205** (80 mg, 29%) was isolated by chromatography over silica gel with hex/MtBE 3:7.

Opt. rot.: $[\alpha]_{\text{D}}^{25} - 20.54$ (*c* 1.090, MeOH).

A sample of (-)-**205** (150 mg, 1.19 mmol) was dissolved in 3.0 mL pyridine and 2-phenylbutyric acid anhydride **179** (1.04 mL, 3.59 mmol) was added at room temperature. The mixture was stirred for 15 h at room temperature. GC analysis of the reaction mixture showed that the reaction had gone to completion. The reaction was quenched with 30.0 mL of water, a small amount of phenolphthalein was added and the stirred mixture was neutralized with 30% NaOH. The aq. solution was extracted with MtBE and the organic solutions were set aside. The aq. solution was acidified with AcOH and the 2-phenylbutyric acid **181** was extracted with MtBE. The ether extracts of **181** were washed with water, dried and concentrated. Short path distillation (0.05 bar, 150 °C) yielded (*R/S*)-**181** (790 mg, 80%) as a colorless oil.

Opt. rot.: $[\alpha]_{\text{D}}^{25} + 3.50$ (*c* 1.630, MeOH).

Based on Horeau's rule, the sign of the optical rotation indicates that (-)-**205** possesses (*R*)-configuration. The absolute configuration of the original epoxyketone (+)-(*E*)-*trans*-**190** can be correlated to the absolute configuration of (-)-(*R*)-**205** and was found to correspond to (*R*)-configuration at both stereogenic carbon atoms of the oxirane ring as illustrated in *Chapter 4.4.3, Scheme 69*.

Cyclization of (+)-(R,R)-(E)-190 with BF₃·Et₂O.

Hexamethyldisilazane (HMDS) (230 mg, 1.43 mmol) was placed in a reactor and 4.0 mL of THF were added. The solution was cooled with an ice/H₂O bath and BuLi 1.6 M in hexane (0.89 mL, 1.43 mmol) was added dropwise keeping the temperature between 5-10 °C. The solution was stirred for 15 min. and then cooled to -60 °C by means of a CO₂/acetone bath. A solution of epoxyketone (+)-(*R,R*)-(*E*)-**190** (200 mg, 1.19 mmol) in 1.0 mL of THF was added dropwise. The mixture was stirred for 15 min. and then BF₃·Et₂O (0.18 mL, 1.43 mmol) was added by syringe. After 20 min. TLC analysis showed no more change in the product distribution. The reaction mixture was poured onto water and extracted with MtBE. The organic layers were combined, washed with water and brine and concentrated. The product mixture contained (-)-(*E*)-**191** (67%), (+)-(*R,R*)-(*E*)-**190** (24%), (*E*)-**210** (6%) and **205** (3%) according to GC analysis. Cyclobutanone (-)-(*E*)-**191** was isolated by chromatography over silica gel with hex/MtBE 1:1. After drying in vacuo (-)-(*E*)-**191** (99 mg, 50%) was obtained as a colorless oil.

Opt. rot.: $[\alpha]_{\text{D}}^{25}$ - 3.92 (*c* 1.020, MeOH).

Enantiomeric excess (chiral GC): 16%

IR (neat): 3435*m*, 2963*m*, 1775*s*, 1462*w*, 1365*w*, 1251*m*, 1143*m*, 1062*s*, 972*m*, 840*s*, 753*w*.

¹H-NMR (300 MHz, CDCl₃): 5.79-5.60 (*m*, 2 H); 4.35 (*m*, 1 H); 3.22-3.11 (*m*, 1 H); 2.98 (*dd*, *J* = 17.5, 7.6 Hz, 1 H); 2.70 (*m*, 1 H); 1.90 (*s*, 1 H); 1.29 (*d*, *J* = 6.1 Hz, 3 H); 1.20 (*d*, *J* = 0.8 Hz, 3 H); 1.05 (*d*, *J* = 1.1 Hz, 3 H).

¹³C-NMR (75 MHz, CDCl₃): 213.9 (*s*); 136.6, 128.3, 128.2, 68.3 (3 *d*); 63.0 (*s*); 47.6, 47.5 (1 *t*); 38.5, 38.4 (1 *d*); 23.5, 22.8, 18.2 (3 *q*).

EI-MS (GC/MS): 168 (1, *M*⁺), 150 (2), 135 (2), 126 (27), 111 (59), 108 (79), 93 (35), 81 (38), 70 (100), 55 (32), 43 (71).

Cyclization of (+)-(R,R)-(E)-190 with Et₃Al.

HMDS (288 mg, 1.79 mmol) was placed in a reactor and 4.0 mL of THF were added. The solution was cooled with an ice/H₂O bath and BuLi 1.6 M in hexane (1.11 mL, 1.79 mmol) was added dropwise. The solution was stirred for 15 min. and then cooled to -60 °C by means of a CO₂/acetone bath. A solution of epoxyketone (+)-(*R,R*)-(*E*)-**190** (200 mg, 1.19 mmol) in 1.0 mL of

THF was added dropwise. The reaction mixture was stirred for 15 min. and Et₃Al (2.00 mL, 1.79 mmol) was added by syringe. After stirring at -60 °C for 30 min. the mixture was analyzed by TLC. In order to complete the reaction, the mixture was warmed to -20 °C and stirred at that temperature for 15 min. TLC analysis now showed that the reaction had gone to completion. The reaction was quenched with water and the mixture was extracted with MtBE. The ether layers were washed with water and brine, dried and concentrated. Chromatography over silica gel with hex/MtBE 1:1 afforded (+)-(*E*)-**191** (56 mg, 28%) as a colorless oil.

Opt. rot.: $[\alpha]_{\text{D}}^{25} + 10.86$ (*c* 1.050, MeOH).

Enantiomeric excess C(3) (¹H-NMR with Pirkel reagent on diketone (E)-212): 46%

Cyclization of (+)-(R,R)-(E)-190 with Me₃SiOTf.

A solution of HMDS (213 mg, 1.50 mmol) in 8.0 mL of THF was cooled to -10 °C by means of a ice/CO₂ bath. BuLi 1.6 M in hexane (0.94 mL, 1.50 mmol) was added dropwise and the solution was stirred for 15 min. (+)-(R,R)-(E)-**190** was added as a solution in 2.0 mL of THF. The reaction mixture was stirred for 15 min. and then cooled to -60 °C in an acetone/CO₂ bath. Trimethylsilyl triflate Me₃SiOTf (0.35 mL, 1.95 mmol) was added dropwise. TLC analysis showed that an approx. 7:3 mixture of cyclobutanone (*E*)-**191** and diketone (*E*)-**210** was formed just minutes after the addition of Me₃SiOTf. The reaction was quenched with water and the mixture was extracted with MtBE. The combined ether layers were washed with water and brine, dried over MgSO₄ and concentrated. Chromatography over silica gel with hex/MtBE 9:1 followed by short path distillation (0.05 mbar, 60 °C) gave (-)-(*E*)-**191** (200 mg, 69%) as colorless oil.

Opt. rot.: $[\alpha]_{\text{D}}^{25} - 2.14$ (*c* 1.260, MeOH).

Diastereomeric excess (chiral GC): 9%

(E)-4,4-Dimethyl-6-(3-methyloxiranyl)-3-oxohex-5-enoic acid methyl ester ((+)-(R,R)-(E)-241).

HMDS (1.21 g, 7.02 mmol) was dissolved in 20.0 mL of THF and the solution was cooled to -10 °C. BuLi 1.6 M in hexane (4.70 mL, 7.50 mmol) was added dropwise and the mixture was stirred for 15 min. A solution of (+)-(R,R)-(E)-**190** (1.18 g, 7.02 mmol) in 4.0 mL of THF was added. After stirring for 20 min. the reaction mixture was cooled to -60 °C by means of an acetone/CO₂ bath. Methyl cyanoformate (0.84 mL, 10.52 mmol) was added in 5 min. and the mixture was stirred at -60 °C for 30 min. The reaction was monitored by TLC analysis.

The reaction mixture was poured onto water and extracted with MtBE. The combined ether layers were washed with water and brine, dried over MgSO₄ and concentrated. Chromatography over silica gel with hex/MtBE followed by short path distillation (0.05 mbar, 100 °C) afforded (+)-(*R,R*)-(*E*)-**241** (810 mg, 51%) as a colorless oil.

Opt. rot.: $[\alpha]_{\text{D}}^{25} + 36.30$ (c 1.485, MeOH).

IR (neat): 2973 m , 1707 s , 1467 w , 1354 m , 1238 w , 1123 m , 1010 m , 971 m , 929 m , 867 m , 812 m , 740 m .

$^1\text{H-NMR}$ (300 MHz, CDCl_3): 6.12 (d , $J=16.4$ Hz, 1 H); 5.52 (dd , $J=7.6, 16.0$ Hz, 1 H); 3.89 (s , 3 H); 3.70 (s , 2 H); 3.25 (d , $J=2.3, 7.6$ Hz, 1 H); 3.09 (m , 1 H); 1.52 (d , $J=5.0$ Hz, 3 H); 1.43 (d , $J=2.3$ Hz, 6 H).

$^{13}\text{C-NMR}$ (75 MHz, CDCl_3): 204.5, 167.7 (2 s); 137.8, 128.6, 58.9, 56.3 (4 d); 52.1 (q); 50.4 (s); 44.2 (t); 23.4, 23.3, 17.3 (3 q).

EI-MS (GC/MS): 226 (1, M^+), 208 (1 $[M-\text{H}_2\text{O}]^+$), 195 (2), 183 (6), 167 (17), 125 (23), 108 (24), 101 (35), 93 (19), 83 (40), 69 (21), 55 (30) 43 (100).

2-((E)-3-Hydroxybut-1-enyl)-3,3-dimethyl-4-oxocyclobutanecarboxylic acid methyl ester (242).

A solution of HMDS (81 mg, 0.50 mmol) in 4.0 mL THF was cooled to 0 °C with an ice/H₂O bath. BuLi 1.6 M in hexane (0.31 mL, 0.50 mmol) was added by syringe and the mixture was stirred for 15 min. β -Ketoester (+)-(*R,R*)-(*E*)-**241** (100 mg, 0.44 mmol) was mixed with 1.0 mL of THF and added dropwise by syringe. The mixture was stirred at 0 °C for 30 min. and then cooled to -60 °C by means of an CO₂/acetone bath. Me₃SiOTf (0.11 mL, 0.60 mmol) was added and stirring was continued for 30 min. The reaction was monitored by TLC. The reaction was quenched with water and the mixture was extracted with MtBE. The ether layers were combined and washed with water and brine. After drying over MgSO₄ and concentration of the ether solution, the products were separated by chromatography over silica gel with hex/MtBE 9:1. Cyclobutanone **242** (22 mg, 17%) and the fragmentation product **243** (9 mg, 11%) were obtained after short path distillation (0.05 mbar, 120 °C for **242** and 0.05 mbar, 80 °C for **243**).

Analytical data for **242**:

$^1\text{H-NMR}$ (300 MHz, CDCl_3): 5.55 (m , 2 H); 4.20 (m , 1 H); 3.98 (m , 1 H); 3.63 (d , $J=1.5$ Hz, 3 H); 3.00 (m , 1 H); 1.11 (m , 6 H); 0.99 (s , 3 H); 0.00 (s , 9 H).

$^{13}\text{C-NMR}$ (75 MHz, CDCl_3): 204.9, 166.8 (2 s); 138.4, 124.6, 124.3, 68.5, 68.2, 64.1, 64.0 (4 d); 62.4 (s); 52.2 (q); 41.5 (d); 24.3, 22.0, 18.6 (3 q); 0.0 (3 q).

Analytical data for **243**:

$^1\text{H-NMR}$ (300 MHz, CDCl_3): 6.20 (m , 1 H); 5.67 (m , 1 H); 5.43 (dd , $J=6.5, 15.3$, 1 H); 4.22 (m , 1 H); 1.64 (d , $J=6.1$ Hz, 6 H); 1.12 (d , $J=6.1$ Hz, 3 H); 0.00 (s , 9 H).

$^{13}\text{C-NMR}$ (75 MHz, CDCl_3): 134.8 (s); 134.7, 124.9, 124.2, 69.0 (4 d); 25.7, 24.3, 17.9 (3 d); 0.0 (3 q).

Carbonic acid [(E)-2,2-dimethyl-1-methylene-4-(3-methyloxiranyl)but-3-enyl] ethyl ester ((R,R)-(E)-247).

HMDS (2.42 g, 15.00 mmol) was placed in a reactor and 50.0 mL of THF were added. The solution was cooled to -10 °C by means of an ice/acetone bath. BuLi 1.6 M in hexane (9.40 mL, 15.00 mmol) was added dropwise to the stirred solution. Epoxyketone (+)-(R,R)-(E)-**190** (2.00 g, 12.00 mmol) was added as a solution in 5.0 mL of THF. The mixture was stirred for 15 min. and then triethylamine (3.00 g, 30.00 mmol) was added and the solution was cooled to -60 °C with an CO₂/acetone bath. Ethyl chloroformate (2.17 g, 20.00 mmol) was added dropwise. After the addition the mixture was slowly warmed to room temperature. GC analysis showed that the reaction had gone to completion. The mixture was poured onto water and extracted with MtBE. The ether layers were washed with water and brine, dried and concentrated. The crude product was purified by chromatography over silica gel with hex/MtBE 8:2 leading to (R,R)-(E)-**247** (1.98 g, 69%) as a colorless oil after short path distillation (0.05 mbar, 120 °C).

IR (neat): 2975w, 1757s, 1652w, 1465w, 1369w, 1217vs, 1142m, 1074m, 1005m, 927w, 860nm, 820w, 778w.

¹H-NMR (300 MHz, CDCl₃): 5.96 (m, 1 H); 5.27 (m, 1 H); 4.94 (d, *J* = 2.7 Hz, 1 H); 4.88 (d, *J* = 2.3 Hz, 1 H); 4.25 (m, 2 H); 3.07 (dd, *J* = 2.3, 8.0, 1 H); 2.92 (m, 1 H); 1.39-1.23 (m, 12 H).

¹³C-NMR (75 MHz, CDCl₃): 160.4, 153.3 (2 s); 140.9, 126.0 (2 d); 100.3, 64.2 (2 t); 59.4, 56.2 (2 d); 41.5 (s); 25.2, 25.0, 17.4, 14.1 (4 q).

EI-MS (GC/MS): 224 (1, *M*⁺), 180 (3), 152 (11), 134 (42), 124 (18), 108 (53), 94 (49), 90 (53), 82 (100), 78 (49), 66 (45), 54 (47).

High res. EI-MS calculated for C₁₄H₂₀O₄: 240.1362; found: 240.1365.

3-((E)-Hydroxybut-1-enyl)-2,2-dimethylcyclobutanone ((-)-(E)-191) (from Carbonic acid [(E)-2,2-dimethyl-1-methylene-4-(3-methyloxiranyl)but-3-enyl ethyl] ester ((R,R)-(E)-247).

Carbonate (R,R)-(E)-**247** (100 mg, 0.42 mmol) was dissolved in 4.0 mL of THF and then cooled to -10 °C by means of an ice/acetone bath. BuLi 1.6 M in hexane (0.92 mL, 1.47 mmol) was added dropwise. The solution was stirred for 15 min. and then cooled to -60 °C with a CO₂/acetone bath. BF₃·Et₂O (0.19 mL, 1.50 mmol) was added dropwise and the clear solution was stirred at -60 °C for 20 min. TLC analysis showed that the carbonate (R,R)-(E)-**247** had been consumed entirely. The mixture was poured onto water and extracted with MtBE. The ether layers were combined, washed with water and brine and concentrated. Chromatography over silica gel with hex/MtBE 1:1 afforded (-)-(E)-**191** (38 mg, 55%) as a colorless oil after drying in vacuo.

Opt. rot.: [α]_D²⁵ - 2.31 (c 1.080, MeOH).

Diastereomeric excess (chiral GC): 10%

(*S,R*)-(*E*)-4-(2,2-Dimethylcyclobutyl)but-3-en-2-ol ((*S,R*)-(*E*)-**252**).

Cyclobutanone (-)-(*E*)-**191** (100 mg, 0.60 mmol, 18% de) was mixed with 1 mL diethylenglycol and hydrazine 85% (0.08 mL, 2.20 mmol) was added. One pellet of solid KOH (112 mg, 2.00 mmol) was added and the solution was heated to 100-120 °C. When the solution became clear and homogeneous, the temperature was raised to reflux (125 °C) for 30 min. The condenser was removed and the volatiles were removed by a constant stream of nitrogen. Heating was continued until the interior temperature reached 185-190 °C. Stirring was continued at this temperature for 2 h. GC analysis showed the formation of product and the complete disappearance of the starting material.

After cooling to room temperature, the reaction mixture was poured onto water and the mixture was extracted with MtBE. The organic layers were combined, washed, dried and concentrated. The crude product was purified by short path distillation (0.05 mmbar, 120 °C) furnishing (-)-(*S,R*)-(*E*)-**252** (70 mg, 76%) as a colorless oil.

Opt. rot.: $[\alpha]_{\text{D}}^{25} + 7.95$ (*c* 1.220, CH₃Cl).

Diastereomeric excess (¹³C-NMR): 18%

IR (neat): 3343s, 2952vs, 2863m, 1460m, 1367s, 1255s, 1143m, 1057s, 971vs, 939m.

¹H-NMR (300 MHz, CDCl₃): 5.66 (*m*, 1 H); 5.45 (*m*, 1 H); 4.28 (*m*, 1 H); 2.53 (*m*, 1 H); 2.01-1.48 (*m*, 5 H); 1.25 (*m*, 3 H); 1.05 (*d*, 3 H); 0.95 (*s*, 3 H).

¹³C-NMR (75 MHz, CDCl₃): 134.1, 134.0, 131.3, 131.2, 68.8, 68.7 (4 *d*); 39.5 (*s*); 32.4 (*t*); 29.9, 23.4, 22.9 (3 *q*); 21.4, 21.3 (1 *t*).

EI-MS (GC/MS): 154 (1, *M*⁺), 139 (1 [*M*-CH₃]⁺), 136 (2 [*M*-H₂O]⁺), 121 (3), 98 (6), 93 (7), 83 (15), 80 (10), 79 (17), 55 (16), 43 (100), 39 (11).

(*E*)-4-(2,2-Dimethylcyclobutyl)but-3-en-2-one ((*S*)-(*E*)-**189**).

Powdered molecular sieve 4 Å (0.1 g) was suspended in 5.0 mL of CH₂Cl₂. Pyridinium chlorochromate (100 mg, 0.46 mmol) was added and the orange suspension was stirred at room temperature for 30 min. Cyclobutane (*S,R*)-(*E*)-**252** (50 mg, 0.32 mmol) was added and stirring was continued for 1 h. TLC analysis showed that complete oxidation to junionone had taken place. Hexane was added to the reaction mixture under vigorous stirring until a black granular solid formed that settled rapidly. The solids were removed by filtration and the clear filtrate was concentrated. Short path distillation (10 mbar, 80 °C) gave (-)-junionone (-)-(*S*)-(*E*)-**189** (48 mg, 99%) as a colorless liquid.

Opt. rot.: $[\alpha]_{\text{D}}^{25} - 1.65$ (*c* 0.605, CH₃Cl).

Enantiomeric excess (chiral GC): 11%

IR (neat): 2952m, 2863w, 1696w, 1671s, 1620m, 1462w, 1360m, 1253s, 1151w, 981m.

$^1\text{H-NMR}$ (300 MHz, CDCl_3): 6.83 (*dd*, $J = 7.3, 16.1$ Hz, 1 H); 5.99 (*dd*, $J = 1.6, 16.1$ Hz, 1 H); 2.74 (*m*, 1 H); 2.26 (*s*, 3 H); 2.02 (*m*, 1 H); 1.92 (*m*, 1 H); 1.78 (*m*, 1 H); 1.63 (*m*, 1 H); 1.13 (*s*, 3 H); 1.01 (*s*, 3H).

$^{13}\text{C-NMR}$ (100 MHz, CDCl_3): 198.6 (*s*); 149.0, 130.6, 47.0 (3 *d*); 40.8 (*s*); 32.6 (*t*); 30.0, 26.9, 23.4 (3 *q*); 20.8 (*t*).

EI-MS (GC/MS): 152 (3, M^+), 137 (13, $[M-\text{CH}_3]^+$), 108 (80), 96 (100), 94 (49), 93 (45), 81 (46), 80 (88), 78 (49), 68 (37), 66 (41), 55 (54), 52 (55).

X-ray crystallographic data for (-)-(R)-(E)-176**Definition of Terms**

Function minimized:	$\Sigma w(F_o^2 - F_c^2)^2$
w	$= [\sigma^2(F_o^2) + (aP)^2 + bP]^{-1}$ and $P = (F_o^2 + 2F_c^2)/3$
F_o^2	$= S(C - RB)/Lp$ and $\sigma^2(F_o^2) = S^2(C + R^2B)/Lp^2$
S	$=$ Scan rate
C	$=$ Total integrated peak count
R	$=$ Ratio of scan time to background counting time
B	$=$ Total background count
Lp	$=$ Lorentz-polarization factor
R-factors:	
R_{int}	$= \Sigma <F_o^2> - F_o^2 / \Sigma F_o^2$ summed only over reflections for which more than one symmetry equivalent was measured.
$R(F)$	$= \Sigma F_o - F_c / \Sigma F_o $ summed over all observed reflections.
$wR(F^2)$	$= [\Sigma w(F_o^2 - F_c^2)^2 / \Sigma w(F_o^2)^2]^{1/2}$ summed over all reflections.

Standard deviation of an observation of unit weight (goodness of fit):

$$[\Sigma w(F_o^2 - F_c^2)^2 / (N_o - N_v)]^{1/2}$$

where N_o = number of observations; N_v = number of variables

Crystal-Structure Determination. A crystal of $C_{21}H_{32}O_5$ (-)-(E)-176, obtained from hexane / MTBE, was mounted on a glass fibre and used for a low-temperature X-ray structure determination. All measurements were made on a *Nonius KappaCCD* area-detector diffractometer²² using graphite-monochromated Mo $K\alpha$ radiation ($\lambda = 0.71073$ Å) and an *Oxford Cryosystems Cryostream 700* cooler. The unit cell constants and an orientation matrix for data collection were obtained from a least-squares refinement of the setting angles of 3464 reflections in the range $4^\circ < 2\theta < 55^\circ$. The mosaicity was $0.576(3)^\circ$. A total of 207 frames were collected using ϕ and ω scans with κ offsets, 180 seconds exposure time and a rotation angle of 2.0° per frame, and a crystal-detector distance of 30.0 mm.

²² R. Hooft, *KappaCCD Collect Software*, Nonius BV, Delft, The Netherlands, 1999.

Data reduction was performed with *HKL Denzo* and *Scalepack*²³. The intensities were corrected for Lorentz and polarization effects, but not for absorption. The space group was determined from packing considerations, a statistical analysis of intensity distribution, and the successful solution and refinement of the structure. Equivalent reflections were merged. Data collection and refinement parameters are given in *Table 1*. A view of the molecule is shown in *Chapter 4.3.5, Figure 26*.

The structure was solved by direct methods using *SIR92*²⁵, which revealed the positions of all non-hydrogen atoms. The asymmetric unit contains two symmetry-independent molecules and substantial differences in the conformations of the two molecules preclude the possibility of additional overlooked crystallographic symmetry. In one of the independent molecules, the atoms from the alkene group through to the diethyl and methylketone groups are disordered. Two positions were defined for each of these atoms and refinement of the site occupation factors yielded a value of 0.535(8) for the major conformation. Bond length and similarity restraints were applied to all chemically equivalent bond lengths and angles involving the disordered atoms. Furthermore, neighboring atoms within and between each disordered conformation were restrained to have similar atomic displacement parameters. The non-hydrogen atoms were refined anisotropically. All of the H-atoms were placed in geometrically calculated positions and refined using a riding model where each H-atom was assigned a fixed isotropic displacement parameter with a value equal to 1.2U_{eq} of its parent atom (1.5U_{eq} for the methyl groups). Refinement of the structure was carried out on F^2 using full-matrix least-squares procedures, which minimized the function $\sum w(F_o^2 - F_c^2)^2$. The weighting scheme was based on counting statistics and included a factor to down weight the intense reflections. Plots of $\sum w(F_o^2 - F_c^2)^2$ versus $F_c / F_c(\text{max})$ and resolution showed no unusual trends. A correction for secondary extinction was applied. One reflection, whose intensity was considered to be an extreme outlier, was omitted from the final refinement.

Neutral atom scattering factors for non-hydrogen atoms were taken from Maslen, Fox and O'Keefe^{28a}, and the scattering factors for H-atoms were taken from Stewart, Davidson and

²³ Z. Otwinowski, W. Minor, in *Methods in Enzymology*, Vol. 276, *Macromolecular Crystallography*, Part A, Eds. C.W. Carter Jr., R.M. Sweet, Academic Press, New York, 1997, pp. 307-326.

²⁴ R.H. Blessing, *Acta Crystallogr., Sect. A* **1995**, *51*, 33-38.

²⁵ A. Altomare, G. Cascarano, C. Giacovazzo, A. Guagliardi, M.C. Burla, G. Polidori, M. Camalli, *SIR92, J. Appl. Crystallogr.* **1994**, *27*, 435.

²⁶ A. Altomare, G. Cascarano, C. Giacovazzo, A. Guagliardi, M.C. Burla, G. Polidori, M. Camalli, *SIR92, J. Appl. Crystallogr.* **1994**, *27*, 435.

²⁷ a) H.D. Flack, G. Bernardinelli, *Acta Crystallogr., Sect. A* **1999**, *55*, 908-915; b) H.D. Flack, G. Bernardinelli, *J. Appl. Crystallogr.* **2000**, *33*, 1143-1148.

²⁸ a) E.N. Maslen, A.G. Fox, M.A. O'Keefe, in 'International Tables for Crystallography', Ed. A.J.C. Wilson, Kluwer Academic Publishers, Dordrecht, 1992, Vol. C, Table 6.1.1.1, pp. 477-486; b) D.C. Creagh, W.J. McAuley, *ibid.* Table 4.2.6.8, pp. 219-222; c) D.C. Creagh, J.H. Hubbell, *ibid.* Table 4.2.4.3, pp. 200-206.

Simpson²⁹. Anomalous dispersion effects were included in F_c ³⁰; the values for f' and f'' were those of Creagh and McAuley^{28b}. The values of the mass attenuation coefficients are those of Creagh and Hubbel^{28c}. All calculations were performed using the *SHELXL97*³¹ program.

Crystallographic Data for (-)-(R)-(E)-176

Crystallized from	hexane / MTBE
Empirical formula	C ₂₁ H ₃₂ O ₅
Formula weight [g mol ⁻¹]	364.48
Crystal colour, habit	colorless, plate
Crystal dimensions [mm]	0.05 × 0.10 × 0.30
Temperature [K]	160 (1)
Crystal system	triclinic
Space group	<i>P</i> 1 (#1)
<i>Z</i>	2
Reflections for cell determination	3464
2 θ range for cell determination [°]	4–50
Unit cell parameters <i>a</i> [Å]	6.3813(3)
<i>b</i> [Å]	9.4373(4)
<i>c</i> [Å]	16.9480(9)
α [°]	89.700(2)
β [°]	81.267(3)
γ [°]	87.576(3)
<i>V</i> [Å ³]	1007.91(8)
<i>F</i> (000)	396
<i>D_x</i> [g cm ⁻³]	1.201
μ (Mo <i>K</i> α) [mm ⁻¹]	0.0840
Scan type	ϕ and ω
2 θ _(max) [°]	50
Total reflections measured	14102
Symmetry independent reflections	3523
<i>R</i> _{int}	0.062

²⁹ R.F. Stewart, E.R. Davidson, W.T. Simpson, *J. Chem. Phys.* **1965**, 42, 3175-3187.

³⁰ J.A. Ibers, W.C. Hamilton, *Acta Crystallogr.* **1964**, 17, 781-782.

³¹ G.M. Sheldrick, *SHELXL97, Program for the Refinement of Crystal Structures*, University of Göttingen, Germany, 1997.

Reflections with $I > 2\sigma(I)$	3122
Reflections used in refinement	3522
Parameters refined; restraints	578; 277
Final $R(F)$ [$I > 2\sigma(I)$ reflections]	0.0482
$wR(F^2)$ (all data)	0.1344
Weights:	$w = [\sigma^2(F_o^2) + (0.0716P)^2 + 0.2553P]^{-1}$ where $P = (F_o^2 + 2F_c^2)/3$
Goodness of fit	1.092
Secondary extinction coefficient	0.051(9)
Final Δ_{\max}/σ	0.007
$\Delta\rho$ (max; min) [$\text{e } \text{\AA}^{-3}$]	0.47; -0.17
$\sigma(d_{\text{C-C}})$ [\AA]	0.00–0.0

4.7 References

- [38] E. D. Hughes, *Trans. Faraday Soc.* **1938**, *34*, 185-202.
- [39] S. Winstein, *Dissertation, California Institute of Technology*, **1938**.
- [40] J. D. Roberts, Wm. G. Young, S. Winstein, *J. Am. Chem. Soc.*, **1942**, 2157-2164.
- [41] L. A. Paquette, C. J. M. Stirling, *Tetrahedron* **1992**, *48*, 7383.
- [42] G. Stork, W. N. White, *J. Am. Chem. Soc.*, **1956**, *78*, 4609-4619.
- [43] J. Staroscik, B. Rickborn, *J. Am. Chem. Soc.*, **1971**, *93*, 3046-3047.
- [44] C. R. Johnson, D. M. Wieland, *J. Am. Chem. Soc.*, **1971**, *93*, 3047-3049.
- [45] G. Stork,; A. F. Kreft, *J. Am. Chem. Soc.*, **1977**, *99*, 3850-3851.
- [46] G. Stork,; A. F. Kreft, *J. Am. Chem. Soc.*, **1977**, *99*, 3851-3853.
- [47] R. M. Magid, O. S. Fruchey, *J. Am. Chem. Soc.*, **1977**, *99*, 8368-8370.
- [48] E. Toromanoff, J. Martel, J. Mathieu, G. Nomine, *Tetrahedron Lett.*, **1972**, *15*, 1491-1496.
- [49] R. M. Magid, *Tetrahedron* **1980**, *36*, 1901.
- [50] S. E. Denmark, L. K. Marble, *J. Org. Chem.*, **1990**, *55*, 1984-1986.
- [51] P. L. Fuchs, R. E. Donaldson, *J. Am. Chem. Soc.*, **1981**, *103*, 2108-2110.
- [52] W. Kirmse, F. Scheidt, H.-J. Vater, *J. Am. Chem. Soc.*, **1978**, *100*, 3945-3946.
- [53] L. A. Paquette, S. L. Schreiber, *J. Am. Chem. Soc.*, **1989**, *111*, 2331-2332.
- [54] S.-I. Murahashi, Y. Tanigawa et al., *J. Am. Chem. Soc.*, **1978**, *100*, 4610-4612.
- [55] C. L. Liotta, *Tetrahedron Lett.*, **1975**, *16*, 523-526.
- [56] W. D. Stohrer, *Angew. Chem.*, **1983**, *95*, 642-643.
- [57] K. N. Houk, M. N. Paddon-Row, N. G. Rondan, *J. Mol. Structure THEOCHEM*, **1983**, *12*, 197-208.
- [58] R. L. Yates, D. Epiotis, F. Bernardi, *J. Am. Chem. Soc.*, **1975**, *97*, 6615-6621.
- [59] M. J. S. Dewar, *J. Am. Chem. Soc.*, **1984**, *106*, 209-219.
- [60] G. Fráter, U. Müller, W. Günther, *Tetrahedron*, **1984**, *40*, 1269-1277.
- [61] G. Fráter, U. Müller, W. Günther, *Helv. Chim. Acta*, **1986**, *69*, 1858-1861.
- [62] A. Sidani, J. Marchand-Brynaert, L. Ghosez, *Angew. Chem.*, **1974**, *86*, 272.
- [63] C. Houge, A. M. Frisque-Hesbain, A. Mockel, L. Ghosez, J. P. Declercq, G. Germain, M. Van Meerssche, *J. Am. Chem. Soc.*, **1982**, *104*, 2920-2921.
- [64] L. Ghosez, F. Mahuteau-Betzer, C. Genicot, A. Vallribera, J.-F. Cordier, *Chem. Eur. J.*, **2002**, *8*, 3411-3422.
- [65] B. M. Trost, T. Yasukata, *J. Am. Chem. Soc.*, **2001**, *123*, 7162-7163.
- [66] M. Yoshida, M. Abdel-Hamid Ismail, H. Nemoto, M. Ihara, *J. Chem. Soc., Perkin Trans. I*, **2000**, 2629-2635.
- [67] J. E. Baldwin, *J.C.S. Chem. Comm.*, **1976**, 734-736.

-
- [68] E. Benzing, *Angew. Chem.*, **1959**, *15*, 521.
- [69] T. Inukai, R. Yoshizawa, *J. Org. Chem.*, **1967**, *32*, 404-407.
- [70] T. Mukaiyama, K. Banno, K. Narasaka, *J. Am. Chem. Soc.*, **1974**, *96*, 7503-7509.
- [71] E. Nakamura, M. Shimizu, I. Kuwajima, J. Sakata, K. Yokoyama, R. Noyori, *J. Org. Chem.*, **1983**, 932-945.
- [72] R. G. Pearson, *J. Chem. Edu.*, **1968**, *45*, 581-587; R. G. Pearson, *J. Chem. Edu.*, **1968**, *45*, 643-648.
- [73] T. L. Ho, *Tetrahedron*, **1985**, *41*, 1-86.
- [74] H. C. Brown, J. Chandrasekharan, P. V. Ramachandran, *J. Am. Chem. Soc.*, **1988**, *110*, 1539-1546; H. C. Brown, B. Singaram, *J. Org. Chem.*, **1984**, *49*, 945-947.
- [75] A. Horeau, *Tetrahedron Lett.*, **1961**, *15*, 506-512.
- [76] R. M. Magid, B. G. Thally, S. K. Souther, *J. Org. Chem.*, **1981**, *46*, 824-825.
- [77] A. F. Thomas, M. Ozainne, *Chem. Commun.*, **1973**, *19*, 746.
- [78] H. O. House, R. L. Wasson, *J. Am. Chem. Soc.*, **1956**, *78*, 4394-4400.
- [79] E. Weitz, A. Scheffer, *Ber. Dtsch. Chem. Ges.*, **1921**, *54B*, 2327-2344.
- [80] M. Frohn, M. Dalkiewicz, Y. Tu, Z.-X. Wang, Y. Shi, *J. Org. Chem.*, **1998**, *63*, 2948-2953.
- [81] J. Herscovici, K. Antonakis, *J. C. S. Chem. Commun.*, **1980**, 561-562.
- [82] M. Yamaguchi, K. Shibato, I. Hirao, *Tetrahedron Lett.*, **1984**, *25*, 1159-1162.
- [83] M. Yamaguchi, I. Hirao, *Chem. Lett.*, **1985**, 337-338.
- [84] S. G. Davies, P. Warner, *Tetrahedron Lett.*, **1985**, *26*, 4815-4818.
- [85] H. H. Wasserman, S. Wolff, T. Oku, *Tetrahedron Lett.*, **1986**, *27*, 4909-4912.
- [86] T.-J. Sturm, A. E. Marolewski, D. S. Rezenka, S. K. Taylor, *J. Org. Chem.*, **1989**, *53*, 2039-2040.
- [87] M. Chini, P. Crotti, L. Favero, M. Pineschi, *Tetrahedron Lett.*, **1991**, *32*, 7583-7586.
- [88] P. Crotti, V. Di Bussolo, L. Favero, F. Macchia, M. Pineschi, *Tett. Lett.*, **1994**, *35*, 6537-6540.
- [89] P. Crotti, V. Di Bussolo, L. Favero, F. Macchia, M. Pineschi, *J. Org. Chem.*, **1996**, *61*, 9548-9552.
- [90] P. Crotti, F. Badalassi, V. Di Bussolo, L. Favero, M. Pineschi, *Tetrahedron*, **2001**, *57*, 8559-8572.
- [91] S. K. Taylor, J. A. Fried, Y. N. Grassl, A. E. Marolewski, E. A. Pelton, T.-J. Poel, D. S. Rezenka, M. R. Whittaker, *J. Org. Chem.*, **1993**, *58*, 7304-7307.
- [92] M. E. Jung, D. C. D'Amico, *J. Am. Chem. Soc.*, **1993**, *115*, 12208-12209.

5. Tables

<i>Table 1.</i> Phenol alkylation with (-)-sparteine using different bases.	18
<i>Table 2.</i> Experimental results with different chiral auxiliaries.	21
<i>Table 3.</i> Results from solid-state alkylation reactions.	22
<i>Table 4.</i> Summary of S _N 2' reactions from the literature.	53
<i>Table 5.</i> Non-bonded vs. electrostatic interactions in S _N 2' reactions by Epiotis et al.	59
<i>Table 6.</i> Absolute configuration of the <i>cis</i> -epoxy-ketone by correlation.	91
<i>Table 7.</i> Epoxide activation with aluminum ester enolates by Taylor et al.	97
<i>Table 8.</i> Cyclization experiments of (<i>R,R</i>)-(<i>E</i>)- 190 with different Lewis acids.	101

6. Figures

Figure 1. a) 300 MHz NMR spectrum of <i>rac</i> - 40 . b) <i>rac</i> - 40 with chiral shift reagent.....	17
Figure 2. Chiral auxiliaries used for the alkylation of 2,6-dimethyl phenol.	20
Figure 3. (-)-sparteine vs. Tröger's base.....	22
Figure 4. Postulated structure of the allyl bromide/ α -isosparteine salt 63	23
Figure 5. Postulated transition state for the phenol alkylation with 63	23
Figure 6. ORTEP plot of allyl bromide/ α -isosparteine salt 63 , benzene molecules omitted.	24
Figure 7. Possible sites of attack on 2,6-dimethyl phenol.	24
Figure 8. IR and VCD spectrum of (<i>R</i>)- 66 in acetonitrile- d_3	27
Figure 9. Simulated VCD curves of the two enantiomers of 66	28
Figure 10. Proposed structure of (<i>R</i>)- 66	28
Figure 11. IR and VCD spectrum of 70 in acetonitrile- d_3	29
Figure 12. Simulated VCD curves of the two enantiomers of 70	29
Figure 13. Proposed structure of (<i>S</i>)- 70 based on the VCD spectrum.	30
Figure 14. Allyl bromide/ α -isosparteine salt 63	32
Figure 15. LUMO distortion in allylic systems by Liotta et al.....	56
Figure 16. Static distortion in the <i>syn</i> and <i>anti</i> transition state by Stohrer.....	56
Figure 17. sp^n -Hybridization of the central carbon atom in the allylic system.	57
Figure 18. Static distortion of the allylic system in the <i>syn</i> and <i>anti</i> transition state.	57
Figure 19. Aromatic transition state in S_N2' reactions proposed by Epiotis et al.	58
Figure 20. Trajectory for nucleophilic <i>syn</i> attack on allylic systems.	58
Figure 21. Preferred transition states for charged and neutral nucleophiles.	59
Figure 22. $A^{1,2}$ and $A^{1,3}$ strain in the allylic system of (<i>S</i>)-(<i>E</i>)- 139	64
Figure 23. Evans-Polanyi plot for the <i>syn</i> -reactions of conformer 1 and 2 of (<i>S</i>)-(<i>E</i>)- 139E	65
Figure 24. HSAB considerations in the S_Ni' reaction.....	74
Figure 25. HSAB effects in alkyl vs. allylic systems.	74
Figure 26. ORTEP plot of the camphanoate derivative of (+)-(<i>E</i>)- 178	76
Figure 27. Interpretation of the results from Horeau's method.	78
Figure 28. Analysis of the cyclobutanone products by chiral GC.....	80
Figure 29. Lowest energy conformer of (+)-(<i>S</i>)-(<i>E</i>)- 140	81
Figure 30. ROA spectra of (+)-(<i>S</i>)-(<i>E</i>)- 140	82
Figure 31. Superimposed experimental ROA spectra of (+)-(<i>S</i>)-(<i>E</i>)- and (-)-(<i>R</i>)-(<i>Z</i>)- 140	82
Figure 32. VCD spectrum of (+)-(<i>S</i>)-(<i>E</i>)- 140	83
Figure 33. Experimental data from the stereoselective S_Ni' reaction.....	84

<i>Figure 34.</i> RAMAN/ROA spectrum of (<i>R,R</i>)-(<i>E</i>)- 190 vs. (<i>R,R</i>)- 208	93
<i>Figure 35.</i> Weakening of the epoxide carbon-oxygen bond by a soft Lewis acid.	96
<i>Figure 36.</i> Analysis of junionone with chiral GC.....	106
<i>Figure 37.</i> Chiral GC of synthetic (+)-junionone vs. natural junionone.....	107

7. Schemes

<i>Scheme 1.</i> Regio- and enantioselective ketone alkylation of allyl enol carbonates by Trost.	5
<i>Scheme 2.</i> Synthesis of chiral, substituted cyclohexenones by Fráter.	6
<i>Scheme 3.</i> Diastereoselective synthesis of cyclohexenones by Meyers et al.	6
<i>Scheme 4.</i> Diastereoselective synthesis of cyclohexenones by Maiti et al.	7
<i>Scheme 5.</i> Diastereoselective Birch reduction alkylation reaction by Schultz et al.	7
<i>Scheme 6.</i> Dehydrobromination- and rearrangement-reaction reported by Schulz et al.	8
<i>Scheme 7.</i> Alkylation-dearomatization of phenols.	9
<i>Scheme 8.</i> C- and O-alkylation of phenoxide ion.	10
<i>Scheme 9.</i> Unpublished phenolate alkylation experiment with (-)-sparteine.	10
<i>Scheme 10.</i> Synthesis of (+/-)-seychellene by Fráter et al.	11
<i>Scheme 11.</i> Regioselective in-situ hydrogenation by Goeke.	11
<i>Scheme 12.</i> Hydrogenolysis of cyclohexadienones by Miller et al.	12
<i>Scheme 13.</i> Regioselective hydrogenation of 4-oxoisophorone enol acetate by Soukup.	12
<i>Scheme 14.</i> O- and C-alkylation of 2,6-dimethylphenol.	13
<i>Scheme 15.</i> Selective hydrogenation of the cyclohexadienone 4,5-double bonds.	14
<i>Scheme 16.</i> Acid catalyzed rearrangement of cyclohexadienones.	15
<i>Scheme 17.</i> By-product from BuLi and toluene.	15
<i>Scheme 18.</i> By-product resulting from dialkylation of 2,6-dimethyl naphthol.	16
<i>Scheme 19.</i> Alkylation of asymmetric 2-methyl-6- <i>tert</i> -butylphenol 64 .	25
<i>Scheme 20.</i> Enantioselective alkylation of 2-methyl-1-naphthol 65 .	25
<i>Scheme 21.</i> Enantioselective alkylation of 1-methyl-2-naphthol 69 .	25
<i>Scheme 22.</i> Synthesis of 1-methyl-2-naphthol 69 .	26
<i>Scheme 23.</i> Enantioselective phenol and naphthol alkylation with sparteine.	31
<i>Scheme 24.</i> Regioselective hydrogenation of cyclohexadienones.	32
<i>Scheme 25.</i> Mechanism of the S _N 2 reaction.	48
<i>Scheme 26.</i> Mechanism of the S _N 2' reaction.	48
<i>Scheme 27.</i> S _N 2 vs. S _N 2' reactions by Stork et al.	49
<i>Scheme 28.</i> S _N 2 and S _N 2' reaction of 1,3-cyclohexadiene mono-epoxide with organo cuprates, by Rickborn et al.	49
<i>Scheme 29.</i> Radical anion mediated mechanism postulated by Johnson et al.	50
<i>Scheme 30.</i> Evidence for <i>anti</i> addition of thiolates by Stork et al.	50
<i>Scheme 31.</i> Evidence for selective <i>syn</i> displacement in unbiased S _N 2' reactions.	51
<i>Scheme 32.</i> S _N i' reaction in the prostaglandin synthesis by Toromanoff.	52

<i>Scheme 33.</i> Enantioselective S _N 2' reaction by Denmark et al.	53
<i>Scheme 34.</i> Cyclobutanone and oxetane through S _N i ring closure by Fráter et al.	60
<i>Scheme 35.</i> Diastereoselective cyclobutanone synthesis through [2+2] addition of optically active ketenes to olefins, by Fráter et al.	60
<i>Scheme 36.</i> Diastereoselective cyclobutanone synthesis, by Ghosez et al.	61
<i>Scheme 37.</i> Synthesis of chiral cyclobutanones by Ghosez et al.	61
<i>Scheme 38.</i> Chiral cyclobutanones by Trost et al.	62
<i>Scheme 39.</i> Chiral cyclobutanone by Ihara et al.	62
<i>Scheme 40.</i> Cyclobutanones by the S _N i', 4- <i>exo-trig</i> ring closure reaction.	63
<i>Scheme 41.</i> 6- <i>Exo-tet</i> ring closure leading to six member rings.	63
<i>Scheme 42.</i> Cyclobutanone vs. oxetane formation in the 4- <i>exo-trig</i> S _N i' reaction.	64
<i>Scheme 43.</i> Mechanistic pathways of the S _N i' reaction leading to cyclobutanones.	66
<i>Scheme 44.</i> Synthesis of the key-intermediate 145 by the Stork enamine synthesis.	67
<i>Scheme 45.</i> (<i>Z</i>)- selectivity of unstabilized phosphonium ylides.	68
<i>Scheme 46.</i> (<i>E</i>)- and (<i>Z</i>)-selectivity of stabilized phosphonium ylides.	68
<i>Scheme 47.</i> Possible reaction mechanisms for the cyclization of keto-ester (<i>E</i>)- 152 .	69
<i>Scheme 48.</i> Chemoselective reduction of the ester function in keto-ester (<i>E</i>)- 152 .	70
<i>Scheme 49.</i> Fluoride ion catalyzed S _N i' reaction by Nakamura et al.	71
<i>Scheme 50.</i> Synthesis of (<i>E</i>)- 170 containing a cyclohexane ring.	71
<i>Scheme 51.</i> Synthesis of methane- and toluenesulfonic-acid ester precursors.	72
<i>Scheme 52.</i> Cyclobutanones through S _N i' reaction of mesylate (<i>E</i>)- 136 .	72
<i>Scheme 53.</i> S _N i' reaction leading to spiro cyclobutanones.	73
<i>Scheme 54.</i> O- vs. C-nucleophilicity in the S _N i reaction.	73
<i>Scheme 55.</i> Enantioselective synthesis of the hydroxy ketone (-)-(<i>R</i>)-(<i>E</i>)- 176 .	75
<i>Scheme 56.</i> Synthesis of (+)-(<i>S</i>)-(<i>E</i>)- 176 with (-)-Ipc ₂ BCl by Midland et al.	76
<i>Scheme 57.</i> Determination of the absolute configuration of (+)-(<i>S</i>)-(<i>E</i>)- 176 by Horeau's empirical method.	77
<i>Scheme 58.</i> Stereoselective S _N 2 displacement by Magid et al.	78
<i>Scheme 59.</i> S _N i' reaction of chiral chloro-ketone (+)-(<i>S</i>)-(<i>E</i>)- 139 .	79
<i>Scheme 60.</i> Separation of (+)-(<i>E</i>)- and (-)-(<i>Z</i>)- 140 over AgNO ₃ impregnated silica gel.	81
<i>Scheme 61.</i> Reaction mechanism of the 4- <i>exo-trig</i> S _N i' reaction.	85
<i>Scheme 62.</i> (-)-Junionone from (-)-(<i>E</i>)-caryophyllene by Thomas et al.	86
<i>Scheme 63.</i> Synthetic route leading to (-)-junionone.	87
<i>Scheme 64.</i> Keto-aldehyde 194 through epoxide rearrangement by House et al.	87

<i>Scheme 65.</i> Construction of (<i>E,E</i>)- 196 by the Wittig reaction followed by I ₂ catalyzed isomerization.	88
<i>Scheme 66.</i> Preparation of the Shi catalyst 200 .	89
<i>Scheme 67.</i> Regio- and enantioselective epoxidation by Shi et al.	89
<i>Scheme 68.</i> Fragmentation reaction leading to optically active alcohol 205 .	90
<i>Scheme 69.</i> Determination of the absolute configuration of 205 by Horeau's method.	90
<i>Scheme 70.</i> Preparation of pure (<i>E</i>)- <i>trans</i> - 190 for ROA spectroscopy.	92
<i>Scheme 71.</i> Attempted, base induced, S _N i' reaction of (<i>R,R</i>)-(<i>E</i>)- 190 .	94
<i>Scheme 72.</i> S _N i' reaction of (<i>R,R</i>)-(<i>E</i>)- 190 after epoxide activation with BF ₃ ·Et ₂ O.	94
<i>Scheme 73.</i> Allyl cation intermediate in the BF ₃ ·Et ₂ O cyclization of (<i>R,R</i>)-(<i>E</i>)- 190E .	95
<i>Scheme 74.</i> Epoxide activation with ZnCl ₂ by Wasserman et al.	96
<i>Scheme 75.</i> Metal salt induced epoxide activation by Crotti et al.	98
<i>Scheme 76.</i> S _N i reaction between ketone enolates and epoxides by Crotti et al.	99
<i>Scheme 77.</i> Reaction of aluminum ester enolates with epoxides by Taylor et al.	99
<i>Scheme 78.</i> Products formed from (<i>R,R</i>)-(<i>E</i>)- 190 with different Lewis acids.	100
<i>Scheme 79.</i> S _N i' reaction of β-keto ester epoxide (<i>E</i>)- 241 .	102
<i>Scheme 80.</i> Possible mechanisms for the S _N i' reaction performed in the prostaglandin synthesis by Toromanoff et al.	102
<i>Scheme 81.</i> Cyclobutanone synthesis from β-keto-ester (<i>R,R</i>)-(<i>E</i>)- 247 with BuLi.	103
<i>Scheme 82.</i> Synthesis of (-)-junionone using Me ₃ SiOTf as the Lewis acid.	104
<i>Scheme 83.</i> Synthesis of (+)-junionone with Et ₃ Al as Lewis acid.	105
<i>Scheme 84.</i> Mechanism of the S _N i' reaction leading to cyclobutanones.	108
<i>Scheme 85.</i> Cyclobutanone vs. oxetane formation in the S _N i and S _N i' reaction.	109
<i>Scheme 86.</i> Total synthesis of (-)-junionone (-)-(<i>S</i>)-(<i>E</i>)- 189 .	109
<i>Scheme 87.</i> Allyl cation intermediate in the cyclization of (<i>R,R</i>)-(<i>E</i>)- 190E .	110
<i>Scheme 88.</i> Stereoselective cyclization of (<i>R,R</i>)-(<i>E</i>)- 190 with Et ₃ Al.	110

8. Acknowledgments

I would like to express my sincere appreciation to *Prof. Dr. Heinz Heimgartner* for accepting me in his group and for helping me to successfully complete this research.

I am much obliged to *Dr. Andreas Goeke* for his fruitful cooperation, for the time he spent with me, and for his many clarifying discussions and suggestions.

Special thanks are due to *Givaudan* for the generous financial support of this work.

I am indebted to *Gerhard Brunner* for his efforts and professional advice, helping me to solve numerous NMR related problems. Also, I would like to thank *Katarina Grman* for performing the chiral GC analysis.

I wish to express my gratitude to *Prof. Dr. Werner Hug* and *Dymitro Dudenko* from the University of Fribourg for performing the RAMAN/ROA measurements and calculations. I would also like to thank *Dr. Anthony Linden* from the University of Zurich for performing the X-ray crystallographic measurements and calculations.

Many thanks to *Dr. Elemér Vass* from the Eötvös Loránd University in Budapest for performing the VCD measurements and calculations.

I would like to thank my parents for their tremendous support in all respects and my brother for all his support and valuable discussions.

Special thanks are extended to the members of the Heimgartner group for the pleasant work atmosphere and for their help and cooperation. I would like to thank *Simon Stamm* for the many valuable discussions and inspiring ideas.

Sincere thanks are due to *Sonja Samanes* for her caring and patience and to *Reto Zollinger* for his loyal friendship.

I would also like to thank *Dr. Christine Famega* for the many encouraging discussions.

Last but not least, I want to thank the members of the student association *Schützenverein Schweizerischer Studierender* for all the great times we spent and for providing me with the kind of social skills, not attainable elsewhere. *Vivat, Crescat, Floreat!*

9. Curriculum Vitae

Name: Lovchik
First name: Martin Alan
Date and place of birth: April 4. 1972 in Zurich, Switzerland
Nationality: Swiss, USA

Education

2002 - present PhD Studies at the University of Zurich under the supervision of Prof. Dr. Georg Fráter and Prof. Dr. Heinz Heimgartner from the Institute of Organic Chemistry. Title: "I. Enantioselective Synthesis of Cyclohexa-2,4-dien-1-ones and Cyclohex-2-en-1-ones from Phenols. II. Cyclobutanes through S_Ni' Ring Closure, a Mechanistic Study".

2001 Master of Science in organic chemistry at the University of Cincinnati, Ohio USA. Titel: "Transition metal catalyzed rearrangement of vinyl cyclobutenes".

1992 Certificate of Proficiency as Laboratory Technician in Zurich, Switzerland

1989-1992 Apprenticeship as Laboratory Technician at Givaudan Duebendorf, Switzerland

1986-1989 Secondary School in Horgen, Switzerland

1981-1986 Elementary School in Horgen, Switzerland

1979-1981 Elementary School in Emsworth, UK

Employment History

1996 – 1999 Laboratory Technician, Givaudan Geneva, Switzerland
Department for Process Development

1992 – 1996 Laboratory Technician, Givaudan Duebendorf, Switzerland
Flavors and Fragrance Research